

JOURNAL OF

CHROMATOGRAPHY

INCLUDING ELECTROPHORESIS AND OTHER SEPARATION METHODS

EDITORS

U.A.Th. Brinkman (Amsterdam)
R.W. Giese (Boston, MA)
J.K. Haken (Kensington, N.S.W.)
K. Macek (Prague)
L.R. Snyder (Orinda, CA)

EDITORS, SYMPOSIUM VOLUMES.

E. Heftmann (Orinda, CA), Z. Deyl (Prague)

EDITORIAL BOARD

D.W. Armstrong (Rolla, MO)
W.A. Aue (Halifax)
P. Bocek (Brno)
A.A. Boulton (Saskatoon)
P.W. Carr (Minneapolis, MN)
N.H.C. Cooke (San Ramon, CA)
V.A. Davankov (Moscow)
Z. Deyl (Prague)
S. Dilli (Kensington, N.S.W.)
H. Engelhardt (Saarbrücken)
F. Erni (Basle)
M.B. Evans (Hatfield)
J.L. Glajch (N. Billerica, MA)
G.A. Guiochon (Knoxville, TN)
P.R. Haddad (Hobart, Tasmania)
I.M. Hais (Hradec Králové)
W.S. Hancock (San Francisco, CA)
S. Hjertén (Uppsala)
S. Honda (Higashi-Osaka)
Cs. Horváth (New Haven, CT)
J.F.K. Huber (Vienna)
K.-P. Hupe (Waldbronn)
T.W. Hutchens (Houston, TX)
J. Janák (Brno)
P. Jandera (Pardubice)
B.L. Karger (Boston, MA)
J.J. Kirkland (Newport, DE)
E. sz. Kováts (Lausanne)
A.J.P. Martin (Cambridge)
L.W. McLaughlin (Chestnut Hill, MA)
E.D. Morgan (Keele)
J.D. Pearson (Kalamazoo, MI)
H. Poppe (Amsterdam)
F.E. Regnier (West Lafayette, IN)
P.G. Righetti (Milan)
P. Schoenmakers (Eindhoven)
R. Schwarzenbach (Dübendorf)
R.E. Shoup (West Lafayette, IN)
R.P. Singh (Wichita, KS)
A.M. Siouffi (Marseille)
D.J. Strydom (Boston, MA)
N. Tanaka (Kyoto)
S. Terabe (Hyogo)
K.K. Unger (Mainz)
R. Verpoorte (Leiden)
Gy. Vigh (College Station, TX)
J.T. Watson (East Lansing, MI)
B.D. Westerlund (Uppsala)

EDITORS, BIBLIOGRAPHY SECTION

Z. Deyl (Prague), J. Janák (Brno), V. Schwartz (Prague)

ELSEVIER

JOURNAL OF CHROMATOGRAPHY

INCLUDING ELECTROPHORESIS AND OTHER SEPARATION METHODS

Scope. The *Journal of Chromatography* publishes papers on all aspects of **chromatography, electrophoresis** and related methods. Contributions consist mainly of research papers dealing with chromatographic theory, instrumental developments and their applications. The section *Biomedical Applications*, which is under separate editorship, deals with the following aspects: developments in and applications of chromatographic and electrophoretic techniques related to clinical diagnosis or alterations during medical treatment; screening and profiling of body fluids or tissues related to the analysis of active substances and to metabolic disorders; drug level monitoring and pharmacokinetic studies; clinical toxicology; forensic medicine; veterinary medicine; occupational medicine; results from basic medical research with direct consequences in clinical practice. In *Symposium volumes*, which are under separate editorship, proceedings of symposia on chromatography, electrophoresis and related methods are published.

Submission of Papers. The preferred medium of submission is on disk with accompanying manuscript (see *Electronic manuscripts* in the Instructions to Authors, which can be obtained from the publisher, Elsevier Science Publishers B.V., P.O. Box 330, 1000 AH Amsterdam, Netherlands). Manuscripts (in English; *four* copies are required) should be submitted to: Editorial Office of *Journal of Chromatography*, P.O. Box 681, 1000 AR Amsterdam, Netherlands, Telefax (+31-20) 5862 304, or to: The Editor of *Journal of Chromatography, Biomedical Applications*, P.O. Box 681, 1000 AR Amsterdam, Netherlands. Review articles are invited or proposed in writing to the Editors who welcome suggestions for subjects. An outline of the proposed review should first be forwarded to the Editors for preliminary discussion prior to preparation. Submission of an article is understood to imply that the article is original and unpublished and is not being considered for publication elsewhere. For copyright regulations, see below.

Publication. The *Journal of Chromatography* (incl. *Biomedical Applications*) has 40 volumes in 1993. The subscription prices for 1993 are:

J. Chromatogr. (incl. *Cum. Indexes, Vols. 601-650*) + *Biomed. Appl.* (Vols. 612-651):

Dfl. 8520.00 plus Dfl. 1320.00 (p.p.h.) (total ca. US\$ 5466.75)

J. Chromatogr. (incl. *Cum Indexes, Vols. 601-650*) only (Vols. 623-651):

Dfl. 7047.00 plus Dfl. 957.00 (p.p.h.) (total ca. US\$ 4446.75)

Biomed. Appl. only (Vols. 612-622):

Dfl. 2783.00 plus Dfl. 363.00 (p.p.h.) (total ca. US\$ 1747.75).

Subscription Orders. The Dutch guildler price is definitive. The US\$ price is subject to exchange-rate fluctuations and is given as a guide. Subscriptions are accepted on a prepaid basis only, unless different terms have been previously agreed upon. Subscriptions orders can be entered only by calendar year (Jan.-Dec.) and should be sent to Elsevier Science Publishers, Journal Department, P.O. Box 211, 1000 AE Amsterdam, Netherlands, Tel. (+31-20) 5803 642, Telefax (+31-20) 5803 598, or to your usual subscription agent. Postage and handling charges include surface delivery except to the following countries where air delivery via SAL (Surface Air Lift) mail is ensured: Argentina, Australia, Brazil, Canada, China, Hong Kong, India, Israel, Japan*, Malaysia, Mexico, New Zealand, Pakistan, Singapore, South Africa, South Korea, Taiwan, Thailand, USA. *For Japan air delivery (SAL) requires 25% additional charge of the normal postage and handling charge. For all other countries airmail rates are available upon request. Claims for missing issues must be made within six months of our publication (mailing) date, otherwise such claims cannot be honoured free of charge. Back volumes of the *Journal of Chromatography* (Vols. 1-611) are available at Dfl. 230.00 (plus postage). Customers in the USA and Canada wishing information on this and other Elsevier journals, please contact Journal Information Center, Elsevier Science Publishing Co. Inc., 655 Avenue of the Americas, New York, NY 10010, USA, Tel. (+1-212) 633 3750, Telefax (+1-212) 633 3764.

Abstracts/Contents Lists published in Analytical Abstracts, Biochemical Abstracts, Biological Abstracts, Chemical Abstracts, Chemical Titles, Chromatography Abstracts, Current Awareness in Biological Sciences (CABS), Current Contents/Life Sciences, Current Contents/Physical, Chemical & Earth Sciences, Deep-Sea Research/Part B: Oceanographic Literature Review, Excerpta Medica, Index Medicus, Mass Spectrometry Bulletin, PASCAL-CNRS, Referativnyi Zhurnal, Research Alert and Science Citation Index.

US Mailing Notice. *Journal of Chromatography* (ISSN 0021-9673) is published weekly (total 52 issues) by Elsevier Science Publishers (Sara Burgerhartstraat 25, P.O. Box 211, 1000 AE Amsterdam, Netherlands). Annual subscription price in the USA US\$ 4446.75 (subject to change), including air speed delivery. Second class postage paid at Jamaica, NY 11431. **USA**

POSTMASTERS: Send address changes to *Journal of Chromatography*, Publications Expediting, Inc., 200 Meacham Avenue, Elmont, NY 11003. Airfreight and mailing in the USA by Publications Expediting.

See inside back cover for Publication Schedule, Information for Authors and information on Advertisements.

© 1993 ELSEVIER SCIENCE PUBLISHERS B.V. All rights reserved.

0021-9673/93/\$06.00

No part of this publication may be reproduced, stored in a retrieval system or transmitted in any form or by any means, electronic, mechanical, photocopying, recording or otherwise, without the prior written permission of the publisher, Elsevier Science Publishers B.V., Copyright and Permissions Department, P.O. Box 521, 1000 AM Amsterdam, Netherlands.

Upon acceptance of an article by the journal, the author(s) will be asked to transfer copyright of the article to the publisher. The transfer will ensure the widest possible dissemination of information.

Special regulations for readers in the USA. This journal has been registered with the Copyright Clearance Center, Inc. Consent is given for copying of articles for personal or internal use, or for the personal use of specific clients. This consent is given on the condition that the copier pays through the Center the per-copy fee stated in the code on the first page of each article for copying beyond that permitted by Sections 107 or 108 of the US Copyright Law. The appropriate fee should be forwarded with a copy of the first page of the article to the Copyright Clearance Center, Inc., 27 Congress Street, Salem, MA 01970, USA. If no code appears in an article, the author has not given broad consent to copy and permission to copy must be obtained directly from the author. All articles published prior to 1980 may be copied for a per-copy fee of US\$ 2.25, also payable through the Center. This consent does not extend to other kinds of copying, such as for general distribution, resale, advertising and promotion purposes, or for creating new collective works. Special written permission must be obtained from the publisher for such copying.

No responsibility is assumed by the Publisher for any injury and/or damage to persons or property as a matter of products liability, negligence or otherwise, or from any use or operation of any methods, products, instructions or ideas contained in the materials herein. Because of rapid advances in the medical sciences, the Publisher recommends that independent verification of diagnoses and drug dosages should be made.

Although all advertising material is expected to conform to ethical (medical) standards, inclusion in this publication does not constitute a guarantee or endorsement of the quality or value of such product or of the claims made of it by its manufacturer.

This issue is printed on acid-free paper.

CONTENTS

(Abstracts/Contents Lists published in Analytical Abstracts, Biochemical Abstracts, Biological Abstracts, Chemical Abstracts, Chemical Titles, Chromatography Abstracts, Current Awareness in Biological Sciences (CABS), Current Contents/Life Sciences, Current Contents/Physical, Chemical & Earth Sciences, Deep-Sea Research/Part B: Oceanographic Literature Review, Excerpta Medica, Index Medicus, Mass Spectrometry Bulletin, PASCAL-CNRS, Referativnyi Zhurnal, Research Alert and Science Citation Index)

REGULAR PAPERS

Column Liquid Chromatography

- Peculiarities of zone migration and band broadening in gradient reversed-phase high-performance liquid chromatography of proteins with respect to membrane chromatography
by B.G. Belenkii, A.M. Podkladenko, O.I. Kurenbin, V.G. Mal'tsev, D.G. Nasledov and S.A. Trushin (St. Petersburg, Russian Federation) (Received March 29th, 1993) 1
- Chiral stationary phases consisting of axially dissymmetric 2'-substituted-1,1'-binaphthyl-2-carboxylic acids bonded to silica gel for high-performance liquid chromatographic separation of enantiomers
by S. Oi, M. Shijo, H. Tanaka and S. Miyano (Sendai, Japan) and J. Yamashita (Tokyo, Japan) (Received April 20th, 1993) 17
- Use of carotenoids in the characterization of octadecylsilane bonded columns and mechanism of retention of carotenoids on monomeric and polymeric stationary phases
by E. Lesellier and A. Tchaplà (Orsay, France) and A.M. Krstulovic (Meudon-la-Forêt, France) (Received March 19th, 1993) 29
- Study of polyorganosiloxanes (native and solvent swollen) for the preparation of narrow (5–15 μm I.D.) and long (1–6 m) open tubular columns in reversed-phase liquid chromatography
by K. Göhlin (Göteborg, Sweden) and M. Larsson (Mölnådal, Sweden) (Received March 22nd, 1993) 41
- Pyrophosphates as biocompatible packing materials for high-performance liquid chromatography
by S. Inoue and N. Ohtaki (Saitama, Japan) (Received April 19th, 1993) 57
- Displacement chromatography on cyclodextrin silicas. IV. Separation of the enantiomers of ibuprofen
by Gy. Farkas, L.H. Irgens, G. Quintero, M.D. Beeson, A. Al-Saeed and Gy. Vigh (College Station, TX, USA) (Received April 28th, 1993) 67
- Fluorescence derivatization reagent for resolution of carboxylic acid enantiomers by high-performance liquid chromatography
by J. Kondo, T. Imaoka, T. Kawasaki, A. Nakanishi and Y. Kawahara (Tokyo, Japan) (Received April 20th, 1993) 75
- High-performance liquid chromatographic analysis of wheat flour lipids using an evaporative light scattering detector
by F.D. Conforti, C.H. Harris and J.T. Rinehart (Blacksburg, VA, USA) (Received April 21st, 1993) 83
- Determination of RDX, 2,4,6-trinitrotoluene and other nitroaromatic compounds by high-performance liquid chromatography with photodiode-array detection
by M. Emmrich (Berlin, Germany), M. Kaiser (Swisttal, Germany) and H. Rüdén and S. Sollinger (Berlin, Germany) (Received March 19th, 1993). 89
- Direct separation of 4-amino-3-(4-chlorophenyl)butyric acid and analogues, GABA_B ligands, using a chiral crown ether stationary phase
by C. Vaccher, P. Berthelot and M. Debaert (Lille, France) (Received March 5th, 1993) 95
- High-performance gel-permeation chromatographic analysis of protein aggregation. Application to bovine carbonic anhydrase
by C. De Felice, K. Hayakawa, T. Watanabe and T. Tanaka (Tokyo, Japan) (Received April 6th, 1993) 101
- High-performance liquid chromatographic determination of the isomeric purity of a series of dioxolane nucleoside analogues
by M.P. Di Marco, C.A. Evans, D.M. Dixit, W.L. Brown, M.A. Siddiqui, H.L.A. Tse, H. Jin, N. Nguyen-Ba and T.S. Mansour (Québec, Canada) (Received April 27th, 1993) 107

(Continued overleaf)

Contents (continued)

Characterization of vitamin D ₃ metabolites using continuous-flow fast atom bombardment tandem mass spectrometry and high-performance liquid chromatography by B. Yeung and P. Vouros (Boston, MA, USA) and G. Satyanarayana Reddy (Providence, RI, USA) (Received April 5th, 1993)	115
Determination of pesticides in drinking water by on-line solid-phase disk extraction followed by various liquid chromatographic systems by S. Chiron and D. Barceló (Barcelona, Spain) (Received April 8th, 1993)	125
Analysis of polyethylene glycols with respect to their oligomer distribution by high-performance liquid chromatography by T. Meyer, D. Harms and J. Gmehling (Oldenburg, Germany) (Received February 22nd, 1993)	135
<i>Gas Chromatography</i>	
Solubility parameters of broad and narrow distributed oxyethylates of fatty alcohols by A. Voelkel and J. Janas (Poznań, Poland) (Received April 27th, 1993)	141
Parallel cryogenic trapping multidimensional gas chromatography with directly linked infrared and mass spectral detection by K.A. Krock, N. Ragunathan and C.L. Wilkins (Riverside, CA, USA) (Received May 3rd, 1993)	153
<i>Planar Chromatography</i>	
Rapid synthesis of isoprenoid diphosphates and their isolation in one step using either thin layer or flash chromatography. by R. Kennedy Keller and R. Thompson (Tampa, FL, USA) (Received May 10th, 1993)	161
<i>Electrophoresis</i>	
Application of capillary electrophoresis to the analysis of the oligomeric distribution of polydisperse polymers by J. Bullock (Malvern, PA, USA) (Received May 11th, 1993)	169
SHORT COMMUNICATIONS	
<i>Column Liquid Chromatography</i>	
Determination and confirmation of benomyl and carbendazim in water using high-performance liquid chromatography and diode array detection by J.S. Dhoot and A.R. del Rosario (Berkeley, CA, USA) (Received May 25th, 1993)	178
<i>Gas Chromatography</i>	
Structure-gas chromatographic retention time models of tetra- <i>n</i> -alkylsilanes and tetra- <i>n</i> -alkylgermanes using topological indexes. A correction by E.J. Kupchik (Jamaica, NY, USA) (Received April 27th, 1993)	182
<i>Planar Chromatography</i>	
Adsorption chromatography on cellulose. X. Adsorption of tryptophan and derivatives from CuSO ₄ -containing eluents by T.K.X. Huynh and M. Lederer (Lausanne, Switzerland) (Received April 29th, 1993)	185
Quantitation of 5-methylcytosine by one-dimensional high-performance thin-layer chromatography by S.A. Leonard, S.C. Wong and J.W. Nyce (Greenville, NC, USA) (Received May 24th, 1993)	189
<i>Electrophoresis</i>	
Validation of a capillary electrophoresis method for the enantiomeric purity testing of fluparoxan by K.D. Altria and A.R. Walsh (Ware, UK) and N.W. Smith (Greenford, UK) (Received May 11th, 1993)	193
Determination of total vitamin C in fruits by capillary zone electrophoresis by M. Chiari, M. Nesi, G. Carrea and P.G. Righetti (Milan, Italy) (Received April 26th, 1993)	197

JOURNAL OF CHROMATOGRAPHY

VOL. 645 (1993)

JOURNAL of CHROMATOGRAPHY

INCLUDING ELECTROPHORESIS AND OTHER SEPARATION METHODS

EDITORS

U.A.Th. BRINKMAN (Amsterdam), R.W. GIESE (Boston, MA), J.K. HAKEN (Kensington, N.S.W.), K. MACEK (Prague),
L.R. SNYDER (Orinda, CA)

EDITORS, SYMPOSIUM VOLUMES

E. HEFTMANN (Orinda, CA), Z. DEYL (Prague)

EDITORIAL BOARD

D.W. Armstrong (Rolla, MO), W.A. Aue (Halifax), P. Boček (Brno), A.A. Boulton (Saskatoon), P.W. Carr (Minneapolis, MN), N.H.C. Cooke (San Ramon, CA), V.A. Davankov (Moscow), Z. Deyl (Prague), S. Dilli (Kensington, N.S.W.), H. Engelhardt (Saarbrücken), F. Erni (Basle), M.B. Evans (Hatfield), J.L. Glajch (N. Billerica, MA), G.A. Guiochon (Knoxville, TN), P.R. Haddad (Hobart, Tasmania), I.M. Hais (Hradec Králové), W.S. Hancock (San Francisco, CA), S. Hjertén (Uppsala), S. Honda (Higashi-Osaka), Cs. Horváth (New Haven, CT), J.F.K. Huber (Vienna), K.-P. Hupe (Waldbronn), T.W. Hutchens (Houston, TX), J. Janák (Brno), P. Jandera (Pardubice), B.L. Karger (Boston, MA), J.J. Kirkland (Newport, DE), E. sz. Kováts (Lausanne), A.J.P. Martin (Cambridge), L.W. McLaughlin (Chestnut Hill, MA), E.D. Morgan (Keele), J.D. Pearson (Kalamazoo, MI), H. Poppe (Amsterdam), F.E. Regnier (West Lafayette, IN), P.G. Righetti (Milan), P. Schoenmakers (Eindhoven), R. Schwarzenbach (Dübendorf), R.E. Shoup (West Lafayette, IN), R.P. Singhal (Wichita, KS), A.M. Siouffi (Marseille), D.J. Strydom (Boston, MA), N. Tanaka (Kyoto), S. Terabe (Hyogo), K.K. Unger (Mainz), R. Verpoorte (Leiden), Gy. Vigh (College Station, TX), J.T. Watson (East Lansing, MI), B.D. Westerlund (Uppsala)

EDITORS, BIBLIOGRAPHY SECTION

Z. Deyl (Prague), J. Janák (Brno), V. Schwarz (Prague)



ELSEVIER
AMSTERDAM — LONDON — NEW YORK — TOKYO

J. Chromatogr., Vol. 645 (1993)

© 1993 ELSEVIER SCIENCE PUBLISHERS B.V. All rights reserved.

0021-9673/93/\$06.00

No part of this publication may be reproduced, stored in a retrieval system or transmitted in any form or by any means, electronic, mechanical, photocopying, recording or otherwise, without the prior written permission of the publisher, Elsevier Science Publishers B.V., Copyright and Permissions Department, P.O. Box 521, 1000 AM Amsterdam, Netherlands.

Upon acceptance of an article by the journal, the author(s) will be asked to transfer copyright of the article to the publisher. The transfer will ensure the widest possible dissemination of information.

Submission of an article for publication entails the authors' irrevocable and exclusive authorization of the publisher to collect any sums or considerations for copying or reproduction payable by third parties (as mentioned in article 17 paragraph 2 of the Dutch Copyright Act of 1912 and the Royal Decree of June 20, 1974 (S. 351) pursuant to article 16 b of the Dutch Copyright Act of 1912) and/or to act in or out of Court in connection therewith.

Special regulations for readers in the USA. This journal has been registered with the Copyright Clearance Center, Inc. Consent is given for copying of articles for personal or internal use, or for the personal use of specific clients. This consent is given on the condition that the copier pays through the Center the per-copy fee stated in the code on the first page of each article for copying beyond that permitted by Sections 107 or 108 of the US Copyright Law. The appropriate fee should be forwarded with a copy of the first page of the article to the Copyright Clearance Center, Inc., 27 Congress Street, Salem, MA 01970, USA. If no code appears in an article, the author has not given broad consent to copy and permission to copy must be obtained directly from the author. All articles published prior to 1980 may be copied for a per-copy fee of US\$ 2.25, also payable through the Center. This consent does not extend to other kinds of copying, such as for general distribution, resale, advertising and promotion purposes, or for creating new collective works. Special written permission must be obtained from the publisher for such copying.

No responsibility is assumed by the Publisher for any injury and/or damage to persons or property as a matter of products liability, negligence or otherwise, or from any use or operation of any methods, products, instructions or ideas contained in the materials herein. Because of rapid advances in the medical sciences, the Publisher recommends that independent verification of diagnoses and drug dosages should be made.

Although all advertising material is expected to conform to ethical (medical) standards, inclusion in this publication does not constitute a guarantee or endorsement of the quality or value of such product or of the claims made of it by its manufacturer.

This issue is printed on acid-free paper.

Printed in the Netherlands

Peculiarities of zone migration and band broadening in gradient reversed-phase high-performance liquid chromatography of proteins with respect to membrane chromatography[☆]

B.G. Belenkii* and A.M. Podkladenko

Institute for Analytical Instrumentation, Russian Academy of Sciences, Rijsky Prospect 26, 198103 St. Petersburg (Russian Federation)

O.I. Kurenbin, V.G. Mal'tsev, D.G. Nasledov and S.A. Trushin

Institute of Macromolecular Compounds, Russian Academy of Sciences, Bolshoy Prospect, St. Petersburg (Russian Federation)

(First received September 30th, 1992; revised manuscript received March 29th, 1993)

ABSTRACT

The peculiarities of zone migration and band broadening in the reversed-phase gradient HPLC of proteins were investigated. In the isocratic mode a critical composition of the mobile phase was found at which all proteins regardless of their molecular mass migrate with equal velocity and have a capacity factor equal to the phase ratio (V_p/V_0), *i.e.*, the same capacity factor as a marker of total accessible volume would have in steric exclusion chromatography. It is shown that steric exclusion conditions are never achieved in gradient HPLC. In the first (adsorption stage) of gradient elution where the separation takes place the velocity of a protein increases until it becomes equal to the velocity of the desorbing solvent front at a critical distance X_0 from column entrance. Strong broadening is characteristic of this stage. In the second (critical) stage the protein travels the remaining distance ($L - X_0$) with the velocity of the solvent. A definition of X_0 is given allowing one very simple calculation of the minimum permissible column length as a function of gradient steepness, mobile phase velocity and protein adsorption parameter. When $x = X_0$ the protein zone has the smallest dispersion. Making $L < X_0$ is especially disadvantageous, as it leads to anomalous bandspreading. The theory of gradient HPLC was refined on this basis and the usefulness of this approach in high-performance membrane chromatography is demonstrated.

INTRODUCTION

In the past 10 years, high-performance liquid adsorption chromatography (HPLAC) of proteins on reversed-phase, ion-exchange, hydro-

phobic and metal chelate sorbents has been developing rapidly. In all types of HPLAC of proteins, in the first stage protein sorption with a capacity factor $k' > 50$ takes place, followed by the selective desorption of a protein in the concentration gradient of a displacer agent. Protein chromatography in the displacer's gradient takes place according to the "all or nothing" principle, which is manifested in a very sharp dependence of capacity factor on displacer concentration [1,2]. This effect is usually explained by the cooperative interaction between

* Corresponding author.

[☆] Presented at the 16th International Symposium on Column Liquid Chromatography, Baltimore, MD, June 14–19, 1992. The majority of the papers presented at this symposium were published in *J. Chromatogr.*, Vols. 631 + 632 (1993).

protein macromolecules and the stationary phase (multi-site adsorption) [3,4]. With few exceptions, proteins are separated with the aid of gradient elution because isocratic elution is possible only when low-capacity ion-exchange and hydrophobic sorbents are used [5,6]. Such sorbents are not characterized by the above sharp transition from unlimited adsorption to complete desorption with a slight increase in the eluting power of the solvent.

An important feature of HPLAC of proteins is that the resolution is independent of the column length or even decreases with increasing column length, which has been reported by several workers [7,8]. This feature makes it possible to use very short columns [9,10] and provides the possibility of chromatography on sorbing membranes: high-performance membrane chromatography (HPMC) [11–15]. In this case sorbing membranes may be considered to be a sorbent layer fixed at the points of particle contact. These membranes, just like the sorbent layer, are characterized by the “interparticle” volume (volume of wide pores through which the flow passes) and the “inner” pore volume (volume of narrow pores filled with stagnant fluid similar to those of perfusion sorbents) [16,17].

The successful development of gradient HPLAC of proteins is based to a considerable extent on the theoretical papers of Regnier and co-workers [4,18] dealing with the mechanism of adsorption chromatography of proteins and on the gradient elution theory developed by Snyder and co-workers [19–26], first for small molecules [19] and later modified for macromolecules [20–26] including proteins [21,22,23]. This theory predicts the retention times and the width of protein peaks and is the basis of process optimization with respect to the degree of separation and the peak capacity [22,24].

However, some important aspects of the elution behaviour have not yet been completely elucidated. First, two problems should be solved. (1) What is the role of steric exclusion in the gradient HPLAC of proteins? In other words, when the eluent composition is programmed, can the zone of desorbed protein migrating along the column acquire the velocity corresponding to the

size-exclusion conditions (SEC) of chromatography? (2) Is there a limit to resolution with decreasing column length and, if there is, on what does this limit depend?

In this paper we attempt to answer these questions and to refine on this basis the theory of gradient HPLAC (and, correspondingly, HPMC) of proteins. As in reversed-phase (RP) HPLC the main specific feature of the HPLAC of proteins (sharp transition from adsorption to desorption) is manifested to the greatest extent, this type of chromatography will be considered experimentally.

THEORY

The measure of the affinity of a protein molecule to the stationary phase is the capacity factor k' , which is the equilibrium ratio of substance mass in sorbent pores, q_p , and in the adsorption layer, \bar{q} , to the substance mass in the mobile phase, q_0 :

$$k' = \frac{q_p + \bar{q}}{q_0} = \frac{V_R - V_0}{V_0} \quad (1)$$

where V_R is the elution volume of the protein and V_0 is the elution volume of a standard which is sterically excluded from the pores and does not interact with their surface.

According to the so-called “three-phase” model [27] in which the equilibrium between the free mobile solution in the interparticle volume, the stagnant liquid in pores and the adsorption layer is considered, the capacity factor may be represented as the product of exclusion and adsorption components:

$$k' = k'_{\text{SEC}}(1 + k_a) \quad (2)$$

where $k_a = \bar{q}/q_p$ is the adsorption constant,

$$k'_{\text{SEC}} = q_p/q_0 = K_{\text{SEC}}(V_p/V_0)$$

K_{SEC} is the equilibrium exclusion distribution coefficient (ratio of substance concentration in pores and in the free solution):

$$K_{\text{SEC}} = C_p/C_0; \quad \kappa = V_p/V_0; \quad k'_{\text{SEC}} = K_{\text{SEC}}\kappa$$

(κ is the ratio of the intraparticle pore volume to the interparticle volume of the column).

It has been shown in papers on the adsorption chromatography of flexible-chain (synthetic) polymers [28–32] on porous sorbents that there is a critical composition of the mobile phase (and an energy of interaction between the segments of macromolecule and the adsorbent surface related to this composition) at which the interphase distribution of all polymers is characterized by the Gibbs energy $\Delta G = -RT \ln K_d = 0$, and the macromolecules regardless of their molecular mass are eluted at $K_d = (C_p + \bar{C})/C_0 = k'/\kappa = 1$, *i.e.*, they have $k' = \kappa$.

At the critical point the exclusion entropy effect is compensated for by the enthalpy effect, *i.e.*, a slight adsorption interaction between the segments of the macromolecule and the inner surface of the adsorbent: $K_{SEC} = 1/(1 + k_a)$, where k_a is the adsorption coefficient.

The critical conditions of protein chromatography may be found (if they exist) by studying the isocratic elution behaviours of several proteins with different molecular masses with a wide range of the mobile phase solvent strength. The phenomenon of critical mobile phase composition and its manifestation in gradient HPLAC of proteins have not been investigated as it is not very evident.

Even the problem of the existence of critical conditions for proteins, *i.e.*, the conditions of chromatography with $k' = k$ has not yet been solved unequivocally. In order to establish the existence of critical conditions, it is necessary to distinguish between the exclusion and the adsorption components of k' , *i.e.*, to determine k' from eqn 1 by using only the exclusion volume V_0 .

However, some workers [12,20] use other definitions of the capacity factor:

$$k'' = \frac{V_R - V_{SEC}}{V_{SEC}} = \frac{q_p - q}{q_p - q_0} = \frac{k'}{1 + \kappa k'_{SEC}} \quad (3)$$

$$k''' = \frac{V_R - V_m}{V_m} = \frac{k' - \kappa}{1 + \kappa} \quad (4)$$

where V_m is the elution volume of the substance

which is not adsorbed but completely penetrates the intraparticle pores and V_{SEC} is the elution volume of the protein in the absence of adsorption, *i.e.*, under size-exclusion conditions. These definitions do not allow one to distinguish either between macromolecules and small molecules (eqn. 4) or between adsorption and penetration into the inner pores (eqn. 3) and hence all manifestations of the critical phenomenon appear to be masked in experiments and manipulations with capacity factors defined in this manner. Moreover, to detect the critical conditions, monofunctional sorbents should be used, *i.e.*, non-specific adsorption should be completely eliminated.

Because the above requirements have not been probably met, the critical conditions in the HPLAC of proteins have not been found even in investigations dealing specially with this problem [33].

In reversed-phase (RP) ion-exchange (IE) and hydrophobic interaction HPLAC, the dependence of k' on the concentration of the displacing agent may be described according to Kopaciewicz *et al.* [4] by the general equation

$$\log k' = \log k_z - z \log C \quad (5)$$

where C is the molar concentration of the displacer, *i.e.*, of an organic solvent in RP-HPLAC, or of a salt in IE-HPLAC or of water in hydrophobic interaction HPLAC.

We shall introduce the concept of critical concentration C_c at which $k' = \kappa$, *i.e.*, $K_{SEC}(1 + k_a) = 1$. Then eqn. (5) can be rewritten in the following form:

$$k' = \kappa \left(\frac{C_c}{C} \right)^z \quad (6)$$

At the high z values (of the order of several tens) which exist in RP-HPLAC the logarithmic dependence of $\log k'$ on the concentration passes into a well known linear dependence:

$$\log k' = \log k_w - S\varphi \quad (7)$$

where φ is the volume fraction of organic solvent or, if the concept of critical concentration is used,

$$\log(k'/\kappa) = S(\varphi_c - \varphi) \quad (8)$$

Retention time in the gradient HPLAC of proteins

In isocratic elution, if eqn. 1 is used the migration velocity of the zone maximum (v) is determined by

$$v = u \cdot \frac{1}{1 + k'} \quad (9)$$

where u is the linear elution velocity (with the assumption that the flow passes only through the interparticle volume). Note that the fundamental eqn. 9 is true only for k' defined by eqn. 1, and not eqn. 3 or 4.

Snyder's theory of gradient elution is based on Freiling's equation [34]:

$$\int_0^{V_g^*} \frac{dV}{V_i} = 1 \quad (10)$$

where V_g^* is the reduced retention volume in gradient elution ($V_g^* = V_g - V_m$), V_g is the experimental retention volume, V_m is the total accessible volume of the column and V_i is the instantaneous reduced retention volume.

The solution of eqn. 10 for RP-HPLC under linear gradient conditions is given [21] by the following equation for the retention time:

$$t_R = \frac{1}{SB} \cdot \log [2.3k'_0 SB(t_{SEC}/t_0) + 1] + t_{SEC} + t_d \quad (11)$$

at $k'(t)$ defined by the equations

$$k' = k_w \cdot 10^{-S\varphi(t)} \quad (12)$$

and

$$\varphi(t) = \varphi_0 + Bt \quad (13)$$

where φ is the volume fraction of the displacing agent (organic solvent), φ_0 is the initial value of φ at the moment of gradient start, B is the gradient steepness, k_w and S are the parameters of protein adsorption, $k'_0 = k_w \cdot 10^{-S\varphi_0}$, t_{SEC} is the time of protein elution under the conditions of size-exclusion chromatography and t_d is the instrumental time lag of a gradient device.

Eqn. 11 makes it possible to attain good

coincidence with experimental data [21], although its theoretical basis (Freiling's equation) is not absolutely rigorous as it was derived for a column of infinite length.

If the more correct Drake procedure [35] is used (see Appendix) then we have the following dependence of migration time on migration distance:

$$t(x) = t_0 + \frac{1}{SB} \cdot \log \left[1 + \frac{k'_0}{\kappa} (E - 1) \right] \quad (14)$$

and hence the retention time is given as $t_R = t(x = L)$, where $E = 10^{SBx/u}$, $k'_0 = k'$ at $\varphi = \varphi_0$, $t_0 = x/u$ is the migration time of a standard substance that is unable to penetrate into inner pores or to be adsorbed on their surface and L is the column length.

It follows from eqn. 14 that the migration velocity of the chromatographic zone depends on the distance x travelled along the column (at $\kappa \ll k'_0$) as follows:

$$v(x) = \frac{E - 1}{(1 + \kappa)E - 1} \cdot u = \frac{(1 + \kappa)(E - 1)}{E(1 + \kappa) - 1} \cdot u_d \quad (15)$$

where u_d is the displacer's velocity, $u_d = u/(1 + \kappa)$, assuming solvent demixing effects to be absent, and u is the mobile phase velocity.

This exponential equation shows that the zone velocity increasing with the distance passed by the zone cannot attain the velocity of the concentration point of the gradient moving at a velocity u_d . However, eqn. 15 enables us to determine the distance X_0 at which the zone velocity $v(x)$ becomes virtually identical with u_d :

$$X_0 = \frac{\lambda u}{SB\kappa} \quad (16)$$

where λ is the parameter characterizing the precision of the fulfillment of the equality $v(X_0) = u_d$. If one inserts X_0 from eqn. 16 instead of x into eqn. 15, it can be seen that $v(X_0) = 0.95u_d$ at $\lambda = 1$ and $v(X_0) = 0.99u_d$ at $\lambda = 2$. These calculations are given for $\kappa = 1$. The theoretical dependence of v on $r = x/X_0$, calculated for $\kappa = 1$ and $\lambda = 1$, is shown in Fig. 1. The value of X_0 plays a fundamental role in the theory of the gradient HPLAC of proteins. It

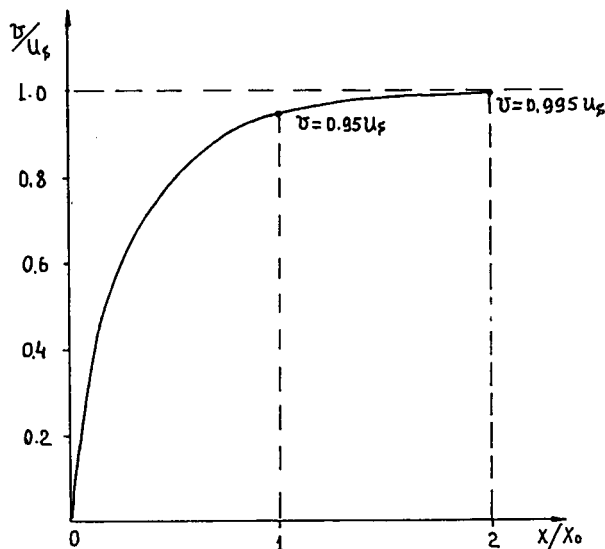


Fig. 1. Ratio of zone velocity (v) to solvent velocity (u_d) as a function of dimensionless migration distance x/X_0 (calculated for $\lambda = 1$ and $\kappa = 1$).

will be shown further that X_0 means the critical distance along the column at which the protein zone comes to the end of its movement in the adsorption mode of chromatography and starts migration according to the laws of critical chromatography.

Eqs. 9 and 15 may be used to obtain the following dependence of the instantaneous capacity factor in gradient elution on the distance x passed along the column:

$$k'(x) = \frac{\kappa E(x)}{E(x) - 1} \quad (\text{at } k' \gg \kappa) \quad (17)$$

where $E(x) = 10^{x/X_0}$ at $\lambda = 1$.

It should be noted that Snyder's theory gives the following expression for the instantaneous capacity factor:

$$k'(x) = \frac{1}{2.3SBt_m}$$

or in our designations and taking into account that $t_m = L/u_d$:

$$\tilde{k}'(x) = \frac{\kappa}{2.3(x/X_0)(1 + \kappa)} \quad (18)$$

Expanding eqn. 17 into a series and taking only the first two terms, which is possible only at $x/X_0 \ll 1$, we can obtain a similar but not identical equation:

$$\tilde{k}'(x) = \frac{\kappa}{2.3(x/X_0)}$$

This means that Snyder's theory of instantaneous capacity factor should work well only for $x \ll X_0$, i.e., either for short columns or only for the upper part of a long column or when S is small, i.e., for small molecules. However, even in this case the definition of k' by eqn. 4 instead of eqn. 1 leads to the wrong results near the critical point ($k' = \kappa$).

At a column length $L > X_0$ the elution time of the protein zone is given in our theory as $t_R = t(x = X_0) + (L - X_0)/u_d$ and hence from eqns. 8, 14 and 16 it follows that

$$t_R = t(\varphi_c) + t_d + \frac{L(1 + \kappa)}{u} \quad (19)$$

where $t(\varphi_c)$ is the time of the gradient to generate the critical concentration:

$$t(\varphi_c) = (\varphi_c - \varphi_0)/B$$

and t_d is the delay time of a gradient device.

Zone spreading in the gradient HPLAC of proteins

Now the relationships of zone spreading in the gradient HPLAC of proteins will be considered. This problem has been investigated in a series of papers by Snyder's group [19,22,23,25]. As the theoretical model developed by these workers has been repeatedly improved, we shall deal with the latest variant [23,25].

The following expression is used for peak standard deviation (in time units):

$$\sigma_t = 0.5J(1 + \tilde{k}')t_m \left[\frac{H(k')}{L} \right]^{1/2} \quad (20)$$

where H is the height equivalent to a theoretical plate (HETP) and \tilde{k}' is the instantaneous value of k' in the middle of the column:

$$k' = \frac{1}{1.15SBt_m} = \frac{1}{1.15b} \quad (21)$$

$t_m = L/u_d$ is the time of the displacer's movement along the column, $H(\tilde{k}')$ is the value of HETP corresponding to $k' = \tilde{k}'$ and J is the empirical factor of additional spreading:

$$J = 0.99 + 1.7b - 1.35b^2 + 0.48b^3 - 0.06b^4 \quad (22)$$

In this model the dependence of HETP on velocity is given by Knox's equation [36]:

$$h = \frac{H}{d_p} = \tilde{A}v^{1/3} + \tilde{B}/v + \tilde{C}v \quad (23)$$

where $v = ud_p/D_m$ is the reduced velocity. It is assumed that the coefficient \tilde{A} does not depend on k' and the dependence of the coefficients \tilde{B} and \tilde{C} on \tilde{k}' is given by

$$\tilde{B} = 1.1 + b'\tilde{k}' \quad (24)$$

and

$$\tilde{C} = \frac{1 - \tilde{x} + \tilde{k}'}{(1 + \tilde{k}')^2 \cdot 15(B - 1.2b'\tilde{x})} \rho \quad (25)$$

where b' is the parameter of surface diffusion ($0 < b' < 0.25$), $\tilde{x} = 1/(1 + \kappa)$ and $\rho = D_p/D_m$ is the ratio of diffusion coefficient in pores and in the free solution. The ρ value is a decreasing function of r_{sp} (ratio of the Stokes protein radius R to the pore radius r) and can be found from the equation

$$\rho = 1 - 1.83r_{sp} + 1.21r_{sp}^3 - 0.38r_{sp}^5 \quad (26)$$

Snyder's model predicts with high precision the width of the protein peak in gradient HPLAC. Thus, the average value of R_w (ratio of experimental to calculated peak width) is in the range $0.83 < R_w < 1.3$, and relative standard deviation of σ_t is 10–33%. For systems that are not complicated by conformational transitions, aggregation, etc. ("well behaved systems") the protein width may be calculated with a relative standard deviation less than 17%. However, when Snyder's model is used, it is necessary to correct the calculated value of σ_t with the aid of an empirical factor J (eqn. 22), the physical meaning of which, unfortunately, has not been elucidated. Moreover, the experimental dependence of HETP on k' and u (see Fig. 3) found by us does not agree with Snyder's model.

We shall determine zone spreading in the gradient chromatography of proteins taking into account both the chromatographic spreading and the gradient contraction of the protein zone. As the migration velocity of the zone changes continuously, the local HETP (HETP at a distance along the column x) depends on the distance passed by the zone. At the column end, the protein zone acquires the velocity $v(x = L)$ and its time dispersion is determined by the equation

$$\sigma_t^2 = \frac{\sigma_L^2(x = L)}{v^2(x = L)} = \frac{\int_0^L H(x) dx}{v^2(x = L)} \quad (27)$$

where $\sigma_L(x = L)$ is the dispersion at the point $x = L$ in length units.

As a result of the concentration gradient of the displacer along the column, the protein zone is subjected to gradient contraction, because the molecules that have diffused to the front boundary of the zone where $\varphi < \varphi_c$ acquire the velocity $v(x + \Delta x)$ and those that have diffused to the rear boundary where $\varphi > \varphi_c$ acquire the velocity $v(x - \Delta x)$. These velocities are lower and higher, respectively, than the velocity of the zone centroid $v(x)$.

The dynamics of the spreading and gradient sharpening of zones may be described by the following differential equation (its derivation is given in the Appendix):

$$H(x) = H_0(x) - \left[4.6\kappa(1 + \kappa) \frac{SB}{u} \cdot \frac{E(x)}{E(x)(1 + \kappa) - 1} \right] \sigma_L^2 \quad (28)$$

To solve eqn. 28, the function $H_0(x)$ should be known. It is determined by the dependence of $H(k')$ on the distance passed along the column through the dependence of the instantaneous capacity factor $k'(x)$ on this distance (eqn. 17).

The general equation for HETP may be written in the following form [37]:

$$H = A*u + B*/u + \sum C*u \quad (29)$$

The character of the dependence of the coefficients A^* , B^* and C^* on k' cannot be considered to be precisely determined because in this case there are theoretical disagreements [37–40], and the scarcity of experimental data does not make it possible to prefer one of these approaches. Moreover, the function $H(k')$ is different for different processes limiting the mass transport velocity: diffusion in the mobile zone, diffusion in the stationary phase (in the immobile zone) and the sorption–desorption reaction.

In the Results and Discussion section we shall show that in RP-HPLC of proteins at linear elution velocities $u > 0.5$ mm/s the first two terms in eqn. 29 related to flow anisotropy (A^*) and molecular diffusion (B^*) may be neglected.

EXPERIMENTAL

Instrumentation

A Kh-Zh-1311 microcolumn gradient chromatograph was used for the chromatography of proteins. It includes two syringe pumps with a variable flow-rate of 1–200 $\mu\text{l}/\text{min}$ and with a syringe volume of 1.5 ml and a fluorimetric detector with a 0.3- μl cell and a 0.5- μl injection valve. Proteins were detected by measuring the fluorescence of tryptophan with excitation at 220 nm and collection of the emitted fluorescence radiation at 320 nm. In some instances detection was carried out with the aid of a Shimadzu SPD2 AM spectrophotometric detector at 280 nm.

Columns

The RP-HPLC of proteins was carried out on PTFE microcolumns (30–200 nm \times 0.5 mm I.D.) packed with Nucleosil 300- C_4 and 500- C_4 (Macherey–Nagel) or with MPS-300- C_4 alkylated macroporous glass (LenChrom). The last sorbent was prepared by Unger *et al.*'s procedure [41] by treating chlorinated macroporous glass with butyl lithium. The columns were packed at a pressure of 12 MPa from a 20% slurry in carbon tetrachloride with subsequent pumping (without pressure release) of 50% aqueous methanol.

Reagents

Water–acetonitrile systems (LiChrosolv, Merck) with the addition of 0.1–0.3% of trifluoroacetic acid (TFA) (Pierce) were used as the mobile phase.

The proteins ribonuclease A, bovine serum albumin (BSA), thyroglobulin, α -chymotrypsinogen A, immunoglobulin A, conalbumin, lactalbumin and γ -globulin were purchased from Serva and the bacterial ribonuclease M from Reakhim.

As a marker of interparticle volume V_0 in size-exclusion chromatography thyroglobulin was used ($M_r = 660\,000$) and as marker of the total accessible volume $V_T = V_0 + V_P$ *p*-aminobenzoic acid (Reakhim) was used with elution with 70% acetonitrile.

RESULTS AND DISCUSSION

The experimental dependence of k' on the composition of the mobile phase obtained in a series of isocratic experiments for several proteins is shown in Fig. 2. At $k' \gg 1$, $\log k'$ changes linearly with displacer concentration, *i.e.*, in accordance with eqn. 7. In the isocratic mode in the region of $k' = \kappa$, transition from adsorption to exclusion chromatography occurs. Just as for flexible chain homopolymers [28–32], there is a critical composition at which all proteins regardless of their molecular mass migrate with $k'/\kappa = 1$. It can be seen from Fig. 2 that the $k'(\varphi)$ dependences for the four proteins under investigation intersect at one point which corresponds to the critical composition of the eluent $\varphi_c = 0.425$.

The only exception is chymotrypsinogen A (curve 5), for which $\varphi_c = 0.46$. As proteins are copolymers of 20 different amino acids, are in a globular form and the globular–random coil transition does not take place in HPLAC, the detection of the identical critical composition of the eluent φ_c for a number of proteins is unexpected. The decrease in k' in the range of $\varphi > \varphi_c$ (*i.e.*, in the size-exclusion mode) is probably determined by the increase in the effective size of the protein molecule with a change in

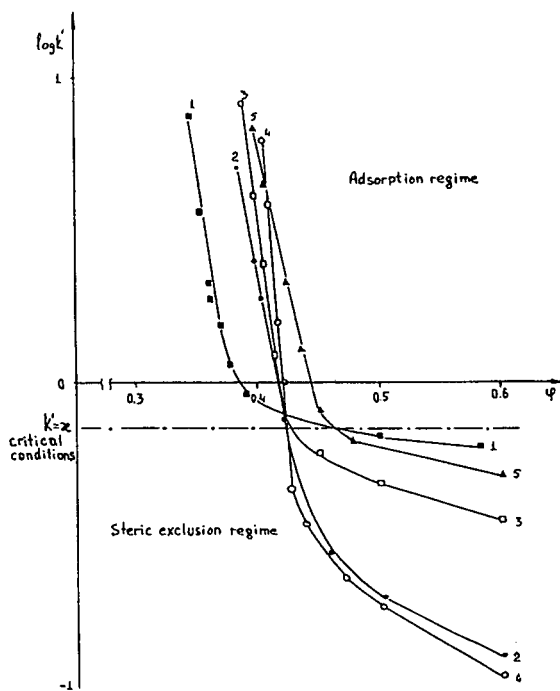


Fig. 2. Logarithmic plot of capacity factor, k' , as a function of volume fraction of acetonitrile in the mobile phase, φ . The data were obtained in isocratic experiments for the following proteins: (1) ribonuclease M ($M_r = 12\,200$), (2) bovine serum albumin (66 500), (3) lactalbumin (17 400), (4) conalbumin (80 000) and (5) chymotrypsinogen A (24 000). Column 150×0.5 mm I.D., packed with Nucleosil 300-C₄ ($x = \kappa = 0.75$).

eluent composition (it expands as the solvent becomes less polar).

In order to check the conclusion that the velocity of the displacer front is the lower limit of the zone migration velocity in gradient elution, experiments were carried out on the stepwise desorption by 70% acetonitrile ($\varphi > \varphi_c$) of proteins previously adsorbed at $\varphi_0 = 0$. The results are given in Table I. It can be seen that in stepwise desorption all proteins migrate at the velocity of the front of the desorbing solvent u_d , whereas under isocratic elution conditions ($\varphi = 0.7$) a size-exclusion effect is distinctly observed (decrease in t_R with increasing molecular mass of protein). These data indicate that under gradient conditions k' cannot (in contrast to Stadalius *et al.*'s opinion [21]) decrease to $k' = k'_{SEC}$ even with a very steep gradient, which means that steric effects do not influence protein separation carried out with the aid of gradient RP-HPLC.

The results presented in Figs. 1 and 2 and Table 1 show that two regions of changes in the composition of the mobile phase in the gradient RP-HPLC of proteins may be distinguished: the precritical region $\varphi \leq \varphi_c$, $x \leq X_0$ in which the protein zone migration obeys eqn. 15 and the critical region $\varphi \geq \varphi_c$, $x \geq X_0$ in which the protein migrates at a virtually constant velocity equal to that of the displacer front $v \approx u_d$. It is important that the velocity of motion of all proteins in the

TABLE I

RETENTION TIMES OF PROTEINS ON A REVERSED-PHASE SORBENT IN STEPWISE DESORPTION AND IN ISOCRATIC ELUTION MODES OF HPLC

Compound	Molecular mass	t_R (min)	
		Stepwise desorption, 10-70% CH ₃ CN	Isocratic elution, >70% CH ₃ CN
Ribonuclease A	19 700	0.76	0.66
α -Chymotrypsinogen A	24 000	0.76	0.62
BSA	66 500	0.74	0.54
γ -Globulin	169 000	0.75	0.52
Immunoglobulin A	400 000	0.74	0.50
Sodium azide	65	—	0.76
Solvent front	—	0.73	—

critical region is the same. Hence no additional zone separation takes place here. However, the additional band spreading occurs as a result of the further increase in the number of random walk steps, *i.e.*, the number of acts of sorption-desorption.

We shall now define the main differences between the model of protein retention proposed here and Snyder's theory. Freiling's equation (eqn. 10) on which Snyder's model is based is a particular case of eqn. A4 obtained on the assumption that the velocity of the chromatographic zone is much lower than that of the displacer u_d . Hence, eqns. 11, 18 and 21 derived by Snyder for the retention time of the protein and instantaneous capacity factor also refer to a particular case of eqns. 14 and 17 and should be rigorously valid only at relatively low values of $r = x/X_0$. They may be obtained from eqns. 14 and 17 by expanding the functions into series taking into account the fact that k' in Snyder's model is not determined from eqn. 1 but as $k'' = (t - t_{SEC})/t_{SEC}$.

For checking eqn. 14, which determines the retention time of the protein in gradient RP-HPLC, the values of k_w and S were obtained for a number of proteins from isocratic experimental data (Table II). These values are compared in Table II with the values of k'_w and S calculated from eqn. 14 by the method of successive approximations according to the results of two gradient experiments with the variation in φ_0 , B and u . Good agreement between the experimen-

tal and calculated data indicates that eqn. 14 is valid.

We shall now consider the experimental data on peak spreading in the RP-HPLC of proteins. The dependence of the isocratic HETP on k' for a number of proteins on the variation in the composition of the mobile phase is shown in Fig. 3. It is clear that in the precritical region ($k' > \kappa \approx 0.8$) HETP increases drastically with increase in k' . The higher the molecular mass (M_r) of the protein, the greater is this increase although the problem of plate height dependence on M_r needs further investigation. These experimental data were found to be consistent with the following dependence of HETP on u and k' :

$$H_0 = A^* + \omega u + \alpha u [k'/(1+k')]^2 \quad (30)$$

To determine the velocity dependences of HETP terms at different k' values, the dependence of H/u on $[k'/(1+k')]^2$ was investigated. It was found that at $u > 0.5$ mm/s the HETP depends linearly on u . Moreover, the value of A^* (0.03 mm $< A^* < 0.06$ mm) is small and may be neglected, just as the term related to molecular diffusion.

Fig. 4 shows the dependence of H/u on $[k'/(1+k')]^2$ for (1) ribonuclease M and (2) conalbumin. It can be seen that this dependence is linear and the results obtained at different elution velocities fall on this line with sufficient precision.

The theoretical basis of the dependence $H(k')$

TABLE II

PARAMETERS OF PROTEIN ADSORPTION ($\log k_w$ AND S) OBTAINED IN ISOCRATIC EXPERIMENTS OR CALCULATED FROM PARALLEL GRADIENT RUNS

Column, 150 mm \times 0.5 mm I.D. (Nucleosil 300-C₄); mobile phase, water-acetonitrile containing 0.1% TFA; acetonitrile content varied.

Protein	$\log k_w$		S	
	Isocratic	Gradient	Isocratic	Gradient
Ribonuclease M	14.2	14.3	38.0	38.1
Lactalbumin	10.1	10.0	23.9	24.0
Conalbumin	27.0	27.5	65.1	64.8

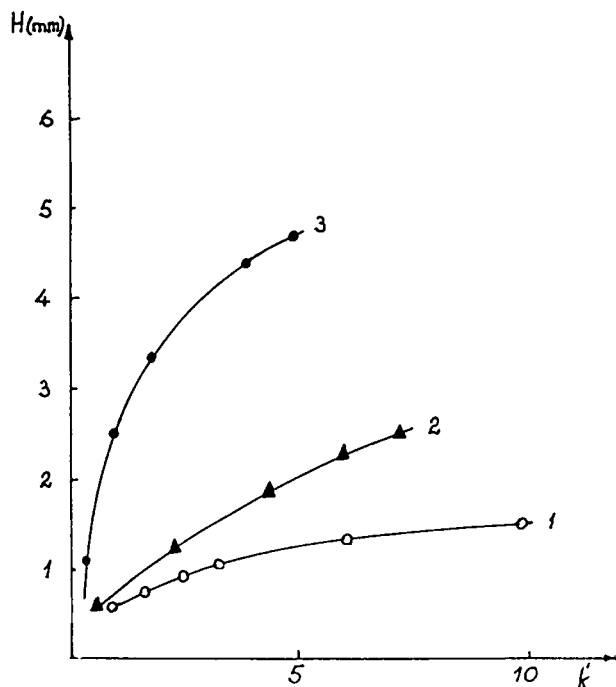


Fig. 3. Experimental dependence of isocratic HETP on capacity factor, k' , for the proteins (1) ribonuclease M ($M_r = 12\,200$), (2) lactalbumin (17 400) and (3) conalbumin (80 000).

stated above and given by eqn. 30 can be found in Giddings' book [42]. In this book the term independent of k' is related to external diffusion mass transport: $\omega = \tilde{\omega}d_p^2/D_m$ and the term proportional to $[k'/(1+k')]^2$ is determined by internal diffusion resistance to mass transport (when adsorption exists) according to eqn. 4.6-44 in ref. 41. This equation may be written by using our designations and a three-phase adsorption model (eqn. 2) as follows:

$$\alpha = \frac{1}{30} \cdot \frac{d_p^2}{D_s} \cdot \frac{k'(1+k_a)}{(1+k')^2}$$

$$= \frac{1}{30} \cdot \frac{d_p^2}{D_s K_{SEC} \kappa} \left(\frac{k'}{1+k'} \right)^2 \quad (31)$$

where D_s is the diffusion coefficient in the stationary phase, D_m is the diffusion coefficient in the mobile phase and d_p is particle diameter of the sorbent.

The isocratic data shown in Fig. 4 were used to determine the values $\alpha_1 = 0.52$ s and $\omega_1 = 0.4$ s

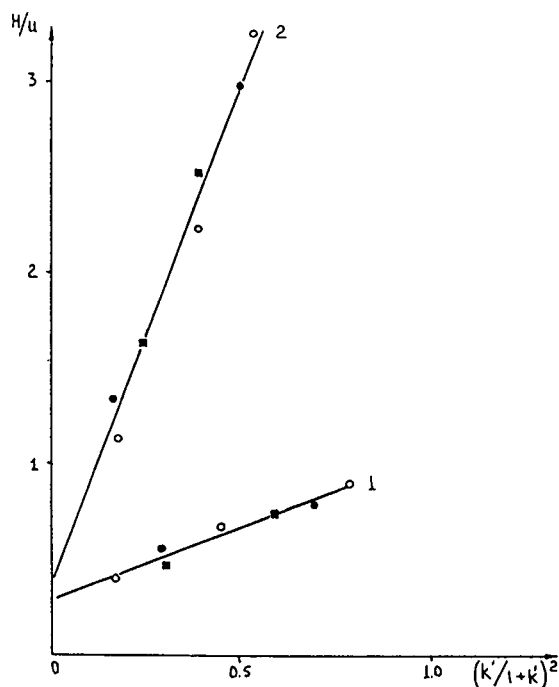


Fig. 4. Ratio of experimental isocratic HETP to linear elution velocity (u) as a function of $[k'/(k'+1)]^2$ for the proteins (1) ribonuclease M and (2) conalbumin. Flow-rate: $\circ = 10$; $\bullet = 20$; $\blacksquare = 30$ $\mu\text{l}/\text{min}$. H/u in s.

for ribonuclease M and $\alpha_2 = 2.4$ s and $\omega_2 = 0.3$ s for conalbumin.

The calculated dependences σ_i^2/t_0 for these two proteins in gradient elution were obtained by using the above values of α and ω and are shown in Fig. 5 as a function of the dimensionless parameter $r = x/X_0$ (solid lines). Fig. 5 also shows the experimental points for gradient conditions of chromatography obtained by the variation in $r = x/X_0$ with the aid of changes in x , B and u . The calculated and experimental values are in relatively good agreement: the average value of $R_w = \sigma_i(\text{exp})/\sigma_i(\text{calc})$ is 1.05 for conalbumin and 1.1 for ribonuclease M, and relative standard deviations of the calculated σ_i are 11 and 15%, respectively. It should be noted that a relatively wide range of r was investigated: $0.1 < r < 3.1$. The fact that the values of σ_i^2/t_0 obtained at different velocities fall on the same curve is additional evidence for the conclusion that the contribution of the terms A^* and B^*/u to the HETP value is negligible.

The type of the dependence of protein zone

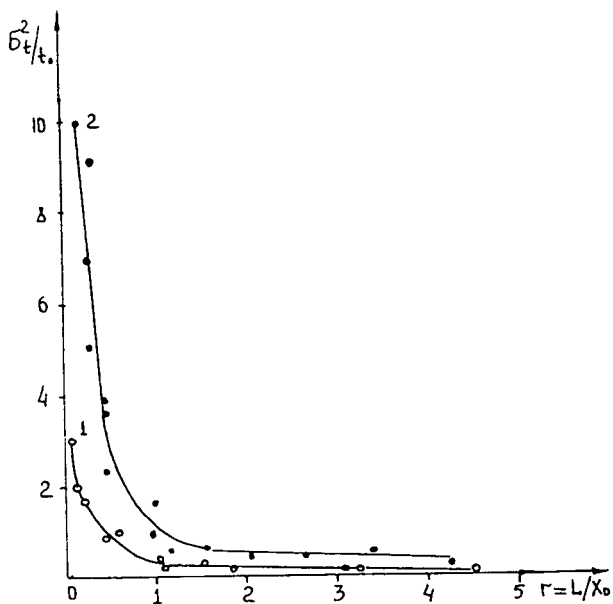


Fig. 5. Ratio of peak variance (σ_t^2) to the time of passage of the mobile phase through the interparticle voids of the column (t_0) as a function of dimensionless column length (L/X_0) in gradient HPLC of proteins. Theoretical dependences were calculated by means of eqn. A17. Experimental points were obtained in gradient runs with varying column length, from rate and gradient steepness. σ_t^2 in s.

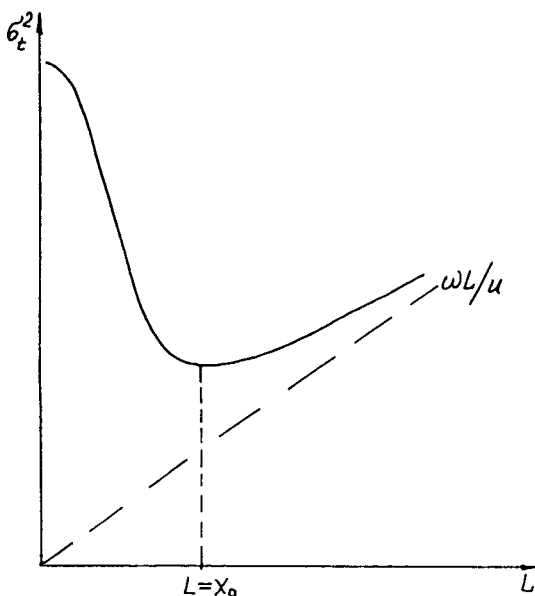


Fig. 6. Graphical representation of the character of the dependence of peak variance on column length in gradient RP-HPLC.

dispersion on column length is shown in Fig. 6. In the precritical region ($L \ll X_0$) the zone is hardly broadened, as it is eluted with $k' \gg \kappa$. At the point $L = X_0$ the variance of the zone is a minimum. At $L > X_0$ there is no gradient compression and the variance becomes proportional to the square root of the column length.

CONCLUSIONS

The relationships considered here are characteristic of columns packed with the usual hydraulically impermeable sorbents for HPLC, which were used in this work. If we pass to perfusion chromatography [16,17,41], in which the eluent moves both in the interparticle volume and in gigantic (giga-dimensions) sorbent pores, it is characterized by the situation in which zone spreading at high elution velocities no longer depends on the eluent velocity, as has been shown elsewhere [43,44]. HPMC on polyglycidyl methacrylate (PGMA-EDM) membranes [11-16] is probably characterized by just this situation because in HPMC [13] the zone width does not change over a relatively wide range of elution velocities. Hence the main features of the HPMC of proteins on the PGMA-EDM membranes include the relationships for the critical chromatography of proteins developed in this paper and the spreading relationships characteristic of perfusion chromatography.

The concept of the critical distance X_0 (eqn. 16) discussed in this paper is of fundamental importance to membrane chromatography. For two proteins with adsorption parameters S_1 and S_2 ($S_2 > S_1$) and corresponding to these parameters critical distances $X_{0,1}$ and $X_{0,2}$ ($X_{0,2} < X_{0,1}$), the distance $X_{0,1}$ will correspond to the optimum thickness of the adsorption layer ($L_{opt} = X_{0,1}$).

At this distance one would obtain the highest separation between peak maxima and the smallest dispersion of peak 1 with peak 2 being slightly broader than it would be at the distance $X_{0,2}$. However, in the case when $L > X_{0,1} > X_{0,2}$ the elution behaviour is much worse, as there is no additional separation, but both peaks become broader. The situation should be extremely bad when $L < X_{0,2} < X_{0,1}$, as in this case the separa-

tion is not at its maximum, but the peaks should be strongly broadened.

Although the column length or membrane thickness may be calculated by means of commercially available software, based on Snyder's theory (Drylab 6), the use of the parameter X_0 proposed in this paper makes all calculations and evaluations extremely simple.

SYMBOLS

A^*	contribution of flow anisotropy to the plate height. In general (eqn. 29) A^* is a function of the linear elution velocity (u). At high flow-rates A^* becomes independent of u and is given as $A^* = 2\lambda d\rho$, where λ is the dimensionless coefficient of eddy diffusion and $d\rho$ is the particle size	k_a	adsorption coefficient (dimensionless) (eqn. 2)
B	steepness of linear gradient (eqn. 12)	k'_{SEC}	steric exclusion capacity factor (eqn. 2)
B^*	coefficient taking into account molecular diffusion in eqn. 29 which describes the dependence of the plate height on elution velocity (u)	K_d	interface distribution coefficient; $K_d = k'/\kappa$
b	dimensionless parameter of Snyder's theory (eqn. 21); $b = SBt_m$	k'', k'''	incorrect definitions of the capacity factor (eqns. 3 and 4)
b'	parameter of surface diffusion (eqn. 25)	k_w	capacity factor (in RP-HPLC) in water mobile phase (organic solvent is absent)
C	molar concentration of the displacing agent (eqn. 5)	k'_0	capacity factor (in RP-HPLC) in the starting eluent in gradient elution ($\varphi = \varphi_0$)
C_c	critical concentration of the displacing agent at which $K_{\text{SEC}}(1 + k_a) = 1$ (eqns. 6 and 8)	J	Snyder's empirical factor of band broadening (eqn. 22)
C^*	coefficient taking into account intraparticle diffusion and adsorption in eqn. 29 which describes the dependence of the plate height on elution velocity (u)	L	column length
D_m	diffusion coefficient in the mobile phase	r	dimensionless distance; $r = L/X_0$ (eqn. A17)
D_s	diffusion coefficient in the stationary phase (eqn. 31)	S	dimensionless protein adsorption parameter (in RP-HPLC) (eqns. 7 and 8)
d_p	particle diameter of the packing material	t	time
E	dimensionless function of x/X_0 (eqns. 14 and 15); $E = 10^{SBx\kappa/u} = 10^{x/X_0}$ ($\lambda = 1$)	t_R	retention time
F	flow-rate (volumetric)	t_{SEC}	retention time in steric exclusion conditions
H	plate height (height equivalent to a theoretical plate, HETP)	t_d	delay time of the gradient device
H_0	plate height in the absence of gradient contraction (eqn. A10)	t_0	time of mobile phase passage through interpartical voids; $t_0 = x/u = V_0/F$
k'	capacity factor (dimensionless) (eqn. 1)	t_m	retention time of a substance which does not interact with the sorbent, but penetrates into its pores
		u	linear elution velocity; $u = xF/V_0$
		u_d	solvent velocity; $u_d = u/(1 + \kappa)$, assuming solvent (displacer) demixing effects are absent
		V_R	retention volume
		V_0	interparticle void volume of the column
		V_p	inner pore volume of the sorbent
		V_{SEC}	retention volume in steric exclusion conditions
		v	migration velocity of the zone maximum (eqn. 9)
		x	distance along the column
		X_0	fundamental parameter of critical distance (definition given by eqn. 16)
		α	auxiliary parameter, taking into account intraparticle diffusion (time units) (eqns. 30 and 31)
		λ	auxiliary parameter in eqn. 16; $\lambda = 1$
		κ	phase ratio; $\kappa = V_p/V_0$

ω	auxiliary parameter (time units) in eqn. 30; $\omega = \tilde{\omega}d_p^2/D_m$
σ	standard deviation
σ_L	peak standard deviation in length units
σ_t	peak standard deviation in time units
τ	auxiliary time variable (eqn. A2)

APPENDIX

If the velocity of zone migration is given as a function of the displacer concentration $v = f(\varphi)u$ and the gradient function $\varphi(t)$ is known, then it is possible to write a differential equation of zone migration in the following form:

$$\frac{dx}{dt} = uf \left[\varphi \left(t - \frac{x}{u_d} \right) \right] \quad (\text{A1})$$

where u_d is the displacer velocity, $u_d = u/(1 + \kappa)$.

The integration of eqn. A1 enables us to obtain the distance x passed by the zone as a function of time t . With this aim a new variable was introduced:

$$\tau = t - x/u_d \quad (\text{A2})$$

in which the additional time x/u_d has been taken into account. This time is necessary for a concentration point of the gradient moving at a constant velocity $u_d = u/(1 + \kappa)$ to overtake the sample which has passed the distance x . Then eqn. A1 becomes

$$u_d \left(1 + \frac{d\tau}{dt} \right) = uf[\varphi(\tau)] \quad (\text{A3})$$

The solution of this equation:

$$t = \int_0^\tau \frac{d\tau}{1 + u/u_d \cdot [\varphi(\tau)]} = F(t) \quad (\text{A4})$$

gives the dependence of the distance x passed by the zone on time t :

$$x = u_d [t - F^{-1}(\tau)] \quad (\text{A5})$$

where $F^{-1}(\tau)$ is the inverse function of $F(\tau)$.

It follows from eqns. 7 and 12 that in RP-HPLC

$$f(\varphi) = \frac{1}{1 + k_w 10^{-S\varphi}} \quad (\text{A6})$$

In this case eqn. A5 has for the linear gradient $\varphi(t) = \varphi_0 + Bt$ the following solution:

$$t(x) = \frac{x}{u} + \frac{1}{SB} \cdot \log \left[1 + \frac{k_0}{\kappa} (E - 1) \right] \quad (\text{A7})$$

where $E = 10^{-SBx\kappa/u}$, $k_0 = k_w 10^{-S\varphi_0}$.

The migration velocity of the chromatographic zone depends on the distance x passed along the column as follows:

$$v(x) = u_d \left[1 - \frac{\frac{\kappa}{(1 + \kappa)} \left(1 - \frac{\kappa}{k_0} \right)}{E - \frac{1}{(1 + \kappa)} \left(1 - \frac{\kappa}{k_0} \right)} \right] \quad (\text{A8})$$

As $\kappa \ll k_0$, eqn. A8 can be simplified to

$$v(x) = \frac{E - 1}{(1 + \kappa)E - 1} \cdot u = \frac{(E - 1)(1 + \kappa)}{(1 + \kappa)E - 1} \cdot u_d \quad (\text{A9})$$

At the column exit the linear velocity of the zone is $v = v(x = L)$ and this is the velocity at which the zone is eluted into the detector. Consequently, if additional gradient zone contraction were not taken into account, the following equation would be valid for time dispersion:

$$\sigma_t^2 = \frac{\sigma_L^2}{v^2(x = L)} = \frac{\int_0^L H_0(x) dx}{v^2(x = L)} \quad (\text{A10})$$

where $H_0(x) = d\sigma_{L,0}^2/dx$ is the local plate height. In reality, because of the concentration gradient of the displacer along the column, the concentration point of the zone located at a distance $x - \sigma_L$ should migrate at a higher velocity than the centroid, and the concentration point $x + \sigma_L$ should migrate more slowly than the zone centre.

Let us now consider the change in the standard deviation of the peak σ_L after a small distance Δx is passed along the column only as a result of the difference between the velocities v (at the point with a coordinate $x + \sigma_L$) and v_x :

$$\Delta\sigma_L = (v_\sigma - v_x) \Delta t = \left(\frac{v_\sigma}{v_x} - 1 \right) \Delta x \quad (\text{A11})$$

At the point $x + \sigma_L$ the local composition of the

mobile phase will correspond to $\varphi(x + \sigma_L) = \varphi_0 + B[t_x - (x + \sigma_L)/u_d]$. Using eqn. A7 for t_x , one may derive the following expression for the local capacity factor at the point $x + \sigma_L$:

$$k'_{(x+\sigma_L)} = k_w 10^{-S\varphi(x+\sigma_L)} = \frac{E 10^{SB\sigma_L(1+\kappa)/u}}{(\kappa/k_0) + E - 1}$$

As usually $\kappa \ll k_0$, the last equation may be written in the simple form

$$k'_{(x+\sigma_L)} = \frac{E \cdot 10^{SB\sigma_L(1+\kappa)/u}}{E - 1} \quad (\text{A12})$$

Hence the velocity v_σ may be given as

$$v_\sigma = \frac{u}{1 + k'_{(x+\sigma_L)}} \\ = u \cdot \frac{E - 1}{E - 1 + E\kappa \cdot 10^{SB\sigma(1+\kappa)/u}} \quad (\text{A13})$$

When σ_L is small, $10^{SB\sigma_L(1+\kappa)/u}$ may be approximated as $1 - 2.3SB\sigma_L(1 + \kappa)/u$.

Applying eqn. A13 for v_σ and eqn. A9 for $v(x)$ and taking into account the above approximation, we obtain from eqn. A11 the following approximate equality:

$$\Delta\sigma_L = -2.3 \cdot \frac{SB\kappa(1 + \kappa)}{u} \cdot \frac{E}{E(1 + \kappa) - 1} \cdot \sigma_L \Delta x \quad (\text{A14})$$

The corresponding change for dispersion is given by

$$d\sigma_L^2 = 2\sigma_L d\sigma_L \\ = -4.6 \cdot \frac{SB\kappa(1 + \kappa)}{u} \cdot \frac{E}{E(1 + \kappa) - 1} \cdot \sigma_L^2 dx \quad (\text{A15})$$

Correcting the local plate height for the front sharpening (eqn. A15), we obtain the following differential equation for real plate height in gradient chromatography:

$$H(x) = \frac{d\sigma_L^2}{dx} = H_0(x) - 4.6\kappa \\ \cdot \frac{SB}{u_d} \cdot \frac{E}{E(1 + \kappa) - 1} \cdot \sigma_{L,0}^2 \quad (\text{A16})$$

where $H_0(x)$ and $\sigma_{L,0}^2$ are the plate height and

dispersion at the point x , respectively, under the condition that gradient contraction is absent.

The solution of eqn. (A16) may be obtained explicitly if we use the dependence of HETP on k' given by eqn. 30. In this case the solution is

$$\sigma_i^2 = 0.434 \cdot \frac{L}{u} \cdot \frac{1}{(E - 1)^2} \left\{ \frac{w(1 + \kappa)^2 + \alpha\kappa^2}{2r} (E^2 - 1) \right. \\ \left. - \frac{2w(1 + \kappa)(E - 1)}{r} + 2.3\omega \right\} \quad (\text{A17})$$

where $E = 10^{-SBL\kappa/u}$ and L is the column length. This solution was obtained taking into account that $\sigma_i^2 = \sigma_L^2/v^2$ (eqn. A10) and $v(x = L)$ being given by eqn. A9.

REFERENCES

- 1 R.A. Barford, B.J. Sliwinski, A.C. Breyer and H.L. Rothbart, *J. Chromatogr.*, 235 (1982) 281.
- 2 M.T. Hearn and B. Grego, *J. Chromatogr.*, 255 (1983) 125.
- 3 N.K. Boardman and S.M. Partridge, *Biochem. J.*, 59 (1955) 543.
- 4 W. Kopaciewicz, M.A. Rounds, J. Fausnaugh and F.E. Regnier, *J. Chromatogr.*, 266 (1983) 3.
- 5 K. Yao and S. Hjertén, *J. Chromatogr.*, 385 (1987) 87.
- 6 Z. Elrassi and Cs. Horváth, *J. Liq. Chromatogr.*, 9 (1986) 3245.
- 7 R. Van der Zee and G.W. Welling, *J. Chromatogr.*, 244 (1982) 134.
- 8 F.E. Regnier, *Science*, 222 (1983) 245.
- 9 R.M. Moore and R.R. Walfers, *J. Chromatogr.*, 317 (1984) 119.
- 10 M. Verzele, Y.-B. Yang and Ch. Dewaele, *Anal. Chem.*, 60 (1988) 1329.
- 11 T.B. Tennikova, B.G. Belenkii and F. Svec, *J. Liq. Chromatogr.*, 13 (1990) 63.
- 12 T.B. Tennikova, M. Bleha, F. Svec, T.V. Almazova and B.G. Belenkii, *J. Chromatogr.*, 555 (1991) 97.
- 13 D. Josic, J. Reusch, O. Baum, K. Loster and W. Reuter, *J. Chromatogr.*, 590 (1992) 59.
- 14 T.B. Tennikova and F. Svec, *J. Chromatogr.*, 590 (1992) 353.
- 15 D. Josic, J. Reusch, K. Loster, O. Baum and W. Reuter, *J. Chromatogr.*, 556 (1991) 341.
- 16 N. Afeyan, N. Gordon, I. Mazsaroff, I. Varady and F. Regnier, *J. Chromatogr.*, 519 (1990) 1.
- 17 C.P. Desilets, M.A. Rounds and F.E. Regnier, *J. Chromatogr.*, 544 (1991) 25.
- 18 X. Geng and F.E. Regnier, *J. Chromatogr.*, 296 (1984) 15.
- 19 L.R. Snyder, in Cs. Horváth (Editor), *High Performance Liquid Chromatography — Advances and Perspectives*, Vol. 1, Academic Press, New York, 1980, pp. 207–320.

- 20 J.P. Larmann, J.J. De Stefano, A.P. Goldberg, R.W. Stout, L.R. Snyder and M.A. Stadalius, *J. Chromatogr.*, 255 (1983) 163.
- 21 M.A. Stadalius, H.B. Gold and L.R. Snyder, *J. Chromatogr.*, 296 (1984) 31.
- 22 M.A. Stadalius, M.A. Quarry and L.R. Snyder, *J. Chromatogr.*, 327 (1985) 99.
- 23 L.R. Snyder and M.A. Stadalius, in Cs. Horváth (Editor), *High Performance Liquid Chromatography. Advances and Perspectives*, Vol. 4, Academic Press, New York, 1986, pp. 193–318.
- 24 K.G. Nugent, W.G. Burton, T.K. Slattery, B.F. Johnson and L.R. Snyder, *J. Chromatogr.*, 443 (1988) 381.
- 25 M.A. Stadalius, B.F.D. Christ and L.R. Snyder, *J. Chromatogr.*, 387 (1987) 21.
- 26 J.L. Glaich, M.A. Quarry, J.F. Vasta and L.R. Snyder, *Anal. Chem.*, 58 (1986) 280.
- 27 E. Kucera, *J. Chromatogr.*, 19 (1965) 237.
- 28 B.G. Belenkii, E.S. Gankina, M.B. Tennikov and L.Z. Vilenchik, *Dokl. Akad. Nauk SSSR*, 231 (1976) 1147.
- 29 M.B. Tennikov, P.P. Nefedov, M.A. Lazareva and S.Ya. Frenkel, *Vysokomol. Soedin., Ser. A*, 19 (1977) 657.
- 30 A.A. Gorbunov and A.M. Skvortsov, *Vysokomol. Soedin., Ser. A*, 30 (1988) 895.
- 31 B.G. Belenkii, *Pure Appl. Chem.*, 51 (1979) 1519.
- 32 A.M. Skvortsov, E.S. Gankina, M.B. Tennikov and B.G. Belenkii, *Vysokomol. Soedin., Ser. A*, 20 (1978) 678.
- 33 R.S. Blanquet, K.M. Bui and D.W. Armstrong, *J. Liq. Chromatogr.*, 9 (1986) 1933.
- 34 E.C. Freiling, *J. Phys. Chem.*, 61 (1957) 543.
- 35 B. Drake, *Ark. Kemi*, 8 (1955) 1.
- 36 J.H. Knox and M. Salem, *J. Chromatogr. Sci.*, 7 (1969) 614.
- 37 S.G. Weber and P.W. Carr, in P.K. Brown and R.A. Hartwick (Editors), *High Performance Liquid Chromatography*, Wiley, New York, 1989, pp. 1–115.
- 38 C. Horváth and H.J. Lin, *J. Chromatogr.*, 126 (1976) 401.
- 39 J.H. Knox and R.P.W. Scott, *J. Chromatogr.*, 282 (1983) 297.
- 40 R.W. Stout, J.J. De Stefano and L.R. Snyder, *J. Chromatogr.*, 282 (1983) 263.
- 41 K. Unger, W. Thomas and Adrian, *Kolloid Z. Z. Polym.*, 251 (1973) 45.
- 42 J.C. Giddings, *Dynamics of Chromatography*, Marcel Dekker, New York, 1965.
- 43 N.B. Afeyan and S.P. Fulton, *J. Chromatogr.*, 544 (1991) 267.
- 44 G. Carta, D.J. Kirwan and M.E. Gregory, in *5th International Symposium on Preparative and Up Scale Liquid Chromatography, Nancy, 1992*, Abstracts, p. 333.

Chiral stationary phases consisting of axially dissymmetric 2'-substituted-1,1'-binaphthyl-2-carboxylic acids bonded to silica gel for high-performance liquid chromatographic separation of enantiomers

Shuichi Oi, Masayuki Shijo, Hideyuki Tanaka and Sotaro Miyano*

Department of Biochemistry and Engineering, Faculty of Engineering, Tohoku University, Aramaki-Aoba, Aoba-ku, Sendai 980 (Japan)

Junzo Yamashita

Department of Chemistry, Tokyo Medical College, Shinjuku, Tokyo 160 (Japan)

(First received February 2nd, 1993; revised manuscript received April 20th, 1993)

ABSTRACT

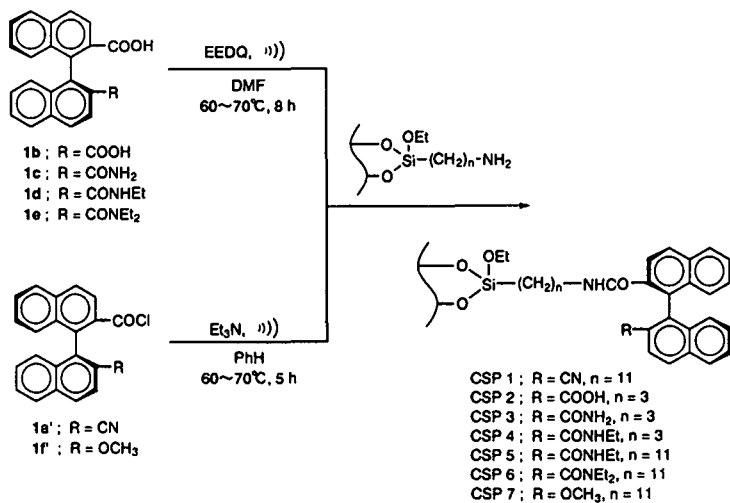
Seven chiral stationary phases (CSPs) were prepared by bonding axially dissymmetric 2'-substituted-1,1'-binaphthyl-2-carboxylic acids to aminoalkylsilanized silica gels through an amide linkage, and the effect of the 2'-substituents (CN, COOH, CONH₂, CONHEt, CONEt₂ and OCH₃) was investigated for the high-performance liquid chromatographic (HPLC) separation of enantiomers. Among these CSPs, that which had a 2'-carboxyl substituent showed the best performance and efficiently discriminated several enantiomeric amino acids, amines and alcohols as their 3,5-dinitrophenyl derivatives, and biaryls bearing 2,2'-polar substituents, by normal-phase HPLC. Stereoselective π -donor \rightarrow acceptor interaction and dipole stacking interaction between the CSPs and the analytes seem to play a critical role in the enantioseparation.

INTRODUCTION

In the 1980s, remarkable progress was made in the direct separation of enantiomers by high-performance liquid chromatography (HPLC) on chiral stationary phases (CSPs) [1]. Various CSPs have been prepared by derivatizing a variety of chiral compounds such as amino acids [2,3], alcohols [4], amines [5], acids [6], hydroxy acids [7], phthalides [8], hydantoins [9], optically active polymeric materials such as polysaccharides [10,11] and the like [1]. Most of the chiral selectors of these CSPs have an element of C-centrochirality for differentiation of enantio-

meric analytes, whereas those with other chiral elements, such as helical chirality of a helicene-carboxylic acid [12] or triarylmethyl methacrylate polymers [13], facial chirality of a paracyclophanecarboxylic acid [14], and P-centrochirality of triarylphosphine oxides [15], have also been reported. On the other hand, axially dissymmetric 1,1'-binaphthyls have been extensively utilized as efficient chiral auxiliaries in a variety of asymmetric reactions and chiral recognitions [16]. Their applications to CSPs, however, have been limited because of the difficulties in obtaining the prerequisite atropisomeric binaphthyls. Among the few examples are chiral binaphthyl crown ethers bonded [17,18] to or coated [19] on silica gel or polystyrene used for

* Corresponding author.



Scheme 1.

the separation of amino acids, and 1,1'-binaphthyl-2,2'-diyl hydrogenphosphate bonded to silica gel used for the resolution of racemic helicenes [20].

In a previous paper, we reported the preparation of several CSPs by using axially dissymmetric 1,1'-bi-2-naphthol and 1,1'-binaphthyl-2,2'-dicarboxylic acid (**1b**) [21]. It was shown that **1b**, rather than 1,1'-bi-2-naphthol, was promising as the chiral selector for the separation of a wide range of enantiomers, but the structures of the **1b**-derived CSPs remained ambiguous except that the starting **1b** was bonded to silica via an amide linkage using the 2-carboxylic function. In this paper, we report the preparation and performance of seven structurally well defined CSPs (CSP 1–CSP 7) which were obtained by bonding 2'-substituted-1,1'-binaphthyl-2-carboxylic acids (**1a–f**) to 3-aminopropyl- and/or 11-aminoundecylsilylanized silica gel (Scheme 1). Based on the chromatographic behaviour of CSP 1–CSP 7, chiral recognition models are presented and the structures of the previously reported **1b**-based CSPs are revised.

EXPERIMENTAL

General

Liquid chromatography was performed using a Shimadzu LC-6A or a JASCO Trirotor-III ap-

paratus equipped with a Shimadzu SPD-6A or a JASCO Uvidec-100-III ultraviolet detector (254 nm). Stainless-steel columns (250 mm × 4.6 mm I.D.) were slurry packed with the packing materials described below using conventional techniques.

IR spectra were measured on a Shimadzu IR-460 grating spectrophotometer. ¹H NMR spectra were recorded on a JEOL JNM-FX 60 or Bruker AC-250T instrument with tetramethylsilane as an internal standard. Optical rotations were recorded on a Union PM-101 automatic digital polarimeter in a 1-cm cell. Melting points were measured on a Yamato MP-21 apparatus and are uncorrected. Microanalyses were carried out in the Microanalytical Laboratory of the Institute for Chemical Reaction Science, Tohoku University.

Materials

The preparation of 11-aminoundecylsilylanized silica gel (Hitachi gel 3056 base; spherical 5-μm particles, microsphere diameter 80–100 Å) (found, C 7.57, H 1.69, N 0.93%; calculated, N 0.92%; 0.66 mmol/g based on N) has been described [22]. 3-Aminopropylsilylanized silica gel was prepared in a similar manner to the 11-amino analogue by treatment of a silica gel (Tosoh silica gel, spherical 5-μm particles, microsphere diameter 100 Å) with 3-aminopropyltriethoxysilane in boiling toluene. Analy-

sis: found, C 8.10, H 2.07, N 1.42%; calculated, 1.01 mmol/g gel based on N. Merck silica gel 60GF₂₅₄ was used for analytical and preparative TLC. Column chromatography was performed by using Nacalai Tesque silica gel 60.

Commercial materials were used as purchased unless stated otherwise. Solvents used for HPLC were distilled before use. Tetrahydrofuran (THF) was distilled from sodium diphenylketyl. Dimethylformamide (DMF) and hexamethylphosphoric triamide (HMPA) were distilled from calcium hydride under reduced pressure. Triethylamine was distilled from calcium hydride. These materials were stored under nitrogen. Water-sensitive reactions were routinely carried out in a nitrogen atmosphere.

Axially dissymmetric 2'-substituted-1,1'-binaphthyl-2-carboxylic acids

The preparation of atropisomerically pure (aS, 1S)-2'-(N-1-phenylethyl)carbamoyl-1,1'-binaphthyl-2-carboxylic acid (**2**), 2'-cyano-1,1'-binaphthyl-2-carboxylic acid chloride (**1a'**) and 1,1'-binaphthyl-2,2'-dicarboxylic acid (**1b**) [23] and (aS)-2'-methoxy-1,1'-binaphthyl-2-carboxylic acid chloride (**1f'**) [24] has been reported previously.

(aS)-2'-Carbamoyl-1,1'-binaphthyl-2-carboxylic acid [(aS)-**1c**]. By treatment with thionyl chloride, (aS, 1S)-**2** (4.02 g, 9.03 mmol) was converted into the acid chloride (aS)-**1a'**, which was then dissolved in ethanol (50 ml) with warming. To the solution was added a solution of KOH (5.1 g) in water (5 ml), and the mixture was heated at reflux for 11 h. After volatiles had been removed under reduced pressure, the residue was dissolved in water (100 ml) and washed with diethyl ether (2 × 30 ml) to remove non-acidic compounds. The aqueous phase was acidified with concentrated HCl and the resulting precipitate was extracted with ethyl acetate (3 × 50 ml). The combined extracts were washed with water (3 × 50 ml) and dried over MgSO₄. After filtration, the solvent was evaporated *in vacuo* and recrystallized from acetonitrile to give 2.44 g (79% yield) of (aS)-**1c** as colourless crystals, m.p. 149–150°C; $[\alpha]_D^{20} - 111^\circ$ (c 1.0, acetone); ¹H NMR (C²HCl₃), δ (ppm) 6.50 and 6.10 (2H, two s's, NH₂), 6.9–9.1 (12H, m, Ar-H); IR

(KBr) (cm⁻¹), 3415, 3185, 1650, 1396, 830, 770. Analysis: found, C 77.34, H 4.62, N, 4.15%; calculated for C₂₂H₁₅NO₃, C 77.40, H 4.43, N 4.10%.

(aS)-2'-Ethylcarbamoyl-1,1'-binaphthyl-2-carboxylic acid [(aS)-**1d**]. To a stirred solution of (aS)-**1b** (6.06 g, 17.7 mmol) in THF (60 ml) was added a solution of 1,3-dicyclohexylcarbodiimide (DCC) (3.66 g, 17.7 mmol) in THF (40 ml) at room temperature for 1 h under a nitrogen atmosphere. The mixture was stirred for 2 h at that temperature and then heated at reflux for 4 h. After cooling to room temperature, triethylamine (2 ml) and ethylamine (1.19 g, 26.5 mmol) were added and the mixture was heated at reflux for 3 h. The mixture was allowed to cool to room temperature, precipitated N,N'-dicyclohexylurea was filtered off and the solids were rinsed with small portions of THF. The solvent was distilled out from the filtrate under reduced pressure and the residue was dissolved in chloroform (100 ml). The solution was washed with concentrated HCl (2 × 100 ml) and then with water (4 × 100 ml) and dried over MgSO₄. After filtration, the solvent was evaporated *in vacuo* to give 7.20 g of a mixture of unchanged (aS)-**1b**, (aS)-**1d** and 2,2'-bis(ethylcarbamoyl)-1,1'-binaphthyl.

As the separation of the mixture as such into each component was difficult, the desired (aS)-**1d** was purified via the methyl ester as follows. The mixture was dissolved in HMPA (50 ml) and then a 25% (w/w) aqueous solution of NaOH (5.6 ml) was added. After stirring for 1 h at room temperature methyl iodide (5.8 ml) was added to the solution and stirring was continued for another 1 h. Then 2 M HCl (100 ml) was added to the mixture and it was extracted with diethyl ether (3 × 50 ml). The combined organic layer was washed with 2 M HCl (2 × 50 ml) and then with water (2 × 50 ml) and dried over MgSO₄. After filtration, the solvent was evaporated *in vacuo* to give 5.7 g of the residue, which was chromatographed on a silica gel column (600 g), eluting with hexane–ethyl acetate (1:1) to give 3.3 g of the methyl ester of (aS)-**1d** [49% yield based on (aS)-**1b**]. This was then dissolved in ethanol (50 ml) with warming, and a solution of KOH (5.0 g) in water (15 ml) was added.

After the mixture had been heated at reflux for 3 h, volatiles were removed under reduced pressure. The residue was dissolved in water (200 ml) and washed with diethyl ether (2×30 ml) to remove non-acidic compounds. The aqueous layer was acidified with concentrated HCl and the resulting precipitate was extracted with ethyl acetate (3×50 ml). The combined organic layer was washed with water (3×50 ml) and dried over MgSO_4 . After filtration, the solvent was removed *in vacuo* to give 2.68 g of (aS)-**1d** as colourless foam [41% yield based on the starting (aS)-**1b**], m.p. 202–203°C; $[\alpha]_D^{20} - 153^\circ$ (c 1.02, acetone); $^1\text{H NMR}$ (C^2HCl_3), δ (ppm) 0.32 (3H, t, CH_3), 2.82 (2H, m, CH_2), 6.4–8.0 (13H, m, Ar-H and NH); IR (KBr) (cm^{-1}), 3750–2600, 3275, 2950, 1697, 1589, 1550. Analysis: found, C 78.28, H 5.03, N 3.89%; calculated for $\text{C}_{24}\text{H}_{19}\text{NO}_3$, C 78.03, H 5.18, N 3.79%.

(aS)-2'-Diethylcarbamoyl-1,1'-binaphthyl-2-carboxylic acid [(aS)-**1e**]. To a stirred solution of (aS)-**1b** (2.80 g, 8.18 mmol) in THF (30 ml) was added a solution of DCC (1.69 g, 8.18 mmol) in THF (20 ml) at room temperature for 1 h under a nitrogen atmosphere. The mixture was stirred for another 2 h at that temperature and then heated at reflux for 4 h. After cooling to room temperature, triethylamine (2 ml) and diethylamine (0.90 g, 12.3 mmol) were added to the mixture, which was then heated at reflux for 3 h. The mixture was allowed to cool to room temperature, precipitated N,N'-dicyclohexylurea was filtered off and the solids were rinsed with small portions of THF. The solvent was distilled out from the filtrate under reduced pressure and the residue was dissolved in chloroform (50 ml). The solution was washed with concentrated HCl (2×50 ml) and then with water (4×50 ml) and dried over MgSO_4 . After filtration, the solvent was evaporated *in vacuo* and recrystallized from ethanol to give 2.27 g of (aS)-**1e** as colourless prisms (70% yield), m.p. 239–240°C; $[\alpha]_D^{20} - 150^\circ$ (c 1.02, acetone); $^1\text{H NMR}$ (C^2HCl_3), δ (ppm) 0.36 (3H, t, CH_3), 1.12 (3H, t, CH_3), 2.6–3.8 (4H, m, CH_2), 6.9–8.1 (12H, m, Ar-H); IR (KBr) (cm^{-1}), 3700–2500, 2950, 1715, 1565. Analysis: found, C 78.48, H 5.91, N 3.84%; calculated for $\text{C}_{26}\text{H}_{23}\text{NO}_3$, C 78.57, H 5.83, N 3.52%.

Preparation of stationary phases

CSP 1. A solution of (aS)-**1a'** (1.74 g, 5.10 mmol) in benzene (50 ml) and triethylamine (10 ml) was added to a slurry of 11-aminoundecylsilylated silica gel (3.30 g) in benzene (70 ml). The slurry was irradiated with ultrasound under a nitrogen atmosphere in the water-bath of an ultrasound laboratory cleaner (35 W, 41 kHz) which was maintained at 70°C. After 5 h of irradiation, the modified silica gel was collected and washed exhaustively with benzene, THF, methanol, acetone and diethyl ether and then dried under reduced pressure to a constant mass to afford 3.82 g of CSP 1. Analysis: found, C 19.41, H 2.07, N 1.26%; calculated, 0.54 mmol/g gel based on C.

CSP 2. A solution of (aS)-**1b** (1.50 g, 4.38 mmol) and 1-ethoxycarbonyl-2-ethoxy-1,2-dihydroquinoline (EEDQ) (1.63 g, 6.62 mmol) in DMF (50 ml) was added to 3-aminopropylsilylated silica gel (3.00 g). The slurry was heated at 70°C for 8 h under ultrasound irradiation as above. The modified silica gel was successively washed with DMF, THF, methanol, acetone and diethyl ether and then dried under reduced pressure to afford 3.40 g of CSP 2. Analysis: found, C 17.89, H 2.41, N 1.32%; calculated, 0.47 mmol/g gel based on C.

CSP 3. CSP 3 (3.29 g) was similarly prepared as above by the treatment of (aS)-**1c** (1.03 g, 2.93 mmol) and 3-aminopropylsilylated silica gel (3.00 g) in the presence of EEDQ (1.50 g, 6.09 mmol). Analysis: found, C 13.88, H 1.81, N 1.60%; calculated, 0.26 mmol/g gel based on C.

CSP 4. CSP 4 (3.13 g) was similarly prepared as above by the treatment of (aS)-**1d** (1.70 g, 4.60 mmol) and 3-aminopropylsilylated silica gel (3.00 g) in the presence of EEDQ (2.50 g, 10.2 mmol). Analysis: found, C 10.56, H 1.41, N 1.53%; calculated, 0.19 mmol/g gel based on C.

CSP 5. CSP 5 (3.58 g) was similarly prepared as above by the treatment of (aS)-**1d** (2.00 g, 5.41 mmol) and 11-aminoundecylsilylated silica gel (3.30 g) in the presence of EEDQ (2.50 g, 10.2 mmol). Analysis: found, C 15.96, H 2.47, N 1.28%; calculated, 0.31 mmol/g gel based on C.

CSP 6. CSP 6 (3.46 g) was similarly prepared as above by the treatment of (aS)-**1e** (2.00 g, 5.03 mmol) and 11-aminoundecylsilylated silica

gel (3.30 g) in the presence of EEDQ (2.50 g, 10.2 mmol). Analysis: found, C 14.11, H 2.31, N 1.21%; calculated, 0.20 mmol/g gel based on C.

CSP 7. CSP 7 (3.73 g) was prepared according to the method used for the preparation of CSP 1 by using (aS)-**1f'** (1.21 g, 3.49 mmol) and 11-aminoundecylsilylanized silica gel (3.30 g). Analysis: found, C 19.52, H 1.84, N 0.75%; calculated, 0.55 mmol/g gel based on C.

Preparation of the derivatized enantiomeric analytes

Typical examples of the preparation of the derivatized enantiomeric analytes for the HPLC analysis are as follows.

N-(3,5-Dinitrobenzoyl)alanine butyl ester (**3a**). To a solution of alanine (50 mg, 0.56 mmol) in 1 M NaHCO₃ (5 ml) was added a solution of 3,5-dinitrobenzoyl chloride (258 mg, 1.1 mmol) in THF (2 ml), and then the mixture was stirred at room temperature for 1 h. After the solution had been acidified with 2 M HCl, the resulting precipitate was extracted with ethyl acetate and dried over MgSO₄. After filtration, the solvent was evaporated *in vacuo* and the residue was treated with butanol containing dry HCl at 100°C for 1 h, and then subjected to TLC to give a sample of **3a**.

N-(3,5-Dinitrobenzoyl)-1-phenylethylamine (**4a**). 1-Phenylethylamine (20 mg, 0.17 mmol) and triethylamine (20 μl) were added to a solution of 3,5-dinitrobenzoyl chloride (76 mg, 0.33 mmol) in THF (1 ml). After the solution had been stirred at room temperature for 10 min, 3-dimethylaminopropylamine (20 μl) was added to remove excess of acid chloride and then the mixture was subjected to TLC to give a sample of **4a**.

1-Phenylethyl 3,5-dinitrophenylcarbamate (**5a**). A solution of 1-phenylethanol (20 mg, 0.16 mmol), 3,5-dinitrophenyl isocyanate (67 mg, 0.32 mmol) and one drop of triethylamine in dioxane (1 ml) was stirred at 100°C for 1 h. To the solution was added 3-dimethylaminopropylamine (20 μl) to remove excess of isocyanate and the mixture was subjected to TLC to give a sample of **5a**.

2,2'-Bis(butylcarbamoyl)-1,1'-binaphthyl (**6e**). A mixture of 1,1'-binaphthyl-2,2'-dicarboxylic

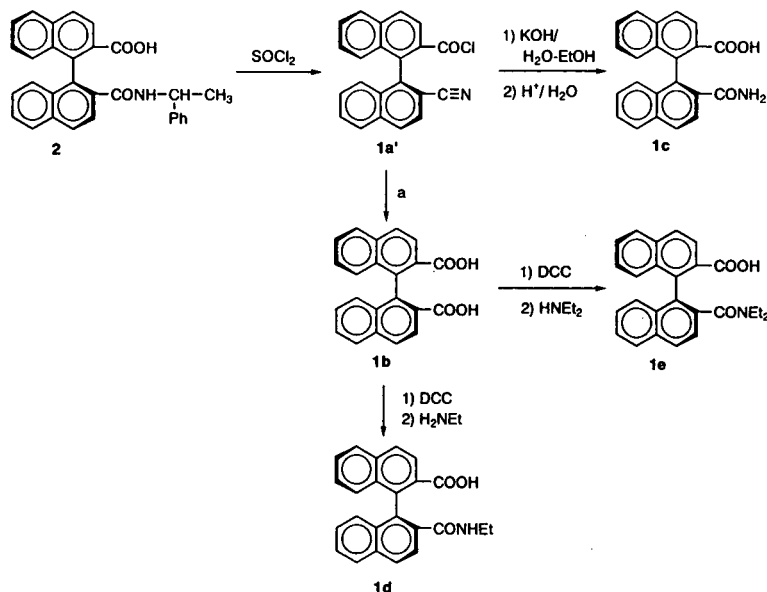
acid (**1b**) (20 mg, 0.06 mmol) in thionyl chloride (0.5 ml) was stirred at 50°C for 1 h. After the excess of thionyl chloride had been distilled out under reduced pressure, butylamine (0.5 ml) was added. The mixture was stirred at room temperature for 10 min and then subjected to TLC to give a sample of **6e**.

Other biaryls used for the derivatization were those prepared in this laboratory and reported elsewhere [25,26].

RESULTS AND DISCUSSION

The preparation of the CSPs was easily accomplished by treating atropisomerically pure 2'-substituted-1,1'-binaphthyl-2-carboxylic acids (**1b–e**) or acid chlorides (**1a'** and **f'**) with 3-aminopropyl- and/or 11-aminoundecylsilylanized silica gel with the aid of a condensing agent, EEDQ or triethylamine, which allowed the covalent bonding of the axially dissymmetric binaphthyl residue to the support via an amide linkage (Scheme 1). From microanalytical results and the increase in mass of the silica gel after bonding the chiral selectors, the contents of the binaphthyl residue of these CSPs were calculated to be in the range 0.19–0.55 mmol/g silica gel. It should be noted that both of the chiral precursors, (aS,1S)-2'-(N-1-phenylethyl)carbamoyl-1,1'-binaphthyl-2-carboxylic acid (**2**) for the synthesis of CSP 1–CSP 6 (Scheme 2) and (aS)-2'-methoxy-1,1'-binaphthyl-2-carboxylic acid (**1f**) for CSP 7, are readily available in substantial amounts as reported previously [23,24]. Treatment of **2** with thionyl chloride gave (aS)-2'-cyano-1,1'-binaphthyl-2-carbonyl chloride (**1a'**) (the von Braun reaction), alkaline hydrolysis of which afforded (aS)-2'-carbamoyl-1,1'-binaphthyl-2-carboxylic acid (**1c**) or (aS)-1,1'-binaphthyl-2,2'-dicarboxylic acid (**1b**), depending on the reaction conditions. Treatment of **1b** with 1,3-dicyclohexylcarbodiimide (DCC) followed by reaction with ethylamine and diethylamine gave (aS)-2'-ethylcarbamoyl- (**1d**) and (aS)-2'-diethylcarbamoyl-1,1'-binaphthyl-2-carboxylic acid (**1e**), respectively (Scheme 2).

The resulting CSPs were slurry packed into 250 × 4.6 mm I.D. stainless-steel columns by using conventional methods. Enantiomeric sam-



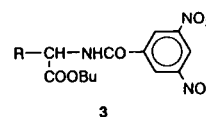
Scheme 2. (a): (1) KOH-aq. EtOH; (2) NaOH-H₂O; (3) H⁺/H₂O (see ref. 23).

ples of amino acids and amines as the 3,5-dinitrobenzamides, alcohols as the 3,5-dinitrophenylcarbamates, 1,1'-bi-2-naphthol and biarylcarboxylic acids as the N-butylamides, are summarized in Scheme 3. They were eluted with hexane–2-propanol mixtures, the composition of which was varied to adjust the capacity factor, k' , in a comparable range, and Table I lists the chromatographic data. Although the analytes examined are relatively limited, inspection of Table I allows the following comments on the structural factors of CSP 1–CSP 7 and their chromatographic behaviour. These CSPs show appreciable selectivity for many of the analytes with separation factors, α , of up to 1.54. Typical chromatograms are shown in Fig. 1.

The elution order is consistent in that, where the absolute stereochemistry of the samples is known, the *S*-enantiomers are eluted prior to the *R*-counterparts on the CSPs bearing a *S*-axial chirality, only two obvious exceptions being the derivatized leucine **3c** on CSP 7 and the 1-phenylethylamine derivative **4a** on CSP 5. The inconsistency of the elution order of the derivatized phenylglycine **3d** compared with the other amino acid derivatives (**3a–c** and **e**) may need some comments here. As will be discussed later, the binaphthyl-based CSPs seem to discriminate

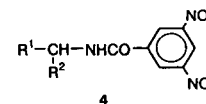
Amino acid derivatives:

R	3
CH ₃ (Alanine)	3a
CH(CH ₃) ₂ (Valine)	3b
CH ₂ CH(CH ₃) ₂ (Leucine)	3c
Ph (Phenylglycine)	3d
CH ₂ Ph (Phenylalanine)	3e



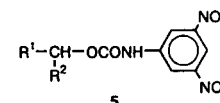
Amine derivatives:

R ¹	R ²	4
CH ₃	Ph	4a
CH ₃	1-Naph	4b
CH ₃	(CH ₂) ₅ CH ₃	4c



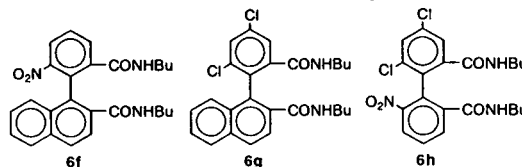
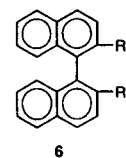
Alcohol derivatives

R ¹	R ²	5
CH ₃	Ph	5a
CH ₂ CH ₃	Ph	5b
(CH ₂) ₂ CH ₃	Ph	5c
CH ₃	(CH ₂) ₅ CH ₃	5d



Biaryl derivatives

R ¹	R ²	6
OH	OH	6a
H	CONHBu	6b
CH ₃	CONHBu	6c
OCH ₃	CONHBu	6d
CONHBu	CONHBu	6e



Scheme 3.

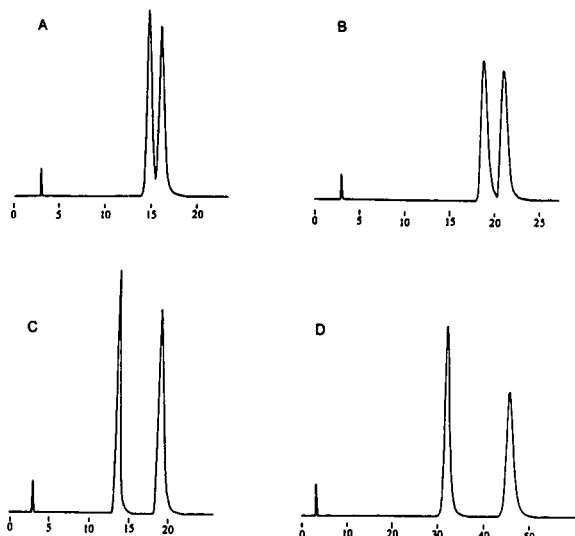


Fig. 1. Chromatographic separation of enantiomers. (A) N-(3,5-Dinitrobenzoyl)alanine butyl ester on CSP 2; (B) N-(3,5-dinitrobenzoyl)-1-phenylethylamine on CSP 2; (C) 1-phenylpropyl 3,5-dinitrophenylcarbamate on CSP 2; (D) 2,2'-bis(butylcarbamoyl)-1,1'-binaphthyl on CSP 3. Chromatographic conditions as in Table I.

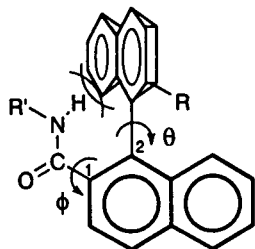
a pair of enantiomers by the spatial arrangement of the steric bulk of the three substituents attached to the chiral carbon centre. For the amino acid derivatives **3**, the smallest substituent is hydrogen throughout **3a–e**, and hence the steric repulsion caused by the R or COOBu group on approach to the chiral selectors should be compared. It seems that the CSPs recognize that the effective exclusion size of the sp^2 -hybridized COOBu group is larger than the sp^3 -hybridized CH_3 (**3a**), $CH(CH_3)_2$ (**3b**), $CH_2CH(CH_3)_2$ (**3c**) and CH_2Ph (**3e**) to elute the *S*-isomers first, but smaller than sp^2 -hybridized Ph (**3d**) to elute the *R*-isomer first. The apparent inversion of the elution order of **6f** is because of the inversion of the substituent priority sequence about the substituents on the biaryl residue. In conclusion, it may be said that axial chirality of the binaphthyl chiral selector is the main determinant for the stereoselectivity, almost irrespective of the 2'-substituent.

CSP 4 and 5 have the same chiral binaphthyl residue but connecting arms of different length. Interestingly, the chromatographic behaviours of the two CSPs are similar for different types of

analytes, except that the k' values on CSP 5 are slightly larger than those on CSP 4. This may be ascribed in part to a higher loading rate of the chiral selector on CSP 5 than on CSP 4. The insensitivity to the length of the connecting arms seems to stem from the structure of the bulky and rigid binaphthyl selector moiety, implying some clues for the chiral discrimination mechanism (see below).

The most characteristic feature of these chiral phases is the good separability of alcohol enantiomers as the 3,5-dinitrophenylcarbamates, whereas the separations of amino acids and amines as the 3,5-dinitrobenzamides are poor to fair. Roughly, the discriminating abilities of these CSPs for the derivatized aryl carbinols **5a–c** decrease in the order CSP 2 > CSP 1 > CSP 7 > CSP 3 > CSP 5 \cong CSP 4 > CSP 6, as judged by the α values. This order is nearly in accordance with the reverse of the bulk of the 2'-substituent, suggesting that steric hindrance imposed by the 2'-substituent reduces the chiral discriminating ability. It seems that the presence of protic hydrogen on the 2'-substituent compensates to some extent the repulsive Van der Waals steric effect via hydrogen bonding between the CSP and analyte, as discussed later.

In a control experiment, derivatization of 1-phenylethanol into the phenylcarbamate, in place of the 3,5-dinitrophenylcarbamate (**5a**), dramatically reduced both k' {from 5.62 [eluted with hexane–2-propanol (90:10)] (Table 1) to 2.35 [eluted with hexane–2-propanol (95:5)]} and α (from 1.28 to 1.00) on CSP 3, showing the critical importance of the π -donor–acceptor interaction between the π -basic naphthalene plane of the CSP and the π -acidic 3,5-dinitrophenyl ring of the analyte. In a previous study, (*aS*)-2'-methoxy-1,1'-binaphthyl-2-carboxylic acid (**1f**) was converted into the (*S*)-1-phenylethylamide (**7a**) (Fig. 2) [27]. An X-ray crystal analysis of **7a** showed that the dihedral angle θ between the two naphthalene planes is 97.5° , and that the –CO–NH–CH– atoms are almost on a same plane, the –CO–NH– linkage being an *s-trans* conformation and the dihedral angle ϕ of C_1 – C_2 – $C=O$ being 52.6° . It has been shown that, for the 1-phenylethyl ester of **1f**, the plane containing the –CO–O–CH– atoms is coplanar



7a; R = OCH₃, R' = (S)-CH(CH₃)Ph

7b; R = CN, COOH, CONH₂, CONHEt, CONEt₂, OCH₃

R' = -(CH₂)_n-Si ← n = 3, 11

Fig. 2. Schematic view of 2'-substituted-1,1'-binaphthyl-2-carboxylic acid derivatives (7).

with the connected naphthalene plane [24], and therefore the deviation of the -CO-NH-CH- plane of 7a from the coplanarity with the connected naphthalene plane is ascribed to the steric repulsion between the other naphthalene plane and the amide hydrogen, as depicted schematically in Fig. 2. This means that the side of the naphthalene plane against the amide hydrogen is severely blocked by the R' group of 7, e.g., the 1-phenylethyl moiety in the case of 7a, which in turn means that the lower side of the -CO-NH-CH- plane is almost completely blocked by the relevant naphthalene ring. Although CSP 1-CSP 7 are carrying the solid silica gel support at the end of the alkyl chain connecting to the amido nitrogen at the 2'-position and conformational changes by dissolution must be taken into account, it may not be unreasonable to assume that the stable conformation of the binaphthyl selectors of the CSPs is similar to that of 7a (Fig. 2, 7b).

On the basis of the chromatographic results (Table I) and the X-ray crystal analysis of the model compound (7a, Fig. 2), a probable chiral discrimination mechanism for the 3,5-dinitrophenyl-derivatized alcohols by the binaphthyl-based CSPs is as shown in Fig. 3. As stated above, the plane containing the -CO-NH-CH- linkage has open space only above the plane of the connected naphthalene nucleus. Hence the most favourable approach of the analyte towards

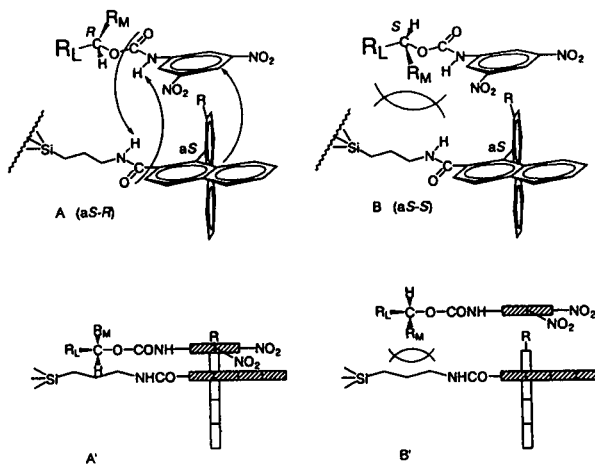


Fig. 3. Chiral discrimination models of alcohol derivatives. (A) Schematic representation of the adsorbate of (R)-alcohol derivatives on (aS)-CSPs; (A') side view of A; (B) schematic representation of the adsorbate of (S)-alcohol derivatives on (aS)-CSPs; (B') side view of B.

the chiral selector should occur from the upper side of the horizontal naphthalene plane, as only this approach can provide two cooperative attractive interactions between the CSP and analyte via the dipole stacking interaction and the π -donor-acceptor interaction. The steric hindrance imposed by the 2'-substituent can be substantially avoided by the approach of the analyte from the direction parallel to the -CO-NH-CH- plane, which is tilted several tens of degrees (*ca.* 50°) from the horizontal naphthalene plane. Obviously, the smaller is the R group on the 2'-position, the easier will be the π -donor-acceptor interaction between the 3,5-dinitrophenyl ring and the horizontal naphthalene ring. However, when the R group bears protic hydrogen, the 2'-substituent may be expected to form hydrogen bonds with one of the two nitro groups of the 3,5-dinitrophenyl ring.

Under these circumstances, inspection of the space-filling CPK (Corey-Pauling-Koltun) molecular models indicates that the most bulky substituent R_L linked to the chiral carbon centre of the analyte is most comfortably located by being arranged parallel to the CSP-connecting chain as shown in Fig. 3A' and B' for steric reasons and probably for lipophilic interaction. Comparison of Fig. 3A' and B' clearly indicates

that the carbamate of (*R*)- R_1R_2CHOH should associate more strongly with the CSP of the (*aS*)-binaphthyl axis than that of the (*S*)-alcohol, because in the former carbamate, the smallest ligand, *i.e.*, hydrogen, on the chiral carbon atom is directed toward the alkyl chain of the CSP (Fig. 3A'), whereas in the latter carbamate, the medium ligand R_M must be disposed toward the CSP against increased steric repulsion (Fig. 3B'). The space between the chiral binaphthyl moiety and the silica gel support given by the trimethylene bridge, $-(CH_2)_3-$, seems to be wide enough to accommodate the relevant analyte moiety, rendering the α value almost independent of the length of the connecting arm.

As can be seen from Fig. 3, the 3,5-dinitrophenyl nucleus of the analyte can overlap with the other two sides of the naphthalene planes of the CSP. These π -donor–acceptor interactions will contribute to the retention, but seem to be non-stereoselective because the chiral moiety of the analyte is disposed apart from the sterically effective bulk of the CSP. In this respect, comparison of the chromatographic behaviours of structurally closely related **4a** and **5a** is of interest. Inspection of Table I reveals that the retention of **4a** is always longer than that of **5a** but the relationship of the stereoselectivity is reversed between the two throughout CSP 1–CSP 7. The longer retention of **4a** may be ascribed to the enhanced, non-stereoselective π -donor–acceptor interaction with the CSPs: the π -acidity of **4a** should be significantly stronger than that of **5a**, as the 3,5-dinitrophenyl nucleus of the former bears an electron-withdrawing carbonyl substituent whereas that of the latter bears a highly electron-donating amino substituent. On the other hand, the lower resolution of **4a** on these CSPs may be ascribed to the lack, or at least the reduction, of the cooperative, stereoselective dipole stacking interaction because of the mismatched direction of the amide dipoles of the analyte and the CSP (Fig. 4). The inferior resolution of the other amines and amino acids as the 3,5-dinitrobenzamines may have the same basis, but at present further explanations of the HPLC results in Table I are difficult because of the too many alternatives for plausible CSP–analyte interactions.

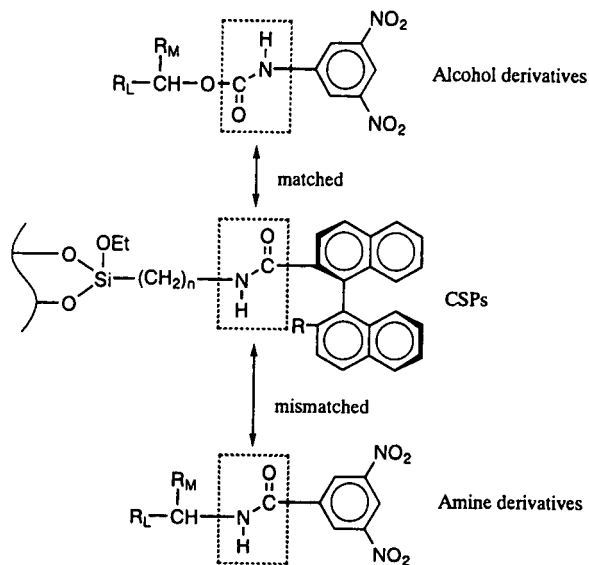


Fig. 4. Matched and mismatched dipole stacking interaction of alcohol and amine derivatives, respectively, on (*aS*)-CSPs.

The chiral discrimination model depicted in Fig. 3 implies that the stronger is the π -donating character of the horizontal naphthalene plane, the better is the separation to be expected. This has been exemplified by the far better chiral discrimination ability of an axially dissymmetric bianthracene-based CSP [28]. Another interesting extension of the model is that the minimum requirement for a CSP to separate enantiomeric alcohols as the 3,5-dinitrophenylcarbamates is a chiral π -donor plane connected to the amide linkage $-\text{CO}-\text{NH}-(\text{CH}_2)_n-\text{Si}\equiv$, the soundness of the idea has also been reported in a preliminary communication by preparing a CSP derived from chiral (*S*)-[10]paracyclophane-13-carboxylic acid [14].

A second characteristic feature of the CSPs is their performance with respect to the axially dissymmetric biaryl enantiomers (**6**). It seems that the presence of polar functional groups, such as hydroxyl or carbamoyl, at both of the 2- and 2'-positions in the biaryl analytes is required for chiral discrimination by the CSPs. Thus, the separability of the biaryl analytes **6** is in the order of 2,2'-bis(butylcarbamoyl)biaryls (**6e–h**) followed by 2'-methoxy-2-butylcarbamoyl-1,1'-binaphthyl (**6d**) and then 1,1'-bi-2-naphthol (**6a**).

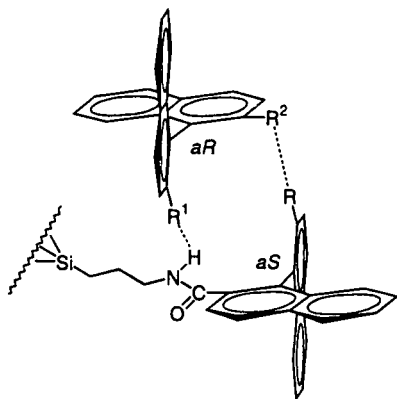


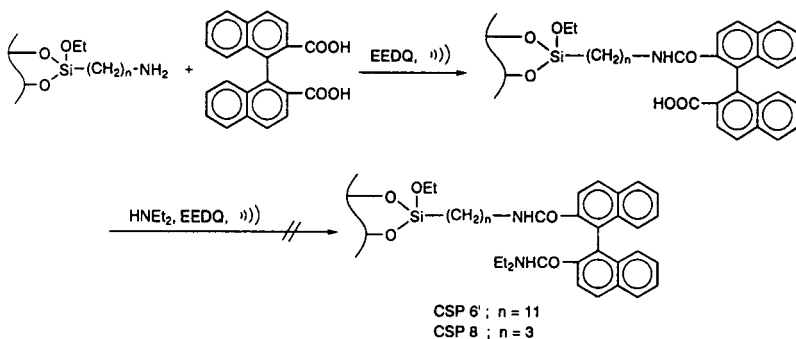
Fig. 5. Chiral discrimination model of (*aR*)-biaryls on (*aS*)-CSPs.

2-Butylcarbamoyl-1,1'-binaphthyl (**6b**) is only partially separable on CSP 3 and CSP 5, but the 2'-methyl analogue (**6c**) shows no indication of separation on these CSPs. The separation of **6e** is a typical example of the discrimination of the biaryl analytes **6** by the biaryl-based CSPs; the separability of **6e** decreases in the order CSP 3 > CSP 2 > CSP 5 > CSP 4 > CSP 7 > CSP 1 > CSP 6. This seems to imply that the hydrogen-bonding ability of the 2'-substituent of the binaphthyl selector is more important than the steric size for the resolution of the biaryl analytes. Fig. 5 shows a probable model for the more retained biaryl analyte, where the hydrogen bonding between the 2,2'-substituents on both the CSP and the heterochiral analyte plays a critical role. A similar chiral discrimination model of 1,1'-bi-2-naphthol on a CSP derived

from *trans*-1,2-diaminocyclohexane has been proposed [29].

Considering the above resolution results for the CSPs for both the C-centrochiral and the axially chiral analytes (Table I), a carboxyl function should be the substituent of choice for the 2'-position (CSP 2), because it is small in size and bears protic hydrogen for hydrogen bonding. On the other hand, CSP 6 is the least effective because the 2'-diethylcarbamoyl group is the largest in bulk and bears no protic hydrogen. In this regard, we previously claimed the preparation of the CSPs (CSP 6' and CSP 8 in Scheme 4) which had a 2'-diethylcarbamoyl substituent on the binaphthyl moiety. The performance of these CSPs, however, was far different from that of CSP 6 prepared in this work, which definitely bears a 2'-diethylcarbamoyl substituent. They were, on the other hand, similar to that of CSP 2, indicating that CSP 6' and CSP 8 had, in fact, a free 2'-carboxyl rather than a 2'-diethylcarbamoyl substituent. It should be considered that the treatment of the binaphthyl-modified silica with diethylamine in the presence of EEDQ retained the 2'-carboxyl group almost intact because of the steric congestion (Scheme 4), and the previously reported structures of CSP 6' and CSP 8 must be revised to those bearing 2'-carboxyl function.

In conclusion, we have reported here that an efficient and stable CSP for the separation of a wide range of enantiomers by HPLC is readily prepared by bonding axially dissymmetric 1,1'-binaphthyl-2,2'-dicarboxylic acid (**1b**) to 3-aminopropylsilanized silica gel [30].



Scheme 4.

ACKNOWLEDGEMENTS

We are grateful to the Ministry of Education, Science and Culture, Japan (Grant-in-Aid No. 02555177), and to Tosoh for financial support.

REFERENCES

- 1 For a general review: W.H. Pirkle and T.C. Pochapsky, *Chem. Rev.*, 89 (1989) 347.
- 2 F. Mikeš, G. Boshart and M. Gil-Av, *J. Chromatogr.*, 122 (1976) 205.
- 3 W.H. Pirkle, J.M. Finn, J.L. Schreiner and B.C. Hamper, *J. Am. Chem. Soc.*, 103 (1981) 3964.
- 4 W.H. Pirkle and D.W. House, *J. Org. Chem.*, 44 (1979) 1957.
- 5 N. Ôi, M. Nagase and T. Doi, *J. Chromatogr.*, 257 (1983) 111.
- 6 N. Ôi, M. Nagase, Y. Inada and T. Doi, *J. Chromatogr.*, 265 (1983) 111.
- 7 Y. Dobashi and S. Hara, *Tetrahedron Lett.*, 26 (1985) 4217.
- 8 W.H. Pirkle and T.J. Sowin, *J. Chromatogr.*, 396 (1987) 83.
- 9 W.H. Pirkle and M.H. Hyun, *J. Chromatogr.*, 322 (1985) 309.
- 10 G. Hesse and R. Hagel, *Liebigs Ann. Chem.*, (1976) 996.
- 11 Y. Okamoto, M. Kawashima and K. Hatada, *J. Am. Chem. Soc.*, 106 (1984) 5357.
- 12 Y.H. Kim, A. Balan, A. Tishbee and E. Gil-Av, *J. Chem. Soc., Chem. Commun.*, (1982) 1336.
- 13 H. Yuki, Y. Okamoto and I. Okamoto, *J. Am. Chem. Soc.*, 102 (1980) 6358.
- 14 S. Ôi and S. Miyano, *Chem. Lett.*, (1992) 987.
- 15 A. Tambuté, A. Begos, M. Lienne, M. Caude and R. Rosset, *J. Chromatogr.*, 396 (1987) 65.
- 16 For a recent review, see C. Rosini, L. Franzini, A. Raffaelli and P. Salvadori, *Synthesis*, (1992) 503.
- 17 L.R. Sousa, G.D.Y. Sogah, D.H. Hoffman and D.J. Cram, *J. Am. Chem. Soc.*, 100 (1978) 4569.
- 18 G.D.Y. Sogah and D.J. Cram, *J. Am. Chem. Soc.*, 101 (1979) 3035.
- 19 T. Shinbo, T. Yamaguchi, K. Nishimura and M. Sugiura, *J. Chromatogr.*, 405 (1987) 145.
- 20 F. Mikes and G. Boshart, *J. Chromatogr.*, 149 (1978) 455.
- 21 J. Yamashita, T. Numakura, H. Kita, T. Suzuki, S. Ôi, S. Miyano, H. Hashimoto and N. Takai, *J. Chromatogr.*, 403 (1987) 275.
- 22 J. Yamashita, H. Kita, M. Tada, T. Numakura, H. Hashimoto and N. Takai, *Nippon Kagaku Kaishi*, (1987) 441.
- 23 S. Ôi, Y. Matsuzaka, J. Yamashita and S. Miyano, *Bull. Chem. Soc. Jpn.*, 62 (1989) 956.
- 24 S. Miyano, S. Okada, H. Hotta, M. Takeda, C. Kabuto and H. Hashimoto, *Bull. Chem. Soc. Jpn.*, 62 (1989) 1528.
- 25 S. Miyano, S. Okada, T. Suzuki, S. Handa and H. Hashimoto, *Bull. Chem. Soc. Jpn.*, 59 (1986) 2044.
- 26 S. Miyano, H. Fukushima, S. Handa, H. Ito and H. Hashimoto, *Bull. Chem. Soc. Jpn.*, 61 (1988) 3249.
- 27 S. Miyano, S. Okada, H. Hotta, M. Takeda, T. Suzuki, C. Kabuto and F. Yasuhara, *Bull. Chem. Soc. Jpn.*, 62 (1989) 3886.
- 28 S. Ôi, M. Shijo and S. Miyano, *Chem. Lett.*, (1990) 59.
- 29 M. Sinibaldi, V. Carunchio, C. Corradini and A.M. Girelli, *Chromatographia*, 18 (1984) 459.
- 30 S. Ôi, M. Shijo, J. Yamashita and S. Miyano, *Chem. Lett.*, (1989) 1545.

Use of carotenoids in the characterization of octadecylsilane bonded columns and mechanism of retention of carotenoids on monomeric and polymeric stationary phases

E. Lesellier* and A. Tchaplà

LETIAM, IUT d'Orsay, Plateau du Moulon, B.P. 127, 91403 Orsay Cedex (France)

A.M. Krstulovic

Synthelabo Recherche (LERS), Recherche Analytique et Contrôle Pharmaceutique, 23–25 Avenue Morane Saulnier, 92360 Meudon-la-Forêt (France)

(First received January 8th, 1993; revised manuscript received March 19th, 1993)

ABSTRACT

Different analyses were performed with 29 commercial octadecylsilane bonded columns in HPLC and subcritical fluid chromatography (SbFC) in order to evaluate the characteristics of stationary phases. Two types of test molecules were used, carotenoids and polycyclic aromatic hydrocarbons. The use of the *cis-trans* isomers of β -carotene allowed the characterization of the stationary phase (monomeric *versus* polymeric) and of the carbon content. The separation of luteine and zeaxanthine depends on the nature of the stationary phase and, in addition, allows the evaluation of the extent of accessibility of residual silanol groups. These results, and those of a study on the effect of temperature, allow a better understanding of the separation mechanisms in the retention of planar and non-planar compounds, and emphasize the similarity between HPLC and SbFC.

INTRODUCTION

Reversed-phase high-performance liquid chromatography (HPLC) now occupies an important place amongst separation methods. Several factors contribute to this situation, in particular the ease of manipulation and the reproducibility of analyses. In addition, the better knowledge of retention mechanisms and the understanding of

the influence of the solvent enable one to obtain increasingly reliable separation predictions.

Along with these developments, new synthesis methods and overlapping of silanol groups have also contributed to the ability to perform certain difficult separations and have improved the transfer of a separation between supports.

Many different parameters govern the choice of a chromatographic support. The diversity of silicas employed [1] (spherical or non-spherical, pore diameter from 60 to 300 Å) and pretreatment (acidic or basic, thermal, cladding with zirconia), bonding treatment (reactivity: chloro,

* Corresponding author.

alkoxy), end-capping (trimethylsilyl) or steric protection (diisopropyl) lead to the appearance of columns on the market which, starting with the carbon chain C₁₈, have very different performances. It is therefore necessary, for a successful separation, to have a better knowledge of the characteristics of the adsorbent employed.

In addition to the classical techniques for the characterization of stationary phases (spectroscopy, microscopy or thermal analysis), which necessitate specialized equipment and/or skills, numerous tests allow for a better definition of the C₁₈ support used and also allow the eventual replacement of one material by another [1,2].

The most often used tests include those employing a homologous series or the coupling of the benzene–anthracene pair for determining the solvophobic power of the chains, the phenyl series for the identification of structure, the selectivity of the pairs N,N-diethyltoluamide–anthracene [3] and caffeine–theophylline for the determination of residual silanols, the measurement of the asymmetry of peaks of N,N-dimethylaniline and the NIST 869 test for polycyclic aromatic hydrocarbons (PAHs) for determining the monomeric or polymeric nature of the phase [4].

Previous studies either in non-aqueous reversed-phase (NARP) liquid chromatography [5] or in subcritical fluid chromatography (SbFC) [6] have shown that the separation of the *cis*–*trans* isomers of carotenes is also dependent on the nature of the stationary phase. This separation cannot generally be achieved on a monomeric support at ambient temperature, in contrast to polymeric supports. Nevertheless, it is apparent that the treatment of columns that are employed specifically for the study of basic products, such as Ultrabase UB 225 bonded with monofunctional silanes, enabled this separation to take place [7]. Further, a different investigation showed the distinctive behaviour of non-oxygenated α - and β -carotenes and the dependence of their retention on the oxygenated groups of the stationary phase [8].

On the basis of this information, we were able to compare different commercial columns in

SbFC employing a mixture of four carotenoids and some of their isomers. In addition, we compared these results with those obtained by the NIST 869 test.

EXPERIMENTAL

Chemicals

HPLC-grade methanol was purchased from Carlo Erba (Milan, Italy) and acetonitrile from Merck (Darmstadt, Germany).

Luteine, zeaxanthine and *cis*- β -carotene were kindly provided by Hoffman La Roche (Basle, Switzerland); all-*trans*- α - and β -carotene were purchased from Sigma (St. Louis, MO, USA).

Carbon dioxide (N45 grade, containing <7 ppm of water) was purchased from Alphagaz (Bois d'Arcy, France).

Apparatus

Subcritical fluid chromatography was performed using equipment manufactured by Jasco (Tokyo, Japan). The two pumps (Model 880-PU) were connected to a SEDERE pulse damper (Touzart et Matignon, Vitry sur Seine, France). The head of the pump used for carbon dioxide was cooled to -2°C by a cryostat (F 10 c; Julabo, Seelbach, Germany). The pulse damper was connected to an injection valve fitted with a 20- μl loop (Model 7125; Rheodyne, Cotati, CA, USA). The column was thermostated in a controlled oven (Crocasil; Cluzeau, Ste. Foy-la-Grande, France), regulated at 25°C by a cryostat (D 8 GH; Haake, Karlsruhe, Germany).

Detection was performed with a UV–Vis detector (Hewlett-Packard Model 1050) with a high-pressure-resistant cell. The eluent was discharged via an automatic back-pressure regulator (Model 880-81). Chromatograms were recorded at 450 nm, using an electronic integrator (CR 6A; Shimadzu, Kyoto, Japan). The flow-rate of the mobile phase was 3.0 ml/min, the output pressure of the fluid was 15 MPa, the temperature was 25°C and the composition of the mobile phase was carbon dioxide–acetonitrile–methanol (65:33.25:1.75, v/v/v).

Liquid chromatography of PAHs was performed using a quaternary pump (PU4100; Unicam, Cambridge, UK), an injection valve

(Rheodyne Model 7125) and a diode-array detector (PU 4121), connected to a PC compatible computer using the PU 6003 software (Unicam). The flow-rate of the mobile phase [water–acetonitrile (15:85)] was 2.0 ml/min. The analyses were carried out at ambient temperature.

The chromatographic columns used in this study were the following: 5- μ m Hypersil ODS (150 \times 4.6 mm I.D.) (Shandon, Sewickley, PA, USA); 10- μ m Partisil ODS3 (250 \times 4.6 mm I.D.) (Whatman, Clifton, NJ, US); 5- μ m Pecosphere HS 5 (150 \times 4.6 mm I.D.) (Perkin-Elmer, Norwalk, CT, USA); 5- μ m Ultrasphere DABS (250 \times 4.6 mm I.D.) (Beckman, San Ramon, CA, USA); 5- μ m Adsorbosphere HS (250 \times 4.6 mm I.D.) (Alltech, Deerfield, IL, USA); 5- μ m Adsorbosphere UHS (250 \times 4.6 mm I.D.) (Alltech); 5- μ m Zorbax ODS (250 \times 4.6 mm I.D.) (DuPont, Wilmington, DE, USA); 3- μ m Ultracarb 3 C 18 (150 \times 4.6 mm I.D.) (Phenomenex, Torrance, CA, USA); 5- μ m Ultrabase UB 225 (250 \times 4.6 mm I.D.) (SFCC Shandon, Eragny, France); 5- μ m LiChrospher 100 RP 18 e (250 \times 4 mm I.D.) (Merck); 5- μ m LiChrospher 100 RP 18 (250 \times 4 mm I.D.) (Merck); 5- μ m Superspher 100 RP 18 e (250 \times 4 mm I.D.) (Merck); 5- μ m Superspher 100 RP 18 (250 \times 4 mm I.D.) (Merck); 5- μ m Hypersil BDS (250 \times 4.6 mm I.D.) (Shandon); 5- μ m Kromasil C₁₈ (150 \times 4.6 mm I.D.) (Eka Nobel, Surte, Sweden); 5- μ m Nucleosil C₁₈ (150 \times 4.6 mm I.D.) (Macherey-Nagel, Düren, Germany); 5- μ m Zorbax Rx (150 \times 4.6 mm I.D.) (DuPont); 5- μ m Bakerbond C₁₈ wide pore (100 \times 4.6 mm I.D.) (Baker, Phillipsburg, NJ, USA); 5- μ m Supelcosil LC-PAH (150 \times 4.6 mm I.D.) (Supelco, Bellefonte, PA, USA); 5- μ m Vydac 201 TP (150 \times 4.6 mm I.D.) (Separations Group, Hesperia, CA, USA); 5- μ m PAH HC/ODS (250 \times 4.6 mm I.D.) (Perkin-Elmer); 5- μ m Vydac 218 TP (250 \times 4.6 mm I.D.) (Separations Group); 5- μ m Suplex pKb (150 \times 4.6 mm I.D.) (Supelco); 5- μ m Pecosphere 5-CR (150 \times 4.6 mm I.D.) (Perkin-Elmer); 5- μ m Inertsil IN 5 ODS2-15F (150 \times 4.6 mm I.D.) (Gasukuro, Tokyo, Japan); 5- μ m Spheri-5 ODS (250 \times 4.6 mm I.D.) (Brownlee Labs., Santa Clara, CA, USA); 5- μ m Vydac 201 HS (150 \times 4.6 mm I.D.) (Separations Group);

5- μ m RP Select B (250 \times 4.6 mm I.D.) (Merck); and 5- μ m Spherisorb ODS 2 (150 \times 4.6 mm I.D.) (Phase Separations, Queensferry, UK).

The void volume was determined as described elsewhere [6].

RESULTS AND DISCUSSION

Comparison of the NIST results in LC and in SbFC

As has been shown by Sander and Wise [4], the selectivity between two PAHs such as benzo[*a*]pyrene (BaP) (planar compound) and tetrabenzonaphthalene (TBN) (non-planar compound) depends on the monomeric or polymeric nature of the stationary phase. However, this test is valid only for very precise mobile phase conditions. Therefore, we wanted to assess the validity of the test for the chromatographic conditions used in this work. Fig. 1 shows the selectivity obtained in HPLC as a function of that obtained in SbFC. A correlation coefficient of 0.975 was obtained, which indicates the good correlation between the results obtained by the two methods. A decrease in the selectivity values of *ca.* 0.2 can, however, be observed in SbFC (Table I). In SbFC, polymeric columns give a selectivity value of ≤ 0.8 (instead of a value of 1.0 for HPLC), whereas monomeric columns give values close to or above 1.5 (instead of a value of 1.7 for HPLC).

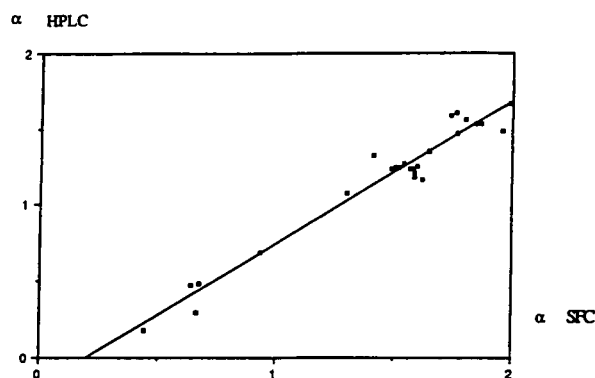


Fig. 1. TBN–BaP selectivity in HPLC vs. SbFC on different commercial columns. The equation of the linear regression is $y = -0.1839 + 0.9309x$. The correlation coefficient is 0.975.

TABLE I

EXPERIMENTAL VALUES AND CHARACTERISTICS OF DIFFERENT COMMERCIAL COLUMNS

The linkage functionality and the carbon content are given when data were available from the manufacturers.

Column	No.	k' (α -carotene)	Selectivity			Linkage functionality ^a	Carbon content (%)
			<i>cis-trans</i> - β -Carotene	TBN–BaP	α -Carotene– zeaxanthine		
Hypersil ODS	1	5.8	1	1.485	6.27	M	8
Partisil ODS 3	2	6.2	1	1.53	0.99	M	10
Pecosphere HS	3	9	1	1.608	2.28	M	8
Ultrasphere DABS	4	11.5	1.04	1.495	5.31		
Adsorbosphere HS	5	16	1.048	1.58	2.69	M	20
Adsorbosphere UHS	6	38	1.052	1.62	2.97	M	30
Zorbax ODS	7	14.5	1.068	1.466	1.046	M	20
Ultracarb 3 ODS	8	8.5	1.082	1.53	1.12	M	22
Ultrabase UB 225	9	13.5	1.84	1.185	4.428	M	19
LiChrospher 100 RP 18 e	10	9.1	1.09	1.238	2.53		22
Hypersil BDS	11	6.6	1.122	1.212	5.83	M	11
Kromasil C ₁₈	12	10.1	1.092	1.153	4.9	M	19
Nucleosil C ₁₈	13	7.2	1.104	1.354	0.625		
Zorbax RX	14	7.7	1.097	1.078	3.82		
Bakerbond C ₁₈ wide pore	15	1.5	1.153	0.183	0.218	P	
Supelcosil LC-PAH	16	2.2	1.181	0.30	0.205	P	8
Vydac 201 TP	17	2.5	1.208	0.476	0.184	P	8
PAH HC/ODS	18	2.4	1.194	0.487	0.155	P	8.5
Vydac 218 TP	19	1.8	1.213	0.69	0.271	P	8
Suplex pKb	20	2.4	1.148	0.815	0.17		
Pecosphere 5-CR	21	10.5	1.07	1.35	4.27	M	12
Superspher 100 RP 18 e	22	12.1	N.m. ^b	1.277	4		
Inertsil IN 50D2-15F	23	7.1	N.m.	1.255	3.7		
Spheri-5 ODS	24	11.4	N.m.	1.238	1.836	P	
Vydac 201 HS	25	6.1	N.m.	1.561	0.541	M	13.5
RP Select B	26	1.9	N.m.	1.331	0.426		
Superspher 100 RP 18	27	11.1	N.m.	1.235	1.148		
LiChrospher 100 RP 18	28	10.4	N.m.	1.148	1.035		
Spherisorb ODS 2	29	5.8	N.m.	1.243	0.883		12

^a M = monofunctional, P = polyfunctional.

^b N.m. = Not measurable.

A similar change in selectivity to those between HPLC and SbFC was observed in HPLC as a function of the organic solvent in either binary aqueous–organic mixtures or in pure organic solvents. A decrease in the water content of the mobile phase leads to a decrease in the BaP–TBN selectivity. If one were to base the

proposed model of Sander and Wise [9] on the presence of slots in the stationary phase which permit the insertion of planar compound, BaP, one could explain this phenomenon.

Indeed, some workers have shown a change in the state of the alkyl chains, collapsed on the silica in the presence of water and more extend-

ed in the mobile phase in the presence of organic solvents [10,11]. The probable unfolding of organic solvents increases either the number or the size of the slots and increases the possibility of penetration of BaP into the stationary phase.

This phenomenon is observed regardless of the type of silane used (mono- or polyfunctional), which implies that there are two types of sites that BaP can penetrate: those created by the network in the bulk of the polymeric phases, which would correspond to a macrostructure of those phases, and the surface sites arising from the state of the grafted chains, either at the surface of the polymeric phases or present in the monomeric phases.

As the changes in the values in this test are identical for NARP chromatography and SbFC, it would appear that the mixture of CO₂ and organic modifier used in SbFC has properties close to those of a non-aqueous mobile phase in NARP.

A study of the variation of the TBN–BaP selectivity in SbFC showed that the addition of modifier results in a decrease in selectivity, which is characteristic of a polymeric-type phase (Fig. 2). These modifiers seem to induce an elongation of the alkyl chains in the mobile phase. It is probable that pure CO₂ solvates the alkyl chains only weakly. The state of the

stationary phase is probably comparable to that observed in liquid chromatography with water-rich mobile phases (collapsed conformation of the alkyl chains).

The extent of the effect of organic modifiers varies depending on the type of modifier used, as shown in a previous study [7]. Modifiers can be classified into three categories on the basis of their dielectric constants: (i) acetonitrile and methanol (>30), (ii) acetone and ethanol (20–30) and (iii) tetrahydrofuran and methylene chloride (<10). The larger the dielectric constant, the smaller is the tendency of the TBN–BaP selectivity towards a polymeric-type phase. This underlines increased solvation and elongation of the chains, as in HPLC with aqueous–organic mixtures [12–21].

Comparison of the selectivity of BaP–TBN and the selectivity of the cis–trans isomers of β -carotene

It must initially be emphasized that it is not possible to measure the value of selectivity between 9- or 13-*cis*- and *trans*- β -carotene, whose separation is difficult with certain columns owing either to the low k' values with some columns or to broad peaks with the particular mobile phase employed. The latter phenomenon has already been observed when using acetonitrile at the modifier. It was also not possible to inject the component separately as we did not have samples of the 9- and 13-*cis* isomers.

We chose to group together the results obtained according to their similarities, because for certain monomeric columns the use of linear regression does not reflect the reality when the selectivity of these isomers is equal to 1, whereas the value of the NIST test for the same columns varies between 1.48 and 1.61 (Fig. 3).

An identical value for the first selectivity and a varying value for the second can only strongly degrade the correlation coefficient, whereas the information given by the two selectivities is in this instance identical. In other words, the phase is monomeric with a low bondage density.

There is a tendency for the selectivity to increase between the *cis*–*trans* isomers of β -carotene when the value of the NIST test decreases. The correlation coefficient is 0.87,

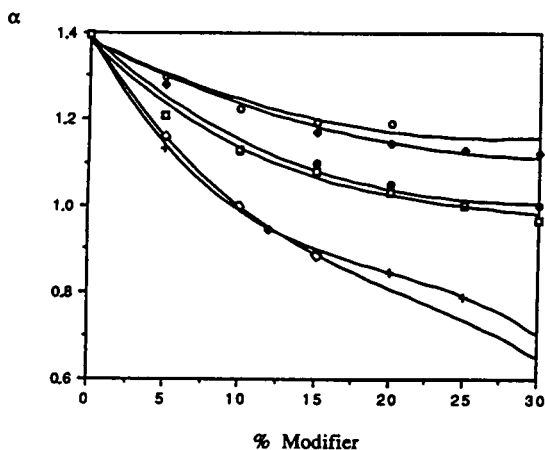


Fig. 2. Selectivity of TBN–BaP in SbFC as a function of the percentage of modifier. Flow-rate, 3.0 ml/min; temperature, 25°C; column, Ultrabase UB 225. ○ = Acetonitrile; ◆ = methanol; ● = acetone; □ = ethanol; + = methylene chloride; ◇ = THF.

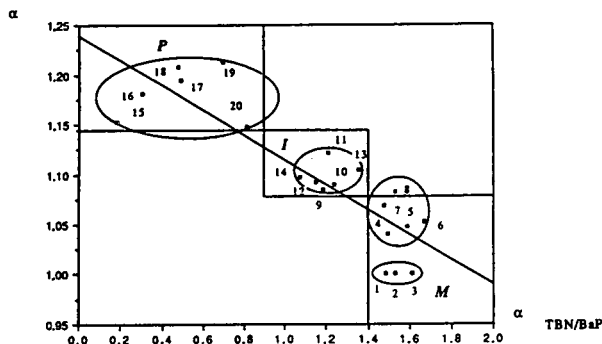


Fig. 3. Selectivity of 9- or 13-*cis*- and *trans* isomers of β -carotene as a function of the selectivity of TBN-BaP in SbFC on different commercial columns. P = polyfunctional; I = intermediate; M = monofunctional. Numbers are column numbers as given in Table I.

which, according to previous statements, shows some correlation between the two criteria. According to Sander and Wise [4], it is possible to separate columns into three categories, monomeric, intermediate and polymeric. This distribution in SbFC corresponds to selectivity values of >1.45 for the first group, 0.9 – 1.45 for the second group and <0.9 for the last group.

Among the monomeric columns, Hypersil ODS (column No. 1, Table I), Pecosphere HS (No. 3) and Partisil 5 ODS3 (No. 2) give a selectivity between the *cis*–*trans* isomers of β -carotene of 1. However, five columns give a selectivity >1 (ca. 1.05) for the *cis*–*trans* isomers of β -carotene but behave as monomeric according to the tests with PAH Zorbax ODS (No. 7), Adsorbosphere HS (No. 5), Adsorbosphere UHS (No. 6), Ultrasphere DABS (No. 4) and Ultracarb (No. 8). These five columns give capacity factors greater than all the other columns, which underlines their high carbon content, and above all takes account of the specific surface area and a carbon load that must be greater than those for the three aforementioned columns. It should be noted that Adsorbosphere UHS gives k' values that are three times greater than those of Ultrabase UB 225 used as a reference, and whose retentivity is already amongst the most important.

As expected, all the polymeric columns, Vydac 201 TP (column No. 16), Vydac 218 TP (No. 18), Supelcosil LC-PAH (No. 15), PAH HC/ODS

(No. 17), Suplex pKb (No. 19) and Bakerbond C_{18} wide pore (No. 14) tested are found in the group of columns that have a polymeric stationary phase.

These structures of these columns allow one to separate the *cis*–*trans* isomers for which the selectivity is between 1.15 and 1.21. It must be noted, however, that despite this elevated value, these columns are less adapted to separations of carotenes under these analytical conditions. This is due to their poor retention, which is indicative of a relatively low carbon content (Table I).

The group of intermediate columns includes Ultrabase UB 225 (column No. 9), Nucleosil C_{18} (No. 13), Hypersil BDS (No. 11), Zorbax Rx (No. 14), Kromasil C_{18} (No. 12) and LiChrospher 100 RP 18 e (No. 10). They give intermediate value for PAHs, which, according to Sander and Wise [4], correspond to a monomeric phase with a high bonding density or a polymeric phase with a low bonding density. One effectively finds among these columns those for which the extent of bonding is important, such as Ultrabase UB 225. It is also interesting that several of these columns (Ultrabase UB 225, Zorbax Rx, Kromasil C_{18} and Hypersil BDS) are stated by the manufacturers as having been specially designed for use with basic products, and often present a high coverage density (Ultrabase UB 225 and Kromasil C_{18} $3.2 \mu\text{mol}/\text{m}^2$, Hypersil BDS $3.6 \mu\text{mol}/\text{m}^2$).

If one looks into the development of the selectivity of the PAHs between initially available supports and those designed for basic products, one realises that the coverage of the silanol groups after bonding (LiChrospher 100 RP 18 e and Superspher 100 RP 18) entails increased selectivity, which shows the development of the support towards a more monomeric natural phase. It could be that the groups used to react with the silanols decrease the depth between the grafts where the BaP becomes trapped, or that the BaP can no longer interact with the silanols. This type of interaction between the silanols and the PAHs has already been reported [22].

Conversely, comparison between thermally treated silicas and silicas that are untreated before bonding (Hypersil, Zorbax and Pecosphere) shows that the selectivity of the PAHs

decreases for treated supports, which gives the columns a more pronounced polymeric character. Even so, it is not really the structure of the phase that is modified but rather the carbon load which leads to an identical development of PAH selectivity, as was shown by Sentell and Dorsey [23].

In addition, it can be emphasized that the three supports designed for basic products (Hypersil BDS and Pecosphere 5 CR) are end-capped or sterically protected (Zorbax Rx). This observation indicates that a detailed understanding of the parameters influencing the separations studied is difficult. An additional parameter that could be of importance is the inorganic impurity content of the silicas used (sodium, aluminium, iron) (Ultrabase UB 225 and Kromasil C₁₈) whose presence can affect the chromatographic properties [1].

It appears nevertheless that the columns treated for the analysis of basic products allow the separation of the *cis-trans* isomer of β -carotene and have an adequate carbon content for this separation and also for the separation of mixtures containing other pigments.

Study of α -carotene–zeaxanthin selectivity

We have previously observed in SbFC that the retention of xanthophylls (luteine and zeaxanthine) greatly depends on the presence of an alcohol as a modifier [8]. A minimum amount of alcohol is necessary for the Ultrabase UB 225 column to ensure rapid elution of its components. Therefore, we deduced that a small amount of alcohol is indispensable for the recovery of the residual silanol groups that interact and strongly retain luteine and zeaxanthine. For this column the selectivity between *trans*- α -carotene and zeaxanthine, with 35% modifier [acetonitrile–methanol (95:5)], is 4.43 (Fig. 4A).

The same analysis carried out on a polymeric column (Supelcosil LC-PAH) gives a totally different result in that the xanthophylls are much more strongly retained than the carotenes, the selectivity of α -carotene–zeaxanthine being 0.205 (Fig. 4B). This result seems surprising as the use of a polymeric stationary phase for

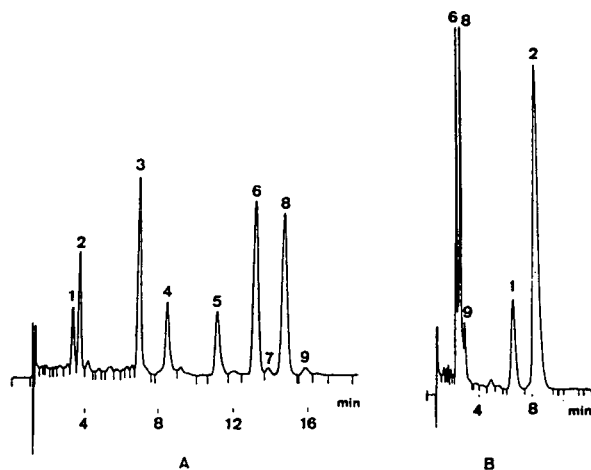


Fig. 4. Chromatograms of a mixture of carotenoids on two different types of stationary phases. Flow-rate, 3.0 ml/min; temperature, 25°C; mobile phase, acetonitrile–methanol–carbon dioxide (33.25:1.75:65, v/v/v). (A) Ultrabase UB 225; (B) Supelcosil LC-PAH. Peaks: 1 = luteine; 2 = zeaxanthine; 3 = β -cryptoxanthine; 4 = lycopene; 5 = all-*trans*- γ -carotene; 6 = all-*trans*- α -carotene; 7 = *cis*- α -carotene; 8 = all-*trans*- β -carotene; 9 = 9-*cis*- β -carotene.

avoiding interactions of products with residual silanols is a recognized practice [24,25]. The addition of butylamine to the mobile phase at a level of 0.25% lowered the capacity factor of luteine from 8.28 to 5.69 and decreased the asymmetry factor of luteine from 2.03 to 1.3. It seems that the xanthophylls interact with certain oxygen atoms carried by the siloxane groups that are more accessible at the stationary polymeric phase/mobile phase interface, rather

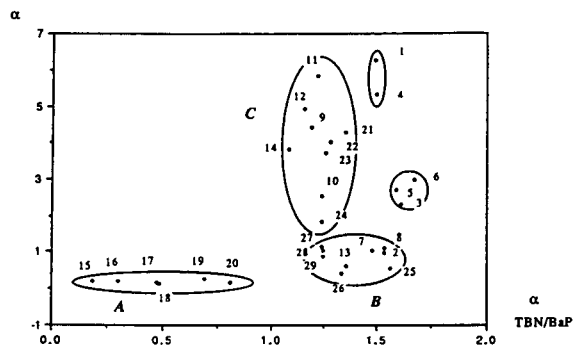


Fig. 5. Selectivity α -carotene–zeaxanthine as a function of the selectivity of TBN–BaP in SbFC for different commercial columns. Numbers are column numbers as given in Table I.

than with the residual silanol groups which are difficult to access with this type of bonding. This behaviour has also been noted in HPLC [25]. We therefore compared this selectivity as a function of that of PAHs (Fig. 5) and established a plan regrouping columns with similar behaviour. Comparison with partial results obtained for the mixture of residual silanols by a different method [3] shows an identical development between the two sources of results, which seems to confirm the hypothesis of the retention mechanism of xanthophylls on polymeric stationary phases.

The first group (A) (15–20) includes polymeric columns that give an inverted retention between the xanthophylls and the carotenes.

Also with these columns the *cis-trans* selectivity of β -carotene is highest. The combination of these two selectivities thus allows the discrimination of this type of support.

The second group (B) (2, 7, 8, 13, 25–29) contains columns that are classified as monomeric or as intermediate according to the NIST 869 test. Included here are the classical silica supports (Nucleosil, Spherisorb ODS 2, LiChrospher 100 RP 18).

The selectivity between α -carotene and zeaxanthine is close to 1, which often lead to co-elution of the carotene and the xanthophylls on these columns. It is possible, however, to suppress this co-elution by altering the amount of alcohol in the mobile phase since the retention of the xanthophylls depends more on the alcohol content than does that of the carotenes. The value of this selectivity shows that the residual silanols are accessible to the xanthophylls on these columns.

The third group (C) (9–12, 14, 21–24) also gives an intermediate PAH selectivity even though most of the supports are monomeric. The elevated value of the α -carotene–zeaxanthine selectivity shows that few of the silanol groups are available to the xanthophylls, which explains their low retention. This result is not surprising since these columns (except the Spheri-5 ODS) are treated for the analysis of basic products and therefore the number of residual silanol present is decreased. It appears that these columns are also those which give a selectivity for the *cis*–

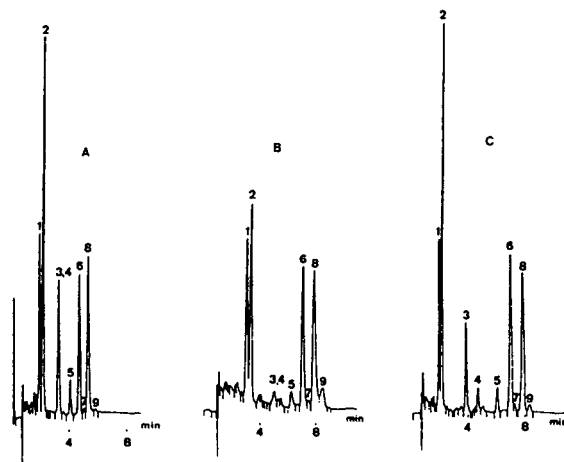


Fig. 6. Chromatograms of a mixture of carotenes on different chromatographic supports used for the analysis of basic products. Analytical conditions as in Fig. 4. (A) LiChrospher 100 RP 18; (B) Pecosphere 5-CR; (C) Zorbax Rx. Peaks: 1 = luteine; 2 = zeaxanthine; 3 = β -cryptoxanthine; 4 = lycopene; 5 = all-*trans*- γ -carotene; 6 = all-*trans*- α -carotene; 7 = *cis*- α -carotene; 8 = all-*trans*- β -carotene; 9 = *cis*- β -carotene.

trans isomers of β -carotene of close to 1.1 with a sufficient retention to obtain, under these conditions (Fig. 6), a complete separation of the compounds studied.

On studying the information obtained regarding these supports, it appears that certain pretreatment of the silica before bonding increases the number of reactive silanols, which leads to a high bonding density phase with homogeneous bonding. These columns therefore have comparable performances and can be used for the separation of complex mixtures of carotenoid pigments.

Two other groups can be distinguished according to this classification, composed of columns classified as monomeric by the NIST 869 test. Amongst these five columns, three give a selectivity close to 3 for the α -carotene–zeaxanthine coupling: Pecosphere HS (No. 3), Adsorbosphere UHS (No. 6), whereas the other two, Hypersil ODS (No. 1) and Ultrasphere DABS (No. 4), have a very high selectivity for the compounds studied.

These results with regard to the Hypersil ODS and the Pecosphere HS columns are surprising, in that these columns are the opposite of the three other columns which are either treated for

basic products (Ultrasphere DAB) or which give a high recovery as attested by the very high capacity factors (Adsorbosphere).

Mechanism of separation of the cis–trans isomers of carotenes

From the results obtained it is possible to propose a separation mechanism for the *cis–trans* isomers of carotenes. As polymeric phases exhibit superior selectivity for this separation, the separation mechanism depends on the shape selectivity, often observed for rigid or planar compounds. The conformation or the order of the bonded chains also plays an important role in this separation, as shown by the results obtained with highly bonded silica or in the presence of different solvents. However, several pieces of information indicate that the separation mechanisms of PAHs and *cis–trans* isomers of carotenes are probably different.

First, for polymeric columns, there does not appear to be a correlation between measured selectivity values within this group, which could indicate that the separation mechanisms between PAHs and carotenes are not identical. The slot model [9] suggests that the planar compounds are retained more than the non-planar compounds, which is the opposite to what is observed for the carotenes, where the linear *trans* isomer is retained less than the bent *cis* isomer, both in SbFC and in NARP HPLC.

Nevertheless, the selectivity of the carotene isomers is highest on a polymeric phase. It is possible that polymeric phases have an irregular thickness depending on the extent of local polymerization. This irregular thickness can lead to the presence of slots, which explains the higher retention of the BaP compared with the TBN and assumes that the surface of this phase has alternating troughs and bumps.

In this instance, owing to the cluttered nature of the interior of the polymeric network together with the tangling of the alkyl chains, it is possible that the carotenes, which are large, rigid molecules, do not penetrate the stationary phase but remain stuck to the surface or only penetrate superficially.

On this uneven surface, the bent form of the *cis* isomers would favour interactions in contrast

to the *trans* compounds, for which none of the surface would be in contact with the adsorbent.

In the same way, high-bonded-density or/and homogeneously bonded monomeric phases (Ultrasphere UB 225, Hypersil BDS, Kromasil C₁₈) could give a surface state similar to that described previously, but whose topology would be less pronounced, explaining the lower values of the selectivity for these phases. The value indicative of the coverage density of bonded groups for these supports is in the region of 3.4 $\mu\text{mol}/\text{m}^2$. The high density would favour rigidity of grafts [26] which could not move apart sufficiently to let the molecules penetrate the interior of the phase.

Dill [27], in his model of retention, emphasized a phenomenon of entropic exclusion (linked with the disruption of a spatial molecular arrangement) of the solute by stationary phases with high coverage density.

The separation mechanism of the *cis–trans* isomers results from an external contact with a stationary phase that covers the silica in the same way but whose surface is more or less regular.

Effect of temperature on the structure of the stationary phase

We investigated the effect of temperature on a polymeric column (Vydac 201 TP) and on a highly bonded monomeric column (Ultrasphere UB 225) and on a monomeric column (Zorbax ODS). There have been several reports of the influence of temperature on the separation of *cis–trans* isomers [5,28] and the unique behaviour of polymeric phases has also been emphasized with the use of homologous series [29] or other test compounds [30,31].

A decrease in temperature leads to a decrease in TBN–BaP selectivity for the three columns studied, as has already been reported by Sander and Wise [32]. On the other hand, Fig. 7 shows that if one observes a phase transition for the monomeric column, Zorbax ODS, and for the Ultrasphere column, the curve of $\log k'$ vs. $1/T$ for BaP is not linear for the polymeric column, Vydac 201 TP, in the temperature range 5–45°C, which shows the existence of a phase transition for this polymeric column. The variation of $\log k'$ for β -carotene shows a change in the slope for

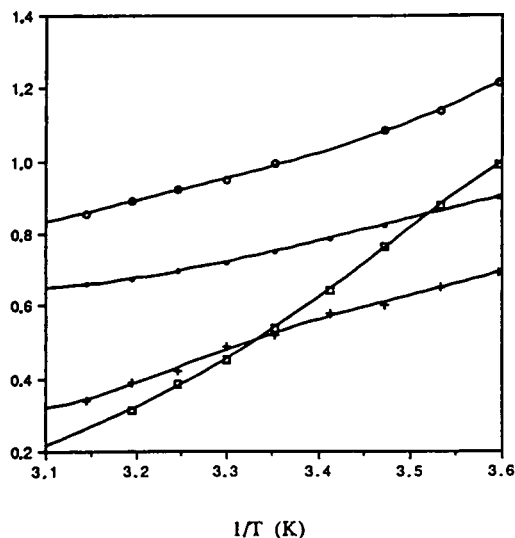
Log k' 

Fig. 7. Variation of the k' as a function of the analytical temperature for different types of linkage. \circ = BaP on Ultrabase UB 225 (15% of acetonitrile as modifier in CO_2); $+$ = BaP on Vydac 201 TP (10% of acetonitrile as modifier in CO_2); \bullet = BaP on Zorbax ODS (15% of acetonitrile as modifier in CO_2); \square = all-*trans*- β -carotene on Vydac 201 TP (10% of acetonitrile as modifier in CO_2).

this column, which seems to confirm this hypothesis. In HPLC, such behaviour has been reported by Jinno *et al.* [33] for a polymeric column using a similar sample, coronene. The same has been observed with smaller test molecules [29–31].

The different results with respect to that of Sander and Wise can be explained by the size of the range studied and the subtlety of the phenomenon. These results further underline the similarity in behaviour between the stationary phases in HPLC and SbFC.

If we now turn to the influence of temperature on the separation of the *cis-trans* isomers of β -carotene, we find that it has little effect for a high-bonded-density phase, whatever the percentage of acetonitrile in the carbon dioxide (Fig. 8). One could propose that the state of the surface is therefore not greatly affected by a change in temperature, either because the high coverage density leads to an increased rigidity of the grafts, or because the variation in temperature induces various opposing phenomena.

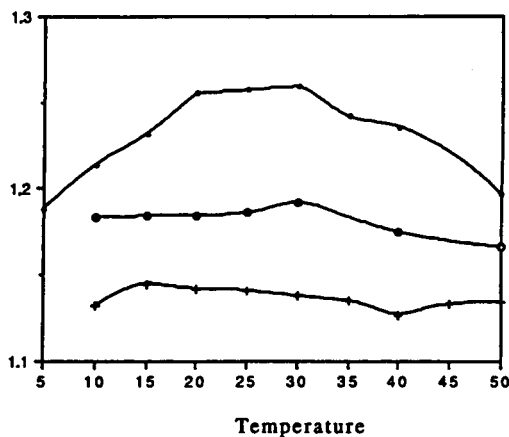
 α 

Fig. 8. Selectivity of fifteen all-*trans-cis* isomers of β -carotene vs. analytical temperature for two types of linkage. \bullet = Vydac 201 TP (10% of acetonitrile as modifier in CO_2); \circ = Ultrabase UB 225 (15% of acetonitrile as modifier in CO_2); $+$ = Ultrabase UB 225 (30% of acetonitrile as modifier in CO_2).

It is, in fact, known that with respect to the bonds there are two types of effects associated with a decrease in temperature: a lengthening of grafts (prevails in *trans* forms of the bonded chains) and an increased rigidity of the chains. These two changes conflict according to the penetrating power of the carotenes into the bulk of the stationary phase.

An increase in selectivity of 50 at 25°C followed by a decrease of 25 at 5°C is seen for the polymeric phase. Even then, one can suggest that there are numerous phenomena occurring. If we consider that the structure of the polymeric stationary phase is made up of a network of variable thickness and of octadecyl chain extremities which form an external layer, it could be that between 50 and 25°C the rigidity of the network increases, as do the local differences in the thickness and topology recognition. In the same way, the swelling of the polymeric phases under the influence of a solvent, like a sponge, has been described by Lochmüller and Kersey [34].

However, between 25 and 5°C, the free grafts take up a *trans* configuration which initiates their stretching and favours penetration of compounds which would in turn decrease the *cis-trans* selectivity.

On the other hand, these two phenomena (between 5 and 25°C and between 25 and 50°C) favour in the same way the insertion of BaP and are in accordance with the continuous increase in the TBN–BaP selectivity observed with a decrease in temperature.

Hence the use of carotenes as test molecules appears to allow the visualization of phenomena unobserved by the use of the selectivity between the PAHs, which further emphasizes the difference in behaviour between these compounds.

CONCLUSIONS

The retention mechanism of carotenes depends on different factors according to the type of compounds studied. The separation of the *cis*–*trans* isomer of carotenes is probably linked to the state of the surface of the stationary phase whereas that of the xanthophylls seems to be governed more by the presence of accessible oxygen groups for the support than that of carotenes. By combining these two criteria of selectivity it seems that it is possible to characterize the nature of the support used.

Polymeric columns give a selectivity between the *cis*–*trans* isomers of β -carotene which is greater than 1.15 and a selectivity between luteine and zeaxanthine which is always greater than 1.2. Monomeric columns with a high carbon content, used in particular for the analysis of basic products, give a value between 1.07 and 1.15 for the first selectivity and a value greater than 2.5 for the second. These columns seem particularly useful for the analysis of carotenoids by SbFC.

ACKNOWLEDGEMENTS

The authors gratefully thank Mrs. Nathalie Huchon and Miss Alexandra Jones for the preparation of the manuscript.

REFERENCES

- 1 K.K. Unger, in K.K. Unger (Editor), *Packings and Stationary Phases in Chromatographic Techniques (Chromatographic Science Series, Vol. 47)*, Marcel Dekker, New York, 1990, pp. 1–2.
- 2 A. Goldberg, *Anal. Chem.*, 54 (1982) 342.
- 3 M.J. Walters, *J. Assoc. Off. Anal. Chem.*, 70 (1987) 465.
- 4 L.C. Sander and S.A. Wise, *J. High Resolut. Chromatogr. Chromatogr. Commun.*, 11 (1988) 383.
- 5 E. Lesellier, C. Marty, C. Berset, A. Tchaplá, *J. High Resolut. Chromatogr.*, 12 (1989) 447.
- 6 E. Lesellier, A. Tchaplá, M.R. Pechard, C.R. Lee and A.M. Krstulovic, *J. Chromatogr.*, 557 (1991) 59.
- 7 E. Lesellier, A.M. Krstulovic and A. Tchaplá, *Chromatographia*, 36 (1993) 275.
- 8 E. Lesellier, A.M. Krstulovic and A. Tchaplá, *J. Chromatogr.*, 641 (1993) 137.
- 9 L.C. Sander and S.A. Wise, *LC·GC*, 6 (1990) 24.
- 10 C.H. Lochmüller, C.H. Hunnicutt and M.L. Mullaney, *J. Phys. Chem.*, 89 (1985) 5770.
- 11 D.E. Martire and R.E. Boehm, *J. Phys. Chem.*, 87 (1983) 1045.
- 12 L.C. Sander, J.B. Callis and L.R. Field, *Anal. Chem.*, 55 (1983) 1068.
- 13 L.C. Sander, C.J. Glinka and S.A. Wise, *Anal. Chem.*, 62 (1990) 1099.
- 14 J. Stahlberg and M. Almgren, *Anal. Chem.*, 57 (1985) 817.
- 15 A.M. Stalcup, D.E. Martire and S. Wise, *J. Chromatogr.*, 442 (1988) 1.
- 16 J.W. Carr and J.M. Harris, *Anal. Chem.*, 58 (1986) 526.
- 17 K. Tani and Y. Susuki, *Chromatographia*, 31 (1991) 347.
- 18 L.A. Cole and J.G. Dorsey, *Anal. Chem.*, 62 (1990) 16.
- 19 P.B. Wright, E. Lamb, J.G. Dorsey and R.G. Kooser, *Anal. Chem.*, 64 (1992) 785.
- 20 P. Shah and L.B. Rogers, *J. Chromatogr.*, 388 (1987) 411.
- 21 S. Heron and A. Tchaplá, *J. Chromatogr.*, 556 (1991) 219.
- 22 A.Y. Fadeev, G.V. Lisichkin, V.K. Runov and S.M. Staroverov, *J. Chromatogr.*, 558 (1991) 31.
- 23 K.B. Sentell and J.G. Dorsey, *J. Chromatogr.*, 461 (1989) 193.
- 24 D. Chan Leach, M.A. Stadalius, J.S. Berus and L.R. Snyder, *LC·GC Int.*, 5 (1988) 22.
- 25 K.S. Epler, L.C. Sander, R.G. Ziegler, S.A. Wise and N.E. Craft, *J. Chromatogr.*, 595 (1992) 89.
- 26 K.B. Sentell and J.G. Dorsey, *Anal. Chem.*, 61 (1989) 930.
- 27 K.A. Dill, *J. Phys. Chem.*, 91 (1987) 1980.
- 28 L.S. Sander and N.E. Craft, *Anal. Chem.*, 62 (1990) 1545.
- 29 S. Heron and A. Tchaplá, *Chromatographia*, 36 (1993) 11.
- 30 L.A. Cole and J.G. Dorsey, *Anal. Chem.*, 64 (1992) 1317.
- 31 L.A. Cole, J.G. Dorsey and K.A. Dill, *Anal. Chem.*, 64 (1992) 1324.
- 32 L.C. Sander and A. Wise, *Anal. Chem.*, 61 (1989) 1789.
- 33 K. Jinno, T. Nagoshi, N. Tanaka, M. Okamoto, J.C. Fetzer and W.R. Biggs, *J. Chromatogr.*, 436 (1988) 1.
- 34 C.H. Lochmüller and M.T. Kersey, *Anal. Chem.*, 60 (1988) 1910.

Study of polyorganosiloxanes (native and solvent swollen) for the preparation of narrow (5–15 μm I.D.) and long (1–6 m) open tubular columns in reversed-phase liquid chromatography

Karin Göhlin*

Department of Analytical and Marine Chemistry, Chalmers University of Technology and University of Göteborg, S-412 96 Göteborg (Sweden)

Marita Larsson

Bioanalytical Chemistry, Astra Hässle AB, S-431 83 Mölndal (Sweden)

(First received December 2nd, 1992; revised manuscript received March 22nd, 1993)

ABSTRACT

Narrow-bore, (5–15 μm), long (up to 6 m), efficient and stable open tubular columns with four different polyorganosiloxane coatings, were prepared by the static coating and the precipitation coating methods. The polysiloxanes were substituted with phenyl- (OV-17-vi and PS-264), methyl- (PS-255), and octadecyl- (PMSC₁₈) groups. They were studied in their regular cross-linked state as well as after swelling with *n*-heptane. Anthracene derivatives were used as model compounds. Column properties such as retention, selectivity and efficiency were investigated in reversed-phase liquid chromatography. GC was used for complementary studies of 50 μm I.D. columns. The highest retention was obtained on the columns coated with OV-17-vi and on the swelled stationary phases. A considerable resolution improvement was obtained in the columns, after swelling with *n*-heptane owing to the increase in retention. More than 10^6 theoretical plates were achieved in 70 min at a k' of 0.46 in a 6 m \times 6 μm I.D. column.

INTRODUCTION

In order to reach high separation power (one million theoretical plates and more), *e.g.* for the separation of complex mixtures, open tubular columns (OTCs) are being developed for liquid chromatography (LC). OTCs have a lower flow resistance compared to conventional packed columns. This feature permits the use of very long columns (up to several meters). Consequently, a higher total number of theoretical plates is obtained. The chromatographic theory

predicts that OTCs should compete with packed columns in resolution and separation speed, when columns of small I.D. (10 μm or less) are used [1–4]. Recently, our group presented a comparison of narrow-bore (5–15 μm I.D.) OTCs and conventional LC columns with the same type of stationary phase: immobilized poly-methyloctadecylsiloxane [5]. These experimental data are in good agreement with the theoretical predictions.

Open tubular LC (OT-LC) columns were in the beginning prepared from soda-lime glass [6–8] and borosilicate glass [9,10]. In 1979, fused silica was introduced as column material [11] and it is now favoured over other materials in gas

* Corresponding author.

chromatography. Fused silica has some advantageous properties, as compared to other glass capillaries, such as greater flexibility, higher inertness and better UV transparency. These characteristics have made fused silica attractive also for packed and open tubular capillary columns in LC. Naturally, practical difficulties are met with capillaries of a few micrometer I.D. To avoid extra-column band-broadening, the injection and detection volumes should be in the nano- to picolitre range. This has been solved by split injections and various on-column detection techniques.

The most common type of polymeric stationary phases used in open tubular column chromatography are polyorganosiloxanes, which contain a linear backbone of siloxane bonds. Polyorganosiloxane stationary phases have been applied earlier for the preparation of narrow-bore columns for LC [12–18]. They have gained popularity due to properties such as easy formation of uniform and stable cross-linked films, high solute diffusivities, and liquid-like behaviour. The preferred combination of column properties narrow tubes, long columns and thick stationary phase films, all place high demands on the coating procedure. A lot of effort has been made in order to improve the methods for the preparation of narrow-bore OTCs. A major problem has been to achieve sufficient retention, owing to the small ratio of surface area to mobile phase volume in an open tube.

Several methods have been used to prepare small-diameter columns for OT-LC. The dynamic coating method, known from gas chromatography, was first used by Hibi *et al.* [10]. They coated borosilicate columns with inner diameters down to 30 μm . The dynamic method is a straightforward method, but very high pressures are required to prepare narrow-bore columns with thick films. In addition, it is difficult to control the film thickness and the uniformity along the tube.

With the static coating method it is easy to regulate and control the film thickness. This method is well-established for the preparation of GC columns and it results in more efficient columns than the dynamic method [19]. For the preparation of narrow-bore (30–50 μm) columns in GC, static coating was initially applied by

Schutjes *et al.* [20]. In OT-LC, the static coating method of polysiloxane stationary phases, was first utilized by Takeuchi *et al.* [21]. It is a relatively time-consuming method and the coating time increases for narrower columns with thicker stationary phase films. To accelerate the static coating technique for narrow-bore capillaries, different procedures have been employed. It has been performed at elevated temperatures [22,23], including the “free-release” static coating method [24], where the coating is done at higher temperatures, but without applying a vacuum at the column end. Another approach to speed up the static coating method, has been to select more volatile solvents for the stationary phase solution. Different variants have been tried, such as mixed solvents [25], liquefied gases [26,27] and freons [12,28].

Dluzneski and Jorgenson [13] introduced a new method for the preparation of narrow-bore columns. It is known as the precipitation coating method and is based on variable solubilities of a stationary phase polymer in selected solvent systems, at different temperatures. The method is fast but it is difficult to control the film thickness, and it has only been shown to work with the vinyl-modified version of the stationary phase OV-17.

The bonding of monomeric reagents to the column wall is an alternative to the polymeric coatings mentioned above. In order to yield sufficient retention it is necessary to increase the surface area of the capillary wall with an etching procedure. That makes the choice of column material important. The high purity of fused silica gives the material some advantageous properties, as mentioned earlier. However, it is difficult to increase the surface area in fused-silica capillaries. Therefore, borosilicate glass is still used in OT-LC for *e.g.* bonded ODS phases [29].

Recently, a new procedure supposed to simplify the preparation of narrow-bore OTCs, was presented by Slais *et al.* [30]. It utilizes a flowing retentive liquid as stationary phase. In addition OT-LC separations have been performed at elevated temperatures in order to obtain high efficiencies in commercially available columns (50–100 μm I.D.) [31,32].

To overcome the problem with low sample

capacity and low column retention in open tubular fused-silica columns, different approaches have been presented in the literature. Tock and co-workers [33,34] used an ammonia solution to convert polyethoxysiloxane films into porous silica layers in fused-silica capillaries. The layer was then modified with silane reagents. Euguchi *et al.* [35] were able to create thick films of acrylate polymers by photopolymerization in transparent fused-silica tubes, and they achieved considerable retention.

An alternative approach is to swell the polymeric coating, which acts as a stationary phase, with a solvent. Swelling of polysiloxanes with non-polar solvents was accomplished in 11–50 μm I.D. OTCs by Folestad and Larsson [36]. The stationary phase volume increased by a factor of 3 to 4. Besides the increase in retention, swelling also affects column selectivity and the diffusion coefficients in the stationary phase. Horká *et al.* [37] showed that immobilized Carbowax 20M stationary phase films in OTCs swelled in mobile phases of methanol and water. However, their primary aim was to improve the mass transfer in the stationary phase and not to increase the retention.

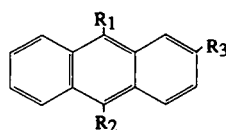
The aim of this work was to prepare and evaluate narrow (5–15 μm I.D.) and long (1–6 m) OTCs for reversed-phase liquid chromatography. The static evaporative and the precipitation coating methods were used to coat the columns with four different polymeric stationary phase films. Polyorganosiloxanes substituted with phenyl, methyl and octadecyl groups were used. In order to increase the retention capacity, which is an obstacle with OTCs, the polymers were also swelled with *n*-heptane. GC was used as a complementary evaluation method. Differences in the preparation methods and chromatographic performance are discussed.

EXPERIMENTAL

Chemicals

The stationary phases used were PMSC₁₈, PS-255, PS-264 and OV-17-vi. PMSC₁₈, a poly-methyloctadecylsiloxane, was synthesized at Max Planck Institut für Kohlenforschung (Mülheim/Ruhr, Germany), and was a generous gift from G. Schomburg and J. Köhler. PS-255 is a

copolymer of dimethylsiloxane and 1–3% methylvinylsiloxane and PS-264 is a copolymer of 92–96% polydimethylsiloxane, 3–7% diphenylsiloxane and 0.5–1% methylvinylsiloxane, both gum phases from Fluka (Buchs, Switzerland). OV-17-vi is a methylphenylsilicone gum with 50% phenyl and 1% vinyl groups from Alltech (Deerfield, IL, USA). As radical initiators for the cross-linking reaction bis(α,α -dimethylbenzyl)peroxide (dicumyl peroxide) or benzoyl peroxide from Merck (Darmstadt, Germany) were used. The following solvents were applied during the coating procedure and in the evaluation work: *n*-pentane, dichloromethane, acetone, *n*-heptane, cyclohexane (analytical-reagent grade) from Merck (Darmstadt, Germany), acetonitrile (LC grade) from Rathburn (Walkerburn, UK), and water from a Milli-Q system from Millipore (Bedford, MA, USA). Anthracene derivatives were used as test compounds (see Fig. 1) and they were dissolved in the mobile phase. The derivatives were synthesized at the Department of Organic Chemistry, University of Göteborg and kindly provided by H.-D. Becker.




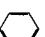
	R1	R2	R3
1	-COOH	-H	-H
2	-(CH ₂) ₃ OH	-H	-H
3	-OCH ₃	-H	-H
4	-H	-H	-H
5	-CH ₃	-H	-H
6	-H	-H	-CH ₃
7	-CH ₃	-CH ₃	-H
8		-H	-H
9	-(CH ₂) ₃ - 	-H	-H
10	-(CH ₂) ₃ -CH ₃	-H	-H

Fig. 1. Anthracene derivatives used as test compounds.

Column preparation

Fused-silica tubing (5 and 10 μm I.D.) from Polymicro Technologies (Phoenix, AZ, USA) was coated mainly by the static coating method as described earlier [14–16]. The stationary phase and the peroxide for the cross-linking reaction were dissolved in *n*-pentane. When the capillaries were coated with the stationary phase OV-17-vi, the precipitation method as described by Dlużneski and Jorgenson [13] was applied. The dimensions of the columns investigated in this work are presented in Table I. Different phase ratios were obtained by varying the stationary phase concentration in the coating solution. The inner diameter of the columns was measured by the electrical resistance over the mercury filled capillary as described by Guthrie *et al.* [38]. The stationary phase film thickness, d_f , in static coating was calculated according to eqn. 1

$$d_f = r \cdot \sqrt{\frac{1}{100/c - 1} + 1} - r \quad (1)$$

where r is the column radius and c is the concentration of the stationary phase in the coating solution (% v/v). To calculate the volumetric concentration a density of 0.98 g ml^{-1} for PS-255 and PS-264 and a density of 0.9 g ml^{-1} for PMSC₁₈ was used.

Instrumental set-up

The chromatographic system was similar to the systems used previously for OT-LC in our laboratory [15,16]. The low volumetric flow-rates and the small injection volumes were created by a simple split arrangement. Splitting ratios up to 1:1 000 000 were used to minimize band broadening from the injection system. The swelling of the stationary phase film was performed according to Folestad and Larsson [36]. During

TABLE I
CHARACTERISTICS OF THE OPEN TUBULAR COLUMNS

Column No.	Internal diameter (μm)	Length (cm)	Stationary phase concentration (% v/v)	Phase ratio ^a	Film thickness (μm)	Type of stationary phase
1	5.7	176	2.17	0.022	0.031	PMSC ₁₈
2	5.8	144	1.10	0.011	0.016	PMSC ₁₈
3	6.0	253	1.10	0.011	0.017	PMSC ₁₈
4	6.0	212	1.10	0.011	0.017	PMSC ₁₈
5	6.3	576	1.10	0.011	0.017	PMSC ₁₈
6	11.1	140	6.25	0.067	0.180	PMSC ₁₈
7	11.3	146	4.26	0.044	0.124	PMSC ₁₈
8	12.6	160	2.17	0.022	0.069	PMSC ₁₈
9	13.3	143	2.17	0.022	0.073	PMSC ₁₈
10	13.8	475	2.17	0.022	0.076	PMSC ₁₈
11	6.6	163	1.01	0.010	0.017	PS-255
12	11.7	184	2.97	0.030	0.089	PS-255
13	11.7	176	2.00	0.020	0.059	PS-255
14	11.9	157	2.00	0.020	0.060	PS-255
15	11.6	146	2.00	0.020	0.059	PS-255
16	6.5	187	1.01	0.010	0.017	PS-264
17	13.0	161	2.00	0.020	0.066	PS-264
18	13.0	179	1.01	0.010	0.033	PS-264
19	13.3	170	1.01	0.010	0.033	PS-264
20	6.5	115	1.00	–	–	OV-17-vi
21	9.2	156	2.00	–	–	OV-17-vi

^a The phase ratio is defined as the stationary to mobile phase volume ratio.

the swelling experiments, the mobile phase was pre-saturated with *n*-heptane. The on-column detection was performed with a laser-induced fluorescence detection system [39,40]. The lasers used were a He–Cd laser Model 4210 NB from Liconix (Sunnyvale, CA, USA) and an argon ion laser Model 2025-05 from Spectra-Physics (Mountain View, CA, USA). The chromatograms were recorded on a Perkin-Elmer 56 strip chart recorder or with a computer system, PC integration pack from Kontron (Zürich, Switzerland).

Procedures

LC capacity factors, k' , were measured at ambient temperature, and 9-anthracenecarboxylic acid and nitromethane were used as unretained solutes. The mobile phase used throughout this study was acetonitrile–water (50:50). The peaks were symmetrical in this study and they were treated as Gaussian. Consequently, the theoretical plate height, H for the test solutes was calculated from eqn. 2

$$H = \frac{Lw_{1/2}^2}{5.54t_R^2} \quad (2)$$

where L is the column length, $w_{1/2}$ is the peak width at half the peak height and t_R is the retention time of the solute. Efficiency measurements at different flow-rates were made. In order to obtain the reduced velocity, ν , the solute diffusion coefficients in the mobile phase, D_m , were calculated from the Wilke–Chang equation [41]. The D_m values in this work are

TABLE II

DIFFUSION COEFFICIENTS IN ACETONITRILE–WATER (50:50), FOR ANTHRACENE DERIVATIVES, CALCULATED ACCORDING TO REF. 41, AT THE TEMPERATURE 298 K

Solute	D_m (cm ² /s)
Anthracene	$8.5 \cdot 10^{-6}$
9-Methylanthracene	$8.0 \cdot 10^{-6}$
9-Phenylanthracene	$6.8 \cdot 10^{-6}$
Propylphenylanthracene	$6.0 \cdot 10^{-6}$
<i>n</i> -Butylanthracene	$6.8 \cdot 10^{-6}$

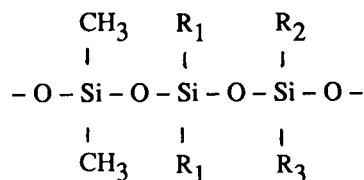


Fig. 2. Polysiloxane backbone, the R groups symbolize various organic substituents (see Table III).

presented in Table II. Gas chromatography was used as a complement to study retention characteristics, efficiency and stability of the stationary phase film. Conventional GC equipment is not suited for columns with I.D. of 10 μm or less. Instead 50 μm I.D. columns were coated in an equivalent way. The GC measurements were performed in accordance with earlier work by us [16].

RESULTS AND DISCUSSION

The polyorganosiloxanes have various organic groups attached to the silicon atoms (Fig. 2), and the composition of the stationary phases used in this study is specified in Table III. The chemical and physical properties of polysiloxanes influence the efficiency, selectivity and stability of the coated columns. The column efficiency is a function of solute diffusion rates in the polymer film, as well as uniformity of the coated film. Selectivity is a function of the pendant groups on the polysiloxane backbone. The influence of selectivity is important since the separation of

TABLE III

COMPOSITION OF THE STATIONARY PHASES STUDIED

Numbers refer to the approximate molar proportion of each substituent group bonded to the siloxane backbone.

Stationary phase	Composition (%)			
	–CH ₃	–C ₆ H ₅	–C ₁₈ H ₃₇	–CH = CH ₂
OV-17-vi	50	50	–	1
PS-264	94	5	–	1
PS-255	99	–	–	1
PMSC ₁₈	83	–	17	–

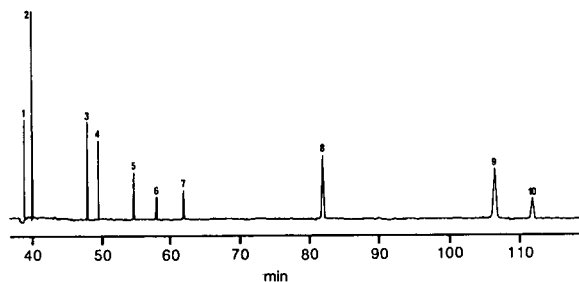


Fig. 3. Separation of anthracene derivatives in column No. 5 ($5.8 \text{ m} \times 6.3 \mu\text{m}$ I.D.) coated with PMSC_{18} and swelled with *n*-heptane. Mobile phase was acetonitrile–water (50:50). Linear flow-rate: 0.25 cm/s. Volumetric flow-rate: 4.6 nl/min. Peaks: 1 = 9-anthracene carboxylic acid; 2 = 9-propanolanthracene; 3 = 9-methoxyanthracene; 4 = anthracene; 5 = 9-methylanthracene; 6 = 2-methylanthracene; 7 = 9,10-dimethylanthracene; 8 = 9-phenylanthracene; 9 = 9-propylene-phenylanthracene; 10 = 9-*n*-butylanthracene.

complex mixtures is facilitated by a variability in selectivity, besides a high efficiency and an adequate retention capacity. The possibility to affect the selectivity in LC with a change in mobile phase composition further increases the potential of high-resolution separations. An example of a high-resolution separation in a polysiloxane-coated OTC is shown in Fig. 3.

Column preparation

The static coating method. The static coating method is the preferred method for polymeric stationary phases in open tubular columns since it is possible to control the film thickness. One of the drawbacks with open tubular fused-silica columns is the low retention capacity. Higher k' values are obtained with thicker stationary phase films. Very thick films in capillary columns were considered in various respects by Grob and Grob [42]. The preferred phase for very thick coatings (up to $5 \mu\text{m}$) was according to them, the gum phase PS-255, due to the low viscous solution. SE-54 (5% methylphenyl, 1% methylvinyl siloxane) was less suitable for coating of very thick films. This observation is in agreement with that of Folestad *et al.* [15]. They were able to coat a $50 \mu\text{m}$ I.D. column with a PS-255 solution of 13.6% (v/v) while it was impossible to prepare homogeneous SE-54 solutions with a concentration over 6%. The stationary phase PS-264 used in this work is a gum phase and has a

similar composition as the SE-54 phase. We were able to coat a series of $50 \mu\text{m}$ I.D. columns with a PS-264 concentration of up to 10.1% (v/v). There is a linear relationship between the capacity factor and the phase ratio in these PS-264 columns, when evaluated in GC. The efficiency, expressed as number of theoretical plates for *n*-alkanes, is comparable to the $50 \mu\text{m}$ I.D. columns coated with PS-255. Thus, it is possible to create thick stationary phase films with the stationary phase PS-264. However, when the internal diameter of the column is decreased the concentration of the stationary phase solution must be increased to provide similar film thickness. The difficulties in filling and evaporation of the solvent increase accordingly.

The main drawback of the static coating method is that it is relatively time consuming. Long coating times increase the risk of Rayleigh instability, which can result in rearrangement of the stationary phase film [43]. In this study the evaporation time was shorter for columns coated with the stationary phase PMSC_{18} as compared to the two gum phases PS-255 and PS-264. The approximate evaporation time in a $2 \text{ m} \times 5 \mu\text{m}$ I.D. column coated with a stationary phase solution of 1% (v/v) was 2 h and 45 min for the gum phases, and 1 h and 40 min for the PMSC_{18} -coated columns. In addition, the capillaries were easier to fill with the PMSC_{18} solution. Typically, the complete coating procedure of a $5 \mu\text{m}$ I.D. column took one working day, after the coating solution was homogenized.

To assess the reproducibility of the static coating method under demanding conditions, two long columns (over 5 m in length) of $6 \mu\text{m}$ I.D. were coated with PMSC_{18} solutions of the same concentration. One of these columns was accidentally broken in halves and was evaluated as two separate columns. The retention and selectivity properties of the "three" columns were equal. These characteristics will be discussed further below. It is generally assumed, that the number of theoretical plates will increase linearly with the length of the column (at constant separation temperature and linear flow velocity). This is exemplified in Fig. 4 where N/m is plotted against the linear flow velocity for the long column and the second half of the

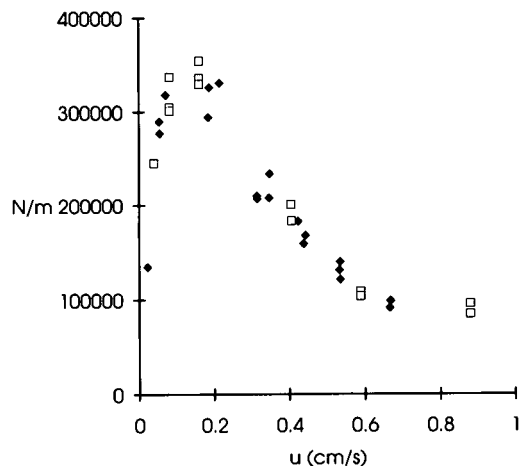


Fig. 4. The number of theoretical plates per meter vs. the linear flow-rate in two 6 μm I.D. PMSC₁₈-coated columns, (□) column No. 4 and (◆) column No. 5. Test solute: 9-phenylanthracene, $k' = 0.26$.

divided column for a retained substance. As can be seen there is good agreement between the two columns. Also, this result is equal to that of column 2, which was coated as a 1.7 m long column. Overall the retention characteristics and efficiency are similar in the columns, which indicates that the reproducibility of the column preparation procedure is appropriate.

To conclude, narrow-bore columns of 5–15 μm I.D. and a length of up to 6 m were successfully prepared. The coating times for all the columns in this work were reasonable compared to for example Van Berkel-Geldof *et al.* [12,17], who showed that static coating of open tubular columns with PS-255 solutions in *n*-pentane at 45°C, required several days. Also under demanding conditions, *i.e.* coating 6 m long columns with an I.D. of 6 μm , the static coating method resulted in efficient columns.

The precipitation coating method. The precipitation coating method [13] is convenient even for very narrow columns. It has resulted in stable columns with inner diameters as narrow as 1.7 μm [44]. The choice of stationary phase is still limited to OV-17-vi, so despite the ease of manipulation and the promptness, the method has not been widespread.

In order to achieve high efficiency in capillary columns it is important to coat the columns with

uniform stationary phase films. Originally, it was shown in GC that OTCs coated with polysiloxanes of high phenyl content yielded a relatively low efficiency. This was thought to be related to the low viscosity of the phenyl-containing phases at that time. However, the OV-17-vi has more of a gum like character and is consequently better suited as stationary phase in open tubular columns. Static coating of a similar type of stationary phase in GC columns gave columns of higher efficiency than the original OV-17 phase [45].

To get a rough estimate of the uniformity of the OV-17-vi films, 50 μm I.D. columns coated with the precipitation method were evaluated, with GC. The efficiency in isothermal separations was evaluated as the number of theoretical plates, N , for *n*-alkanes and in temperature-programming as Trennzahl (TZ) according to Grob *et al.* [46]. At the same k' value and the same linear flow-rate, N values in the OV-17-vi coated columns were 4–5 times lower compared to 50 μm I.D. columns coated with PS-255, evaluated earlier by us [47]. The separation efficiency expressed as Trennzahl was approximately 20 and 10 in PS-255 and OV-17-vi coated columns, respectively, at the same elution temperature.

A low efficiency in GC is generally assumed to be associated with an irregular distribution of the stationary phase film. Other parameters that influence the column efficiency with the precipitation method, according to Dluzneski [44] are the precipitation time and the time for removal of solvent. He also observed that there was a large difference in viscosity for different batches of OV-17-vi. However, there was no significant difference in the obtained efficiency in LC, for the narrow-bore OV-17-vi coated columns, as compared to the other stationary phases in this work.

Immobilization and column stability

The degree of stationary phase immobilization was estimated by GC measurements of k' values for *n*-alkanes, before and after rinsing the column with organic solvents. Such measurements have been performed earlier in our lab-

oratory for the stationary phases PS-255 [15] and PMSC₁₈ [16], in 50 μm I.D. columns. It was found that the extractable part of the stationary phase was 8–10% in PS-255-coated columns and somewhat higher, 10–30%, in PMSC₁₈-coated columns. A stationary phase similar to OV-17-vi coated with the static coating method and evaluated in GC showed a 20% loss of stationary phase [48]. Dluzneski [44] estimated the extractability of the OV-17-vi stationary phase by the measurement of k' values in LC. He showed that the extractability depended on the percentage of peroxide used for cross-linking. At the recommended concentration, 1% peroxide (w/w of the polymer), the loss of stationary phase was 16–34%.

In this study the stationary phases PS-264 and OV-17-vi were coated in 50 μm I.D. columns and evaluated by GC to estimate the degree of cross-linking. For PS-264 the extractable part was 3–12% and in the OV-17-vi columns coated with the precipitation coating method it was 1–30%. The loss of stationary phase in columns coated with the precipitation method increased with the film thickness. This differs from the observations for the other stationary phases, where the removable part seemed to be independent of d_f .

In order to study the stability of the stationary phases in LC, columns have been stored with mobile phase inside for several years. The columns have also been used in an indirect detection mode with basic dyes as visualizing agents [49]. The mobile phases used were up to 90% buffer of pH 3, and various additives *e.g.* methylene blue, tetramethylammonium chloride, and ion-pairing agents such as *n*-pentane sulfonic acid. These conditions are comparable to the ageing experiments performed on polymer-coated silica particles by Hetem *et al.* [50]. For example, in our column 17 the k' values for the anthracene derivatives were the same in 1989, when the column was prepared, and in 1992 after storage with mobile phase (acetonitrile and water) and separations under the demanding conditions described above. No influence on the peak shape could be observed. Consequently the stability of the polymer coated columns is high.

Retention and selectivity characteristics

Swelling. To increase the retention in OTCs, the polymeric stationary phase can be swelled with an organic solvent. The extent of swelling depends on the similarity (polarity) of the stationary phase and the solvent, and the degree of cross-linking in the stationary phase. It has been shown [36] that PS-255 and SE-54 coated in 50 μm I.D. columns, swell 3–4 times (by volume in *n*-heptane). The swollen stationary phases exhibited good stability. Dluzneski [44] tried to swell narrow-bore OTC coated with OV-17-vi. He used *n*-heptane as a swelling agent, but the k' value for 9-methyl anthracene was lower after the presumed swelling, probably partly owing to extraction of the stationary phase. Pretorius and Lawson [51] studied the swelling of polysiloxane stationary phases in batch experiments. Their results showed that OV-17 swelled 62% in hexane as compared to polydimethylsiloxane which swelled 130% in the same solvent. Additionally, their result showed that dichloromethane was a better swelling agent for OV-17. In order to achieve stable systems the mobile phase needs to be pre-saturated with the swelling agent. The high solubility of dichloromethane in a mixture of acetonitrile and water is unfavourable. A better choice of mobile phase is methanol and water and some preliminary experiments with this combination have been performed [52].

The PMSC₁₈ stationary phase has been investigated earlier in OT-LC by us [5,16]. The retention characteristics of the PMSC₁₈ stationary phase are favourable but the capacity factors are still comparatively low. In this study swelling of the PMSC₁₈ film with *n*-heptane was performed. The swelling of the stationary phase films in the 50 μm I.D. columns was measured by the difference in I.D. before and after swelling. The film thickness increased with a factor 3–4 and the swelling factor S_v , calculated according to ref. 36, was 2.3–2.5. Thus the swelling of PMSC₁₈ is similar to the swelling of PS-255 studied earlier [36]. The increase in retention after swelling of the PMSC₁₈ was approximately 5 times and 6 times for fluorene and phenylfluorene, respectively (Table IV). This increase is smaller as compared to the increase of 12–16 times on gum

TABLE IV

SWELLING EFFECTS IN 50 μm I.D. PMSC₁₈ COATED COLUMNS

Column I: 58.7 μm I.D., 151 cm long and a film thickness of 0.65 μm . Column II: 49.7 μm I.D., 196 cm long and a film thickness of 0.27 μm . The mobile phase used was acetonitrile–water (50:50). k' values for fluorene derivatives before and after swelling with *n*-heptane, and selectivity factor $\alpha = (k'_{\text{phenylfluorene}})/(k'_{\text{fluorene}})$ before and after swelling with *n*-heptane.

Column	k'_{fluorene}	$k'_{\text{phenylfluorene}}$	k'_{fluorene} , swelled	$k'_{\text{phenylfluorene}}$, swelled	α	α , swelled
I	0.22	0.35	1.07	2.02	1.59	1.83
II	0.46	0.72	2.24	4.10	1.57	1.89

phases for the same solutes [36]. Since the degree of swelling is similar the reason could be that the influence of *n*-heptane in the film is smaller for the more lipophilic PMSC₁₈ than for PS-255. The increase in retention for the anthracene derivatives in these 50 μm I.D. columns was 7–10 times. As expected the selectivity in the columns changed after the swelling.

Retention. Capacity factors of anthracene derivatives on cross-linked polysiloxanes of varying composition are presented in Table V. The relative standard deviation was 1–4% for the k' values measured in the flow-rate interval of 0.03–2.5 cm/s. The highest capacity factors for these solutes were observed on columns coated with the stationary phase OV-17-vi, which contains 50% phenyl. Swelling the polymeric stationary phase with *n*-heptane resulted in increased retention for all types of stationary phases. The relative standard deviation for the k'

value measurements was 2–7% for the swelled stationary phases, over a larger flow-rate interval (up to 5 cm/s).

The gum phases PS-255 and PS-264 coated in 10 μm I.D. columns showed the largest increase in retention for the anthracene derivatives, 10–20 times. The only exception was the column with the thickest film (No. 12), which showed a k' enhancement of 5–10 times. The k' increase for PMSC₁₈-coated columns was 3–13 times. In general solutes with higher k' showed a larger increase in retention after swelling, in the same column.

Measurements of the internal diameter of the column before and after swelling with *n*-heptane in two of the 10 μm I.D. columns (columns 6 and 17) showed that the increase in film thickness was approximately 2.5 times. However, the real phase ratio in the small-diameter columns is unknown (see the part about immobilization). In

TABLE V

CAPACITY FACTORS FOR ANTHRACENE AND 9-PHENYLANTHRACENE IN 10 AND 5 μm I.D. OPEN TUBULAR COLUMNS

The columns were coated with polysiloxane stationary phases of different composition. The concentration of the stationary phase solution was 2% in the 10 μm I.D. and 1% in the 5 μm I.D. columns. Mobile phase acetonitrile–water (50:50).

Stationary phase	10 μm I.D. columns		5 μm I.D. columns	
	$k'_{\text{anthracene}}$	$k'_{9\text{-phenylanthracene}}$	$k'_{\text{anthracene}}$	$k'_{9\text{-phenylanthracene}}$
PMSC ₁₈	0.07	0.22	0.08	0.27
PS-255	0.05	0.15	0.05	0.08
PS-264	0.08	0.28	0.03	0.07
OV-17-vi	0.38	1.82	0.50	2.35

addition differences in the cross-linking density could affect the swelling.

Capacity factors, at the same nominal phase ratio, were higher in the 5 μm I.D. columns than in the 10 μm I.D. columns, for PMSC₁₈ [16] and OV-17-vi. For example we found that the k' values in the 5 μm I.D. column, coated with a 1% solution, were higher than in the 10 μm I.D. column coated with a 2% solution. However, this has been observed earlier [13], where concentrations of 1% or less of OV-17-vi, gave unexpectedly high k' values.

The 5 μm I.D. columns coated with PS-255 and PS-264 have a lower retention capacity than expected. Furthermore, the selectivity and the increase in retention after swelling in these columns were lower compared to the 10 μm I.D. columns. Grob and Grob [53] noticed that a thick stationary phase film could be almost completely removed by rinsing in spite of cross-linking. They suggested that the rinsing solvent swells the stationary phase and for thick films the expansion could fill a large part of the tubing. Under these conditions the solvent moves with friction, which could be sufficient to tear away a considerable part of the stationary phase. For thinner films there will remain a free space inside the tubing so the solvent can flow with a lower resistance. We always rinse the columns with organic solvents (e.g. dichloromethane and *n*-pentane) to remove the extractable part of the stationary phase before LC testing. Sometimes the result is a temporary plugging of the narrow-

bore columns. This occurred e.g. in the 5 μm I.D. column coated with PS-264. High pressures were used to remove the plug and it is possible that part of the stationary phase was torn off.

Selectivity. The selectivity factors, for the anthracene derivatives on the different stationary phases used, are presented in Fig. 5a and b. For the phenyl-containing stationary phases, the influence of the phenyl-group in 9-propylphenylanthracene was larger compared to the phenyl-group in 9-phenylanthracene. This may be explained by the structure of the two compounds. Intramolecular interactions of the aromatic rings in 9-phenylanthracene are hindered when the phenyl group is located directly on the anthracene molecule. Fig. 5b illustrates the increased similarity between the columns after swelling.

To estimate the contribution from substituents, we calculated the difference in Gibbs free energy ($\Delta(\Delta G)$) from retention data, see eqn. 3

$$\Delta(\Delta G) = RT \ln \alpha \quad (3)$$

where R is the gas constant and T is the thermodynamic temperature (296 K). Group selectivity calculations for a methyl group, derived from 9,10-dimethylantracene vs. anthracene and from 9-methylantracene vs. anthracene, gave identical values of the selectivity contribution in a column, approximately 900 J/mol.

In Fig. 6 the contribution from the phenyl

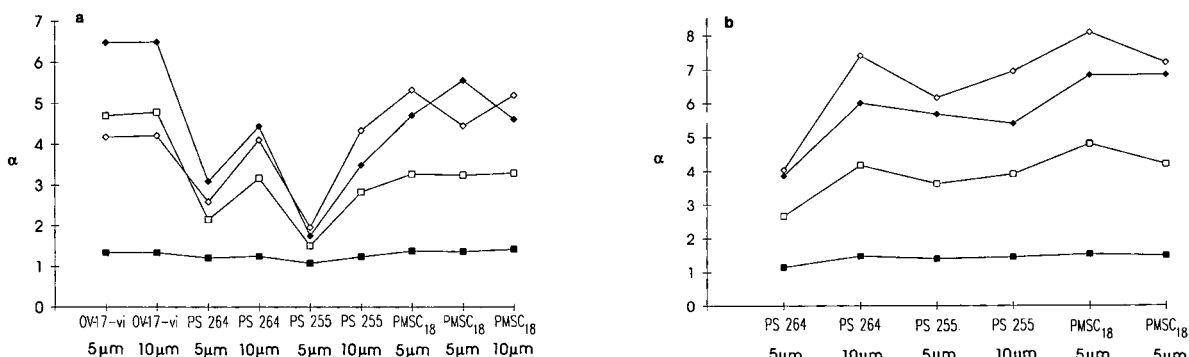


Fig. 5. Selectivity factors, α , in columns coated with different stationary phases and of different internal diameter. The α -values are calculated against anthracene. ■ = 9-Methylantracene; □ = 9-phenylanthracene; ◆ = 9-propylphenylanthracene; ◇ = 9-*n*-butylanthracene. (a) Before swelling with *n*-heptane. (b) After swelling with *n*-heptane.

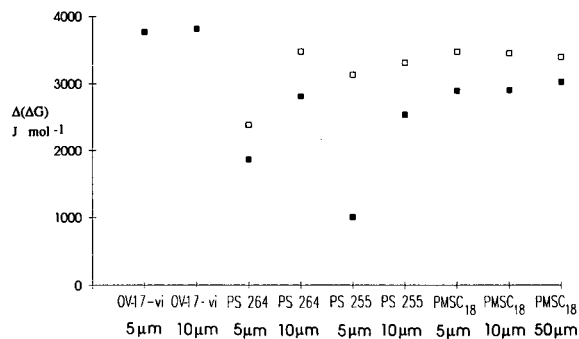


Fig. 6. The difference in Gibbs free energy, $\Delta(\Delta G)$ (J/mol), for a phenyl group in the different columns. $\Delta(\Delta G)$ was calculated from 9-phenylanthracene and anthracene. ■ = Before swelling, □ = after swelling.

group in 9-phenylanthracene is shown. The phenyl groups in the stationary phase OV-17-vi show a higher selectivity towards the phenyl substituted anthracene. Whereas the PS-264 stationary phase, containing a smaller fraction of phenyl groups, has about the same selectivity as the PMSC₁₈ stationary phase.

The methylene group selectivity for columns with different stationary phases and internal diameters is shown in Fig. 7. Different values were obtained when the methylene group selectivity was calculated from 9-butylanthracene and 9-methyl anthracene compared to propylphenylanthracene and 9-phenylanthracene. This may be explained by the different environment for the methylene group units. Evidently the selectivity effect of a methylene unit is different when it is

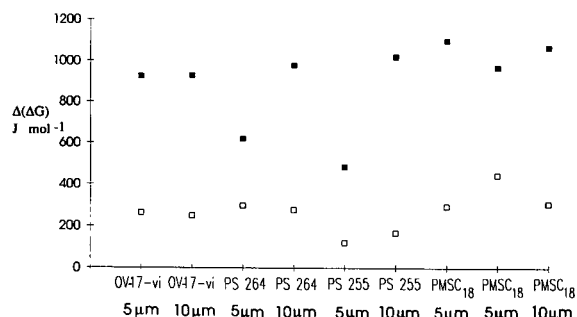


Fig. 7. The difference in Gibbs free energy, $\Delta(\Delta G)$ (J/mol), for a methylene group in the different columns. $\Delta(\Delta G)$ was calculated in two ways: (□) from 9-propylphenylanthracene and 9-phenylanthracene and (■) from 9-*n*-butylanthracene and 9-methylanthracene.

located on an aromatic ring as compared to an alkyl chain.

Columns coated with the same stationary phase in general show the same selectivity. Notable in Figs. 5–7 is the anomalous behaviour of the 5 μm I.D. columns coated with gum phases as discussed above. Also, the order of 9-propylphenylanthracene and 9-*n*-butylanthracene was reversed in two of the 5 μm I.D. columns coated with PMSC₁₈. These two columns were the last to be prepared and the dissimilarity could be caused by a change in the polymer composition owing to ageing.

To conclude, it was seen that polysiloxane stationary phase composition affects the selectivity for the anthracene derivatives. Overall, the same selectivity factors were obtained in the polysiloxanes after swelling with *n*-heptane. This indicates that the organic solvent dominates the retention mechanism in the swelled columns.

Retention and selectivity, comparison with other publications. Even if conventional liquid chromatography has a high accuracy, precision and repeatability within one laboratory, retention results between laboratories, or even on nominally identical systems, can vary significantly. Differences in the stationary phase materials, and methods to measure the void volume are two of the problems.

The gum phases PS-255 and PS-264 have been evaluated earlier in OT reversed-phase LC [12,15,17]. Comparison of k' values and selectivity factors for anthracene derivatives from different groups are presented in Table VI. It can be seen that the obtained retention in the columns coated by Van Berkel-Geldof *et al.* [12] is higher compared to columns prepared in our laboratory. In our work and in ref. 15 the columns were rinsed with pentane and dichloromethane while the columns in ref. 12 were rinsed with a mixture of acetonitrile and water, before LC tests. Consequently, a larger part of the stationary phase could be extracted in the former case, which leads to a lower retention. It is however important to rinse out the extractable part of the stationary phase, especially to diminish the risk of plugging when the columns are swelled with *n*-heptane. The mobile phase composition was not the same in the different

TABLE VI

COMPARISON OF THE RETENTION AND SELECTIVITY DATA ON THE GUM PHASES PS-255 AND PS-264 FROM DIFFERENT PUBLICATIONS

The columns were coated with the static coating technique. In this work acetonitrile–water (50:50) and in refs. 12 and 15 acetonitrile–water (40:60) was used.

Stationary phase	I.D. (μm)	Phase ratio ^b	$k'_{\text{anthracene}}$		Selectivity ^a	Ref.
			Acetonitrile–water (40:60)	Acetonitrile–water (50:50)		
PS-255	11.7	0.030		0.077	1.2	This work, column no. 12
PS-255	10.5	0.032	0.97		1.3	12
PS-255	11.6	0.050	0.14			15
PS-255	28.5	0.042	1.3			12
PS-264	13.0	0.020			1.3	This work, column no. 17
PS-264	25.1	0.059			1.3	12

^a Selectivity factors for 9-methylanthracene vs. anthracene.

^b Stationary to mobile phase volume ratio.

papers. However, the selectivity factors for 9-methylanthracene shown in Table VI are similar. This agrees with our previous observations with 50 μm I.D. columns where acetonitrile–water (50:50) and (40:60) gave the same α for 9-methylanthracene vs. anthracene.

The phase ratios in the columns coated with OV-17-vi are unknown, but according to Dlużneski and Jorgenson [13] higher stationary phase concentrations will result in columns with a larger amount of stationary phase. The k' values can be compared to those obtained for 9-methylanthracene in 10 μm I.D. columns in the method description [13]. The k' value for 9-methylanthracene in a column coated with a 2% solution is approximately 1.2 with a mobile phase composition of acetonitrile–water (35:65). In our 10 μm I.D. column k' was 0.5 for the mobile phase composition 50:50, which agrees reasonably well.

Kinetic performance efficiency

To determine the kinetic performance in chromatographic columns it is necessary to use solutes that show the column at its best, *i.e.* give symmetrical peaks [54]. The anthracene solutes are a good choice in this respect.

A rough estimate of the diffusion coefficients in the different stationary phases (D_s value) was

obtained by comparing experimental data with the Golay equation by use of a curve-fitting procedure. D_s values in 10 μm I.D. columns coated with PMSC₁₈ were $1 \cdot 10^{-8}$ – $4 \cdot 10^{-8}$ cm^2/s and in the PS-255 coated columns they were $5 \cdot 10^{-9}$ – $8 \cdot 10^{-9}$ cm^2/s for 9-phenylanthracene. In the 5 μm I.D. columns coated with PMSC₁₈ the obtained D_s values were smaller. In column 5 the D_s value was approximately $1 \cdot 10^{-9}$ cm^2/s .

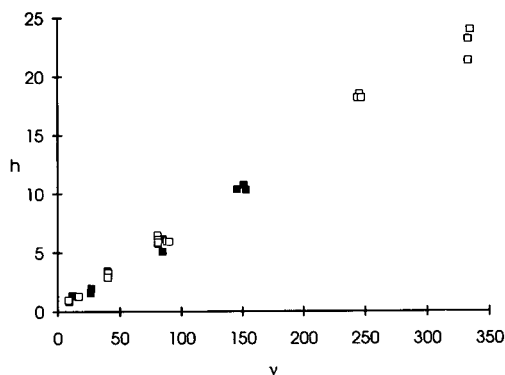


Fig. 8. Reduced plate height, h , vs. reduced flow-rate, v , in the columns coated with OV-17-vi. ■ = column No. 20 with an internal diameter of 6.5 μm . Test solute was 9-phenylanthracene with a k' value of 2.4. □ = Column No. 21 with an internal diameter of 9.2 μm . Test solute was 9-propylphenylanthracene with a k' value of 2.5. D_m values used to calculate the reduced velocity are shown in Table II.

After swelling and assuming an increase in film thickness of 2.5 times in column 6 the obtained D_s value was $1 \cdot 10^{-8}$ cm²/s. Again the real film thickness in these columns is unknown. However, estimating the loss in film thickness to 10% gave approximately the same D_s value in the columns.

In OV-17-vi coated columns the nominal film thickness is unknown. However, Fig. 8 shows the experimentally obtained reduced plate height ($h = H/d_c$, d_c = column diameter) vs. the reduced velocity ($\nu = ud_c/D_m$, u = linear velocity) for the two columns coated with OV-17-vi, for solutes of approximately the same k' value. The major advantage of reduced parameters rather than absolute ones, is that they readily allow comparisons of columns with different internal diameters and for solutes with different diffusion coefficients. As can be seen there is an excellent agreement between the efficiency in the two columns.

In Fig. 9, h is plotted vs. ν for three of the stationary phases: PMSC₁₈, OV-17-vi and one of the gum phases, PS-264. Different solutes were chosen to obtain the same k' value ($k' = 0.36$). A h_{\min} of 0.5 was achieved, which corresponds to 180 000 plates/m in the PMSC₁₈ column, 217 000

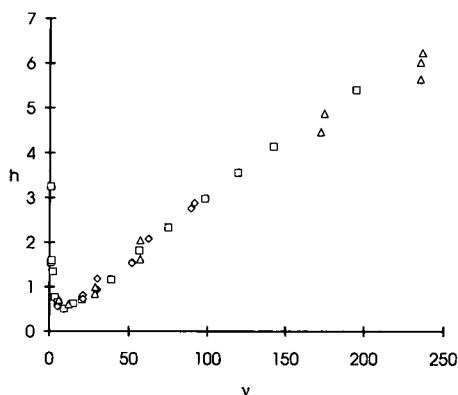


Fig. 9. Comparison of the reduced plate height vs. reduced velocity for columns coated with the different stationary phases. \square = Column No. 6 (1.4 m \times 11.1 μ m I.D.) coated with PMSC₁₈, 9-methylanthracene, $k' = 0.36$. Δ = Column No. 21 (1.6 m \times 9.21 μ m I.D.) coated with OV-17-vi, anthracene, $k' = 0.38$. \diamond = Column No. 17 (1.6 m \times 13 μ m I.D.) coated with PS-264, 9-*n*-butylanthracene, $k' = 0.36$. D_m values used to calculate the reduced velocity are shown in Table II.

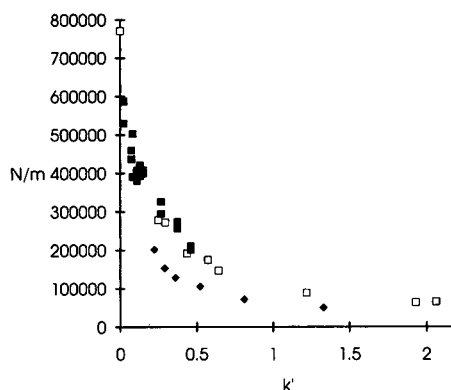


Fig. 10. The number of theoretical plates/m vs. k' . The linear velocity of the mobile phase was 0.2 cm/s. PMSC₁₈-coated columns. \blacksquare = Column No. 5 (5.8 m \times 6.3 μ m I.D.) before swelling and \square = after swelling with *n*-heptane. \blacklozenge = Column No. 6 (1.4 m \times 11.1 μ m I.D.).

plates/m in the OV-17-vi column and 154 000 plates/m in the PS-264-coated column.

Certainly, the obtained number of theoretical plates and the low h values in the OTCs are impressive. However, one must not forget the dependence of efficiency on k' at these low k' values. The rapid drop in N with increased k' values is illustrated, by experimentally obtained data, in Fig. 10.

When the quality of a separation should be judged, both the performance and the time must be considered along with the experimental conditions. To consider time, the rate of production of effective theoretical and theoretical plates (N_{eff} and N , respectively) was studied in the columns. N per unit time is facilitated by high flow-rates and low k' values. In the 10 μ m I.D. columns this number is approximately 300 plates/s, whereas in the 5 μ m I.D. columns up to 2000 plates/s could be reached at low k' values. N_{eff} depends on the k' value and the highest N_{eff} was, consequently, obtained in the swelled stationary phases, and in the columns coated with OV-17-vi. Concurrently the retention time increases yielding N_{eff} /s in the same order of magnitude as for the columns with lower k' values. In addition the obtained resolution vs. the retention time for the last eluting component in the pair could be plotted, as recommended by Etre and March [55]. Such plots are shown in Fig. 11. The solute

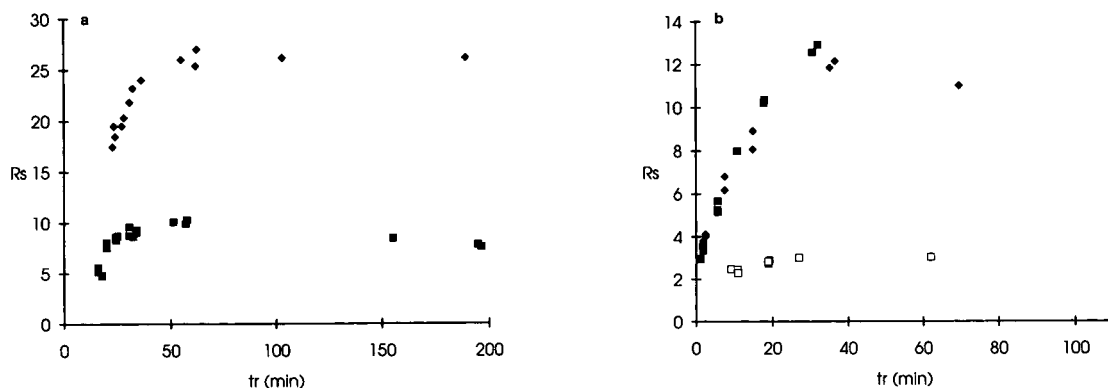


Fig. 11. Resolution for the solute pair 9-methylanthracene and anthracene vs. the retention time of 9-methylanthracene. (a) Column No. 5 (5.8 m × 6.3 μm I.D.) coated with PMSC₁₈ (■) before swelling and (◆) after swelling with *n*-heptane. (b) Column No. 17 (1.6 m × 13 μm I.D.) coated with PS-264, (□) before swelling and (◆) after swelling with *n*-heptane. (■) Column No. 21 (1.6 m × 9.2 μm I.D.) coated with OV-17-vi.

pair is 9-methylanthracene and anthracene, which has approximately the same α value for all the stationary phases. The swelling of the stationary phase increases the resolution considerably due to the increase in k' value (Fig. 11a and b). The obtained resolution in the 6.3 μm I.D. column (Fig. 11a) is higher as compared to the 13 μm I.D. column (Fig. 11b). In Fig. 11b the high resolution obtained in a OV-17-vi coated column, possessing a high retention

capacity, is also shown. This also illustrates the large influence on resolution from the retention capacity.

CONCLUDING REMARKS

Chromatographers have explored Golay's model of open tubular columns, aiming at an improved resolution. In gas chromatography and supercritical fluid chromatography open tubular

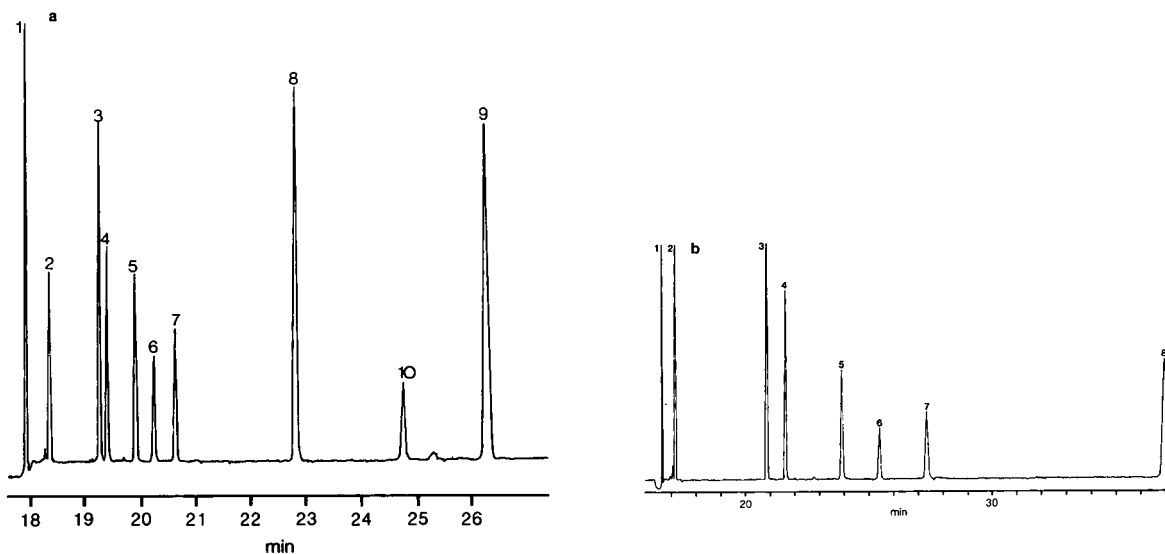


Fig. 12. Separations of anthracene derivatives. PMSC₁₈-coated column No. 5 (5.8 m × 6.3 μm I.D.) at approximately the same mobile phase velocity. Linear flow-rate: 0.55 cm/s. Volumetric flow-rate: 10 nl/min. Other separation conditions as in Fig. 4. (a) before swelling and (b) after swelling with *n*-heptane.

columns are widely used nowadays. In liquid chromatography however, the columns need to be very narrow to be able to show the excellent performance suggested in theory. Analytical requirements of the stationary phase and the columns are defined polarity, variable phase ratio, long-term chemical stability and mechanical strength. The columns prepared and evaluated in this work agree well with the requirements stated above. It is shown that the static coating method (the preferred method for coating OTCs) works well even for very long (6 m) and narrow ($6\ \mu\text{m}$) columns. High efficiency was achieved in our columns, e.g. more than 10^6 theoretical plates. The time of the complete coating procedure is reasonable. The swelling of the stationary phase to increase the k' values was here shown to work well in narrow-bore OTCs and stable systems were achieved. The swelling of the stationary phase also influences the selec-

tivity of the column. Fig. 12 shows the efficient separation obtained in a long narrow column and the differences in resolution before and after swelling with *n*-heptane. In Fig. 13 the excellent retention properties of OV-17-vi columns for these solutes is shown. The influence of the high amount of phenyl groups in the stationary phase film is visualized by the elution order of the anthracene derivatives substituted with phenyl groups. Also, it illustrates that the efficient mass transfer in these columns can be used to achieve fast separations.

REFERENCES

- 1 J.H. Knox and M.T. Gilbert, *J. Chromatogr.*, 186 (1979) 405.
- 2 G. Guiochon, *Anal. Chem.*, 53 (1981) 1318.
- 3 F.J. Yang, *J. Chromatogr. Sci.*, 20 (1982) 241.
- 4 J.W. Jorgenson and E.J. Guthrie, *J. Chromatogr.*, 255 (1983) 335.
- 5 K. Göhlin, A. Buskhe and M. Larsson, *Chromatographia*, in press.
- 6 D. Ishii, T. Tsuda and T. Takeuchi, *J. Chromatogr.*, 185 (1979) 73.
- 7 T. Tsuda, K. Tsuboi and G. Nakagawa, *J. Chromatogr.*, 214 (1981) 283.
- 8 D. Ishii and T. Takeuchi, *J. Chromatogr. Sci.*, 22 (1984) 400.
- 9 T. Tsuda, K. Hibi, T. Nakanishi, T. Takeuchi and D. Ishii, *J. Chromatogr.*, 158 (1978) 227.
- 10 K. Hibi, D. Ishii, I. Fujishima, T. Takeuchi and T. Nakanishi, *J. High Resolut. Chromatogr. Chromatogr. Commun.*, 1 (1978) 21.
- 11 R. Dandeneau and E.H. Zerener, *J. High Resolut. Chromatogr. Chromatogr. Commun.*, 2 (1979) 351.
- 12 O. van Berkel-Geldof, J.C. Kraak and H. Poppe, *J. Chromatogr.*, 499 (1990) 345.
- 13 P.R. Dluzneski and J.W. Jorgenson, *J. High Resolut. Chromatogr. Chromatogr. Commun.*, 11 (1988) 332.
- 14 A. Farbrot, S. Folestad and M. Larsson, *J. High Resolut. Chromatogr. Chromatogr. Commun.*, 9 (1986) 117.
- 15 S. Folestad, B. Josefsson and M. Larsson, *J. Chromatogr.*, 391 (1987) 347.
- 16 K. Göhlin and M. Larsson, *J. Microcol. Sep.*, 3 (1991) 547.
- 17 O. van Berkel, H. Poppe and J.C. Kraak, *Chromatographia*, 24 (1987) 739.
- 18 J.W. Jorgenson, E.J. Guthrie, R.L. St. Claire III, P.R. Dluzneski and L.A. Knecht, *J. Pharm. Biomed. Anal.*, 2 (1984) 191.
- 19 G.A.F.M. Rutten and J.A. Luyten, *J. Chromatogr.*, 74 (1972) 177.
- 20 C.P.M. Schutjes, E.A. Vermeer, J.A. Rijks and C.A. Cramers, *J. Chromatogr.*, 253 (1982) 1.

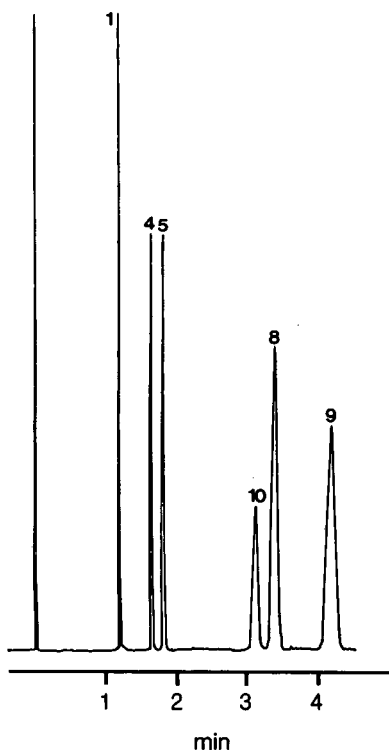


Fig. 13. Fast separation of anthracene derivatives in an OV-17-vi coated column No. 21 ($1.6\ \text{m} \times 9.2\ \mu\text{m}$ I.D.). Linear flow-rate: 2.2 cm/s. Volumetric flow-rate: 84 nl/min. Other separation conditions as in Fig. 4.

- 21 T. Takeuchi, H. Kitamura, T. Spitzer and D. Ishii, *J. High Resolut. Chromatogr. Chromatogr. Commun.*, 6 (1983) 666.
- 22 R.C. Kong and M.L. Lee, *J. High Resolut. Chromatogr. Chromatogr. Commun.*, 6 (1983) 319.
- 23 F.I. Onuska, *J. Chromatogr.*, 289 (1984) 207.
- 24 B. Xu and N.P.E. Vermeulen, *Chromatographia*, 18 (1984) 520.
- 25 R.C. Kong and M.L. Lee, *Chromatographia*, 17 (1983) 451.
- 26 T. Wännman, L. Blomberg and S. Schmidt, *J. High Resolut. Chromatogr. Chromatogr. Commun.*, 8 (1985) 32.
- 27 K. Janák, V. Kahle, K. Tesarik and M. Horká, *J. High Resolut. Chromatogr. Chromatogr. Commun.*, 8 (1985) 843.
- 28 S.R. Sumpter, C.L. Woolley, E.C. Huang, K.E. Markides and M.L. Lee, *J. Chromatogr.*, 517 (1990) 503.
- 29 R.L. St. Claire III, D.M. Dohmeier and J.W. Jorgenson, *J. Microcol. Sep.*, 3 (1991) 303.
- 30 K. Slais, M. Horká and K. Kleparnik, *J. Chromatogr.*, 605 (1992) 167.
- 31 G. Liu, N.M. Djordjevic and F. Erni, *J. Chromatogr.*, 592 (1992) 239.
- 32 G. Liu, N.M. Djordjevic and F. Erni, *J. Chromatogr.*, 598 (1992) 153.
- 33 P.P.H. Tock, G. Stegemann, R. Peerboom, H. Poppe, J.C. Kraak and K.K. Unger, *Chromatographia*, 24 (1987) 617.
- 34 P.P.H. Tock, C. Boshoven, H. Poppe, J.C. Kraak and K.K. Unger, *J. Chromatogr.*, 477 (1989) 95.
- 35 S. Euguchi, J.G. Kloosterboer, C.P.G. Zegers, P.J. Schoenmakers, P.P.H. Tock, J.C. Kraak and H. Poppe, *J. Chromatogr.*, 516 (1990) 301.
- 36 S. Folestad and M. Larsson, *J. Chromatogr.*, 394 (1987) 455.
- 37 M. Horká, K. Janák and M. Krejčí, *J. Microcol. Sep.*, 3 (1991) 217.
- 38 E.J. Guthrie, J.W. Jorgenson, L.A. Knecht and S.G. Bush, *J. High Resolut. Chromatogr. Chromatogr. Commun.*, 6 (1983) 566.
- 39 S. Folestad, L. Johnson, B. Josefsson and B. Galle, *Anal. Chem.*, 54 (1982) 925.
- 40 S. Folestad, B. Josefsson and B. Galle, *J. Chromatogr. Sci.*, 23 (1985) 273.
- 41 C.R. Wilke and P. Chang, *Am. Inst. Chem. Eng. J.*, 1 (1955) 264.
- 42 K. Grob and G. Grob, *J. High Resolut. Chromatogr. Chromatogr. Commun.*, 6 (1983) 133.
- 43 K.D. Bartle, C.L. Woolley, K.E. Markides, M.L. Lee and R.S. Hansen, *J. High Resolut. Chromatogr. Chromatogr. Commun.*, 10 (1987) 128.
- 44 P.R. Dlužneski, *Ph.D. Thesis*, The University of North Carolina at Chapel Hill, Chapel Hill, NC, 1987.
- 45 B.W. Wright, P.A. Peaden and M.L. Lee, *J. High Resolut. Chromatogr. Chromatogr. Commun.*, 5 (1982) 413.
- 46 K. Grob, G. Grob and K. Grob, Jr., *J. Chromatogr.*, 156 (1978) 1.
- 47 K. Göhlin and M. Larsson, *J. Chromatogr.*, 634 (1993) 31.
- 48 P.A. Peaden, B.W. Wright and M.L. Lee, *Chromatographia*, 15 (1982) 335.
- 49 S. Folestad, K. Göhlin, A.P. Larsson and A. Wallin, in preparation.
- 50 M.J.J. Hetem, J.W. de Haan, H.A. Claessens, C.A. Cramers, A. Deege and G. Schomburg, *J. Chromatogr.*, 540 (1991) 53.
- 51 V. Pretorius and K. Lawson, *J. High Resolut. Chromatogr. Chromatogr. Commun.*, 9 (1986) 335.
- 52 K. Göhlin, unpublished results.
- 53 K. Grob and G. Grob, *J. High Resolut. Chromatogr. Chromatogr. Commun.*, 6 (1983) 153.
- 54 P.A. Bristow and J.H. Knox, *Chromatographia*, 10 (1977) 279.
- 55 L.S. Ettre and E.W. March, *J. Chromatogr.*, 91 (1974) 5.

Pyrophosphates as biocompatible packing materials for high-performance liquid chromatography

Senya Inoue* and Nobuyuki Ohtaki

Central Research Laboratory, Kanto Chemical Co., Inc., 1-7-1, Inari, Soka-City, Saitama 340 (Japan)

(First received February 1st, 1993; revised manuscript received April 19th, 1993)

ABSTRACT

Crystalline pyrophosphates of Mg, Ca, Sr, Mn and Zr were developed as new packing materials for high-performance liquid chromatography. They were synthesized as porous and rigid spheres based on a spray-pyrolysis method, followed by heat treatment. The pyrophosphate (PPi) packing materials thus obtained had high mechanical strength. All PPi columns tested showed similar chromatographic behaviours of basic proteins. In contrast, the chromatographic behaviour of acidic proteins, nucleotides and nucleic acids depended on the kind of PPi column: β -Ca₂P₂O₇, α -Sr₂P₂O₇ and Mn₂P₂O₇ columns showed similar chromatographic behaviour, whereas β -Mg₂P₂O₇ and ZrP₂O₇ columns showed no retention of most acidic proteins including phosphoproteins. Based on this property, a successful single-step separation of γ -globulin from other serum proteins by the β -Mg₂P₂O₇ column was achieved. The β -Mg₂P₂O₇ column could not retain nucleotides and the ZrP₂O₇ column could not retain nucleic acids.

INTRODUCTION

Various phosphates have been reported concerning their use as packing materials for high-performance liquid chromatography (HPLC). The chromatographic properties of calcium phosphates such as brushite [1,2], monetite and octacalcium phosphate [1] and calcium phosphate gel [3,4] have been studied. Hydroxyapatite (HAP) has been successfully used for the separation and purification of biomolecules [5,6]. Studies on zirconium phosphate ion exchangers dealt with crystalline material [7] and amorphous gels of variable composition [8].

A few attempts have been made to utilize a gel of magnesium pyrophosphate as a packing material [9,10]. However, the degree of hydration varied with ageing and the particles became smaller with time, so that the gel needed to be used immediately after preparation. In addition,

the flow characteristics were too poor for its direct use in chromatographic columns.

No report has been published on the use of any sintered, crystalline pyrophosphate (PPi) packing materials in HPLC. Such pyrophosphates of alkaline earth metals are promising packing materials because of their high mechanical strength and stability at elevated pH and temperatures. This paper reports new preparations of crystalline pyrophosphates of calcium (CaPP; Ca₂P₂O₇), magnesium (MgPP; Mg₂P₂O₇), strontium (SrPP; Sr₂P₂O₇), manganese (MnPP; Mn₂P₂O₇) and zirconium (ZrPP; ZrP₂O₇) with a rigid spherical shape based on a spray-pyrolysis method. Their chromatographic properties were evaluated with proteins, nucleotides and nucleic acids.

EXPERIMENTAL

Materials

Lysozyme (chicken egg white) was obtained from Merck (Darmstadt, Germany). The follow-

* Corresponding author.

ing proteins were obtained from Sigma (St. Louis, MO, USA): cytochrome *c* (horse heart), ribonuclease A (bovine pancreas), α -chymotrypsinogen A (bovine pancreas), papain (papaya latex), α -chymotrypsin (bovine pancreas), myoglobin (horse skeletal muscle), haemoglobin (bovine blood), γ -globulin (human; prepared from Cohn fractions II and III), γ -globulin (bovine; prepared from Cohn fractions II and III), catalase (bovine liver), conalbumin (chicken egg white; iron poor), conalbumin (chicken egg white; iron complex), transferrin (human; apo type), transferrin (human; holo type), transferrin (bovine; apo type), transferrin (bovine; holo type), β -lactoglobulin A (bovine milk), β -lactoglobulin B (bovine milk), albumin (human serum), phosvitin (egg yolk), α -casein (bovine milk), β -casein (bovine milk), ovalbumin (chicken egg), α -lactalbumin (bovine milk) and trypsin inhibitor (soybean).

Adenosine-5'-monophosphate (AMP), adenosine-5'-diphosphate (ADP) and adenosine-5'-triphosphate (ATP) were obtained from Yamasa Shoyu (Chiba, Japan).

DNA (calf thymus) and tRNA (baker's yeast) were obtained from Sigma.

Preparation of pyrophosphates

Analytical-reagent grade chemicals and distilled water were used throughout. As starting materials for spray-pyrolysis, five kinds of slurries with composition of CaPP, SrPP, MgPP, MnPP and ZrPP were prepared by vigorously mixing solution A with solution B as summarized in Table I. After the reaction, additional methanol

TABLE I
SOLUTIONS USED FOR PREPARATION OF PYROPHOSPHATE SLURRY

Slurry	Solution A	Solution B
$\text{Ca}_2\text{P}_2\text{O}_7$	$\text{Ca}(\text{OH})_2$ in water	$\text{H}_4\text{P}_2\text{O}_7$ in methanol
$\text{Sr}_2\text{P}_2\text{O}_7$	$\text{Sr}(\text{OH})_2$ in water	$\text{H}_4\text{P}_2\text{O}_7$ in methanol
$\text{Mg}_2\text{P}_2\text{O}_7$	$3\text{MgCO}_3 \cdot \text{Mg}(\text{OH})_2 \cdot 3\text{H}_2\text{O}$ in water	$\text{H}_4\text{P}_2\text{O}_7$ in water
$\text{Mn}_2\text{P}_2\text{O}_7$	$\text{MnCO}_3 \cdot n\text{H}_2\text{O}$ in water	$\text{H}_4\text{P}_2\text{O}_7$ in water
ZrP_2O_7	$\text{ZrO}(\text{NO}_3)_2 + \text{HNO}_3$ in water	H_3PO_4 in methanol

or methanol–water mixed solution was added in order to adjust the slurry to a suitable concentration for spraying and to a desirable pyrolysis temperature by the combustion of methanol. The PPI slurry thus obtained was spray-pyrolysed by the method developed in our laboratory for HAP preparation [11]. The spherical powders produced were then heat treated at 800°C for 4 h in air. Only particles of 4–10 μm classified using an air classifier were used as packing materials.

Preparation of comparative hydroxyapatite sample

In order to compare PPI chromatography with HAP chromatography, a spherical HAP packing material was prepared by spray-pyrolysing a slurry with an HAP composition, classifying the powdery product (4–10 μm), and heat treating it at 800°C in air [11,12].

Analysis of products

The crystalline phases of both the spray-pyrolysed powders and the heat-treated powders were identified by X-ray diffraction analysis using $\text{Cu K}\alpha$ radiation with a RAD III instrument (Rigaku, Tokyo, Japan). The crystallinity was evaluated from the broadening of X-ray line profiles. The shape and size of the powders and products were observed with an Alpha 25 scanning electron microscope (SEM) (Akashi, Tokyo, Japan). The specific surface area of the products was measured by the BET method from measurement of the adsorption of nitrogen at liquid nitrogen temperature. The pore size distribution of the products was determined with a Pore Sizer 9310 mercury porosimeter (Micromeritics, Norcross, GA, USA).

Chromatographic procedure

The spherical PPI packing materials and comparative HAP sample were packed in a stainless-steel tube (100 mm \times 8 mm I.D.) under a 100–300 kg/cm^2 pressure using the slurry packing method.

All chromatographic measurements were carried out at room temperature with a system consisting of a model L-5000 LC controller, a Model 655A-11 HPLC pump, a Model 655A-21

variable-wavelength UV detector and a Model D-2500 integrator (Hitachi, Tokyo, Japan).

Samples of proteins, nucleotides and nucleic acids dissolved in 0.001 M sodium phosphate buffer (pH 6.8) were applied to the PPI columns. The bound samples were then eluted with linear gradients starting from 0.001 M sodium phosphate buffer (pH 6.8) at a flow-rate of 1 ml/min. The gradients were $4.83 \cdot 10^{-3}$ M/min for protein elution and $3.25 \cdot 10^{-3}$ M/min for nucleotide and nucleic acid elution. The sample elution was monitored at 280 nm for proteins and at 260 nm for nucleotides and nucleic acids. The column was re-equilibrated by washing for 30 min with the initial buffer.

RESULTS AND DISCUSSION

Properties of pyrophosphates obtained using the spray-pyrolysis method

The droplets produced by spraying a PPI slurry were instantaneously dried and sintered into a spherical and porous material by the heat of combustion of the vaporized methanol. All the spray-pyrolysed materials contained two phases of amorphous and crystalline states. By heat treating these spray-pyrolysed materials at 800°C for 4 h, the completely crystallized products were

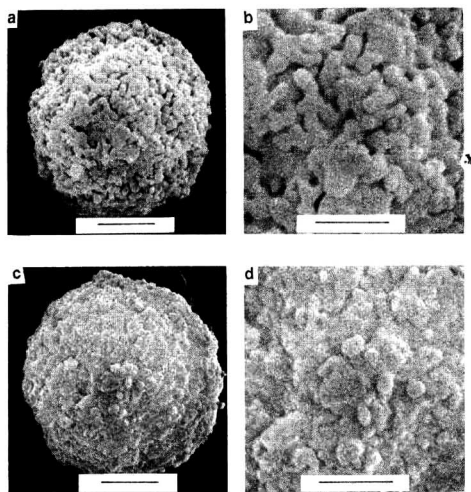


Fig. 1. Scanning electron microphotographs of the appearance and surface texture of the products of (a and b) β -MgPP and (c and d) ZrPP. The bar indicates 2 μ m in (a) and (c) and 1 μ m in (b) and (d).

obtained as β -Mg₂P₂O₇ (β -MgPP), β -Ca₂P₂O₇ (β -CaPP), α -Sr₂P₂O₇ (α -SrPP), Mn₂P₂O₇ (MnPP) and ZrP₂O₇ (ZrPP).

Fig. 1a and c show the appearance of the β -MgPP and ZrPP products. The surface texture of ZrPP (Fig. 1d) consisted of a denser aggregate of fine (0.1–0.4 μ m) primary particles than that of the β -MgPP product (Fig. 1b). The other three PPI products showed an appearance similar to the β -MgPP product.

The data on specific surface area and pore size distribution are summarized in Table II. The ZrPP product had a larger specific surface area and a smaller pore size than those of the other PPI products. The other four PPI products were not very different from each other in these properties.

Chromatography of proteins

Elution behaviour. Table III shows the elution molarities of the tested proteins with isoelectric points (pI) between 4.3 and 11.4, obtained by using the five kinds of PPI columns. The comparative data on the HAP column, obtained under the same chromatographic conditions are given in the last column.

The basic proteins with pI > 7 were retained by and eluted from all the PPI columns. The chromatographic properties of the β -MgPP, β -CaPP and α -SrPP columns were similar to each other and to those of the HAP column. Within the concentration range 0.02–0.19 M, the elution order of the basic proteins was almost the same between the three columns. The properties of the MnPP column were also similar to those of

TABLE II
PROPERTIES OF HEAT-TREATED PYROPHOSPHATE PRODUCTS

Product	Crystal system	Specific surface area (m ² /g)	Pore size distribution (Å)
β -Mg ₂ P ₂ O ₇	Monoclinic	1.3	1500–4000
β -Ca ₂ P ₂ O ₇	Tetragonal	4.6	500–2000
α -Sr ₂ P ₂ O ₇	Orthorhombic	1.8	400–2000
Mn ₂ P ₂ O ₇	Monoclinic	2.3	1000–3000
ZrP ₂ O ₇	Cubic	44.3	50–200

TABLE III
ELUTION OF PROTEINS FROM PYROPHOSPHATES AND HYDROXYAPATITE

For details of measurements, see Experimental.

Protein	pI	Elution molarity (M)					
		β -MgPP (monoclinic)	β -CaPP (tetragonal)	α -SrPP (orthorhombic)	MnPP (monoclinic)	ZrPP (cubic)	HAP (hexagonal)
Trypsin inhibitor	4.3-4.6	N.r. ^a	0.04	0.02	0.02	N.r.	0.04
α -Lactalbumin	4.5	N.r.	0.03	0.02	0.03	N.r.	0.04
Ovalbumin	4.6	N.r.	0.02	0.01	0.02	N.r.	0.02
β -Casein		N.r.	0.18	0.24	>0.8	0.11	0.11
α -Casein		N.r.	0.32	0.30	>0.8	>0.8	0.20
Phosvitin	4.8	N.r.	>0.8	>0.8	>0.8	N.r.	>0.8
Albumin	4.7-4.9	N.r.	0.05	0.04	0.04	N.r.	0.06
β -Lactoglobulin A	5.1	0.15	0.12	0.12	0.24	0.23	0.19
β -Lactoglobulin B	5.2	0.18	0.13	0.14	0.25	0.26	0.20
Holo-transferrin (human)	5.2	N.r.	0.02	0.02	0.06	0.09	0.06
Apo-transferrin (human)	5.5	N.r.	0.02	0.01	0.06	0.09	0.06
Catalase	5.5	0.02	0.06	0.07	0.09	N.r.	0.09
Conalbumin (iron complex)	6.0-6.8	0.08	0.10	0.06	0.11	0.12	0.12
Conalbumin (iron poor)	6.0-6.8	0.06	0.08	0.04	0.11	0.12	0.11
Haemoglobin	6.8-7.0	0.06	0.08	0.05	0.11	0.11	0.09
Myoglobin	8.1-8.2	0.02	0.04	0.02	0.06	0.08	0.08
α -Chymotrypsin	8.1-8.6	0.08	0.11	0.08	0.13	0.22	0.13
Papain	8.8-9.5	0.05	0.07	0.05	0.07	0.10	0.08
α -Chymotrypsinogen A	9.5	0.09	0.12	0.09	0.13	0.21	0.13
Ribonuclease A	9.5-9.6	0.08	0.09	0.06	0.13	0.27	0.11
Cytochrome <i>c</i> (reduced)	10.1	0.15	0.17	0.13		0.43	0.19
Cytochrome <i>c</i> (oxidized)		0.17	0.19	0.14	0.23	0.46	0.21
Lysozyme	11.0-11.4	0.08	0.12	0.08	0.12	0.19	0.12

^aN.r. indicates no retention under the experimental conditions.

the above three PPI columns. However, this column was chemically unstable for repeated use in HPLC. The ZrPP column had a high binding ability for basic proteins, and molarities about twice those of the other PPI columns were required for the elution of proteins with pI > 9.5. For the elution of cytochrome *c*, two peaks due to reduced and oxidized components were resolved by the PPI columns examined, except for the MnPP column.

Acidic proteins, on the other hand, showed various retention behaviours depending on the kind of PPI. The β -CaPP, α -SrPP and MnPP columns could retain most of the tested acidic proteins with pI < 7, and their chromatography was similar to that of HAP. The chromatograms of acidic proteins obtained using the MnPP

column, however, showed an increase in the baseline with a gradient of phosphate concentration, which is probably due to the unstable chemical properties of this column. In contrast, the β -MgPP and ZrPP columns could not retain the acidic proteins with pI < 6 except for a few proteins: the β -MgPP column retained only β -lactoglobulin A and β -lactoglobulin B, whereas the ZrPP column retained transferrins and β -lactoglobulins A and B. β -Lactoglobulins A and B, in spite of their acidic proteins, required elution molarities higher than those for most basic proteins during all PPI chromatography. It is interesting that the β -MgPP and ZrPP columns could not retain phosphoproteins which interact strongly with the HAP matrix because of the presence of the phosphate groups on the mole-

cule [6]. With these properties, one can expect the β -MgPP and ZrPP columns to be applied to the group separation of basic proteins from most acidic proteins.

As Table III reveals, the correlations between the elution molarity and pI among the basic proteins are weak in all instances. The same kind of weak correlations among the acidic proteins can be obtained, except for β -lactoglobulins A and B, with regard to β -CaPP, α -SrPP and MnPP chromatography. Hence it is suggested that PPI chromatography is not very sensitive to the total charge per protein molecule. On the other hand, it appears that the PPI crystals, in addition to HAP, can discriminate among the different structures existing in protein molecules with very similar dimensions, shapes, isoelectric points, etc., although the crystal structure of PPI is different from that of HAP. For example, all the PPI columns separated β -lactoglobulins A and B, which are known to have a slight difference in the primary structure of each protein.

Figs. 2 and 3 illustrate chromatograms of

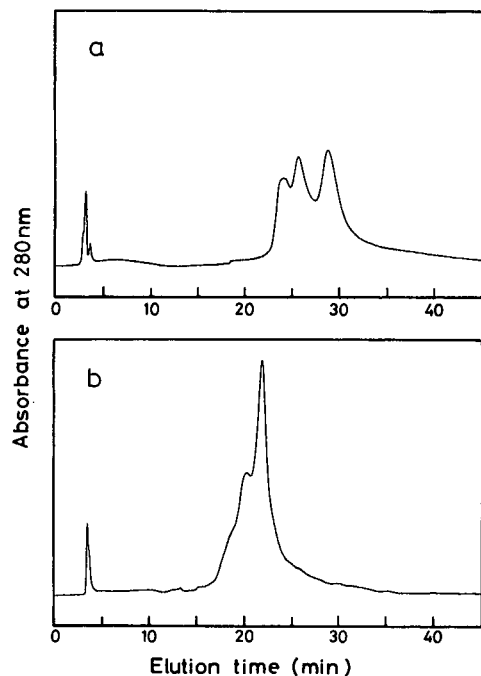


Fig. 2. Chromatograms of haemoglobin obtained using (a) ZrPP and (b) β -CaPP columns. Elution conditions: gradient, $4.83 \cdot 10^{-3}$ M/min from 0.001 to 0.3 M sodium phosphate buffer (pH 6.8); flow-rate, 1 ml/min.

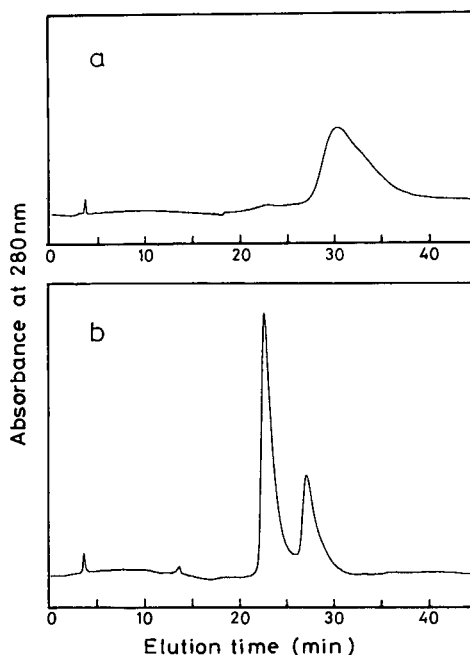


Fig. 3. Chromatograms of conalbumin (iron poor) obtained using (a) ZrPP and (b) β -CaPP columns. Elution conditions as in Fig. 2.

proteins with pI values near 7. For bovine haemoglobin, the ZrPP column gave a good resolution of three peaks (Fig. 2a). The chromatographic resolution obtained using the other PPI columns was inferior to this; Fig. 2b, obtained using the β -CaPP column, is a typical example. For the elution of conalbumin (iron-poor), only one peak was obtained using the ZrPP column (Fig. 3a), whereas two peaks were resolved by the β -CaPP column (Fig. 3b).

Fig. 4 illustrates chromatograms of γ -globulin (bovine) obtained using the PPI columns and a comparative HAP column. It was found that each column gave a characteristic elution profile and different chromatographic resolution among the different components of γ -globulin. For example, the chromatographic resolution obtained using the β -CaPP column (Fig. 4b) is superior to that obtained using the α -SrPP and HAP columns (Fig. 4c and f). During ZrPP chromatography, a different elution profile was obtained consisting of two major sharp peaks (Fig. 4e).

The β -CaPP and α -SrPP columns gave different chromatograms for transferrin (bovine; holo

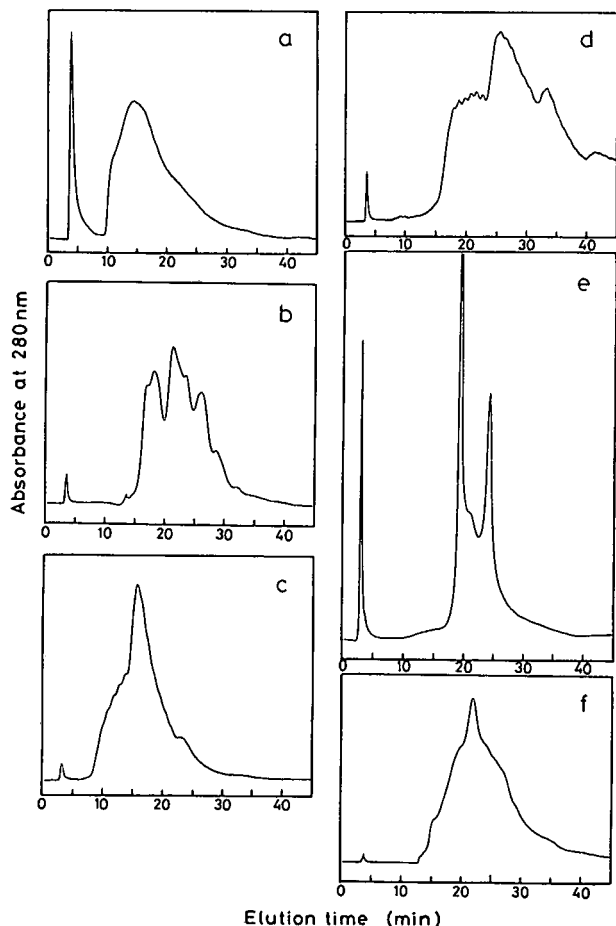


Fig. 4. Chromatograms of γ -globulin (bovine) obtained using (a) β -MgPP, (b) β -CaPP, (c) α -SrPP, (d) MnPP, (e) ZrPP and (f) HAP columns. Elution conditions as in Fig. 2.

type). The chromatogram of transferrin using the β -CaPP column consisted of two major peaks with sharp profiles and some smaller peaks on both sides (Fig. 5a). In contrast, the chromatogram of transferrin using the α -SrPP column showed a broad peak profile overall, which consisted of many different components eluted within the concentration range 0.02–0.12 M (Fig. 5b).

Application to separation of γ -globulin from other serum proteins. A mixture of γ -globulin (human), albumin (human serum), transferrin (human; apo type) and transferrin (human; holo type) was applied to the β -MgPP column. The elution was carried out as described in Fig. 6.

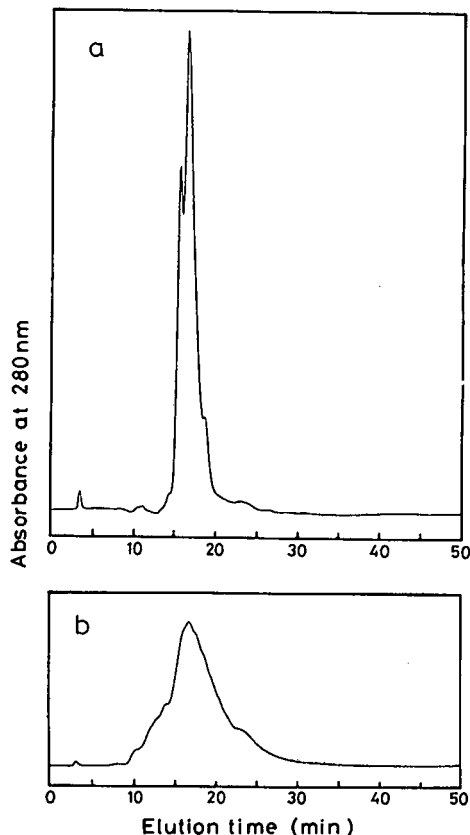


Fig. 5. Chromatograms of transferrin (bovine; holo type) obtained using (a) β -CaPP and (b) α -SrPP columns. Elution conditions as in Fig. 2.

Samples from the peaks thus obtained were identified based on their typical elution molarity and profile by running the single compounds separately. As was expected, the chromatographic separation of γ -globulin from the other serum proteins was achieved (Fig. 6). Albumin and two transferrins were completely eluted with the initial buffer (peak 1), whereas γ -globulin was eluted in the concentration range 0.02–0.19 M (peak 2).

Chromatography of nucleotides and nucleic acids

As Table IV reveals, PPI chromatography of nucleotides (*i.e.*, AMP, ADP and ATP) and nucleic acids (*i.e.*, DNA and tRNA) depended on the kind of PPI column. For example, the retention behaviours of nucleotides and nucleic acids were similar on the β -CaPP, α -SrPP and

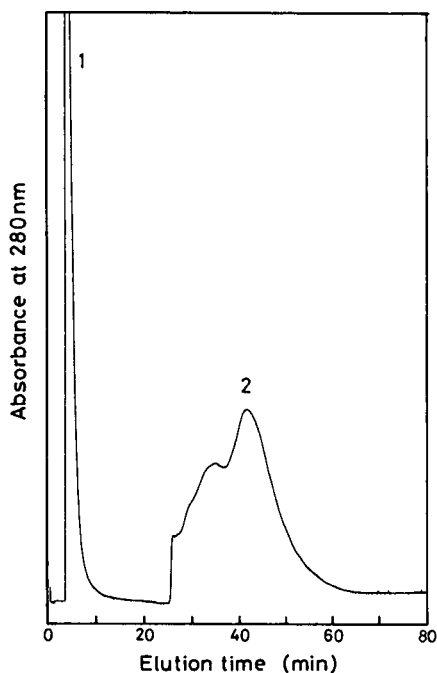


Fig. 6. Separation of a protein mixture containing albumin (human serum), transferrin (human; apo type), transferrin (human; holo type) and γ -globulin (human) using the β -MgPP column. The concentration of sodium phosphate (pH 6.8) was maintained at 0.001 M for 15 min, then a 60-min linear gradient from 0.001 to 0.3 M was started. Peak 1 is due to albumin and two transferrins and peak 2 is due to γ -globulin.

HAP columns. The β -MgPP column could not retain nucleotides but retained nucleic acids, whereas the ZrPP column retained nucleotides but could not retain nucleic acids. However, all chromatograms of the nucleotides obtained using the ZrPP column consisted of a similar profile with two broad peaks and with almost the same retention times between the three nucleotides. Hence it is suggested that the ZrPP crystal cannot discriminate between nucleotides based on the difference in the number of phosphate groups.

DNA retention on the β -MgPP and MnPP columns was stronger than that on the other PPI and HAP columns.

Fig. 7 illustrates the chromatogram of tRNA obtained using the β -CaPP column. Within the main broad peak eluted at about 0.1–0.3 M, good chromatographic resolution was obtained among different components.

From these results, it can be suggested that the difference in crystal structure and component metal ion among the PPI crystals affects the adsorption of nucleotides and nucleic acids: adsorption takes place when the conditions of positively charged adsorbing sites, characterized not only by the geometric arrangement of the metal ion but also by the electrochemical property of the metal ion, are suitable for the adsorp-

TABLE IV

ELUTION OF NUCLEOTIDES AND NUCLEIC ACIDS FROM PYROPHOSPHATES AND HYDROXYAPATITE

For details of measurements, see Experimental.

Sample	Elution molarity (M)					
	β -MgPP (monoclinic)	β -CaPP (tetragonal)	α -SrPP (orthorhombic)	MnPP (monoclinic)	ZrPP (cubic)	HAP (hexagonal)
AMP	N.r. ^a	N.r.	N.r.	N.r.	<0.01	N.r.
ADP	N.r.	<0.01	0.02	0.02	<0.01	0.3
ATP	N.r.	0.05	0.09	0.02	<0.01	0.08
tRNA	0.03–0.11 ^b	0.11–0.31	0.04–0.14	0.01–0.09	N.r.	0.01–0.15
DNA	>0.8	0.13–0.18	0.16–0.24	>0.8	N.r.	0.21–0.29

^a N.r. indicates no retention under the experimental conditions.

^b For nucleic acids with a broad chromatographic profile, the molarity range, not the molarity at the highest peak, is indicated.

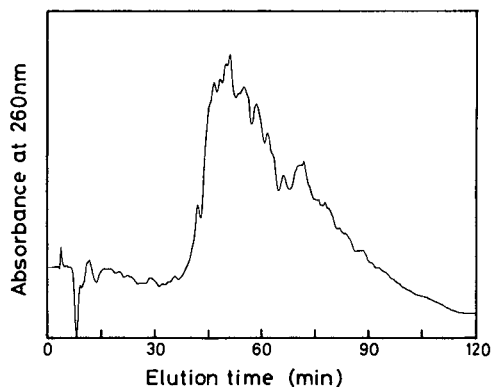


Fig. 7. Chromatogram of tRNA obtained using the β -CaPP column. Elution conditions: gradient, $3.25 \cdot 10^{-3} M/min$ from 0.001 to 0.4 M sodium phosphate buffer (pH 6.8); flow-rate, 1 ml/min.

tion of a molecule with negative phosphate groups.

Influence of surface structure of the PPI crystal

PPI is an inorganic crystal composed of a definite lattice of metal ions and pyrophosphate groups, and its surface presents a complex mosaic of charge depending on the structure of the PPI crystal. Hence the adsorption of molecules such as proteins should depend on the structure of the PPI crystal and the kind of metal ion.

Ca and Sr ions are metal components that can form pure single-cation HAP [*i.e.*, $Ca_{10}(PO_4)_6(OH)_2$ and $Sr_{10}(PO_4)_6(OH)_2$, respectively]. Hence the possibility cannot be excluded that β -CaPP and α -SrPP crystals may be hydrolysed to orthophosphates in a phosphate buffer, followed by further precipitate formation of HAP on their PPI crystal surfaces. If that is the case, then their chromatography should be similar to that on HAP. In fact, the β -CaPP and α -SrPP columns did show elution behaviours similar to that in HAP chromatography with regard not only to basic proteins but also to acidic proteins, nucleotides and nucleic acids.

In contrast, Mg, Mn and Zr ions cannot form pure single-cation HAPs and can only be partially substituted in a parent HAP crystal [13]. Thus, the surfaces of β -MgPP, MnPP and ZrPP would maintain their intrinsic crystal structures under the conditions of this experiment. Their chro-

matographic behaviours should differ from that of HAP, and they should also differ between these three columns. In fact, various elution behaviours of acidic proteins, nucleotides and nucleic acids were obtained, depending on the kind of PPI column, as described in the previous sections. However, with regard to basic proteins, similar chromatographic behaviour between the three columns was obtained, which was also similar to that of HAP.

Moreover, it is interesting that the above-mentioned chromatographic properties of ZrPP are similar to those of zirconium oxide under the condition of the presence of a strong Lewis base such as fluoride or phosphate in the mobile phase [14,15].

A reasonable explanation has not yet been obtained for the different chromatographic effects between PPI crystals with different structures and also between PPI crystals and HAP crystal. It cannot be concluded that PPI crystal surfaces change to the HAP crystal structure by hydrolysis in a buffer merely because the elution behaviour of basic proteins during all PPI chromatography is similar to that of HAP. A possible interpretation of these experimental results might be as follows. The basic proteins are adsorbed by electrostatic interaction. Hence, even though there is a slight discrepancy in geometric arrangement between adsorption groups on the molecule and adsorbing sites on the crystal, a molecule with a flexible structure can be adsorbed on the crystal by slightly modifying the molecular shape. This implies that the PPI crystal does not necessarily need to have the same geometric arrangement of adsorbing sites as the HAP structure. Further, as far as HAP and PPI crystals are concerned, the negatively charged adsorbing sites are always formed by oxygen atoms belonging to the phosphate or pyrophosphate ions. This seems to explain the similar values of the elution molarity for the same basic proteins between the PPI columns and also between the HAP and PPI columns. In contrast, the acidic proteins are considered to be adsorbed in a specific manner by complexation of their adsorption groups to adsorbing sites that are formed by metal ions on the crystal, so that the adsorption is more strongly influenced by the

difference in the geometric arrangement between adsorbing sites and adsorption groups. Moreover, it is likely that the difference in metal ions among the PPI crystals causes the different elution behaviour for the same acidic protein.

In conclusion, it can be expected from the experimental results that these pyrophosphates will provide useful packing materials for specific applications such as the single-step separation of γ -globulin from other serum proteins, which can be achieved using the β -MgPP column. Moreover, β -MgPP and ZrPP crystals seem to be suitable materials for the group separation of basic proteins from acidic proteins or nucleic acids. Except for the MnPP column, the PPI columns prepared by the spray-pyrolysis method in this study were mechanically strong enough to stand as many as 100 chromatographic cycles.

REFERENCES

- 1 M. Spencer and M. Grynopas, *J. Chromatogr.*, 166 (1978) 423.
- 2 H.W. Siegelman and E.F. Firer, *Biochemistry*, 3 (1964) 418.
- 3 D. Keilin and E.F. Hartree, *Proc. R. Soc. London, Ser. B*, 124 (1938) 297.
- 4 M. Koike and M. Hamada, *Methods Enzymol.*, 22 (1971) 339.
- 5 A. Tiselius, S. Hjertén and Ö. Levin, *Arch. Biochem. Biophys.* 65 (1956) 132.
- 6 G. Bernardi and T. Kawasaki, *Biochim. Biophys. Acta*, 160 (1968) 301.
- 7 A. Clearfield and G.D. Smith, *J. Inorg. Nucl. Chem.*, 30 (1968) 327.
- 8 C.B. Amphlett, *Inorganic Ion-Exchangers*, Elsevier, Amsterdam, 1964, pp. 84–136.
- 9 G.C. Schito and A. Pesce, *Giornale di Microbiologia*, 13 (1965) 31.
- 10 G. Fadda, A. Turano and C. Salvadori, *G. Microbiol.*, 16 (1968) 169.
- 11 S. Inoue and A. Ono, *J. Ceram. Soc. Jpn., Int. Ed.*, 95 (1987) 713.
- 12 S. Inoue and N. Ohtaki, *J. Chromatogr.*, 515 (1990) 193.
- 13 D. McConell, *Apatite*, Springer, New York, 1973, pp. 33–37.
- 14 J.A. Blackwell and P.W. Carr, *J. Chromatogr.*, 549 (1991) 59.
- 15 J.A. Blackwell and P.W. Carr, *J. Chromatogr.*, 596 (1992) 27.

Displacement chromatography on cyclodextrin silicas

IV. Separation of the enantiomers of ibuprofen

Gyula Farkas^{*}, Leif H. Irgens^{**}, Gilberto Quintero^{***}, Michelle D. Beeson,
Arif Al-Saeed and Gyula Vigh^{*}

Department of Chemistry, Texas A and M University, College Station, TX 77843-3255 (USA)

(First received February 12th, 1993; revised manuscript received April 28th, 1993)

ABSTRACT

A displacement chromatographic method has been developed for the preparative separation of the enantiomers of ibuprofen using a β -cyclodextrin silica stationary phase. The retention behavior of ibuprofen was studied in detail: the $\log k'$ vs. polar organic modifier concentration, the $\log k'$ vs. pH, the $\log k'$ vs. buffer concentration and the $\log k'$ vs. $1/T$ relationships; also, the α vs. polar organic modifier concentration, the α vs. pH, the α vs. buffer concentration and the $\log \alpha$ vs. $1/T$ relationships have been determined in order to find the carrier solution composition which results in maximum chiral selectivity and sufficient, but not excessive solute retention ($1 < k' < 30$). 4-*tert*-Butylcyclohexanol, a structurally similar but more retained compound than ibuprofen, was selected as displacer for the separation. Even with an α value as small as 1.08, good preparative chiral separations were observed both in the displacement mode and in the overloaded elution mode, up to a sample load of 0.5 mg.

INTRODUCTION

In previous parts of this series [1-3] and a related paper [4], we demonstrated that preparative liquid chromatographic separations of geometrical isomers, positional isomers and enantiomers can be achieved in the displacement mode of operation using columns packed with commercially available β -cyclodextrin silica stationary phase [5,6]. Because these papers and the references cited therein present a detailed review of the characteristics and use of the β -cyclodextrin silica stationary phase and the displacement chromatographic technique, the

reader is referred to them for an introductory discussion. Recent work with the displacement chromatographic separation of chiral compounds led us to a method development scheme which will be discussed in this paper using the non-steroidal anti-inflammatory agent α -methyl-4-[2-methylpropyl]benzeneacetic acid, ibuprofen, as a model substance. The major steps of the method development scheme are (a) selectivity maximization, (b) retention optimization, (c) displacer selection, (d) completion of the displacement chromatographic separation, and (e) evaluation of the purity of the pooled material by fraction analysis.

Because the production rate in preparative chromatography increases dramatically with the value of the selectivity factor, α [7], and because the α values for enantiomer separations on native β -cyclodextrin silica are generally low (1.03 to 1.15) [8], selectivity optimization is the first and the most crucial step of any separation

* Corresponding author.

** Present address: Chinoin Pharmaceutical Company, Budapest, Hungary.

*** Present address: DuPont de Nemours, Belle, WV, USA.

Present address: Tennessee Valley Authority, Chattanooga, TN, USA.

method development scheme. In the reversed-phase mode, chiral separations on cyclodextrin silicas are believed to occur due to the balanced concerted action of inclusion complex formation, hydrogen bond formation, and steric hindrance between the bonded cyclodextrin moiety and the solute [9]. These interactions—and consequently, solute retention and separation selectivity—are influenced by the type and the concentration of the polar organic modifier in the eluent, the type, the concentration and the pH of the buffer, and the temperature of the eluent. Therefore, these parameters have to be investigated in detail in order to select chromatographic conditions which lead to maximized chiral selectivity and appropriate solute retention ($1 < k' < 30$). Then a suitable displacer can be selected based on its relative retention vis-a-vis the more retained ibuprofen enantiomer. This is followed by the completion of the displacement chromatographic run, the collection and the analysis of the enantiomer fractions, and the calculation of the yield and the production rate as a function of the enantiomeric purity of the pooled fraction.

EXPERIMENTAL

The equipment used for these studies was built from commercially available components as described in refs. 1–3. 5- μm β -cyclodextrin silica, Cyclobond I (ASTEC, Whippany, NJ), was slurry-packed into 250 mm \times 4.6 mm I.D. stainless-steel columns (BST, Budapest, Hungary). The column temperature was controlled within $\pm 0.5^\circ\text{C}$ using a water jacket, by a Type UF3 circulating water bath (Science/Electronics, Dayton, OH, USA).

Racemic and *S*(+)-ibuprofen standards were obtained from Aldrich (Milwaukee, WI, USA), along with the displacers and buffer components. HPLC grade methanol, acetonitrile and tetrahydrofuran were purchased from J.T. Baker (Philipsburg, NJ, USA). Aqueous pH standards (pH 4 and 7) were purchased from Fisher Scientific (Fair Lawn, NJ, USA). Water was obtained from a Milli-Q unit (Millipore, Bedford, MA, USA). All chemicals were used as received, without further purification. The carrier and

displacer solutions were freshly prepared using the weighing method described in Part 1 [1].

RESULTS

Retention studies of ibuprofen

Because ibuprofen is a weak acid with $\text{p}K_a = 5.39$ [10], the retention of the ibuprofen enantiomers—and the value of the chiral selectivity factor—are influenced by the type and the concentration of the polar organic modifier, the pH, the buffer concentration, the concentration of the tailing-reducing additive (triethylamine), and the temperature of the eluent. Therefore, the effects of all these factors were individually studied as described below.

Preliminary work indicated that acetonitrile was a good eluent modifier for the analytical separation of the enantiomers of ibuprofen on the native β -cyclodextrin silica stationary phase [3,4,19]. Therefore, acetonitrile was used in the first phase of the selectivity studies and the retention studies. In order to reduce peak tailing, triethylamine (TEA) was added to every eluent, as usual [6]. First, the effects of the acetonitrile concentration were studied in 70 mM citrate–acetonitrile–water eluents. The apparent pH of the eluents was adjusted to 4.0 and 6.0, respectively, by adding a few μl of concentrated sodium hydroxide solution to the hydroorganic eluent and monitoring the pH with a combined glass electrode, standardized against pH 4 and 7 aqueous pH standards [11].

The k' values of (*S*)-(+)–ibuprofen, the more strongly retained enantiomer, are shown as solid lines plotted against the left axis in Fig. 1. The retention behavior of ibuprofen is unexpected: as long as there is more than 20% (v/v) acetonitrile in the eluent, the anionic form of ibuprofen is more retained (in pH 6 eluents) than the free acid form (in pH 4 eluents); the opposite of what is observed on octadecyl silica stationary phases [12] operated in the reversed-phase mode. On octadecyl silicas, weak acids are more retained when the pH of the eluent is below the $\text{p}K_a$ value of the solute (*i.e.*, the acids are not dissociated). However, extrapolation of the k' vs. acetonitrile concentration curves to zero

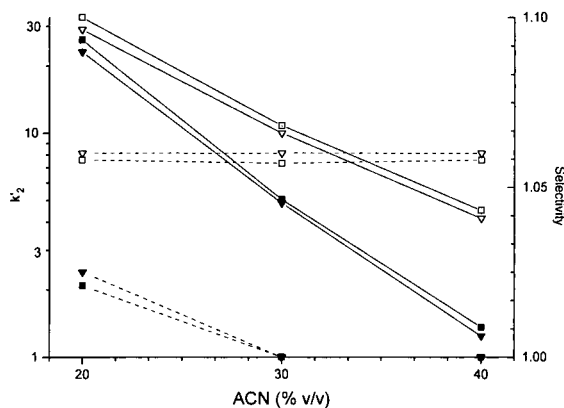


Fig. 1. The capacity factor of (*S*)-(+)-ibuprofen (solid lines plotted against the left axis) and the chiral selectivity factor for the separation of the (*S*)-(+)- and (*R*)-(-)-enantiomers of ibuprofen (dotted lines plotted against the right axis) as a function of the acetonitrile concentration (% v/v), TEA concentration (mM), and pH of the eluent. Total citrate concentration: 70 mM. Full symbols = pH 4, open symbols = pH 6, ∇ = 0 mM TEA, \square = 30 mM TEA. Column temperature: 30°C, eluent flow rate: 1 ml/min.

acetonitrile concentration shows that the neutral form of the weak acid solute is more retained than its dissociated form, in agreement with our previous findings in HPLC [13] and capillary electrophoresis [14]. The slope of the $\log k'$ vs. % (v/v) acetonitrile curve is lower at pH 6 than at pH 4, indicating that the intermolecular interactions between the anion and the β -cyclodextrin are weakened by the polar organic modifier to a lesser degree than those which exist between the non-dissociated weak acid and the β -cyclodextrin. Therefore, ibuprofen separations which utilize a higher pH eluent are more rugged and less sensitive to slight variations in the concentration of the polar organic modifier of the eluent than those which use a low pH eluent. This behavior is clearly an asset for preparative separations.

The chiral selectivity (α) values which were observed for the ibuprofen enantiomers are shown as dotted lines plotted against the right axis of Fig. 1. At pH 6, the chiral selectivity values are much higher than at pH 4, and they do not vary with the acetonitrile concentration in the range tested, as they do at pH 4. This behavior permits the control of solute retention

over a broad range of k' , without a concomitant loss of chiral selectivity, by changing the acetonitrile concentration of the eluent.

Triethylamine (TEA) is a widely used masking agent in β -cyclodextrin silica-based separations [6,15,16,19]. Therefore, the influence of the TEA concentration on the separation of ibuprofen enantiomers was studied as well. Increasing amounts of TEA were added to the 70 mM citrate–acetonitrile–water eluents to produce 5, 10 and 30 mM TEA concentrations. The final pH of the eluents was adjusted by adding a few μ l of a concentrated sodium hydroxide solution, as before. It can be seen in Fig. 1 that as the TEA concentration is increased from 0 mM (triangle symbols) to 30 mM (square symbols), the k' values of the solutes, whether almost neutral (ibuprofen at pH 4), or anionic (ibuprofen at pH 6), remain more or less unchanged, both at high and low pH values, and in both the acetonitrile rich and the acetonitrile poor eluents. However, the peak shape improves as the TEA concentration is increased from 0 through 5 mM to 10 mM. No further improvement is seen when the concentration is raised to 30 mM. Selectivity remains the same, both at low pH and at high pH, as the TEA concentration is changed from 0 mM (triangle symbols) to 30 mM (square symbols). However, as discussed above, peak shape is better when the TEA concentration of the eluent is 10 mM or higher. Therefore, unless stated otherwise, the eluents always contained 10 mM TEA in the rest of the experiments.

In order to investigate briefly the effects of the type of buffer anion on the selectivity, citrate was replaced with acetate. The shape of the α vs. % (v/v) acetonitrile concentration curve obtained was similar to the one in Fig. 1 [4]. However, the pH of the eluent had to be increased to pH 6.8 to obtain selectivities comparable to those shown in Fig. 1. As neither the buffer capacity of the eluent nor the long-term stability of the column are as good at this higher pH with acetate as the buffer anion as at pH 6 with citrate as the buffer anion, all further studies were carried out with the citrate buffer.

The observations summarized in Fig. 1 for the weakly acidic ibuprofen solute are very impor-

tant, because they indicate that (i) when the eluent pH is sufficiently higher than the pK_a value of the chiral weak acid (e.g. one or more pH units), k' can be varied over almost two orders of magnitude, without sacrificing the chiral selectivity of the system, by simply varying the concentration of the organic modifier, and (ii) higher α values can be achieved at the higher pH values where the solubilities (a prime consideration in preparative separations) of the weak acids are higher due to their ionic nature.

Because ibuprofen is mostly anionic at pH 6, it could be expected that solute retention, and perhaps chiral selectivity, would be influenced by the concentration of the buffer anion. Therefore, the analytical citrate concentration was systematically varied using 30% (v/v) acetonitrile: water eluents, while the apparent pH was maintained at 6.0. The $\log k'$ values of the more retained enantiomer, (*S*)-(+) -ibuprofen (solid line), are plotted on the left axis in Fig. 2, as a function of the logarithm of the analytical citrate concentration.

Over the range studied, the retention of non-charged solutes, e.g. that of the 4-*tert*-butylphenol increases very slightly (results not shown), reminiscent of a weak salting-out effect in ordinary reversed-phase HPLC [17], but that

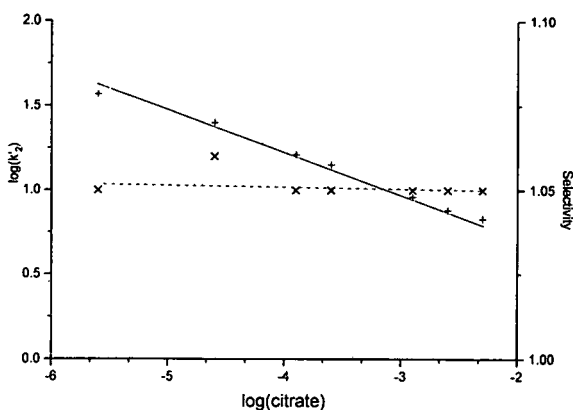


Fig. 2. The capacity factor of (*S*)-(+) -ibuprofen (solid line plotted against the left axis) and the chiral selectivity factor for the separation of the (*S*)-(+) - and (*R*)-(-) -enantiomers of ibuprofen (dotted line plotted against the right axis) as a function of the analytical citrate concentration (M) of the eluent. Eluent: 30 % (v/v) acetonitrile, 10 mM TEA, pH 6. Symbols: + = k' of (*S*)-(+) -ibuprofen, x = α values. Other conditions as in Fig. 1.

of the anionic ibuprofen decreases by almost an order of magnitude as the citrate concentration is varied from 0.5 mM to 10 mM. Chiral selectivity (dotted line), plotted on the right axis in Fig. 2, on the other hand, does not decrease with the citrate concentration. Thus, the concentration of the buffer anion is a powerful variable for the control of the separation of anionic chiral solutes: it can be used to greatly vary solute retention without compromising chiral selectivity.

It could be expected that on native β -cyclodextrin silicas—as in ordinary reversed-phase chromatography—the type and the concentration of the polar organic modifier in the eluent would also influence solute retention and chiral selectivity. Therefore, a series of common water-miscible organic solvents were tested as eluent components [19]. The concentration ranges studied were selected such that the k' values for the more retained (*S*)-(+) -ibuprofen enantiomer fell between 1 and 30. Once again, the observed k' and α values are plotted against the left and right axes of Fig. 3, respectively.

It can be seen in Fig. 3 that the elution strengths of the various organic solvents parallel their usual reversed-phase behavior: the slopes of the $\log k'$ vs. % (v/v) modifier concentration

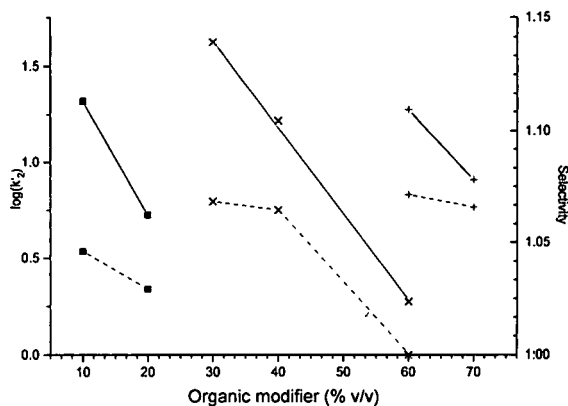


Fig. 3. The capacity factor of (*S*)-(+) -ibuprofen (solid lines plotted against the left axis) and the chiral selectivity factor for the separation of the (*S*)-(+) - and (*R*)-(-) -enantiomers of ibuprofen (dotted lines plotted against the right axis) as a function of the organic modifier concentration (% v/v) of the eluent. Total citrate concentration: 5 mM, TEA concentration 5 mM, pH 6.8, temperature: 25°C. Symbols: + = methanol, x = acetonitrile, ■ = tetrahydrofuran.

lines of the various solvents are similar, indicating that similar retention can be achieved with any of these solvents when used at the appropriate concentration. However, the selectivity plot in Fig. 3 shows that chiral resolution strongly varies with the concentration of the different organic modifiers; selectivity is improved and a limiting maximum value is approached as the water concentration of the eluent is increased. The more hydrophobic the polar organic solvent, the lower its concentration must be in order to secure the limiting α value. Therefore, the behavior shown in Fig. 3 allows one to consider other solvent-related factors as well, such as the solubility of the analyte in the chosen polar modifier, the volatility of the modifier, its purity, price, etc., in selecting the type of the organic modifier to be used for a given preparative chiral separation.

Finally, the effects of the eluent temperature on both solute retention and chiral selectivity were investigated. The $\log k'$ vs. $1/T$ and the $\log \alpha$ vs. $1/T$ curves are plotted against the left and right axes in Fig. 4, respectively. There is a significant increase in the k values (approximately half an order of magnitude) and in the chiral selectivity (approximately 0.07 α units) as the column temperature is decreased from 37°C to 0°C.

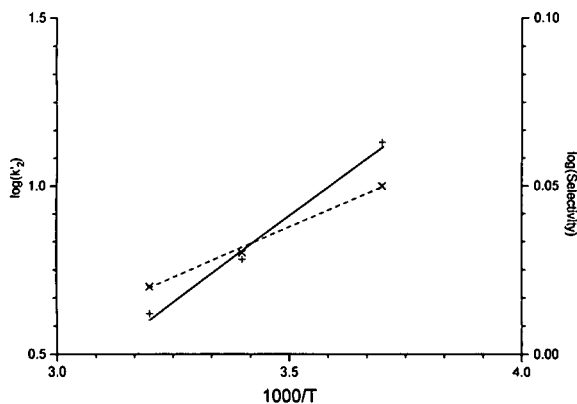


Fig. 4. The capacity factor of (S)-(+)-ibuprofen (solid line plotted against the left axis) and the chiral selectivity factor for the separation of the (S)-(+)- and (R)-(-)-enantiomers of ibuprofen (dotted line plotted against the right axis) as a function of the inverse absolute temperature of the eluent. Conditions as in Fig. 2. Symbols: + = k' of (S)-(+)-ibuprofen, x = α values.

It can be concluded from the retention studies that there are two types of eluent parameters which can be changed to optimize the separation of weak acid chiral solutes on native β -cyclodextrin silica columns. The first type of parameter (the organic modifier and its concentration, the pH and the temperature of the eluent) will change both the k' and the α values; the second type of parameter (the buffer concentration of the eluent) will only change k' , without compromising the value of α . Therefore, one can, and should, maximize the value of α using the eluent parameters which belong to the first group, then adjust the retention of the solute to the desired level using the parameters which belong to the second group. These observations can also be utilized for the selection of the displacer; after maximizing chiral selectivity for the weak acid solute, its retention can be decreased by increasing the buffer concentration to a value that is lower than the capacity factor of an otherwise suitable non-charged displacer.

Preparative chromatographic separation of the ibuprofen enantiomers in the overloaded elution mode and in the displacement mode of operation

The retention and the selectivity studies discussed above allowed us to select separation conditions which represent a reasonable compromise between separation selectivity, the length of time required to complete the separation and the achievable yield and production rate values. The carrier solution selected contained 10 mM TEA, 10 mM citrate and 35% (v/v) acetonitrile in a pH 6.5 solution. The separations were completed at 4°C, at a flow-rate of 0.2 ml/min, using two Cyclobond-I columns connected in series (2 \times 250 mm \times 4.6 mm I.D.), yielding a chiral selectivity, α value of 1.08. Because it was known from previous studies [4,19] that 4-*tert*-butylcyclohexanol has favorable retention and adsorption characteristics on the Cyclobond I column, it was selected as a possible non-charged displacer for the separation of the ibuprofen enantiomers.

Several displacement mode and overloaded elution mode separations were completed by doubling the ibuprofen sample load from 62.5

μg /injection upwards, until the amount of the (*R*)-(–)ibuprofen enantiomer (at 95% enantiomeric purity) produced in the separation began to decrease. As discussed in [4], the concentration of the 4-*tert*-butylcyclohexanol displacer was kept at 2 mM for all of these separations; this concentration falls onto the strongly non-linear region of the Langmuirian adsorption isotherm. Fractions measuring 20 to 90 μl were collected throughout the separations and analyzed for enantiomeric purity using another Cyclobond-I column.

The reconstructed displacement chromatogram of the last sample where production still improved with the load (a nominal 500- μg sample) is shown in Fig. 5. With the 2 mM 4-*tert*-butylcyclohexanol displacer, the bands of the two enantiomers reach the 0.4 mM (for the (*R*)-(–)-enantiomer) and the 0.6 mM (for the (*S*)-(+) -enantiomer) concentration levels. The reconstructed chromatogram for the overloaded elution mode separation of a similar sample—obtained under the same conditions as the displacement chromatogram—is shown in Fig. 6 (nominal 500- μg sample). The peak concentrations of the enantiomers are much lower than in the displacement mode: 0.24 mM and 0.14 mM,

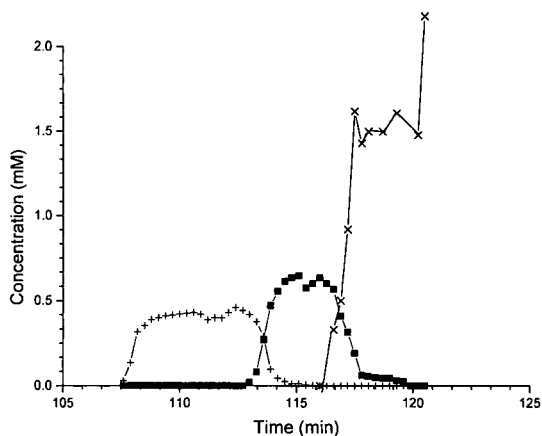


Fig. 5. The reconstructed displacement chromatogram of a nominal 500 μg ibuprofen sample using two Cyclobond I columns, connected in series. The displacer is a 2 mM solution of 4-*tert*-butylcyclohexanol, which is dissolved in a carrier solution of 10 mM TEA, 10 mM citrate, 35 % (v/v) acetonitrile, pH 6.5, 4°C, 0.2 ml/min. Symbols: + = (*R*)-(–)-ibuprofen, ■ = (*S*)-(+) -ibuprofen, × = 4-*tert*-butylcyclohexanol displacer.

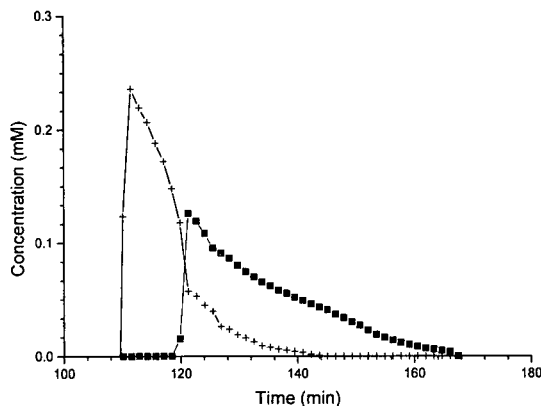


Fig. 6. The reconstructed overloaded elution mode chromatogram of a nominal 500 μg ibuprofen sample using two Cyclobond I columns connected in series. The eluent is the same as the carrier solution in the displacement mode separation (10 mM TEA, 10 mM citrate, 35 % (v/v) acetonitrile, pH 6.5, 4°C, 0.2 ml/min). Symbols: + = (*R*)-(–)-ibuprofen, ■ = (*S*)-(+) -ibuprofen.

respectively. There is a strong decrease in the concentration of the less retained enantiomer as soon as the elution of the more retained enantiomer begins, in agreement with the predictions of the ideal model of overloaded elution mode chromatography [18].

The reconstructed displacement chromatogram permits the calculation of the enantiomer productions (mg) and the % recoveries as a function of the % enantiomeric purity of the

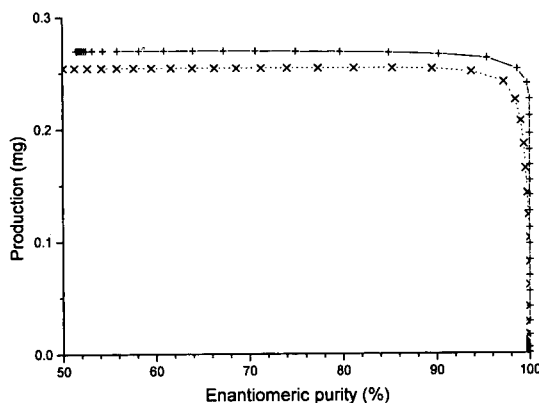


Fig. 7. Production (mg) of the (*R*)-(–)- and the (*S*)-(+) -ibuprofen enantiomers as a function of the % enantiomeric purity of the pooled fractions obtained from the displacement chromatographic separation. Conditions as in Fig. 5. Symbols: + = (*R*)-(–)-enantiomer, × = (*S*)-(+) -enantiomer.

collected fractions. The productions are shown in Fig. 7 for the less retained enantiomer (solid line) and the more retained enantiomer (dotted line), respectively. The % recoveries are shown in Fig. 8, again for the less retained enantiomer (solid line) and the more retained enantiomer (dotted line), respectively. Since the purpose of this separation is chiral resolution, the enantiomeric purities rather than the chemical purities are used in the figures. For the less retained enantiomer, the enantiomeric purity and the chemical purity are identical. For the more retained enantiomer, the chemical purity is less than the enantiomeric purity, because the tail-end of the band of the more retained enantiomer is contaminated by the displacer. However, because the 4-*tert.*-butylcyclohexanol displacer is non-ionic, its traces can be easily removed from the anionic second enantiomer by an additional ion exchange step.

For the corresponding overloaded elution mode separation the calculated enantiomer productions (mg) and % recoveries are shown in Figs. 9 and 10, respectively, for the less retained enantiomer (solid line) and the more retained enantiomer (dotted line).

It can be seen from Fig. 7 that in the displacement mode a little more material can be produced at the 95% enantiomeric purity level from the less retained enantiomer (0.27 mg), than

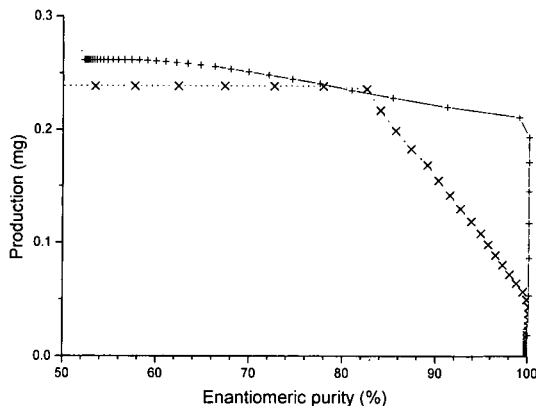


Fig. 9. Production (mg) of the (R)-(-) and the (S)-(+)-ibuprofen enantiomers as a function of the % enantiomeric purity of the pooled fractions obtained from the overloaded elution mode separation. Conditions as in Fig. 6. Symbols: + = (R)-(-)-enantiomer, x = (S)-(+)-enantiomer.

from the more retained enantiomer (0.25 mg). This difference in production is more pronounced in the overloaded elution mode: 0.22 mg can be produced from the less retained enantiomer (solid line), 0.10 mg from the more retained enantiomer (dotted line in Fig. 9). This means that while under the given conditions both the displacement mode and the overloaded elution mode separations yield quite commensurable amounts of pure material for the first enantiomer, the overloaded elution mode yields less of the second enantiomer than does the

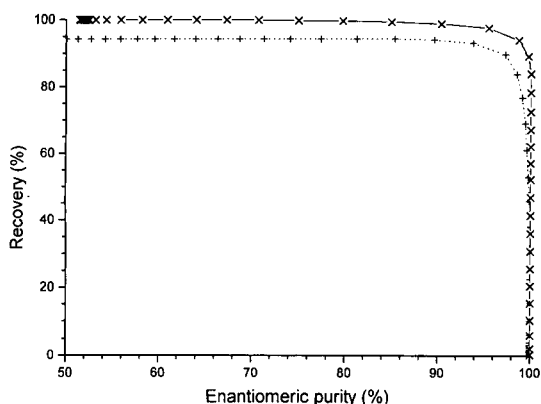


Fig. 8. Recovery (%) of the (R)-(-) and the (S)-(+)-ibuprofen enantiomers as a function of the % enantiomeric purity of the pooled fractions obtained from the displacement chromatographic separations. Conditions as in Fig. 5. Symbols: x = (R)-(-)-enantiomer, + = (S)-(+)-enantiomer.

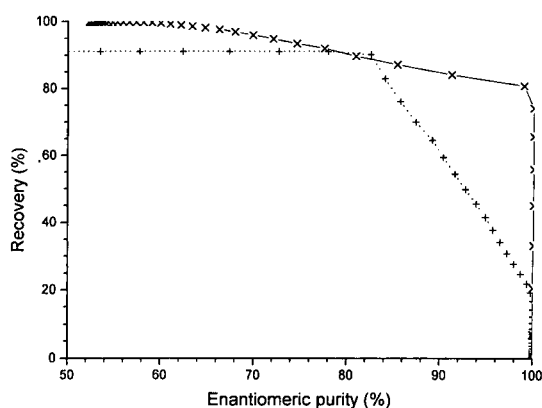


Fig. 10. Recovery (%) of the (R)-(-) and (S)-(+)-ibuprofen enantiomers as a function of the % enantiomeric purity of the pooled fractions obtained from the overloaded elution mode separation. Conditions as in Fig. 6. Symbols: x = (R)-(-)-enantiomer, + = (S)-(+)-enantiomer.

displacement mode. These observations are fully supported by the % recovery vs. enantiomeric purity curves (Figs. 8 and 10): at the 95% enantiomeric purity level less material is recovered in the elution mode than in the displacement mode, but the difference is more pronounced for the more retained enantiomer than for the less retained enantiomer. When it comes to production rates, under the given conditions, the displacement mode fares worse in the case of the less retained enantiomer (due to column regeneration time), but the two techniques have more comparable production rates for the second enantiomer (due to low recovery in the overloaded elution mode).

CONCLUSIONS

A displacement chromatographic method has been developed for the separation of the enantiomers of ibuprofen by a native β -cyclodextrin silica stationary phase on the basis of independent selectivity maximization and retention control. The $\log k'$ vs. polar organic modifier concentration, the $\log k'$ vs. pH, the $\log k'$ vs. buffer concentration and the $\log k'$ vs. $1/T$ relationships have been determined, along with the α vs. polar organic modifier concentration, the α vs. pH, the α vs. buffer concentration and the $\log \alpha$ vs. $1/T$ relationships in order to select the carrier solution composition which results in maximum chiral selectivity and sufficient, but not excessive retention for the less retained enantiomer ($1 < k' < 30$). 4-*tert.*-Butylcyclohexanol, which is a non-charged substance with a structure similar to that of the analyte, is more retained than the more strongly adsorbed enantiomer of ibuprofen, and has a suitable, Langmuirian adsorption isotherm [4,19], could be used as displacer for the separation. A comparison of the productions (mg) and % recoveries as a function of the % enantiomeric purity of the pooled fractions indicates that under the given conditions the displacement mode and the overloaded elution mode separations perform quite comparably for the less retained enantiomer, but the displacement mode performs better for the more retained enantiomer.

ACKNOWLEDGEMENTS

Partial financial support by the National Science Foundation (CHE-8919151), the Texas Coordination Board of Higher Education TATR Program (Grant Number 3376), the Minority Access for Research Careers, National Institute of Health Program (Grant Number 5F31GM11689), and the Dow Chemical Company is gratefully acknowledged. The authors are indebted to ASTEC for the beta-cyclodextrin silica stationary phase used in this study.

REFERENCES

- 1 Gy. Vigh, G. Quintero and Gy. Farkas, *J. Chromatogr.*, 484 (1989) 237.
- 2 Gy. Vigh, G. Quintero and Gy. Farkas, *J. Chromatogr.*, 484 (1989) 251.
- 3 Gy. Vigh, G. Quintero and Gy. Farkas, *J. Chromatogr.*, 506 (1990) 481.
- 4 Gy. Vigh, G. Quintero and Gy. Farkas, in J. Nikelly and Cs. Horváth (Editors), *Analytical Biotechnology (ACS Symposium Series, Vol. 434)*, American Chemical Society, Washington, D.C., 1990, pp. 181-197.
- 5 D.W. Armstrong, *U.S. Patent*, 4,539,399 (1985).
- 6 *Cyclobond Handbook*, Astec, Whippany, N.J., 1990.
- 7 A. Felinger and G. Guiochon, *J. Chromatogr.*, 591 (1992) 31.
- 8 D.W. Armstrong, *Anal. Chem.*, 59 (1987) 84A.
- 9 D.W. Armstrong and W. DeMond, *J. Chromatogr. Sci.*, 22 (1984) 411.
- 10 C.D. Herzfeldt and R. Kummel, *Drug Development and Industrial Pharmacy*, 9 (1983) 767.
- 11 R.G. Bates, *Determination of pH. Theory and Practice*. Wiley-Interscience, New York, 1973.
- 12 L.R. Snyder, J.L. Glajch and J.J. Kirkland, *Practical HPLC Method Development*, Wiley, N.Y., 1988.
- 13 M.D. Beeson and Gy. Vigh, *J. Chromatogr.*, 634 (1993) 197.
- 14 Y. Rawjee, D.U. Staerk and Gy. Vigh, *J. Chromatogr.*, 635 (1993) 291.
- 15 D.W. Armstrong, W. DeMond and B.P. Czech, *Anal. Chem.*, 57 (1985) 481.
- 16 D.W. Armstrong, X. Yang, S.M. Han and R.A. Menges, *Anal. Chem.*, 59 (1987) 2594.
- 17 B.L. Karger, J.N. LePage and N. Tanaka, in Cs. Horváth (Editor), *High-Performance Liquid Chromatography. Advances and Perspectives*, Vol. 1, Academic Press, New York, 1980, p. 113.
- 18 S. Golshan-Shirazi and G. Guiochon, *Anal. Chem.*, 61 (1989) 1368.
- 19 L.H. Irgens, *Ph.D. Thesis*, Texas A and M University, College Station, TX, 1991.

Fluorescence derivatization reagent for resolution of carboxylic acid enantiomers by high-performance liquid chromatography

Junichi Kondo*, Toshi Imaoka, Takao Kawasaki, Akio Nakanishi and Yukinori Kawahara

Product Development Laboratories, Sankyo Co. Ltd., 2-58 Hiromachi 1-chome, Shinagawa-ku, Tokyo 140 (Japan)

(First received December 30th, 1992; revised manuscript received April 20th, 1993)

ABSTRACT

A novel chiral fluorescence derivatization reagent, (–)-2-[4-(1-aminoethyl)phenyl]-6-methoxybenzoxazole (APMB), was synthesized from 4-(6-methoxy-2-benzoxazolyl)acetophenone in several steps. Enantiomeric carboxylic acids were readily condensed with the chiral reagent in the presence of 2,2'-dipyridyl disulphide and triphenylphosphine. The diastereomeric amides formed were separated on a normal- and a reversed-phase column and were sensitively detected fluorimetrically, at 375 nm with excitation at 320 nm in normal-phase chromatography and at 380 nm with excitation at 320 nm in reversed-phase chromatography. The detection limit of (–)-APMB derivative of 2-phenylpropionic acid was 10 fmol at a signal-to-noise ratio of 3.

INTRODUCTION

The stereoisomers of racemic drugs are often readily distinguished by biological systems, and may have different pharmacokinetic properties and different pharmacological or toxicological effects. The development of racemic drugs raises issues of acceptable manufacturing control of synthesis and impurities, adequate pharmacological and toxicological assessment, proper characterization of metabolism and distribution and appropriate clinical evaluation. Therefore, stereospecific analysis becomes a key technique in chiral drug development.

High-performance liquid chromatography (HPLC) has been most widely used for chiral separations. A chiral separation can be performed in either a direct mode, using chiral stationary phases or chiral mobile phases, or an

indirect mode, using a chiral derivatization reagent [1]. A chiral derivatization reagent that has an appropriate chromophore or fluorophore is a useful tool for trace analysis of biological specimens with respect to selectivity, sensitivity and versatility. Therefore, many chiral derivatization reagents have been developed for the resolution of enantiomeric drugs by HPLC [2–22].

This paper deals with the synthesis of (–)-2-[4-(1-aminoethyl)phenyl]-6-methoxybenzoxazole (APMB) as a novel chiral derivatization reagent and its applicability to the resolution of enantiomeric carboxylic acids, which include non-steroidal anti-inflammatory drugs (NSAIDs), by HPLC.

EXPERIMENTAL

Materials and chemicals

All chemicals for synthesis were of guaranteed-reagent grade and all organic solvents for chromatographic purposes were of special grade

* Corresponding author.

for HPLC, obtained from Wako (Osaka, Japan). 4-Isobutyl- α -methylphenylacetic acid (ibuprofen) and 6-methoxy- α -methyl-2-naphthaleneacetic acid (naproxen) were purchased from Funakoshi (Tokyo, Japan), 2-phenylpropionic acid from Norse Laboratories (Newburyport, CA, USA) and 2-fluoro- α -methyl-4-biphenylacetic acid (flurbiprofen) from Sigma (St. Louis, MO, USA). Water was purified with a Milli-Q water purification unit (Millipore, Bedford, MA, USA).

Instruments

A Hitachi (Tokyo, Japan) Model 650-40 spectrofluorimeter was used for the measurement of fluorescence spectra. The HPLC system consisted of a Shimadzu (Kyoto, Japan) Model LC-5A HPLC pump equipped with a Reodyne (Cotati, CA, USA) Model 7125 sample injector and a Shimadzu Model RF-550 fluorescence HPLC monitor; the system was linked to a Shimadzu Model C-R6A chromatographic integrator.

Synthesis of chiral derivatization reagent

The following methods were used for analysis of the synthetic products. Proton nuclear magnetic resonance (^1H NMR) spectra were measured using a Model JNM-GSX400 spectrometer (JEOL, Tokyo, Japan) at 400 MHz, chemical shift values being expressed in ppm downfield from tetramethylsilane as an internal standard. A Perkin-Elmer (Norwalk, CT, USA) Model 1750 infrared spectrometer was used for infrared spectral measurements. Mass spectra were measured with a Model DX-300 mass spectrometer (JEOL) in the electron impact mode.

2-[4-(1-Hydroxyiminoethyl)phenyl]-6-methoxybenzoxazole (2). To a solution of 4-(6-methoxy-2-benzoxazolyl) acetophenone (**1**) (10.1 g), which was prepared by condensation of ethyl 4-acetylbenzimidate hydrochloride and 2-amino-5-methoxyphenol [21], in 95% ethanol (500 ml), was added hydroxylamine hydrochloride (7.0 g) and sodium acetate (8.2 g). The mixture was refluxed for 1 h, then poured into ice-water. The resulting precipitate was filtered and recrystal-

lized from 90% ethanol to give faint reddish needles of **2**; 6.3 g, yield 57%, m.p. 212°C. Elemental analysis: calculated for $\text{C}_{16}\text{H}_{14}\text{N}_2\text{O}_3$, C 68.08, H 5.00, N 9.92; found, C 68.16, H 5.20, N 9.94%. ^1H NMR ($[\text{D}_6\text{H}_6]$ dimethyl sulphoxide; DMSO- d_6), ppm: 2.21 (3H, s, CH_3), 3.86 (3H, s, OCH_3), 7.02 (1H, dd, $J=2.4, 8.8$ Hz, benzoxazole-5H), 7.42 (1H, d, $J=2.4$ Hz, benzoxazole-7), 7.69 (1H, d, $J=8.8$ Hz, benzoxazole-4), 7.88 and 8.14 (each 2H, each d, $J=8.5$ Hz, phenyl), 11.48 (1H, s, oxime-OH). Mass spectrum: m/z 282 (M^+ , base peak). IR (KBr): 1638, 1609, 1489, 1411, 1323, 1143, 1113, 998, 925 cm^{-1} .

(\pm)-2-[4-(1-Aminoethyl)phenyl]-6-methoxybenzoxazole (3a). To a solution of **2** (4.7 g) in methanol (300 ml) was added 10% Pd-C (3.0 g) and ammonium formate (10.5 g) [23] and the mixture was refluxed for 30 min. After the removal of Pd-C by filtration, the resulting solution was evaporated *in vacuo*. The residue was dissolved in 5% HCl (100 ml) and washed with ethyl acetate (100 ml). The pH of the aqueous layer was adjusted to 13–14 with 10% NaOH. Ethyl acetate (200 ml) was added to the alkaline solution to extract the amine. The ethyl acetate layer was then washed with water (100 ml), dried over anhydrous sodium sulphate and evaporated *in vacuo* to give racemic APMB (**3a**), 3.6 g.

(-)-2-[4-(1-Aminoethyl)phenyl]-6-methoxybenzoxazole (3b). To a solution of **3a** (3.6 g) in ethanol (50 ml) was added (*S*)-(-)- α -methoxy- α -trifluoromethylphenylacetic acid (3.5 g) and the mixture was allowed to stand overnight at 5°C. The resulting precipitate was collected by filtration and fractionally crystallized from ethanol four times. The free amine that dissociated with 5% NaOH was extracted with ethyl acetate. The organic layer was washed with water, dried over anhydrous sodium sulphate and evaporated *in vacuo*. Recrystallization of the crude product from ethanol gave faint pale yellow crystals of **3b**; 0.5 g, yield 14%, m.p. 74°C. Elemental analysis: calculated for $\text{C}_{16}\text{H}_{16}\text{N}_2\text{O}_2$, C 71.62, H 6.01, N 10.44; found, C 70.91, H 5.85, N 10.34%. ^1H NMR (DMSO- d_6), ppm: 1.33 (3H, d, $J=6.6$ Hz, CH_3), 3.32 (2H, bs, NH_2), 3.85 (3H, s, OCH_3), 4.08 (1H, q, $J=6.6$ Hz,

CHCH₃), 7.00 (1H, dd, $J=2.2$, 8.7 Hz, benzoxazole-5), 7.41 (1H, d, $J=2.2$ Hz, benzoxazole-7), 7.59 (2H, d, $J=8.2$ Hz, phenyl), 7.66 (1H, d, $J=8.7$ Hz, benzoxazole-4), 8.07 (2H, d, $J=8.2$ Hz, phenyl). Mass spectrum: m/z 268 (M^+), 253 (base peak). IR (KBr): 3436, 1619, 1488, 1319, 1145, 837, 815 cm^{-1} . $[\alpha]_D = -14.2^\circ$ ($c=1.0$, methanol). The optical purity of (-)-APMB was checked on a TSK gel Enantio P1 chiral stationary phase column (Tosoh, Tokyo, Japan) with *n*-hexane–1,2-dichloroethane–2-propanol (6:3:1, v/v/v) as the mobile phase, after derivatization with 3,5-dinitrobenzoyl chloride.

Preparation of (S)-(+)-2-phenylpropionic acid derivative as fluorescence reference

The authentic (-)-APMB derivative of (S)-(+)-2-phenylpropionic acid was synthesized on a preparative scale in order to evaluate its reactivity and fluorescence properties. To a solution of (S)-(+)-phenylpropionic acid (0.4 mmol) and 2,2'-dipyridyl disulphide (0.4 mmol) in 20 ml of dichloromethane were added (-)-APMB (0.4 mmol) and triphenylphosphine (0.4 mmol). The resulting solution was allowed to stand at room temperature for 1 h, followed by washing with 5% HCl, 5% NaHCO₃ and water. After drying with anhydrous sodium sulphate, the resulting solution was evaporated *in vacuo*. The residue was purified on a silica gel column with *n*-hexane–ethyl acetate (1:1, v/v) as eluent. The main fraction was evaporated *in vacuo* to give the product; 0.11 g, yield 69%, m.p. 179°C. Elemental analysis: calculated for C₂₅H₂₄N₂O₃, C 74.98, H 6.04, N 7.00; found, C 74.92, H 6.32, N 6.97%. ¹H NMR (C²HCl₃), ppm: 1.42 (3H, d, $J=7.1$ Hz, CH₃), 1.52 (3H, d, $J=6.9$ Hz, CH₃), 3.60 (1H, q, $J=7.1$ Hz, COCHCH₃), 3.89 (3H, s, OCH₃), 5.14 (1H, m, $J=7.1$, 7.8 Hz, CH₃CHNH), 5.57 (1H, d, $J=7.8$ Hz, NHCO), 6.96 (1H, dd, $J=2.3$, 8.8 Hz, benzoxazole-5), 7.11 (1H, d, $J=2.3$ Hz, benzoxazole-7), 7.20 (2H, d, $J=8.3$ Hz, phenyl), 7.2–7.4 (5H, m, phenyl), 8.07 (2H, d, $J=8.3$ Hz, phenyl). Mass spectrum: m/z 400 (M^+), 252 (base peak). IR (KBr): 3279, 1640, 1533, 1489, 1348, 1224, 1150, 843, 702 cm^{-1} .

Analytical derivatization of carboxylic acids

In a 4-ml amber-coloured screw-capped vial were placed 100 μl of a dichloromethane solution of carboxylic acids (1–200 nmol/ml), 100 μl of a dichloromethane solution of (-)-APMB (0.8 $\mu\text{mol/ml}$), 100 μl each of a dichloromethane solution of 2,2'-dipyridyl disulphide (1.6 $\mu\text{mol/ml}$) and triphenylphosphine (1.6 $\mu\text{mol/ml}$). After being mixed, the reaction solution was allowed to stand for 20 min at room temperature. The solvent was evaporated to dryness with a stream of nitrogen and the residue was dissolved in 400 μl of mobile phase to make a sample solution and a 10- μl aliquot of the sample solution was injected into the HPLC system.

Chromatographic conditions

In the normal-phase mode, resolution of the resulting diastereomers was accomplished using a TSK gel silica-60 column (5- μm particle size, 25 \times 0.46 cm I.D.) (Tosoh) with *n*-hexane–ethyl acetate–2-propanol–acetic acid (900:50:50:1, v/v) as the mobile phase. The mobile phase was pumped isocratically at 1 ml/min. The excitation and emission wavelengths were adjusted to 320 and 375 nm, respectively.

In the reversed-phase mode, with a TSK gel ODS-80TM column (5- μm particle size, 15 \times 0.46 cm I.D.) (Tosoh) and acetonitrile–water–acetic acid (600:400:1, v/v/v), good separations were achieved at ambient temperature and a flow rate of 1 ml/min. The excitation and emission wavelengths were adjusted to 320 and 380 nm, respectively.

RESULTS AND DISCUSSION

Synthesis of fluorescence derivatization reagent

Some fluorescence derivatization reagents have been reported for the resolution of carboxylic acid enantiomers [2–11]. However, few chiral derivatization reagents have strong fluorescence to permit the more sensitive detection of trace amounts of carboxylic acid enantiomers. It has already been demonstrated that a series of 2-phenylbenzoxazole derivatives possess strong fluorescence, and hence some of them were applicable as sensitive fluorescence probes for

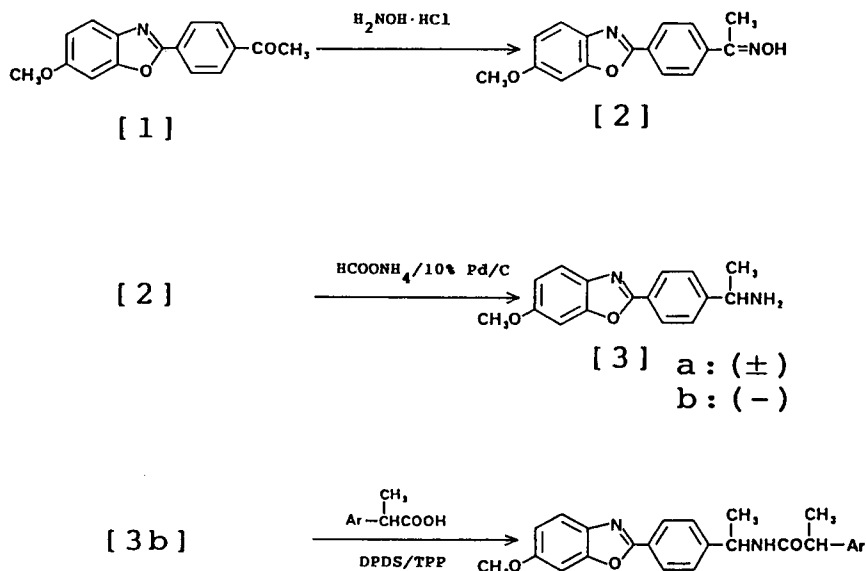


Fig. 1. Synthesis scheme for the chiral fluorescence derivatization reagent, (-)-APMB (3b), and derivatization of 2-arylpropionic acid with (-)-APMB. DPDS = 2,2'-dipyridyl disulphide; TPP = triphenylphosphine.

the trace analysis of organic compounds [10, 24–26]. Our attention became directed toward substituted 2-phenylbenzoxazoles, especially with electron-donating substituents, as new fluorescent probes for the sensitive determination of trace amounts of drugs by HPLC. For this purpose we synthesized a novel fluorescence chiral derivatization reagent, APMB, which has ethylamine as a reactive functional group toward carboxylic acid. The synthetic route to (-)-APMB is shown in Fig. 1. Reaction of 4-(6-methoxy-2-benzoxazolyl)acetophenone with hydroxylamine provided the hydroxyimino derivative, which on treatment with ammonium formate and 10% Pd-C was easily converted into the ethylamine. Optical resolution of (\pm)-APMB was accomplished by repeated fractional crystallization of the (*S*)-(-)- α -methoxy- α -trifluoromethylphenylacetic acid salt from ethanol, to give (-)-APMB. The optical purity of this reagent was 99.90%, as judged by chromatographic separation using TSK gel Enantio P1 with *n*-hexane–1,2-dichloroethane–2-propanol (6:3:1, v/v/v) as the mobile phase after derivatization with 3,5-dinitrobenzoyl chloride, as shown in Fig. 2.

(-)-APMB was stable at room temperature for at least 3 months with protection from

humidity and light, and the dichloromethane solution was also stable for at least 1 week when stored in a refrigerator.

Fluorescence properties of (-)-APMB derivative

As shown in Table I, the excitation and emission spectra of the (-)-APMB amide of (*S*)-(+)-2-phenylpropionic acid were measured in water and various solvents, which have been widely used as components of mobile phases in

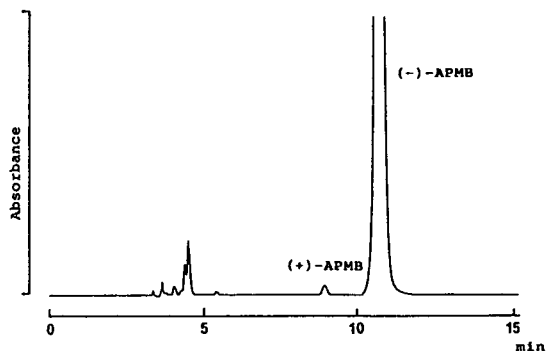


Fig. 2. Chromatograms of 3,5-dinitrobenzoyl derivative of the chiral fluorescence derivatization reagent (-)-APMB (3b). HPLC conditions: column, TSK gel Enantio P1; mobile phase, *n*-hexane–1,2-dichloroethane–2-propanol (6:3:1, v/v/v); flow-rate, 1.0 ml/min; detection, UV at 325 nm; column temperature, 40°C.

TABLE I

FLUORESCENCE SPECTRAL PROPERTIES OF (–)-APMB AMIDE OF (S)-(+)-2-PHENYLPROPIONIC ACID IN VARIOUS SOLVENTS

Solvent	Fluorescence		RFI ^a
	λ_{ex} (max.) (nm)	λ_{em} (max.) (nm)	
<i>n</i> -Hexane	316	374	78
Toluene	320	366	73
Dichloromethane	318	374	94
Ethyl acetate	317	368	94
Tetrahydrofuran	318	370	91
Ethanol	316	377	99
Methanol	318	378	99
Acetone	334	373	42
Acetonitrile	317	374	100
Water	316	394	78

^a RFI = Relative fluorescence intensity (acetonitrile = 100).

HPLC. The fluorescence intensity was not affected by the polarity of the solvent.

The effects of water concentration and pH on the fluorescence intensity were also investigated. The fluorescence intensity was almost a maximum and was constant at water concentrations of 0–90% in aqueous acetonitrile. The most intense fluorescence was constant between pH 3 and 12.

These results suggest that the polarity of the solvent, water concentration and pH have no influence on the fluorescence intensity, which will allow a wide choice of mobile phases in normal- or reversed-phase HPLC.

Derivatization of carboxylic acids with (–)-APMB

Various derivatization reactions of carboxylic acids with amines have been developed in the area of peptide synthesis. Of these methods, Mukaiyama *et al.* [27] reported that oxidation–reduction condensation using 2,2′-dipyridyl disulphide and triphenylphosphine produced peptides in high yields with high optical purity under mild reaction conditions. The fluorescence intensity–time profile of the reaction of (S)-(+)-2-phenylpropionic acid with (–)-APMB was investigated in the presence of 2,2′-dipyridyl di-

sulphide and triphenylphosphine in dichloromethane at room temperature. Under these conditions, the rate of formation of the fluorescent amide was rapid and the derivatization reaction was completed almost quantitatively by evaporation with a stream of nitrogen within 10 min, as shown in Fig. 3.

No racemization of the product or derivatization reagent occurred, even when reaction time was prolonged to 2 h.

Chromatographic separation

In general, normal-phase chromatography is more suitable than reversed-phase chromatography for the separation of diastereomeric amides, because it is sufficiently substantiated that the hydrogen bonding between an amide group and the stationary phase is important for the efficient resolution of diastereomers [7,28,29]. In this study, we attempted to separate the diastereomers formed from (–)-APMB and 2-arylpropionic acids by normal- and reversed-phase chromatography. Table II gives the capacity factors (k'), separation factors (α) and resolutions (R_s) for the diastereomeric amides derived from 2-arylpropionic acids with (–)-APMB on normal- and reversed-phase columns.

Fig. 4 shows typical chromatograms of a reaction mixture of 2-arylpropionic acids with (–)-APMB obtained by normal- and reversed-phase HPLC. The diastereomers were found to be

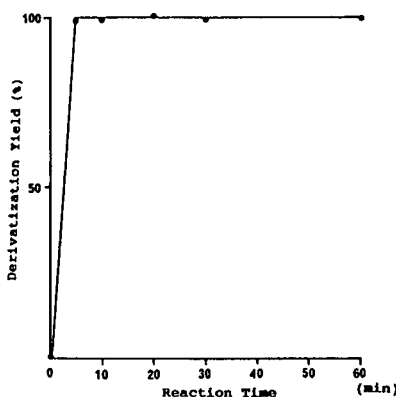


Fig. 3. Time course for the derivatization of (S)-(+)-2-phenylpropionic acid with (–)-APMB: 10 nmol/ml of (S)-(+)-2-phenylpropionic acid was treated with 0.8 μ mol/ml of (–)-APMB in the presence of DPDS and TPP at room temperature.

TABLE II

HPLC SEPARATIONS OF DIASTEREOMERIC AMIDES DERIVED FROM 2-ARYLPROPIONIC ACIDS WITH (-)-APMB

2-Arylpropionic acid	Enantiomer	NP-HPLC			RP-HPLC		
		k'	α	R_s	k'	α	R_s
2-Phenylpropionic acid	<i>R</i>	2.00	1.95	10.2	3.07	1.11	1.27
	<i>S</i>	3.89			2.76		
Ibuprofen	<i>R</i>	1.42	2.17	10.7	12.16	1.21	3.80
	<i>S</i>	3.08			10.03		
Naproxen	<i>R</i>	2.55	1.84	10.1	5.57	1.19	2.72
	<i>S</i>	4.61			4.67		
Flurbiprofen	<i>R</i>	1.75	2.42	9.8	8.97	1.24	4.58
	<i>S</i>	4.24			7.22		

readily resolvable on both normal and reversed stationary phases. No exceptions were observed in the elution order of each pair of enantiomers. In normal-phase chromatography, (*S*)-arylpropionic acids were eluted before the corresponding (*R*)-enantiomers. On the other hand, the elution order of (*R*)- and (*S*)-arylpropionic

acids was reversed on the reversed-phase column.

Excess of the derivatization reagent was eluted with the solvent front and small degradation peaks of the reagent were observed in the reversed-phase chromatogram. In contrast, under the normal-phase chromatographic conditions employed, excess of (-)-APMB was strongly retained in the column and not eluted. Therefore, a simple clean-up procedure, such as acidic liquid-liquid extraction to remove the excess of reagent, may be necessary to avoid interference of the excess of reagent in some applications.

The amides obtained were highly responsive to a fluorescence detector; the detection limits of the authentic derivative obtained from the reaction of (*S*)-(+)-2-phenylpropionic acid with (-)-APMB on the normal- and reversed-phase columns were 10 fmol at a signal-to-noise ratio of 3. This result shows that the sensitivity of (-)-APMB is better than those of 1-(1-naphthyl)ethylamine [8], 1-(4-dimethylamino-1-naphthyl)ethylamine [4] and 1-(1-anthryl)- and 1-(2-anthryl)ethylamine [7].

A calibration graph of peak area versus concentration of (*S*)-(+)-phenylpropionic acid labelled with (-)-APMB was plotted. A good linear detector response (linear regression coefficient = 0.999) was observed in the range 0.5–200 pmol injected on-column.

Multiple derivatization ($n = 5$) of (\pm)-flurbi-

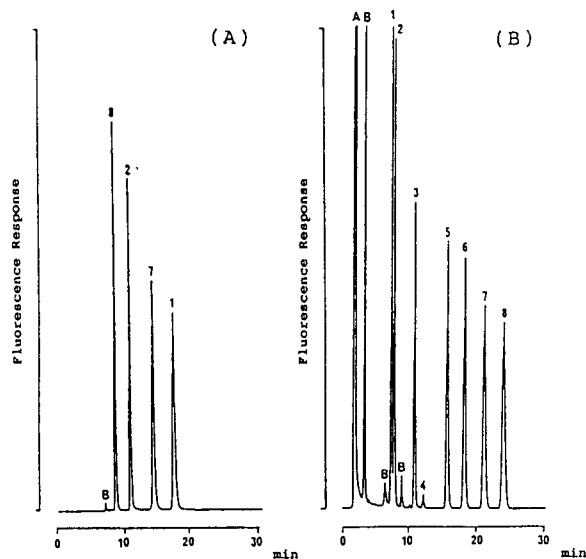


Fig. 4. Chromatograms of (-)-APMB derivatives of 2-arylpropionic acids. (A) Normal-phase HPLC; (B) reversed-phase HPLC. Peaks: 1 = (*S*)-2-phenylpropionic acid; 2 = (*R*)-2-phenylpropionic acid; 3 = (*S*)-naproxen; 4 = (*R*)-naproxen; 5 = (*S*)-flurbiprofen; 6 = (*R*)-flurbiprofen; 7 = (*S*)-ibuprofen; 8 = (*R*)-ibuprofen; A = (-)-APMB; B = degradation peak of the reagent.

TABLE III
REPRODUCIBILITY OF THE PROPOSED METHOD

Carboxylic acid	Relative standard deviation (%) ^a		
	1.25 pmol	5 pmol	10 pmol
(S)-Flurbiprofen	5.62	2.13	0.65
(R)-Flurbiprofen	6.38	3.14	0.51
(S)-Ibuprofen	5.28	2.28	1.04
(R)-Ibuprofen	4.00	2.81	0.75

^a n = 5.

profen and (±)-ibuprofen followed by HPLC gave peak areas with relative standard deviations of 0.5–6.8% in the range 1.25–25 pmol of the racemic acids analysed, as shown in Table III.

The newly synthesized reagent is of great use for the separation of enantiomeric carboxylic acids by HPLC. The proposed method is expected to be suitable for the resolution of enantiomeric carboxylic acids, and its high sensitivity may provide much more precise information on the determination of enantiomeric carboxylic acids, including NSAIDs that have a structure containing 2-arylpropionic acid, in biological fluids.

REFERENCES

- M. Zief and L.J. Crane (Editors), *Chromatographic Chiral Separations (Chromatographic Science Series, Vol. 40)*, Marcel Dekker, New York, 1988.
- C.G. Scott, M.J. Petrin and T. McCorkle, *J. Chromatogr.*, 125 (1976) 157.
- J. Goto, M. Hasegawa, S. Nakamura, K. Shimada and T. Nambara, *J. Chromatogr.*, 152 (1978) 413.
- J. Goto, N. Goto, A. Hikichi, T. Nishimaki and T. Nambara, *Anal. Chim. Acta*, 120 (1980) 187.
- J.M. Maitre, G. Boss and B. Testa, *J. Chromatogr.*, 299 (1984) 397.
- H. Weber, H. Spahn, E. Mutshler and W. Moehrke, *J. Chromatogr.*, 307 (1984) 145.
- J. Goto, M. Ito, S. Katsuki, N. Saito and T. Nambara, *J. Liq. Chromatogr.*, 9 (1986) 683.
- A. Avgerinos and A.J. Hutt, *J. Chromatogr.*, 415 (1987) 75.
- S. Narita and T. Kitagawa, *Anal. Sci.*, 5 (1989) 361.
- H. Spahn and P. Langguth, *Pharm. Res.*, 7 (1990) 1262.
- T. Toyo'oka, M. Ishibashi and T. Terao, *Analyst*, 117 (1992) 727.
- W.H. Pirkle and M.S. Hoeksta, *J. Org. Chem.*, 39 (1974) 3904.
- W.H. Pirkle and C.W. Boeder, *J. Org. Chem.*, 43 (1978) 1950.
- K.J. Miller, J. Gal and M.M. Ames, *J. Chromatogr.*, 307 (1984) 335.
- C.R. Clark and J.M. Barksdale, *Anal. Chem.*, 56 (1984) 958.
- W. Lindner, G. Uray and C. Leitner, *J. Chromatogr.*, 316 (1984) 605.
- J. Gal and A.J. Sedman, *J. Chromatogr.*, 314 (1984) 275.
- K. Shimada, E. Haniuda, T. Oe and T. Nambara, *J. Liq. Chromatogr.*, 10 (1987) 3161.
- N. Nimura and T. Kinoshita, *J. Chromatogr.*, 352 (1986) 169.
- N. Nimura, A. Toyama and T. Kinoshita, *J. Chromatogr.*, 316 (1984) 547.
- D.J. Aberhart, J.-A. Cotting and H.-J. Lin, *Anal. Biochem.*, 151 (1985) 88.
- S. Einarsson, B. Josefson, P. Moller and D. Sanchez, *Anal. Chem.*, 59 (1987) 1191.
- M.K. Anwer and A.F. Spatola, *Synthesis*, (1980) 929.
- H. Naganuma, J. Kondo and Y. Kawahara, *J. Chromatogr.*, 532 (1990) 65.
- G. Schladiz-Keil, H. Spahn and E. Mutschler, *J. Chromatogr.*, 345 (1985) 99.
- K. Shimada and T. Mizuguchi, *J. Chromatogr.*, 606 (1992) 133.
- T. Mukaiyama, R. Matsueda and M. Suzuki, *Tetrahedron Lett.*, (1970) 1901.
- T. Nambara, S. Ikegawa, M. Hasegawa and J. Goto, *Anal. Chim. Acta*, 101 (1978) 111.
- J. Goto, M. Hasegawa, S. Nakamura, K. Shimada and T. Nambara, *J. Chromatogr.*, 152 (1978) 413.

High-performance liquid chromatographic analysis of wheat flour lipids using an evaporative light scattering detector

Frank D. Conforti*, Carolyn H. Harris and Janet T. Rinehart

Department of Human Nutrition and Foods, Wallace Hall, Virginia Tech, Blacksburg, VA 24061 (USA)

(First received November 12th, 1992; revised manuscript received April 21st, 1993)

ABSTRACT

A high-performance liquid chromatographic method which utilized an evaporative light scattering detector for separation of starch and non-starch lipids of unbleached soft red winter wheat flour is described. Separation of the major starch and non-starch lipids was achieved in 60 min using a Lichrosorb Si-60 silica cartridge system and ternary gradient system. The evaporative light scattering detector gave a flat stable baseline, reproducible results and also eliminated the "solvent fronts" in which peaks of interest would have co-eluted. The technique was found useful in identifying the lipids and their relative mass percentages that were present in the flour.

INTRODUCTION

The analysis of cereal lipids is a complex and detailed procedure which is time consuming and in many cases insensitive as well as non-reproducible. In the past thin-layer chromatography (TLC) and quantification for fatty acid methyl esters by gas chromatography (GC) analysis have been the methods of choice for detection of non-starch and starch lipids in wheat flour [1,2]. The introduction of evaporative light scattering detection (ELSD) by Christie [3] to separate lipid classes in animal tissues by high-performance liquid chromatography (HPLC) demonstrated that this type of detector is very useful for analyzing lipids. ELSD gives a very stable baseline and is insensitive to solvent changes and gradients. One of the difficulties encountered with the evaporative light scattering detector is that the detector response is linear in the range of 10–200 μg and drops off drastically below 10 μg making it difficult to quantify lipid classes

present in this lower range. With proper calibration curves, consistent instrument set up, and sufficient sample size, direct quantification is possible [4,5]. Only a few applications of HPLC of lipids in cereals have been reported [6,7]. Christie and Morrison [7] reported a method using HPLC to separate polar lipid classes in cereal grains using an evaporative light scattering detector. The method failed to separate all of the lipid classes present in the flour and some difficulty was encountered with the separation of the glycolipids and less polar phospholipids. In addition, individual simple lipids were not resolved and emerged together at the start of the analysis when a complex lipid extract from wheat flour was analyzed. This made it necessary to extract out the glycolipid fraction prior to HPLC analysis. Moreau [8] introduced a method which separated the major classes of plant lipids from corn coleoptiles by HPLC using ELSD adapted from a procedure which originally used flame ionization as a means for detection [9]. Flame ionization detection has also been reported elsewhere for detection of phospholipids [10–12].

* Corresponding author.

Since flame ionization detectors are no longer commercially available, ELSD has presently become the detection method used most often in separation of lipids by HPLC [5]. It seemed possible that the method described by Moreau [8] could be adapted to separate the major plant lipid classes in cereal grains. The objectives of this research were: (1) to develop an HPLC procedure using ELSD which would successfully separate all the lipid classes present in soft wheat flour without prior fractionation of the individual glycolipids and phospholipids, (2) to identify each lipid class present, and (3) to acquire a relative mass percent of each lipid present.

EXPERIMENTAL

Extraction

Lipids were extracted from unbleached soft red winter wheat flour with water-saturated 1-butanol (WSB) [1,2]. The flour sample contained 1.5% lipid by soxhlet determination for percent fat [13]. Non-starch lipids were extracted from 3 g of flour with 30 ml of solvent at 20°C in a 50-ml teflon tube for 15 min mixed at 5-min intervals, centrifuged at 5900 g for 15 min and the supernatant transferred to a 250-ml evaporator flask. The solvent was then removed using a rotary evaporator under nitrogen at 60°C. After complete removal of all the water and solvent the residue was redissolved in 700 μ l of chloroform-methanol (2:1). The flask was rinsed down several times and the residue was filtered through a 0.45- μ m PTFE filter prior to HPLC analysis. The non-starch extract was then placed in a vial, loaded in the autosampler, and 12 μ l injected. The flour pellet was re-extracted three times with WSB to remove the interstitial lipid solution, and these extracts were discarded before proceeding with the extraction of the starch lipids.

Starch lipids were removed by adding 16 ml of WSB to the washed pellet, heated in a boiling water bath (90–100°C), changing the solvent every hour for 3 hours (three extractions) and the combined hot extracts were taken for analysis. The extracts were centrifuged and the solvent was removed with a rotary evaporator. The residue was redissolved in 700 μ l of chloroform-

methanol (2:1), and filtered as described above. An aliquot of 15 μ l was injected into the HPLC system.

Materials and reagents

Pure reference standards of monogalactosyldiglyceride, digalactosyldiglyceride, lysophosphatidylcholine, lysophosphatidylethanolamine, sterylglucoside, and acylated sterylglucoside were purchased from Matreya (Pleasant Gap, PA, USA). All other standards were purchased from Sigma (St. Louis, MO, USA). Standards were stored frozen in the dark and made up fresh daily to contain 50–100 μ g of each lipid class standard in chloroform-methanol (2:1). PTFE tubes (50 μ l) were used in the extraction process and HPLC-grade solvents were purchased from Fisher Scientific (Raleigh, NC, USA).

Chromatographic conditions

Lipid extracts were separated on a 100 \times 3 mm Chromsep 7 Micron Lichrosorb Si-60 Silica Cartridge System (Chrompack, Raritan, NJ, USA). The guard column was integrated in the Chromsep cartridge holder. The gradient system in Table I was adopted as optimal for separation of the major lipid classes.

TABLE I

TERNARY GRADIENT SYSTEM FOR LIPID CLASS SEPARATION

Time (min)	Flow-rate (ml/min)	Composition of mobile phase ^a		
		% A	% B	% C
0	0.5	100	0	0
5	0.5	95	5	0
10	0.5	85	15	0
15	0.5	40	60	0
33	0.5	40	51	9
48	0.5	40	51	9
53	0.5	40	60	0
58	0.5	100	0	0
80	0.5	100	0	0

^a A = Hexane-tetrahydrofuran (99:1), B = isopropanol, C = water.

All solvents were degassed and filtered prior to analysis. Helium was used as a sparge gas at 20 ml/min during the analysis.

Instrumentation

The HPLC system consisted of a Waters 600E controller with dual pumps, Waters 700E Wisp auto-sampler (Waters Assoc., Milford, MA, USA), and NEC Powermate Data acquisition controller with analysis software. The ELSD apparatus was obtained from Varex (Burtonville, MD, USA). The drift tube temperature was set at 60°C (40°C exhaust temperature). Nitrogen was used as the nebulizing gas at a flow of 45 mm (10 psi).

Calibration curves

Solutions of known concentrations of PE, LPE, LPC, MGDG, and DGDG (for abbreviations see Table II) were analyzed by the described HPLC procedure. Calibration curves were prepared using 10–200 µg of each standard

by plotting the concentration *versus* the peak area response of the ELSD.

Statistical analysis

Data were analyzed by the statistical analysis system [14]. Results were reported as the means of three observations and standard deviation for each non-starch and starch lipid class present in the sample. Linear regression was used to determine correlation coefficients (*r*) for each calibration curve of the individual standards.

RESULTS

Solvent systems such as chloroform–methanol, 2-propanol, and water-saturated 1-butanol were tested for the extraction of both the non-starch and starch lipids. Chloroform–methanol and 2-propanol did not yield consistent results from extraction to extraction. Water saturated 1-butanol demonstrated to be the best solvent in producing the most consistent results with complete extraction. It has been previously cited that

TABLE II
RELATIVE MASS PERCENTS FOR EACH LIPID CLASS

Each value is the mean of three observations ± standard deviation.

Peak No.	Lipid class	Abbrev.	Non-starch	Starch
1	Steryl ester + triglycerides	SE + TG	11.5 ± 0.2	4.7 ± 0.6
2	Triglycerides	TG	12.2 ± 0.6	0.4 ± 0.0
3	Free sterol	ST	4.1 ± 0.2	ND ^a
4	Free fatty acid	FFA	31.7 ± 0.8	6.0 ± 0.3
5	Unknown	UNK	3.5 ± 0.3	ND
6	Acylated sterylglucoside	ASG	2.5 ± 0.2	ND
7	Monogalactosyldiglyceride	MGDG	6.4 ± 0.4	ND
8	Monogalactosylmonoglyceride	MGMG	3.4 ± 0.3	ND
9	Sterylglucoside	SG	1.8 ± 0.1	ND
10	Digalactosyldiglyceride	DGDG	11.7 ± 0.8	ND
11	N-Acylphosphatidylethanolamine	NAPE	1.8 ± 0.1	ND
12	N-Acyllysophosphatidylethanolamine	NALPE	0.1 ± 0.0	ND
13	Phosphatidylethanolamine	PE	3.5 ± 0.1	ND
14	Phosphatidylglycerol	PG	2.0 ± 0.0	ND
15	Lysophosphatidylethanolamine	LPE	0.8 ± 0.0	10.2 ± 0.5
16	Phosphatidylcholine	PC	0.7 ± 0.1	1.0 ± 0.1
17	Lysophosphatidylglycerol	LPG	0.0	0.1 ± 0.0
18	Lysophosphatidylcholine	LPC	2.3 ± 0.2	77.6 ± 0.6

^a ND = None detected.

water-saturated 1-butanol is generally considered the best solvent for extraction of wheat lipids [15].

The extracted residue was redissolved in chloroform–methanol (2:1) since the digalactosyldiglyceride was not soluble in such solvents as hexane–chloroform (1:1) or chloroform alone. The digalactosyldiglyceride peak was either very broad or sometimes not present when either hexane–chloroform (1:1) or chloroform were used. Lipid extracts when redissolved in chloroform–methanol (2:1) resulted in sharp, well resolved peaks.

Different duration times of the ternary gradients were attempted to shorten the HPLC run. The results indicated variation in retention times between each analysis. With strict adherence to the conditions described in Table I these problems were eliminated.

Standards were injected individually as well as in a mixture to determine retention times and resolution of peaks. Retention times did not vary after 200 injections, nor was there any increase in backpressure. Loss of resolution occurred most often due to fluctuations in backpressure from dirty pump seals or the necessity to clean the nebulizer and drift tube on the detector.

The non-starch lipid fraction consisted of seventeen major peaks (Fig. 1) when analyzed by HPLC–ELSD. The exhaust and tube tem-

peratures were kept at a minimum to prevent the free fatty acid peak from being volatilized [16]. The non-starch lipids (Table II) included: (SE + TG), TG, ST, FFA, UNK, ASG, MGDG, MGMG, SG, DGDG, NAPE, NALPE, PE, PG, LPE, PC, and LPC. The identity of each peak was confirmed from the retention time of each corresponding lipid class standard and the enhancing technique of the lipid class peak. Data was in agreement with previous research [15,17] on the composition of lipids in wheat flour. Research has demonstrated that samples dissolved in polar solvents would cause the triacylglycerols to sometimes elute as a double peak with a portion of the TG co-eluting with SE [3]. Since it was found essential to dissolve the non-starch and starch residues in a polar solvent such as chloroform–methanol (2:1) it may be concluded that the first peak in the chromatographs contain both SE and TG.

Seven major peaks were resolved when the starch lipids were separated (Fig. 2). They included (Table II): SE + TG, TG, FFA, LPE, PC, LPG and LPC. Research [17,18] has shown that the starch lipid of wheat flour contains approximately 6–10% FFA, 77% LPC, 10% LPE and very little or no triglycerides, diacyl lipids and monoacyl lipids. The starch lipids shown in Fig. 2 were extracted with hot WSB

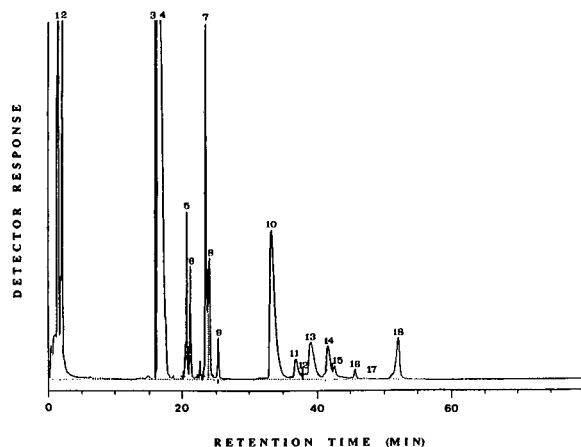


Fig. 1. Separation of non-starch lipids in soft wheat flour on a Lichrosorb Si 60 silica column by HPLC–ELSD. See text for conditions. See Table II for identification of each numbered peak.

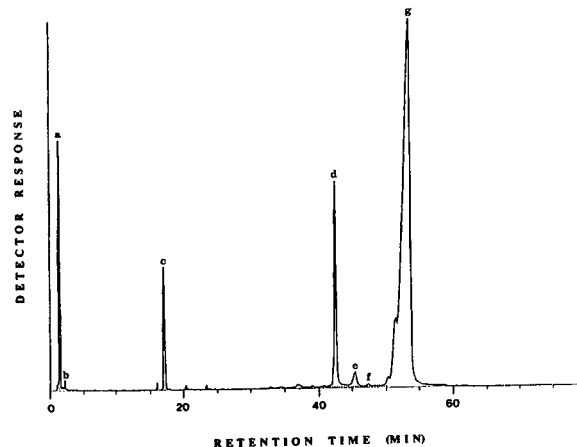


Fig. 2. Separation of starch lipids from soft red winter wheat flour on a Lichrosorb Si 60 silica column by HPLC–ELSD. (a) SE + TG; (b) TG; (c) FFA; (d) LPE; (e) PC; (f) LPG and (g) LPC.

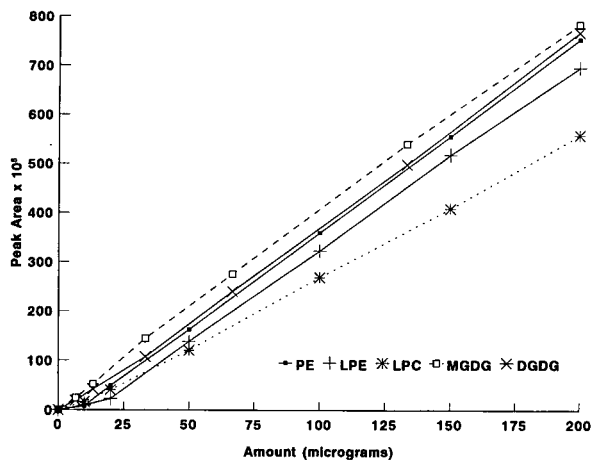


Fig. 3. Calibration curves for phospholipids and glycolipids by HPLC with an evaporative light scattering detector.

after first removing the non-starch lipids. The starch lipids may contain some residual non-starch lipids since it is not protein-free starch. This may explain the presence of the first peak (SE + TG) and the high percentage of the FFA. Extensive research has concluded that the FFA and other monoacyl lipids are non-starch lipids absorbed into the starch lipid granules, therefore, forming surface lipid artifacts [17].

Calibration curves of PE, LPE, LPC, MGDG, and DGDG are shown in (Fig. 3). Linear relationships ($r > 0.99$) between peak area in integrator counts and amounts of phospholipids and glycolipids were found in the 10–200 μg range. The sigmoidal relationship holds and tails off for component amounts below 10 μg [3]. The response of the glycolipids resembles those for phospholipids.

DISCUSSION

The proposed HPLC–ELSD method for separation of non-starch and starch lipids in wheat flour was found to have the following advantages over conventional methods: better resolution and efficiency, a stable baseline, high sensitivity, detection limits in the 10–200 μg range, and good reproducibility. This HPLC–ELSD method was also adaptable for direct analysis of both polar and non-polar lipids in wheat flour without

prior fractionation of the glycolipids. The column cartridge system is fairly inexpensive and easily replaced. Once lipid extraction was achieved with the aid of an autosampler and data handling station the completion of the analysis was automated.

The 22-min re-equilibration between the end of one gradient and the injection of the next sample is crucial to eliminate variations in the retention times and adequate separation of peaks. Use of a ternary gradient clearly resolved the major peaks in both the non-starch and starch extracts.

The lower tube and exhaust temperature allowed detection of the free fatty acids without volatilization. Cleaning of the pump seals, detector nebulizer and drift tube were essential for good reproducibility of day to day runs.

In order to use this HPLC method for quantification it is necessary to prepare different calibration curves for each component in the sample. It is also essential to set up the detector parameters as well as the elution profile exactly the same way each day to maintain reproducibility.

Although it has been reported that starch lipids can be extracted from flour after first removing the non-starch lipids in practice it is best to extract them from pure protein-free washed starch to avoid contamination with any residual non-starch lipids in the flour protein [15].

The lipid data presented in Table II is a representation of only relative mass percents. The possibility of using this application for quantification of the lipid classes present in wheat flour is presently being explored.

ACKNOWLEDGEMENTS

We thank Mark Alley, Agronomy Department, Virginia Tech, for providing wheat samples used in this experiment. We especially thank Robert Moreau, Eastern Regional Research Center, USDA, Philadelphia, PA, for providing publications related to separations of plant lipids by HPLC and helpful discussions related to this subject.

REFERENCES

- 1 W.R. Morrison, D.L. Mann, S. Wong and A.M. Coventry, *J. Sci. Food Agric.*, 26 (1975) 507.
- 2 W.R. Morrison, S.L. Tan and K.D. Hargin, *J. Sci. Food Agric.*, 31 (1980) 329.
- 3 W.W. Christie, *J. Lipid Res.*, 26 (1985) 507.
- 4 S.L. Melton, *J. Am. Oil Chem. Soc.*, 69 (1992) 784.
- 5 P. van der Meeren, J. Vanderdeelen, M. Huys and L. Baert, *J. Chromatogr.*, 447 (1988) 436.
- 6 T.N. Tweeten, D.L. Wetzel and O.K. Chung, *J. Am. Oil Chem. Soc.*, 58 (1981) 664.
- 7 W.W. Christie and W.R. Morrison, *J. Chromatogr.*, 436 (1988) 510.
- 8 R.A. Moreau, in P.J. Quinn and J.L. Harwood (Editors), *Plant Lipid Biochemistry Structure and Utilization*, Portland Press, London, 1990, p. 20.
- 9 R.A. Moreau, P.T. Asmann and H.A. Norman, *Phytochemistry*, 29 (1990) 2461.
- 10 M.D. Grieser and J.N. Geske, *J. Am. Oil Chem. Soc.*, 66 (1989) 1484.
- 11 F.C. Phillips and O.S. Privett, *J. Am. Oil Chem. Soc.*, 58 (1981) 590.
- 12 F.C. Phillips, W.L. Erdahl and O.S. Privett, *Lipids*, 17 (1982) 992.
- 13 *Approved Methods of the AACC*, American Association of Cereal Chemists, St. Paul, MN, 1983, AACC Method 30-25.
- 14 *SAS Procedures Guide, Version 6*, SAS Institute, Cary, NC, 3rd ed., 1990.
- 15 W.R. Morrison, in Y. Pomeranz (Editor), *Advances in Cereal Science and Technology*, Vol. II, American Association of Cereal Chemists, St. Paul, MN, 1978, pp. 221–348.
- 16 K.D. Mukherjee and N. Weber, *CRC Handbook of Chromatography: Analysis of Lipids*, CRC Press, Boca Raton, FL, 1993, p. 41.
- 17 W.R. Morrison, in Y. Pomeranz (Editor), *Wheat Chemistry and Technology*, Vol. I, American Association of Cereal Chemists, St. Paul, MN, 1988, p. 392.
- 18 T. Galliard and P.J. Barnes, in P. Mazliak, C. Benveniste, C. Costes and R. Douce (Editors), *Biogenesis and Function of Plant Lipids*, Elsevier, 1980, p. 191.

Determination of RDX, 2,4,6-trinitrotoluene and other nitroaromatic compounds by high-performance liquid chromatography with photodiode-array detection

Monika Emmrich*

Institut für Hygiene, Freie Universität Berlin, Hindenburgdamm 27, 12200 Berlin (Germany)

Manfred Kaiser

Bundesinstitut für Chemisch-Technische Untersuchungen, Grosses Cent, 53913 Swisttal (Germany)

Henning Rüden and Stefan Sollinger

Institut für Hygiene, Freie Universität Berlin, Hindenburgdamm 27, 12200 Berlin (Germany)

(First received July 28th, 1992; revised manuscript received March 19th, 1993)

ABSTRACT

An HPLC method with photodiode-array detection was developed for the determination of RDX, TNT and the most important aromatic nitro compounds. Three mobile phases, isocratic methanol–water (50:50), a methanol–water gradient and a methanol–water gradient containing 2% of tetrahydrofuran were tested. Under the isocratic conditions used diaminonitrotoluene and the tetranitroazoxytoluene isomers cannot be measured within one HPLC run whereas this could be achieved with the two gradient systems. Good separations are achieved with the gradient systems with different elution orders for the nitrated benzene, toluene and aminonitrotoluene isomers.

INTRODUCTION

Residues of 2,4,6-trinitrotoluene (TNT), one of the most widely used explosives, are often accompanied by co-contaminants resulting from manufacturing impurities of the explosive, from hydrolysis or from biotransformation. Manufacturing impurities include 2,4- and 2,6-dinitrotoluene and dinitro- and trinitrobenzene [1]. Many bacteria and fungi are capable of reducing the nitro groups to amines, hence important biodegradation products are 2-amino-4-nitro- and 4-amino-2-nitrotoluene, the aminodinitro-

toluenes 4-amino-2,6- and 2-amino-4,6-dinitrotoluene and the diaminonitrotoluenes 2,4-diamino-6-nitro- and 2,6-diamino-4-nitrotoluene [1,2,3]. In addition, 2,2',6,6'-tetranitro-4,4'-azoxytoluene and in trace amounts 4,4',6,6'-tetranitro-2,2'-azoxytoluene have been observed as transformation products [4,5].

As these substances can be found in the environment (*e.g.*, soil), efficient and rapid analytical procedures for these compounds are necessary. Gas chromatography with flame ionization detection (FID) or as a more sensitive method electron-capture detection (ECD) is often used to determine these substances [6,7]. However, for the separation of thermally unstable and non-volatile compounds, high-per-

* Corresponding author.

formance liquid chromatography (HPLC) with ultraviolet detection is ideally suited [8,9] and offers adequate detection limits for nitroaromatic compounds [10]. Environmental samples are very complex and the extracts may contain substances that co-elute with the nitroaromatic compounds. Hence the use of HPLC in combination with photodiode-array detection is advantageous, because peak identification is more reliable with the additional information from the UV spectrum. The spectra may be helpful in searching for particular pollutants in samples and give a first identification of the substances present. Further, by comparison of the various UV spectra at the peak front edge, peak apex and peak end edge, one can obtain information about homogeneity. Therefore, an HPLC method in combination with diode-array detection for rapid and efficient analysis was developed for hexahydro-1,3,5-trinitro-1,3,5-triazine (RDX), TNT and its most important derivatives.

EXPERIMENTAL

Apparatus

The HPLC measurements were carried out on a Waters (Milford, MA, USA) Model 600E multi-solvent delivery system equipped with a Waters Model 700 automatic sample injection module and a Waters Model 990 photodiode-array detector. For separation a Merck LiChrospher 100 RP-18 column (25 cm × 4 mm I.D.) with a particle diameter of 5 μm in combination with a precolumn filled with the same material was used. The flow-rate was 1 ml/min and the volume injected was 20 μl. The mobile phase was a methanol–water programmed gradient starting with 35% methanol increased to 70% in 35 min and to 100% in the following 10 min. The column was then flushed for a further 5 min with pure methanol and re-equilibrated for 10 min. For a different elution order of the compounds a secondary gradient from methanol–water containing 2% of tetrahydrofuran (THF) to methanol was used.

Chemicals

RDX, TNT, 2-amino-4,6-dinitro- and 4-amino-2,6-dinitrotoluene (2A-4,6DNT, 4A-

2,6DNT), 2,4-diamino-6-nitro- and 2,6-diamino-4-nitrotoluene (2,4DA-6NT, 2,6DA-4NT), 4,4',6,6'-tetranitro-2,2'-azoxytoluene (2,2'-Azoxy) and 2,2',6,6'-tetranitro-4,4'-azoxytoluene (4,4'-Azoxy) were prepared at the Bundesinstitut für Chemisch-Technische Untersuchungen (Swisttal, Germany). 1,4-Dinitrobenzene (1,4-DNB) and 2,6-dinitrotoluene (2,6-DNT) were obtained from Riedel-de Haën (Seelze, Germany) and 4-amino-2-nitrotoluene (4A-2NT) from Aldrich (Steinheim, Germany). The other reference compounds nitrobenzene (NB), 1,2- and 1,3-dinitrobenzene (1,2-DNB, 1,3-DNB), the nitrotoluene isomers (2-NT, 3-NT and 4-NT), the 2,3-, 2,4- and 3,4-dinitrotoluene iso-

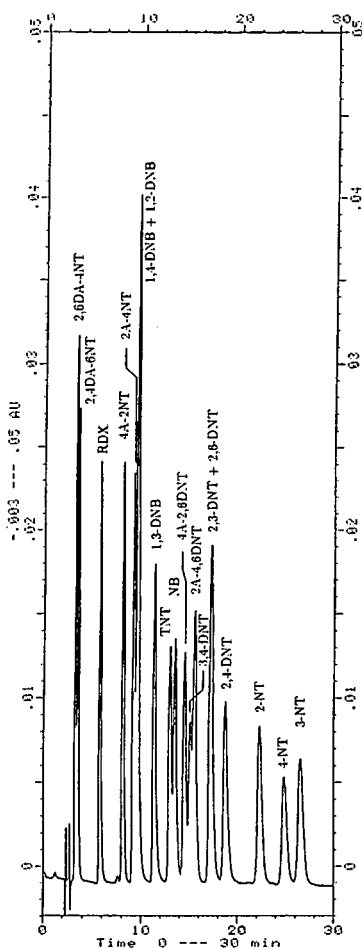


Fig. 1. Chromatogram of RDX, TNT and the nitroaromatic compounds with methanol–water (50:50) as mobile phase and detection at 254 nm.

mers (2,3-DNT, 2,4-DNT and 3,4-DNT) and 2-amino-4-nitrotoluene (2A-4NT) were purchased from Merck (Darmstadt, Germany). All chemicals were used as received. They were dissolved in methanol, with the exception of RDX, 2,2'-Azoxy and 4,4'-Azoxy, which were dissolved in acetonitrile and further diluted with methanol.

For mobile phase preparation, gradient-grade methanol, THF and water for chromatography were purchased from Merck.

RESULTS

Isocratic conditions

Common HPLC methods described in the literature [11,12] use reversed-phase columns with methanol–water under isocratic conditions. These methods have been optimized for the separation of explosives such as TNT, RDX, HMX, Tetryl and trinitrobenzene [9], but little is

known about the elution order and separation of TNT and its degradation products. Therefore, RDX, TNT and the most important related nitroaromatic compounds were tested on a Li-Chrospher 100 RP-18 reversed phase column using methanol–water (50:50) as the mobile phase. A chromatogram recorded at 254 nm is shown in Fig. 1 and the retention times (t_R) are summarized in Table I. Under these conditions 2,6DA-4NT and 2,4DA-6NT are not retained and coincide with the solvent peak. In contrast, 2,2'-Azoxy and 4,4'-Azoxy do not elute within 70 min. To measure all these compounds one has to make several HPLC runs with different isocratic conditions.

Gradient programmed conditions

These compounds can be measured altogether in one chromatographic run with the use of a gradient programmed HPLC method. Fig. 2 shows a chromatogram obtained at 254 nm with

TABLE I

RETENTION TIMES, t_R , FOR METHANOL–WATER (50:50), A METHANOL–WATER GRADIENT AND A METHANOL–WATER GRADIENT CONTAINING 2% OF THF

Compound	t_R (min)		
	Methanol–water (50:50)	Methanol–water gradient	Methanol–water gradient + 2% THF
2,6DA-4NT	3.3	5.2	6.2
2,4DA-6NT	3.6	6.4	8.4
RDX	5.8	11.1	16.3
4A-2NT	8.3	17.6	18.3
1,4-DNB	9.7	18.0	17.1
2A-4NT	9.3	19.0	19.2
1,2-DNB	9.7	19.5	20.6
1,3-DNB	11.5	20.3	20.2
TNT	13.1	23.0	24.1
NB	13.7	23.4	21.2
4A-2,6DNT	14.7	25.4	28.5
2A-4,6DNT	15.8	26.1	29.3
3,4-DNT	15.3	26.3	26.2
2,6-DNT	17.4	27.2	27.2
2,3-DNT	17.4	27.9	28.0
2,4-DNT	19.0	28.2	27.7
2-NT	22.6	30.7	28.8
4-NT	25.2	32.0	29.7
3-NT	26.9	32.8	30.7
4,4'-Azoxy	–	46.7	47.1
2,2'-Azoxy	–	48.8	48.9

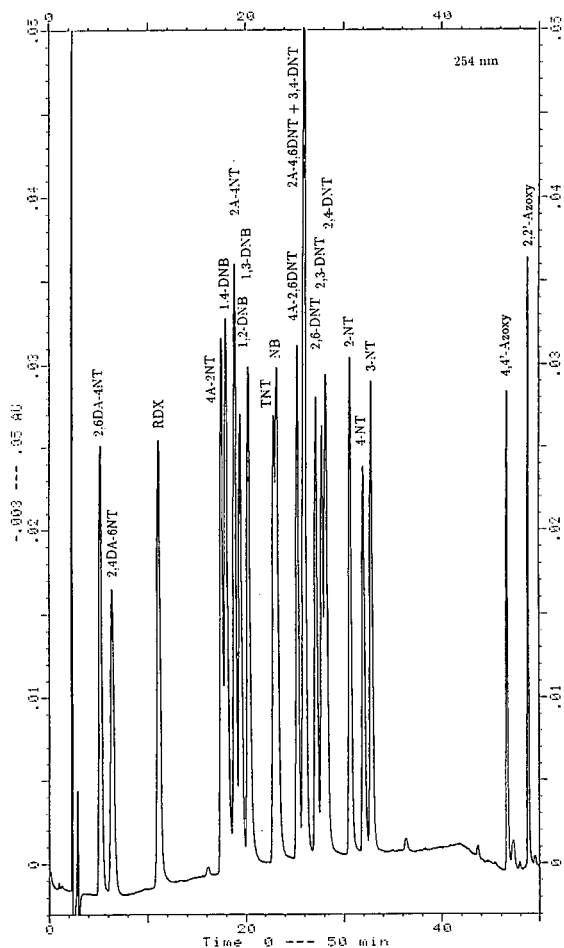


Fig. 2. Chromatogram of RDX, TNT and the nitroaromatic compounds with a gradient programmed mobile phase of methanol–water with detection at 254 nm.

a standard solution containing 6–12 ng/ μ l of each of the 21 substances. Retention times are summarized for the RP-18 column in Table I. Under the experimental conditions, the compounds are nearly completely separated. The two diaminonitrotoluene isomers are eluted first, followed by the nitramine RDX. The two aminonitrotoluene and the three dinitrobenzene isomers elute close together, but they are well separated. TNT and NB have nearly the same retention times and coincide. Then the aminodinitrotoluenes are eluted, but 2A-4,6DNT appears at the same time as 3,4-DNT, followed by the other DNT isomers. Of the mononitrotoluenes, 2-NT is eluted first, followed by 4-NT and 3-NT. 4,4'-Azoxy and 2,2'-Azoxy elute

relatively late at 46.7 and 48.8 min, respectively. If it is desired to shorten the analysis time, 4,4'-Azoxy and 2,2'-Azoxy will elute earlier without changing the elution sequence and separation of the other compounds if the methanol concentration is increased rapidly to 100% after 35 min.

In Table II the different UV absorbance maxima are summarized together with the molar absorptivities (ϵ) for all substances.

The reproducibility of the method was tested by making repeated injections of a standard solution of the compounds. The relative standard deviations of the mean retention times for each compound determined for ten injections are summarized in Table III. The relative standard deviations of the peak retention times are very low and the method has good reproducibility.

For checking the linearity of the detector six different concentrations were tested, each with a minimum of four injections. The calibration graphs with intercept a and slope b are given in Table III for a wavelength of 254 nm. They were calculated as regression lines based on a least-

TABLE II

ABSORBANCE MAXIMA, λ_{\max} (nm), AND MOLAR ABSORPTIVITIES, ϵ_{\max} (10^3 cm²/mol), IN THE MEASURED RANGE 210–350 nm

Compound	λ_{\max}	ϵ_{\max}	λ_{\max}	ϵ_{\max}	λ_{\max}	ϵ_{\max}
2,6DA-4NT	210	29.8	240	13.4	338	3.6
2,4DA-6NT	213	30.8	239	11.9	350	1.7
RDX	210	11.0				
4A-2NT	234	15.0				
1,4-DNB	259	13.5				
2A-4NT	226	12.3	249	11.8	287	4.6
1,2-DNB	210	11.3				
1,3-DNB	233	15.6				
TNT	227	17.4				
NB	258	7.4				
4A-2,6DNT	232	20.6	367	1.9		
2A-4,6DNT	226	17.4				
3,4-DNT	215	11.8	260	5.8		
2,6-DNT	210	9.0	233	8.5		
2,3-DNT	210	10.0	254	5.0		
2,4-DNT	241	12.7				
2-NT	210	6.2	256	5.1		
4-NT	210	6.6	273	8.8		
3-NT	210	7.8	263	6.9		
4,4'-Azoxy	239	34.0				
2,2'-Azoxy	227	23.5	313	18.7		

TABLE III

CALIBRATION GRAPHS AND REPRODUCIBILITY (WAVELENGTH 254 nm) FOR RDX, TNT AND THE NITRO-AROMATIC COMPOUNDS

Compound	Concentration (ng/ μ l)		Calibration graph ^a		r^2	R.S.D. ^b ($n = 36$) (%)
	Min.	Max.	a	b		
RDX	0.41	78	-9	596	1.000	1.3
4A-2NT	0.30	58	-128	836	1.000	1.4
1,4-DNB	0.20	38	-812	1565	0.999	1.5
2A-4NT	0.22	43	-366	1218	0.999	1.4
1,2-DNB	0.31	60	-680	749	0.999	1.6
1,3-DNB	0.17	33	-671	1703	0.998	1.5
TNT	0.22	42	-216	1030	1.000	0.9
NB	0.22	43				
4A-2,6DNT	0.28	54	-32	764	1.000	1.3
2A-4,6DNT	0.24	47	-232	942	1.000	1.4
3,4-DNT	0.24	46				
2,6-DNT	0.26	50	-99	782	1.000	1.0
2,3-DNT	0.32	62	-4	520	0.999	1.1
2,4-DNT	0.16	30	-304	1645	0.999	1.1
2-NT	0.33	64	-139	676	1.000	0.9
4-NT	0.31	59	-207	565	1.000	0.9
3-NT	0.31	60	-235	704	1.000	0.9
4,4'-Azoxy	0.08	16	-16	1489	1.000	0.2
2,2'-Azoxy	0.11	22	-10	1161	1.000	0.1

^a $y = a + bx$.^b Relative standard deviation of retention time.

squares fit. With values between 0.998 to 1.000 for the squared regression coefficients (r^2) all compounds show good linearity. The slope b calculated for 254 nm is a measure of the sensitivity and will have other values for different wavelengths, depending on the UV spectrum.

The detection limit based on the amount required to give a response three times the standard deviation of the noise is in the range 40–80 pg/ μ l. With an injection volume of 20 μ l a minimum amount of 0.8–1.6 ng of each compound is needed.

Influence of THF

TNT is one of the most often used explosives and frequently its measurement is of special interest. In unknown and complex systems such as environmental samples TNT might be accom-

panied by co-contaminants. NB interferes with TNT and the accurate determination of TNT can be affected. Therefore, another HPLC system that offers the detection of TNT without co-elution of NB was developed. A ternary mobile phase mixture was used, consisting of water and methanol mixed with 2% of THF with the same gradient programme as mentioned above.

A chromatogram with methanol–THF–water as mobile phase is shown in Fig. 3. The retention times are given in Table I. The elution order with methanol–THF–water as mobile phase is different from that with methanol–water. There is now an excellent separation of TNT and NB in about 2 min, with NB eluting first. Further, the addition of 2% of THF has a significant influence in RDX, which is retarded by about 5 min and now elutes before 1,4-DNB. The retention times of 3,4-DNT, 2,6-DNT, 2,4-DNT and 2,3-DNT

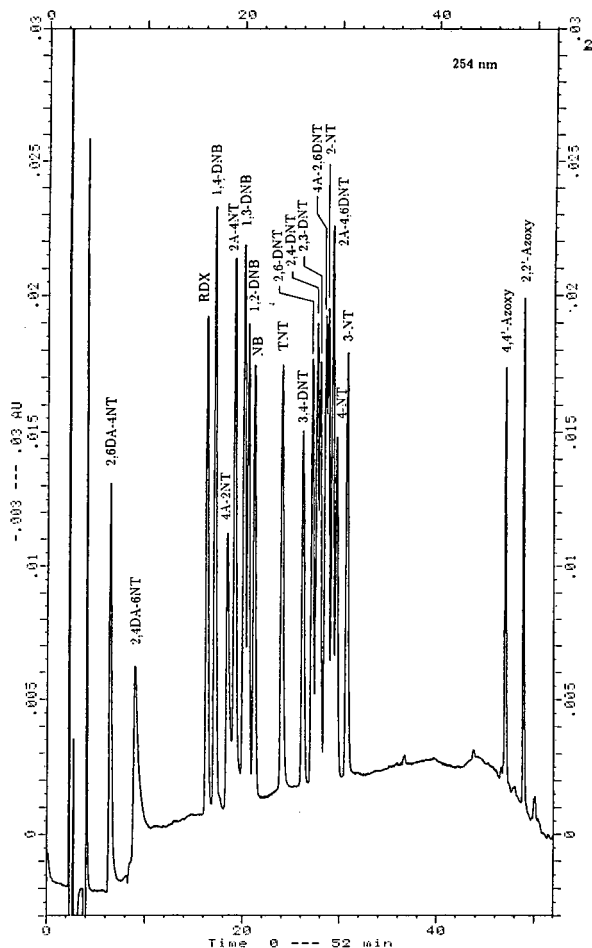


Fig. 3. Chromatogram of RDX, TNT and the nitroaromatic compounds with a gradient programmed mobile phase of methanol–water containing 2% of THF with detection at 254 nm.

are nearly the same. With the methanol–water gradient system 4A-2,6DNT elutes after TNT and NB whereas 2A-4,6DNT coincides with 3,4-DNT. When 2% of THF is added to the mobile phase both are retained about 3 min longer and elute close together with 2-NT. Likewise, the elution order of 4A-2NT and 1,4-DNB changes and 4A-2NT now elutes in front of 2A-4NT.

CONCLUSIONS

With the developed HPLC-method with a methanol–water gradient as the mobile phase, the determination of RDX, TNT and other relevant compounds within one HPLC run is

possible. This cannot be achieved under isocratic conditions and one has to use different solvent strengths, e.g., 20% methanol, to separate 2,4DA-6NT from 2,6DA-4NT, 50% methanol for TNT and its derivatives and 75% methanol for 2,2'-Azoxy and 4,4'-Azoxy [11].

The behaviour of the compounds on a reversed-phase RP-18 column with and without the addition of THF to methanol–water was investigated. The separation for TNT and NB is excellent when THF is added, but the performance for the dinitrotoluene isomers, the aminodinitrotoluenes and 2-NT is better when the methanol–water gradient system alone is used. Hence it might depend on the complexity of the sample matrix and the compounds of interest which of the two systems, methanol–water or methanol–THF–water, is to be preferred. In combination with photodiode-array detection one can obtain further information of peak identity.

REFERENCES

- 1 D. Layton, B. Mallon, W. Mitchell, L. Hall, R. Fish, L. Perry, G. Snyder, K. Bogen, W. Malloch, C. Ham and P. Dowd, *Conventional weapons demilitarization: A health and environmental effects data base assessment; Explosives and their co-contaminants, Final Report, Phase II*, US Army Medical Research and Development Command, Fort Detrick, Frederick, MD, 1987.
- 2 B. Greene, D.L. Kaplan and A.M. Kaplan, *Technical Report Natick/TR-85/046*, US Army Natick Research and Development Center, Natick, MA, 1985.
- 3 F.W. Parrish, *Appl. Environ. Microbiol.*, 34 (1977) 232–233.
- 4 N.G. McCormick, F.E. Feeherry and H.S. Levinson, *Appl. Environ. Microbiol.*, 31 (1976) 949–958.
- 5 W.D. Won, R.J. Heckly, D.J. Glover and J.C. Hoffsommer, *Appl. Microbiol.*, 27 (1974) 513–516.
- 6 J. Feltes, K. Levsen, D. Volmer and M. Spiekermann, *J. Chromatogr.*, 518 (1990) 21–40.
- 7 R.J. Spanggord, B.W. Gibson, R.G. Keck, D.W. Thomas and J.J. Barkley, *Environ. Sci. Technol.*, 16 (1982) 229–232.
- 8 S.D. Harvey, R.J. Fellows, D.A. Cataldo and R.M. Bean, *J. Chromatogr.*, 518 (1990) 361–374.
- 9 T.F. Jenkins and M.E. Walsh, *Report AMXTH-TE-FR-86102*, US Army Toxic and Hazardous Materials Agency, 1987.
- 10 K. Bratin, P.T. Kissinger, R.C. Briner and C.S. Bruntlett, *Anal. Chim. Acta*, 130 (1981) 295–311.
- 11 D.L. Kaplan and A.M. Kaplan, *Anal. Chim. Acta*, 136 (1982) 425–428.
- 12 M.E. Walsh and T.F. Jenkins, *Anal. Chim. Acta*, 231 (1990) 313–315.

Direct separation of 4-amino-3-(4-chlorophenyl)butyric acid and analogues, GABA_B ligands, using a chiral crown ether stationary phase

Claude Vaccher, Pascal Berthelot and Michel Debaert*

Laboratoire de Pharmacie Chimique, Université de Lille II, BP 83, 3 Rue du Pr. Laguesse, 59006 Lille Cédex (France)

(Received March 5th, 1993)

ABSTRACT

The direct resolution of baclofen (β -*p*-chlorophenyl- γ -aminobutyric acid) and a series of four analogues was achieved by HPLC on an enantioselective crown ether column, CR(+). Chromatography was carried out with perchloric acid as mobile phase and methanol as organic modifier. The effects of temperature, pH, eluent composition and substituents are discussed. The absolute configuration is attributed. The best results were obtained with baclofen ($\alpha = 1.48$; $R_s = 8.07$).

INTRODUCTION

The neutral amino acid γ -aminobutyric acid (GABA) is an inhibitory neurotransmitter concerned with the control of neuronal activity in the mammalian central nervous system and with the regulation of many physiological mechanisms [1]. Within the central and peripheral nervous systems, GABA has been shown to act through at least two distinctly different receptor sites [2]. These are termed GABA_A and GABA_B receptors, with different binding properties [3,4]. Until now, β -*p*-chlorophenyl-GABA (baclofen) was the only selective agonist for the GABA_B receptor. Analogues of baclofen have been synthesized and tested for GABA_B receptor affinity [5,8]. The enantiomers of baclofen were found to have different properties, the (*R*)-(-)-enantiomer being about 100 times more active than the (*S*)-(+)-enantiomer [3,6]. We

recently described [7] potent and specific GABA_B receptors antagonists [5]: β -(substituted benzo[*b*]furyl)GABA (1–4), analogues of baclofen, now commercially available as racemates (1 and 2 from Tocris Neuramin, Langford, Bristol, UK) (Fig. 1).

Stereoselective analyses of mixtures of enantiomers of amino acids, such as GABA, have largely employed high-performance liquid chromatography (HPLC) [9]. Separation is possible directly through the use of chiral eluents [chiral solvating agents (CSAs)] or chiral stationary

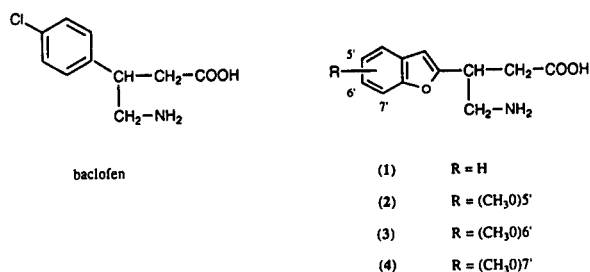


Fig. 1. Structures of baclofen and compounds 1–4.

* Corresponding author.

phases (CSPs) or indirectly through derivatization, leading to diastereomers, with chiral reagents [chiral derivatizing agents (CDAs)].

Baclofen has been extensively studied in analytical chromatography using HPLC with UV [10,11], fluorimetric [12] or radioactivity [13] detection, TLC [14], GC–MS [15] and GLC [16]. For optical resolution of the baclofen enantiomers, GC with electron-capture detection on a CSP [17], HPLC with UV detection on a Pirkle-type CSP after achiral derivatization [18], UV detection on a normal phase after chiral derivatization [19], fluorimetric detection after chiral derivatization [20,21], radioactivity detection [22] using a CSA and polarimetry on a CSP [18] have been described. A recently introduced phase uses a chiral crown ether moiety as chiral selector to resolve amino acids; discrimination between enantiomers relies on the formation of two diastereoisomeric inclusion complexes between the ammonium ion moiety of the amino acid and the chiral crown ether entity of the stationary phase. An acidic mobile phase ensures the protonation to form the ammonium ion which fits in the cavity. Perchloric acid is recommended because of the better resolution and low UV absorption. In this paper we describe the direct separation of baclofen and an optimization study on compounds 1–4.

EXPERIMENTAL

Chromatography

Analytical HPLC was carried out with an LKB Model 2249 metering pump. Detection was performed with a Hewlett-Packard HP 1040 photodiode-array spectrophotometer connected to an HP 9000 S300 computer. The detection wavelengths were 200, 220 and 225 nm. The column was a 150 × 4 mm I.D. Crownpack CR(+) (5 μm) column (Daicel Chemical Industries, Baker, Paris, France). The sample loop was 10 μl and was made using a Rheodyne Model 7125 injector. Elution was carried out isocratically using perchloric acid as the mobile phase diluted to obtain the required pH. An organic modifier (methanol) was included in the mobile phase. The flow-rate was 0.9 ml/min. The temperature of the column was controlled

by circulating water through a jacket surrounding the column. Temperature was measured in the water-bath and was in the range 10–40°C.

Reagents and materials

Baclofen was kindly supplied by Ciba-Geigy. Compounds 1–4 were prepared as described previously [7]. Water was purified through a Milli-Q unit (Millipore). Methanol was of gradient grade from Merck and perchloric acid was of analytical-reagent grade from Prolabo. The required pH was obtained after dilution as described in the technical notice: concentrated acid (70%, 13.6 g) was diluted with 1 l of water to give a solution of pH 1, and further dilutions furnished solutions of pH 2 (100 ml to 1 l), pH 1.3 (500 ml to 1 l) and pH 1.1 (794 ml to 1 l). All the solutions were filtered (0.45 μm), degassed and purged with helium. All amino acids were dissolved in the mobile phase to a concentration of about 1.6 mM (which corresponds to $1.6 \cdot 10^{-8}$ mol injected) and passed through a 0.45-μm membrane filter prior to injection.

RESULTS AND DISCUSSION

The enantiomeric separation of baclofen and compounds 1–4 on the crown ether CSP is summarized in Table I. For baclofen adequate resolution can easily be achieved (Figs. 2 and 3). The lower the temperature, the better the resolution becomes (α and R_s increase). Moreover, a high temperature (40°C) and addition of methanol (10%) give excellent results. A faster run could be obtained with sufficient resolution and enantioselectivity, but the limiting parameter was the column pressure [<2200 p.s.i. (1 p.s.i. = 6894.76 Pa)]. The designation of k'_s and k'_R as the first and second peaks under similar conditions was verified by chromatographing authentic samples of the enantiomers of baclofen (Fig. 3). The elution of the *R* isomer prior to the *S* isomer was the expected order of elution for almost all amino acids on the CR(+) column (Daicel information). Using the crown ether phase we were able to determine the minor enantiomer of baclofen at levels of less than 1%.

For the (benzo[*b*]furanyl)-GABA compounds 1–4, addition of methanol as an organic modifier

TABLE I

ANALYTICAL, HPLC: CAPACITY FACTORS (k') SELECTIVITY OF RESOLUTION (α) AND RESOLUTION (R_s) OF BACLOFEN AND COMPOUNDS 1–4

Capacity factor $k' = (t_x - t_0)/t_0$, separation factor $\alpha = (t_2 - t_0)/(t_1 - t_0)$ and peak resolution $R_s = 2(t_2 - t_1)/(w_1 + w_2)$, where w = peak width at baseline, t_0 = retention time of an unretained compound and t_x retention times of compounds (S or R).

Compound	Mobile phase ^a	Temperature 30°C				Temperature 40°C			
		k'_S	k'_R	α	R_s	k'_S	k'_R	α	R_s
Baclofen	A	25.4	42.0	1.65	8.07	17.4	25.8	1.48	6.11
	B	8.4	16.1	1.92	8.01	7.2	11.3	1.57	5.78
1	B	37.57		1	–	20.75		1	–
	C	53.91		1	–				
	D	64.54		1	–				
	B	53.74	60.43	1.12	1.99	29.16	32.62	1.12	1.75
2	B					28.68	30.87	1.07	1.06
3	B					31.32	33.58	1.07	1.21
4	B								

^a A = HClO₄ (pH 2); B = HClO₄ (pH 2)–CH₃OH (90:10);

C = HClO₄ (pH 1.3)–CH₃OH (90:10); D = HClO₄ (pH 1.1)–CH₃OH (90:10).

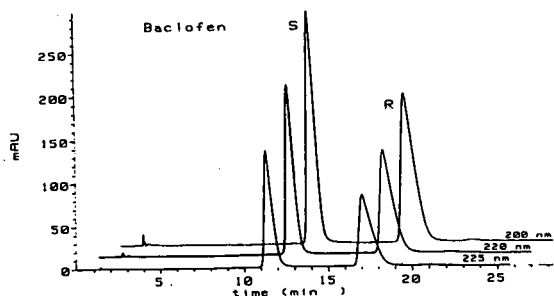


Fig. 2. Chromatograms of baclofen at three different wavelengths (225, 220 and 200 nm). Pseudo-three-dimensional representation. Eluent, HClO₄ (pH 2)–CH₃OH (90:10); temperature, 30°C; for other conditions, see Experimental.

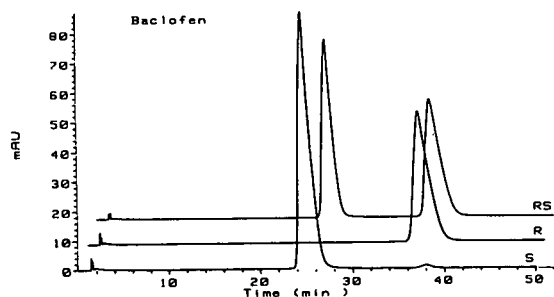


Fig. 3. Chromatograms of racemic (R,S)-baclofen and (R)- and (S)-enantiomers ($\lambda = 225$ nm). Pseudo-three-dimensional representation. Eluent, HClO₄ (pH 2); temperature, 40°C; for other conditions, see Experimental.

and an increase in temperature were necessary to decrease the capacity factors k' . Under the same eluting conditions (40°C, eluent B), 1–4 are much more retained ($k'_S = 20.75, 29.16, 28.68$ and 31.32 , respectively) than baclofen ($k'_S = 7.2$). These compounds should be more hydrophobic than baclofen but the literature data for the log P values of chlorophenyl and benzofuranyl moieties are very similar (2.81 and 2.67 respectively, where P is the partition coefficient measured in n -octanol–water) [23]. With 1–4, hydrogen bonding is possible between the ammonium group and the oxygen of the benzofuran ring [24], which could perhaps explain the increase in retention times. Compound 1 (without a methoxy group) is much less retained than 2–4 but poor resolution (shoulder) was observed even at low temperature (10 or 20°C) and low pH (1.1), where the product seems to be definitely retained on the stationary phase. These differences in retention behaviour are almost certainly due to differences in the hydrophobic nature between 1 ($k' = 20.75$) and 2–4 ($k'_S = 29.16, 28.68$ and 31.32 , respectively) (40°C, eluent B) (Fig. 4) and 1 ($k' = 37.57$) and 2 ($k'_S = 53.74$) (30°C, eluent B). This may be due to the hydrophobicity of the methoxy moiety [23].

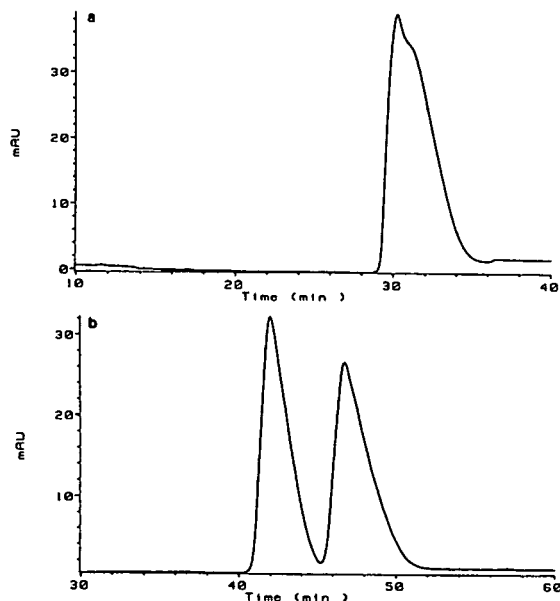


Fig. 4. Chromatograms of (a) **1** and (b) **2** ($\lambda = 225$ nm). Eluent, HClO_4 (pH 2)– CH_3OH (90:10); temperature, 40°C ; for other conditions, see Experimental.

Steric bulk may be another factor that affects the separation; it can either enhance or decrease the enantioselectivity. This depends on whether or not a bulky group prevents the ammonium group from forming a strong inclusion complex. The presence of the methoxy moiety on the heteroaromatic ring seems necessary to observe separation (**1**, $\alpha = 1$) (Fig. 4) and the position of this group changes the enantioselectivity (**2–4**, $\alpha = 1.12$, 1.07 and 1.07 , respectively) (40°C , eluent B). The 5-substitution seems more favourable (Fig. 5). The data in Table I also show that **1** is progressively more retained with decreasing pH.

Preparative separation of the enantiomers of baclofen was easily achieved by HPLC after two-step derivatization [19]. Hydrolysis of the diastereoisomers obtained led to the corresponding enantiomers, whose optical purity was measured by chiral HPLC. The same procedure was applied to the benzo[*b*]furanyl-GABA compounds **1–4**. Attribution of the absolute configuration of their diastereoisomers was made by comparison with baclofen diastereoisomers (relative ^1H and ^{13}C NMR chemical shifts, analytical HPLC) [25]. After hydrolysis the recovered enantiomers have a configuration fully in accordance with the order of elution; the least and most retained enantio-

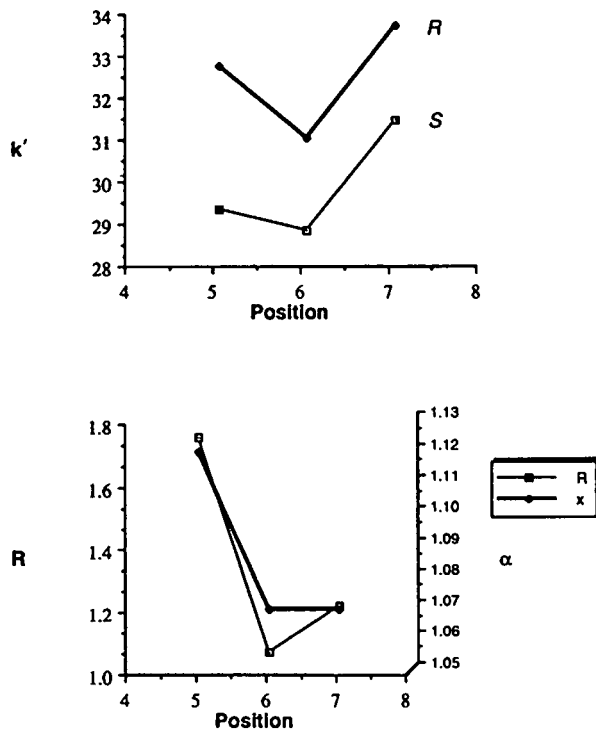


Fig. 5. Variations of the capacity factor (k'), enantioselectivity (α) and resolution (R), with the methoxy position in compounds **2–4**.

mers are *S* and *R*, respectively. The good separation of the optical isomers of **2** makes the chromatographic method suitable for determining optical purity and for studies on pharmacological distribution.

ACKNOWLEDGEMENTS

We gratefully acknowledge Ciba-Geigy (Rueil-Malmaison, France; Basle, Switzerland) for the generous provision of (*R,S*)-(\pm)-baclofen, (*R*)-(-)-baclofen hydrochloride and (+)-(*S*)-baclofen hydrochloride.

REFERENCES

- 1 H. Möhler, *Arzneim. Forsch./Drug Res.*, 42 (1992) 211.
- 2 N.G. Bowery, *Trends Pharmacol. Sci.*, 3 (1982) 400.
- 3 D.R. Hill and N.G. Bowery, *Nature*, 290 (1981) 149.
- 4 N.G. Bowery, G.W. Price, A.L. Hudson, D.R. Hill, G.P. Wilkin and M.J. Turnbull, *Neuropharmacology*, 23 (1984) 219.

- 5 N.G. Bowery, *Trends Pharmacol. Sci.*, 10 (1989) 401.
- 6 H.R. Olpe, H. Demiéville, V. Baltzer, W.L. Bencze, W.P. Koella, P. Wolf and H.L. Hass, *Eur. J. Pharm.*, 52 (1978) 133.
- 7 P. Berthelot, C. Vaccher, A. Musadad, N. Flouquet, M. Debaert and M. Luyckx, *J. Med. Chem.*, 30 (1987) 743.
- 8 N.G. Bowery and G.D. Pratt, *Arzneim. Forsch./Drug Res.*, 42 (1992) 215.
- 9 M. Lienne, M. Caude, A. Tambute and R. Rosset, *Analisis*, 15 (1987) 431.
- 10 B. Sallerin-Caute, B. Monsarrat, Y. Lazorthes, J. Cros and R. Bastide, *J. Liq. Chromatogr.*, 11 (1988) 1753.
- 11 V. Das Gupta, *J. Liq. Chromatogr.*, 10 (1987) 749.
- 12 E.W. Wuis, R.J.M. Dirks, T.B. Vree and E. Van der Kleyn, *J. Chromatogr.*, 337 (1985) 341.
- 13 W. Dieterle, J.W. Faigle and H. Mory, *J. Chromatogr.*, 168 (1979) 27.
- 14 D. Krauss, H. Spahn and E. Mutscheler, *Arzneim. Forsch./Drug Res.*, 38 (1988) 1533.
- 15 C.G. Swahn, H. Beving and G. Sedvall, *J. Chromatogr.*, 162 (1979) 433.
- 16 G. Kochak and F. Honc, *J. Chromatogr.*, 310 (1984) 319.
- 17 A. Sioufi, G. Kaiser, F. Leroux and J.P. Dubois, *J. Chromatogr.*, 450 (1988) 221.
- 18 D.F. Smith and W.H. Pirkle, *Psychopharmacology*, 89 (1986) 392.
- 19 C. Vaccher, P. Berthelot, N. Flouquet and M. Debaert, *J. Chromatogr.*, 542 (1991) 502.
- 20 E.W. Wuis, E.W.J. Beneken Kolmer, L.E.C. Van Beijsterveldt, R.C.M. Burgers, T.B. Vree and E. Van der Kleyn, *J. Chromatogr.*, 415 (1987) 419.
- 21 H. Spahn, D. Krauss and E. Mutschler, *Pharm. Res.*, 5 (1988) 107.
- 22 R.P. Weatherby, R.D. Allen and G.A.R. Johnston, *J. Neurosci. Methods*, 10 (1984) 23.
- 23 R.F. Rekker, *The Hydrophobic Fragmental Constant (Pharmacochemistry Library, Vol. 1)*, Elsevier, Amsterdam, 1977, p. 48.
- 24 P. Berthelot, C. Vaccher, N. Flouquet, M. Luyckx, C. Brunet, T. Boulanger, J.P. Fripiat, D.P. Vercauteren, M. Debaert, G. Evrard and F. Durant, *Eur. J. Med. Chem.*, 26 (1991) 395.
- 25 C. Vaccher, P. Berthelot, S. Ebrik, M.P. Vaccher, N. Flouquet and M. Debaert, in preparation.

High-performance gel-permeation chromatographic analysis of protein aggregation

Application to bovine carbonic anhydrase

Claudio De Felice

Endocrine Research Laboratory, National Children's Medical Research Centre, 3-35-31 Taishido, Setagaya-ku, Tokyo 154 (Japan)

Kou Hayakawa*

Metabolism Research Laboratory, National Children's Medical Research Centre, 3-35-31 Taishido, Setagaya-ku, Tokyo 154 (Japan)

Takayuki Watanabe and Toshiaki Tanaka

Endocrine Research Laboratory, National Children's Medical Research Centre, 3-35-31 Taishido, Setagaya-ku, Tokyo 154 (Japan)

(First received January 4th, 1993; revised manuscript received April 6th, 1993)

ABSTRACT

Protein association in bovine carbonic anhydrase (bCA) was investigated by high-performance gel-permeation chromatography (HPGPC). It was shown that bCA undergoes a time-dependent aggregation after freezing and storing at -20°C . The addition of 50% ethylene glycol or glycerol prevented the aggregation. The HPGPC data were confirmed by the use of cross-linking with subsequent sodium dodecyl sulphate–polyacrylamide gel electrophoretic analysis. The esterase activity of the aggregated bCA was comparable to that of the monomer, suggesting that the observed protein association does not affect the esterase catalytic centre of bCA. This study illustrates how HPGPC can be a convenient and reliable tool for monitoring storage-induced aggregation of proteins.

INTRODUCTION

Many proteins show aggregation or changes in solubility under certain solvent conditions [1,2]. As aggregation can directly affect the chromatographic behaviour of proteins in high-performance liquid chromatography (HPLC), and possibly limit analysis and purification, a systematic

analysis of protein–protein interactions is important to produce optimized separations in both analytical- and preparative-scale operation [3]. To date, chromatographic studies of protein aggregation have chiefly been performed by size exclusion [4,5], although hydrophobic interaction chromatography has recently been applied to the aggregation of β -lactoglobulin A [3].

A high-performance gel-permeation chromatographic (HPGPC) method with non-ionic detergent in the eluent has previously been re-

* Corresponding author.

ported to be a convenient, sensitive and high-yield technique for protein separation according to molecular mass [6]. In this study, an application of this HPGPC method to the analysis of protein aggregation by use of bovine carbonic anhydrase (bCA) was investigated.

EXPERIMENTAL

Chemicals and reagents

Carbonic anhydrase (carbonate dehydratase; carbonate hydro-lyase; EC 4.2.1.1) from bovine erythrocytes was obtained from two sources: Sigma carbonic anhydrase (Lot No. 115F94102) was from Sigma (S. Louis, MO, USA), and Boehringer Mannheim carboanhydrase (Lot No. 13026121-31) was purchased from Boehringer Mannheim Yamanouchi (Tokyo, Japan). Dimethyl suberimidate dihydrochloride (DMS) was purchased from Sigma, veronal buffer from Whittaker Bioproducts (Walkersville, MD, USA), triacetin (glycerol triacetate), sodium acetate, anhydrous and bromothymol blue from Wako (Osaka, Japan) and Nonidet P-40 from Nacalai Tesque (Kyoto, Japan).

Determination of bCA by HPGPC

A Model 2150 HPLC pump with a Model 2152 LC controller (Pharmacia LKB, Uppsala, Sweden) was utilized. Sample injection was carried out with a U6K universal liquid chromatographic injector (Millipore, Milford, MA, USA) with a 2-ml loop. A line filter (GL Sciences, Tokyo, Japan) was inserted between the injector and the column. The flow-rate was 0.4 ml/min with a column inlet pressure of *ca.* 40–50 kg/cm² when two JASCO Bio-Fine GFCSI150-K columns (300 × 7.9 mm I.D.) and a glass column (GlasPac Column TSK G 3000SW, 300 × 8 mm I.D.; Pharmacia LKB Biotechnology, Bromma, Sweden) were used. When using a column consisting of the usual type of stainless-steel tube (Shimpack Diol-300, 250 × 7.9 mm I.D.; Shimadzu, Kyoto, Japan), the flow-rate was 1.2 ml/min with a column inlet pressure of *ca.* 100–150 kg/cm². A sodium phosphate buffer (0.1 M NaH₂PO₄, pH 6.0) solution containing sodium chloride (0.3 M), glycerol (30%, v/v) and the non-ionic detergent Nonidet P-40 (NP-40)

(0.15%, v/v) was utilized as the eluent. Detection of bCA was carried out with a UV detector (Model 655A-21; Hitachi, Tokyo, Japan) at 280–290 nm with a range of 0.64 absorption units full-scale (a.u.f.s.). A synthetic polymer gel column (TSK 4000 PW, 300 × 7.5 mm I.D.; Tosoh, Tokyo, Japan) was also tested.

Aggregation regime of bCA

A solution of 0.1 g/ml of bCA in 0.6 M sodium phosphate buffer (pH 6.0) containing 0.6 M sodium chloride, 2.5% (v/v) glycerol and 0.15% (v/v) NP-40 was stored in aliquots of 0.1 ml at –20°C for 12 h. Under the described conditions, a two-peak chromatogram was obtained by HPGPC.

Sodium dodecyl sulphate–polyacrylamide gel electrophoresis (SDS-PAGE)

SDS-PAGE was performed according to the procedure of Laemmli [7] using 7.5% and 12% acrylamide concentrations. Proteins were detected by Coomassie Brilliant Blue staining.

Cross-linking analysis

To confirm aggregation, DMS was used as a cross-linking agent at a final concentration of 1 mg/ml according to the procedure of Hitchcock [8]. After reaction for 30 min, samples were analysed by SDS-PAGE. Acrylamide concentrations of 7.5% and 12% were used.

Assay of carbonic anhydrase and esterase activity

The carbon dioxide hydration activity was assayed according to the procedure of Armstrong *et al.* [9]. The esterase activity of bCA was characterized by the hydrolysis of the ester triacetin. The reaction was monitored by the liberation of acetic acid. This product was measured by salting-out reversed-phase HPLC, as described previously [10], except that acetate was detected by UV absorption at 210 nm. Esterase activities of both aggregated and monomeric bCA were assayed. Specific activity was expressed as picomoles of acetate liberated per minute per milligram of protein.

Protein content

Protein concentrations were assayed by using a BCA protein assay kit from Pierce (Rockford, IL, USA). BSA was used as a standard protein.

Statistical analysis

The statistical evaluation of the difference in esterase activity between aggregated and monomeric bCA was carried out by Wilcoxon's test. *p* values less than 0.05 were considered to be significant.

RESULTS AND DISCUSSION

A high-recovery protein separation system containing a non-ionic detergent (NP-40) and 2.5% (v/v) glycerol has been developed previously [6]. However, the bCA peak was asymmetric under the conditions originally described. Sufficient peak symmetry could be obtained only by using high glycerol concentrations (30%, v/v) (Fig. 1), and no further improvement in resolution was achieved by changing the phosphate (0.05, 0.15 M), chloride (0.2, 0.4 M) or NP-40 (0.1, 0.2%, v/v) concentrations or by adding 0.1 M sodium sulphate.

A two-peak chromatogram was observed after freezing and storage of bCA (0.1 g/ml) in a

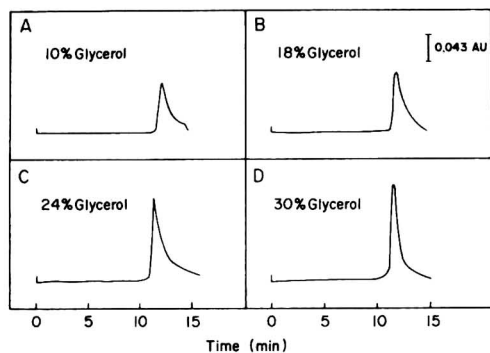


Fig. 1. Effect of different glycerol concentrations in the eluent on the peak shape of bCA chromatogram. A TSK G 3000 SW column (300 × 8 mm I.D.) was used. The eluent conditions except glycerol concentration were as described under Experimental. bCA (0.1 mg) was injected into the HPGPC system. Glycerol concentration: (A) 10; (B) 18; (C) 24; (D) 30% (v/v).

glycerol-phosphate-chloride solution at -20°C for 12 h (Fig. 2B). A two-peak chromatogram was also observed using a Tosoh TSK 4000 PW column (data not shown). As under the same conditions similar chromatographic patterns with both silica and synthetic polymer gel columns were observed, it seems unlikely that mechanisms other than gel permeation play a role in this chromatographic separation.

Reproducible bCA aggregation was obtained under the following incubation conditions: solution composition 0.1 g/ml bCA, 0.6 M NaH_2PO_4 , 0.6 M NaCl, 0.15% (v/v) NP-40 and 2.5% (v/v) glycerol, storage temperature -20°C and storage time 12 h. A time course analysis was also carried out: the percentage of bCA multimers, as assessed by the aggregated/monomer peak-height ratio, increased during the first 3 h, before reaching a peak-height plateau rate

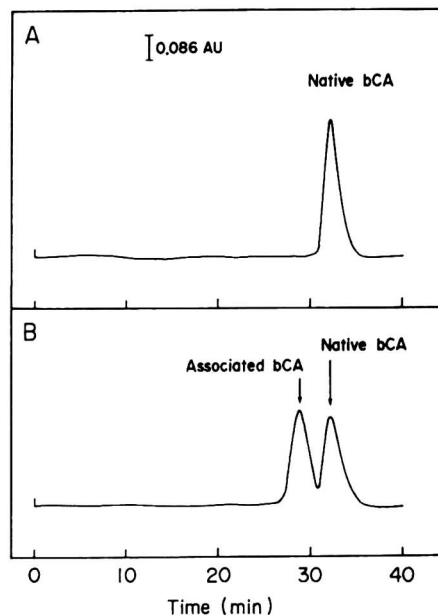


Fig. 2. Separation of aggregated bCA and bCA monomer. A three-column system (as described previously [6]) was used: a TSK G 3000 SW column (300 × 8 mm I.D.) and two JASCO Bio-Fine GFC SI 150-K columns (300 × 7.9 mm I.D.) were joined in series. Other conditions were as described under Experimental. Frozen-stored and freshly dissolved samples of bCA (0.5 mg) were injected into the HPGPC system.

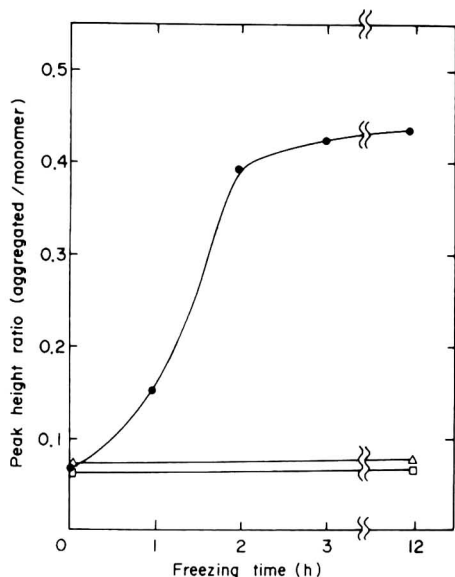


Fig. 3. Time course analysis of aggregation in bCA and the preventive effect of glycerol and ethylene glycol on the formation of bCA multimer species. Protein aggregation was analysed with the Shimpack Diol-300 column as described under Experimental. Peak heights were measured manually. ● = bCA, aggregation regimen as described under Experimental; □ = bCA, addition of 50% (v/v) glycerol; △ = bCA, addition of 50% (v/v) ethylene glycol.

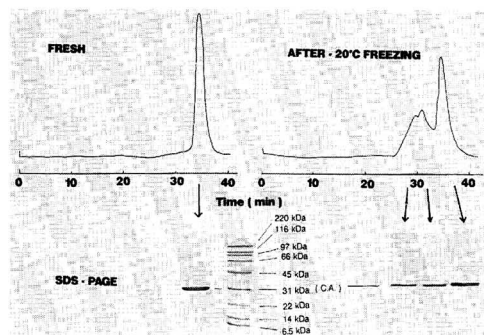


Fig. 4. SDS-PAGE analysis of associated bCA and bCA monomer. Fractionation was carried out by separating bCA (1 mg) with a three-column system as described in Fig. 2. Samples of 0.02 ml of protein peak fractions were analysed by SDS-PAGE at an acrylamide concentration of 12%. Protein bands were detected by Coomassie Brilliant Blue staining. Molecular mass standards for SDS-PAGE (Bio-Rad Labs.) were used. kDa = kilodalton.

of about 0.45 (Fig. 3). On the other hand, in the presence of 50% (v/v) glycerol or 50% (v/v) ethylene glycol, multimer species were not detectable (Fig. 3). Moreover, a two-peak chromatogram was not observed when the samples were frozen and stored at -80°C for as long as 3 weeks. The results of a standard SDS-PAGE analysis of the proteins in the HPGPC peak fractions are shown in Fig. 4. After boiling with 1% (w/v) SDS in Laemmli sample buffer the apparently higher-molecular-mass fraction, *i.e.*, the faster eluting peak, contained only M_r 31 000 bCA monomer (Fig. 4, bottom right). On the other hand, the inability of NP-40, a milder detergent than SDS, to separate the aggregated bCA into monomer suggests the presence of a hydrophobic interaction mechanism under the observed aggregation. In order to confirm aggre-

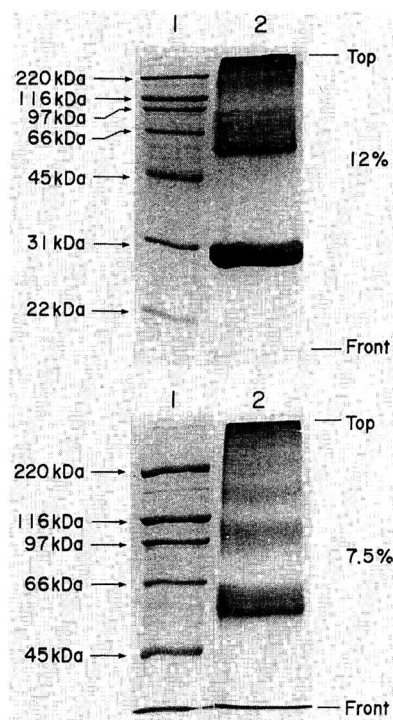


Fig. 5. Demonstration of bCA multimer species formation by cross-linking method. Details of the procedure are described under Experimental. Lanes: 1 = standard proteins (Bio-Rad Labs.); 2 = two-peak bCA treated with DMS. Top, 12% acrylamide; bottom, 7.5% acrylamide. Aliquot samples of 0.01 mg of bCA were analyzed.

gation, a cross-link analysis was carried out as described under Experimental. SDS-PAGE results of cross-linking confirmed the presence of multimer species, mainly dimers in two-peak bCA (Fig. 5). In contrast, no corresponding multimer bands were detectable in single-peak bCA (data not shown). Cross-linked dimer species migrated in a broad band at an apparent molecular mass of 54 000–66 000, while trimers and tetramers were detectable in fainter bands (Fig. 5, bottom).

In order to identify functional changes possibly related to aggregation, the hydrolytic activities of the bCA multimers on triacetin were determined and compared with the bCA monomer. As shown in Table I, the esterase activity of the multimeric species did not differ significantly from that of the bCA monomer. The preserved esterase activity of the bCA multimers indicates that the aggregation occurs without affecting the esterase catalytic centre of the enzyme. There-

TABLE I
COMPARISON OF ESTERASE ACTIVITIES BETWEEN MONOMERIC AND ASSOCIATED bCA

Esterase activity using triacetin as substrate was measured as described under Experimental. Specific activity was expressed as picomoles of acetate liberated per minute per milligram of protein. No statistically significant difference was observed between the esterase activities of aggregated bCA and bCA monomer (Wilcoxon's test, $p > 0.05$).

Sample No.	Monomeric bCA	Associated bCA
1	24.7	31.0
2	19.8	22.6
3	43.5	38.0
4	42.7	28.6
5	36.5	28.9
6	38.1	27.3
7	31.1	35.3
8	35.1	33.2
9	31.0	25.3
Mean \pm S.D.	30.0 \pm 4.9	33.6 \pm 7.9

fore, the presence of intact bCA enzymatic activity despite aggregation suggests that the observed phenomenon consistently differs from that occurring under denaturing conditions, such as in the presence of guanidine hydrochloride, in which the catalytic activity is significantly lost [2]. Moreover, the observation of the formation of bCA multimer species after freezing and storage at -20°C but not at -80°C may provide additional insight into the development of methods to avoid aggregation in enzyme solutions.

Thus, given the combined characteristics of high sensitivity, analytical speed and wide commercial availability of its components, this HPGPC method has been shown to be a simple, applicable and useful tool for the systematic analysis of protein-protein interactions.

ACKNOWLEDGEMENTS

This work was supported by the Ministry of Health and Welfare Japan and Sumitomo Pharmaceuticals, Osaka, Japan. One of the authors (C.D.F.) is on a post-doctoral fellowship from the Science and Technology Agency (STA), Japan.

REFERENCES

- 1 R.R. Burgess, in D.L. Oxender and C.F. Fox (Editors), *Protein Engineering*, Alan R. Liss, New York, 1987, pp. 71–82.
- 2 J.L. Cleland and D.I.C. Wang, *Biochemistry*, 29 (1990) 11072–11078.
- 3 N. Grinberg, R. Blanco, D.M. Yarmush and B.L. Karger, *Anal. Chem.*, 61 (1989) 514–520.
- 4 J. Porath and P. Flodin, *J. Chromatogr.*, 3 (1960) 103.
- 5 D.H. Atha and G.K. Ackers, *Arch. Biochem. Biophys.*, 164 (1974) 392.
- 6 K. Hayakawa, C. De Felice, T. Watanabe and T. Tanaka, *J. Chromatogr.*, 616 (1993) 327–332.
- 7 U.K. Laemmli, *Nature*, 227 (1970) 680.
- 8 S.E. Hitchcock, *Biochemistry*, 14 (1975) 5162.
- 9 J.M. Armstrong, D.V. Myers, J.A. Verpoorte and J.T. Edsall, *J. Biol. Chem.*, 241 (1966) 5137–5149.
- 10 J. Oizumi and K. Hayakawa, *Biochem. J.*, 271 (1990) 45–49.

High-performance liquid chromatographic determination of the isomeric purity of a series of dioxolane nucleoside analogues[☆]

M.P. Di Marco*, C.A. Evans, D.M. Dixit, W.L. Brown, M.A. Siddiqui, H.L.A. Tse, H. Jin, N. Nguyen-Ba and T.S. Mansour

BioChem Therapeutic Inc., 531 Boulevard des Prairies, Laval, Québec, H7V 1B7 (Canada)

(First received January 12th, 1993; revised manuscript received April 27th, 1993)

ABSTRACT

Racemic (\pm)-*cis*-2 hydroxymethyl-4-(cytosin-1'-yl)-1,3-dioxolane analogue (BCH-204) exhibited high levels of anti-HIV activity, but also showed cytotoxicity at the active concentration. To examine the possibility of enantiomerically separating the HIV activity from the cytotoxicity in the dioxolane nucleosides, high-performance liquid chromatography using chiral stationary phase columns was examined. The successful separation of dioxolane compounds was demonstrated utilizing optimum conditions of columns, solvents, flow-rates and temperature. In the reversed-phase mode, the cyclodextrin columns Cyclobond I SP and RSP were used to separate the enantiomers of *cis*- and *trans*-(\pm) dioxolane-C, and the protein column α -AGP was successful in separating enantiomerically *cis*-(\pm) dioxolane-G and *cis*- and *trans*-enantiomeric forms of (\pm)-dioxolane-A. In the normal-phase mode, one of the cellulose columns, Chiralcel OJ, successfully separated enantiomerically (\pm)-dioxolane-T nucleosidic analogue.

INTRODUCTION

The enantiomeric resolution of BCH-189 by high-performance liquid chromatography (HPLC) using the chiral column Cyclobond I Ac [1] produced the promising nucleoside analogue 3TC, which is just completing Phase II clinical trials for the treatment of HIV infection and AIDS. 3TC has an unnatural sugar configuration and was found to be considerably less toxic than the (+)-enantiomer owing to the higher selectivity of the drug for HIV reverse transcriptase over mammalian DNA polymerases [2,3]. Other in-

teresting nucleoside analogues, 1,3-dioxolanes, where the 3'-thia moiety is replaced with oxygen, have been developed by Belleau *et al.* [2]. Both pyrimidine and purine 1,3-dioxolane nucleoside analogues, such as BCH-203, BCH-204 (related racemic diastereoisomers), BCH-344 [4], BCH-571 and BCH-187 (Fig. 1), have shown very interesting anti-HIV properties [5]. Therefore, it was necessary to resolve their enantiomers and study their pharmacological profiles. Further, we have developed a chiral synthesis of these compounds, which requires controlling two epimerizable acetal centres [6]. HPLC was used to evaluate the diastereomeric and enantiomeric purities of key synthetic intermediates and the final products prior to biological evaluation.

HPLC is a useful tool in enantiomeric separations. The availability of many different kinds of

* Corresponding author.

[☆] Dedicated to the memory of the late Professor Bernard Belleau.

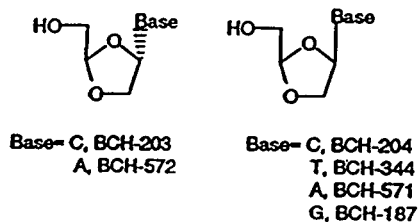
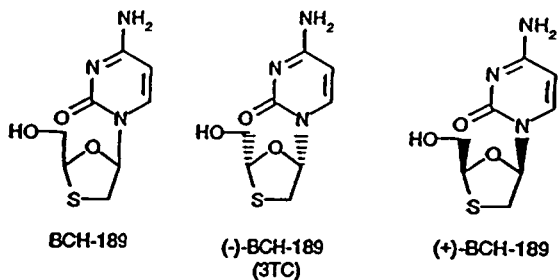


Fig. 1. 1,3-Dioxolane nucleosides with anti-HIV activity.

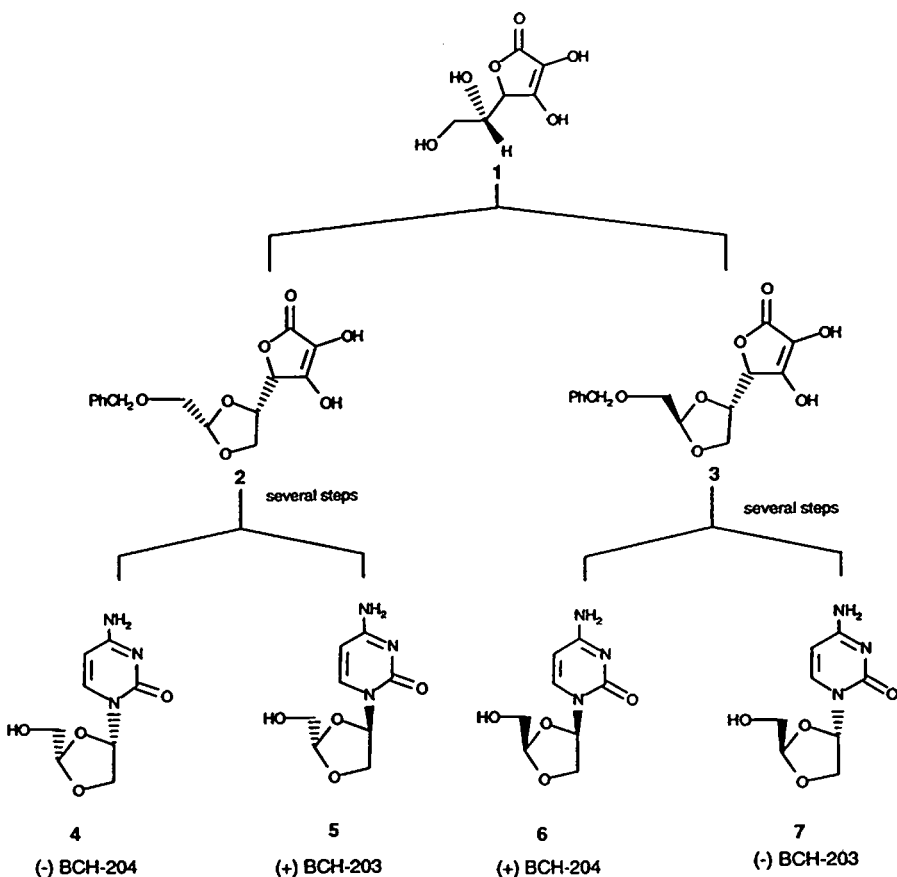


Fig. 2. Synthesis of BCH-203 and BCH-204 stereoisomers from L-ascorbic acid.

chiral stationary phases (CSPs) gives chromatographers a wide choice in the selection of CSPs for optimizing enantiomeric separations. In this respect, we have developed procedures using CSPs with suitable mobile phases to monitor the chiral purity of these intermediates and to achieve the resolution of 1,3-dioxolane nucleosides on preparative scale.

EXPERIMENTAL

Materials

The racemic dioxolane compounds, BCH-204, BCH-203, BCH-187, BCH-344, BCH-571 and BCH-572 (Fig. 1) and compounds 1–7 (Fig. 2), were synthesized in our laboratories. The columns Cyclobond I RSP and SP (each 250 × 4.6 mm I.D.) were purchased from Astec (Whippany, NJ, USA), Chiralcel OJ (250 × 4.6 mm)

from Regis (Morton Grove, IL, USA) and α -AGP from Richard Scientific (Novato, CA, USA). The mobile phase solvents were of HPLC grade from BDH (Montreal, Canada). Triethylamine was purchased from BDH and treated by titrating a 0.05% aqueous solution and adjusting it to pH 7.0 with glacial acetic acid. Buffers were purchased from J.T. Baker (Montreal, Canada) and treated accordingly. Water was of HPLC grade obtained from a Millipore–Waters Milli-Q water-purification system.

Methods

HPLC was performed at various temperatures with a Waters Model 600 multi-solvent delivery system, a WISP 712 automatic injector and a Waters UV detector. The integrator was a Waters Model 740 data module.

RESULTS AND DISCUSSION

One of the important factors in choosing the chiral column and the mode of HPLC for the analysis of a particular compound is the solubility characteristic of that compound [7]. Because BCH-204 is readily soluble in water, reversed phase HPLC was examined. One of the reversed phase chiral columns chosen was in the cyclodextrin series. Cyclobond columns were first evaluated at different concentrations of triethylammonium (TEAA) buffer solutions and various pH values. Separation was achieved with a more derivatized cyclodextrin column than its native column, β -cyclodextrin (Cyclobond I). This derivatized column, called Cyclobond I RSP [(*R,S*-hydroxypropyl ether)], has secondary hydroxypropyl residues, which allow further stereospecific hydrogen bonding, enhancing separations of nucleosides [8]. Decreasing the concentration of TEAA provided a separation of enantiomers, but was not optimum. An organic modifier acetonitrile, was chosen to enhance the separation. Acetonitrile has been reported to have a greater affinity than methanol for the cyclodextrin cavity [8]. Fig. 3 demonstrates the HPLC conditions used for the separation of BCH-204.

Further development of this chromatographic

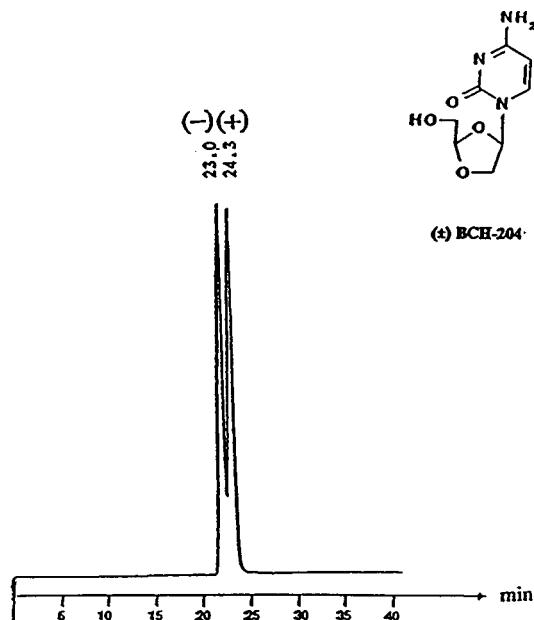


Fig. 3. Resolution of (\pm)-BCH-204. Column, Cyclobond I RSP (250 \times 4.6 mm I.D.); flow-rate, 0.22 ml/min at 0°C; mobile phase, acetonitrile–water (5:95) containing 0.05% of TEAA (pH 7.1) (isocratic); detection, 265 nm; injection, 10 μ l of a 1 mg/ml solution.

method was needed when the racemic *trans* form of BCH-204 (BCH-203) had to be separated. Ideally, these two compounds had to be resolved on the same column and under the same conditions in order to calculate the diastereomeric and enantiomeric excess to help to optimize synthetic procedures, as will be demonstrated later. To achieve enantioselectivity for both of these compounds a second Cyclobond I SP column was added in series with the Cyclobond I RSP column. The combination of Cyclobond I SP and Cyclobond I RSP columns was chosen because there was a better resolution for BCH-204 with the Cyclobond I RSP and a better resolution for BCH-203 with the Cyclobond I SP. The concentration of the organic modifier, acetonitrile, was lowered from 5% to 3%, while the other conditions, flow-rate, temperature and buffer concentrations, remained the same. Fig. 2 illustrates why both racemic compounds had to be evaluated under the same conditions.

The chiral synthesis of all the stereoisomers of cytosine dioxolane nucleosides BCH-203 and

BCH-204 was achieved starting from L-ascorbic, (1), which provided, in the desired non-selective manner, all the nucleosides in optically pure form for biological testing (Fig. 2). As shown in Fig. 4, all four enantiomers could be resolved in a single chromatogram with all pure stereoisomers of BCH-203 and BCH-204 obtained by the synthetic route superpositioned. However, as there was no baseline separation of the enantiomers of BCH-204 and BCH-203, an accurate determination of the enantiomeric excess or peak purity could not be achieved owing to the tailing of some of the peaks. However, this type of HPLC technique can establish, with further baseline separation, the enantiopurity (% ee) of each of the analogues (4, 5, 6 and 7 in Fig. 2). The chiral synthesis allows the assignment of the absolute configuration of the stereoisomers. Further, generation of optically pure 4 and 5 relied on the efficient separation of diastereoisomers 2 and 3 by fractional crystallization; therefore, an HPLC method was developed to assess the diastereomeric excess of 2 and 3. An analytical separation of 2 and 3 was achieved on a reverse-phased Whatman Partisil ODS-3 (5 μ m) column

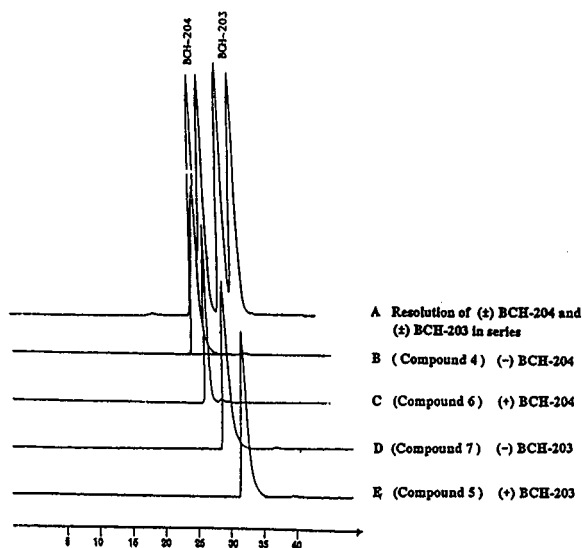


Fig. 4. Resolution of (\pm)-BCH-204 and (\pm)-BCH-203 with columns connected in series. Conditions as in Fig. 3, except that two columns, Cyclobond I RSP and Cyclobond I SP columns (each 250×4.6 mm I.D.), were placed in series and the mobile phase was acetonitrile-water (3:97) containing 0.05% of TEAA (pH 7.1) (isocratic).

(250×4.6 mm I.D.). Fig. 5 shows the chromatogram for (A) the diastereomeric compounds and also the analytical chromatograms after the compounds had been separated preparatively (same column packing but 250×22.5 mm I.D.). Compound 2 was obtained in 96.5% purity with a retention time of 31.5 min (Fig. 5B) and 3 in 97.2% purity with a retention time of 33.0 min (Fig. 5C). The high diastereomeric purity of 2 and 3 indicates that this HPLC method is suitable for evaluating the optical purity of dioxolane intermediates early in the synthetic scheme.

Even though the α -AGP (α -acid glycoprotein) protein column did not successfully separate BCH-203 and BCH-204 [(\pm)-dioxolane-C], other dioxolane compounds, such as the purine analogues, showed optimum peak resolutions. α -AGP consists of a long chain of 181 amino acid residues and 5 carbohydrate units (45% of the total molecule by mass) [9]. This carbohydrate moiety of α -AGP gives the protein a very acidic character [10]. This protein column thus possesses numerous binding sites [11] and is suitable for the enantiomeric resolution of many nucleosides. One such nucleoside, BCH-187 [*cis*-2-hydroxymethyl-4-(guanin-9'-yl)-1,3-dioxolane], achieved excellent separations when a charged modifier, such as 5 mM TBAB (tetra-*n*-butylammonium bromide), was added to the sodium phosphate buffer solution of the mobile phase with two α -AGP columns connected in series. TBAB in the mobile phase strongly induces chiral selectivity [12]. Quaternary ammonium compounds such as TBAB increase the retention time and cause competition between the solute and TBAB in binding to the protein column [12]. Initially, in developing the chiral HPLC method for this compound, changing the pH or adding uncharged modifiers such as methanol, 2-propanol or acetonitrile [12] did not succeed in separating these enantiomers, but on the addition of a small amount of TBAB, resolution was achieved as shown in Fig. 6.

Another purine analogue, BCH-571 [*cis*-2-hydroxymethyl-4-(adenin-9'-yl)-1,3-dioxolane], could also be separated on the α -AGP column, but a normal phosphate buffer mobile phase, without the addition of uncharged or charged

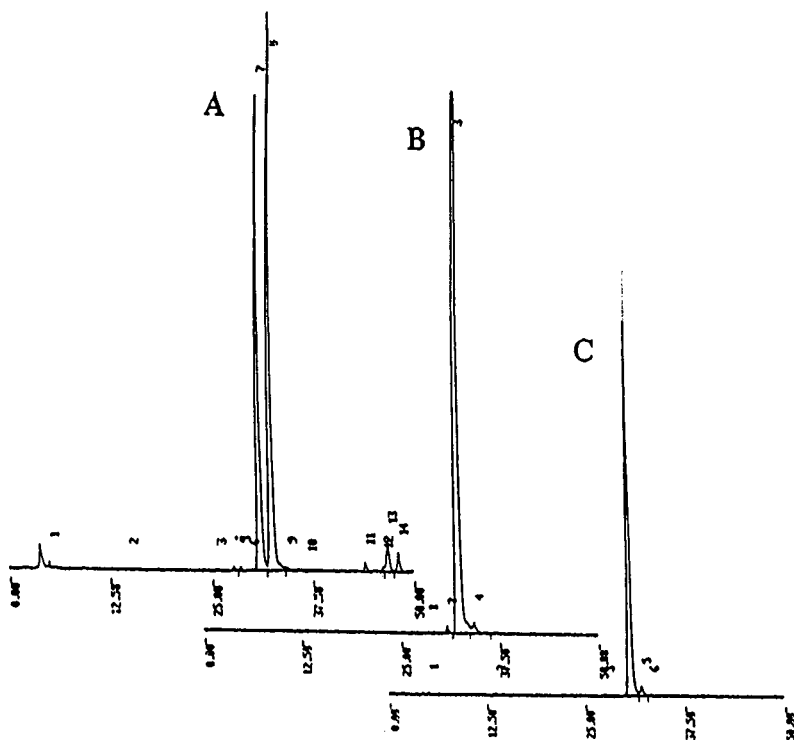


Fig. 5. Chromatograms of (A) diastereoisomers 2 and 3, (B) compound 2 (96.5%) and (C) compound 3 (97.2%). Column, Partisil ODS, 5 μm (250 \times 4.6 mm I.D.); flow-rate, 1.0 ml/min; mobile phase, (A) acetonitrile + 0.04%TFA, (B) 0.04% TFA (aqueous), linear gradient from 10 to 50% in 50 min; UV detection at 265 nm.

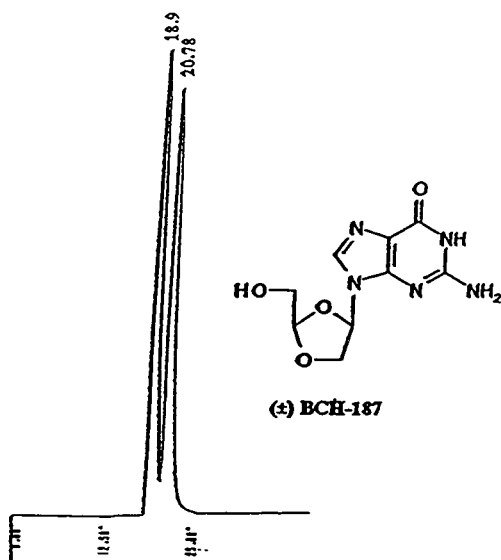


Fig. 6. Separation of (+)-BCH-187. Columns, two chiral α -AGP (100 \times 4.0 mm I.D.) in series; temperature, ambient; flow-rate, 0.15 ml/min; mobile phase, 0.02 M NaH_2PO_4 -5 mM TBAB (pH 7.0) (isocratic); detection, UV at 270 nm.

modifiers, was needed to separate these enantiomers successfully. The results of this separation are shown in Fig. 7. Both of these nucleosides, BCH-187 and BCH-571, were separated at room temperature.

The dioxolane nucleoside BCH-572 [*trans*-2-hydroxymethyl-4-(adenin-9'-yl)-1,3-dioxolane] was also resolved on the α -AGP column. The resolution of this compound with a mobile phase of pure phosphate buffer (pH 7.0) did not result in the separation of enantiomers; however, the addition of 0.1 M NaCl [12] to the mobile phase and decreasing the temperature slightly to 15°C improved the resolution of BCH-572; the optimum HPLC conditions for this nucleoside are demonstrated in Fig. 8.

For these three purine dioxolane nucleosides we have shown that by adding various uncharged modifiers to the mobile phases and decreasing the temperature, one can optimize enantiomeric

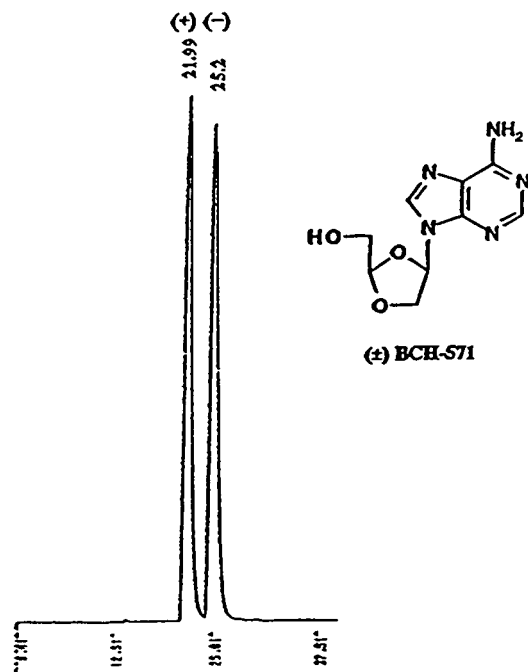


Fig. 7. Enantiomeric resolution of (\pm)-BCH-571. Conditions as in Fig. 6, but with mobile phase 0.02 M NaH₂PO₄ (pH 7.0).

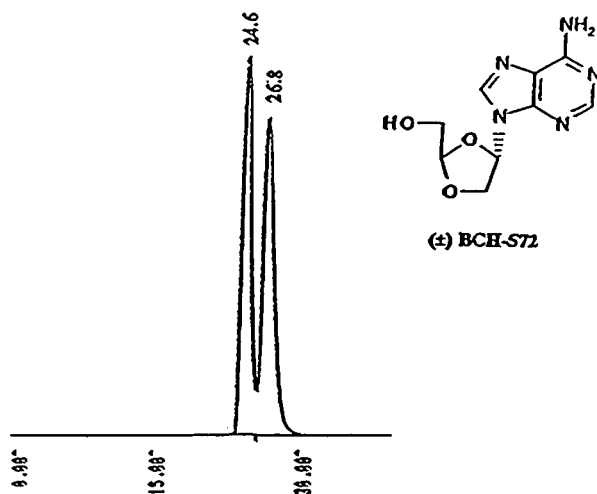


Fig. 8. Enantiomeric separation of (\pm)-BCH-572. Conditions as in Fig. 6, except the temperature was lowered to 15°C and the mobile phase was 0.02 M NaH₂PO₄-0.1 M NaCl (pH 7.0).

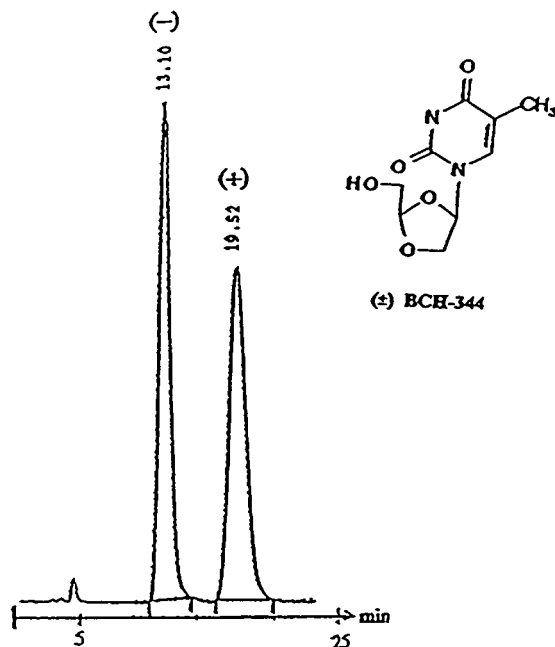


Fig. 9. Chiral separation of (\pm)-BCH-344. Column, Chiralcel OJ (250 \times 4.6 mm I.D.) temperature, ambient; flow-rate, 1 ml/min; mobile phase, 2-propanol-*n*-hexane (35:65) (isocratic); detection, UV at 260 nm; recorder chart speed, 0.25 cm/min; injection, 10 μ l of a 1 μ g/ μ l solution.

separations using just one type of chiral column. Table I gives a summary of mobile phase solutions that were used for each compound before succeeding in separating their enantiomers.

The previous dioxolane nucleosides were all separated by HPLC in the reversed-phase mode, except for one particular nucleoside [BCH-344; *cis*-2-hydroxymethyl-4-(thymine-1'-yl)-1,3-dioxolane-T], which was not successfully separated on reversed-phase chiral columns. However, as it was soluble in organic solvents, normal-phase chiral stationary phases were examined. Many normal-phase chiral columns were studied, and a cellulose column, Chiralcel OJ (250 \times 4.6 mm I.D.), was found to be the most successful. Chiralcel OJ is one of a series of cellulose columns which consist of a poly- β -D-1,4 glucoside with a *p*-toluoyl ester derivative modified on the free hydroxy group [13]. This makes the CSP selective for one of the enantiomers of

TABLE I

METHOD DEVELOPMENT WITH SOLVENTS FOR SEPARATIONS OF ENANTIOMERS OF BCH-187, BCH-571 AND BCH-572 USING CHIRAL α -AGP COLUMNS IN SERIES

Buffer = 0.02 M NaH₂PO₄ adjusted to pH 7.0 with NaOH or HCl. NR = no resolution achieved. α = separation factor, k'_2/k'_1 (k'_2 and k'_1 = capacity factors of first and second peaks, respectively).

Solvent	BCH-187	BCH-571	BCH-572
Buffer (pH 7.0)	NR	Resolution achieved, $\alpha = 1.15$	NR
CH ₃ CN/buffer (10:90)	NR	NR	NR
2-Propanol-buffer (8:92)	NR	NR	NR
Methanol-buffer (5:95)	NR	NR	NR
Buffer-5 mM TBAB (pH 7.0)	Resolution achieved, $\alpha = 1.1$	NR	NR
Buffer-5 mM DMOA ^a (pH 7.0)	NR	NR	NR
Buffer-0.1 M NaCl (pH 7.0)	NR	NR	Resolution achieved, $\alpha = 1.1$
Temperature	Ambient	Ambient	15°C

^a DMOA = N,N,-dimethyloctylamine, 95% pure (Aldrich).

BCH-344. A baseline separation was achieved using as the mobile phase 2-propanol-*n*-hexane (35:65) giving a separation factor (α) between two resolved enantiomeric peaks [12] of about 1.5 (Fig. 9).

CONCLUSIONS

We have demonstrated a successful method development for the chiral separation of nucleoside analogues and important intermediates by HPLC. The results of biological tests [6] confirmed the importance of resolving and assessing the chiral purity of 1,3-dioxolane nucleosides. As research progresses in the development of new antivirals, we expect that concurrent development in HPLC methodology will facilitate the understanding of the impact of chirality on biological activity and host toxicity.

ACKNOWLEDGEMENTS

The authors thank Nancy Jolin, Louise Bernier and Josee Dugas of the BioChem Therapeutic Research HPLC group and Mr. Paulo Bouca and his staff of BioChem Immunostystems for their technical assistance. They also acknowledge

the computational department of Glaxo Group Research (GGR) for the X-ray analysis of compound 2 and the virology department of GGR for biological testing. They further thank Dr. G. Dionne and Dr. C. Vezina of BioChem Therapeutics for their encouragement and Dr. J.W. Gillard for reviewing the paper.

REFERENCES

- 1 J.A.V. Coates, N. Cammack, H. J. Jenkinson, I. M. Mutton, B. A. Pearson, R. Storer, J.M. Cameron and C.R. Penn, *Antimicrob. Agents Chemother.*, 36 (1992) 202.
- 2 B. Belleau, D. Dixit, N. Nguyen-Ba and J.L. Kraus, in *5th International AIDS Conference, 1989*, p. 515.
- 3 M.A. Wainberg, M. Stern, R. Martel, B. Belleau and H. Soudeyns, in *5th International AIDS Conference, 1989*, p. 552.
- 4 D.W. Norbeck, S. Spanton, S. Broder and H. Mitsuya, *Tetrahedron Lett.*, 30 (1989) 6263.
- 5 H.O. Kim, S.K. Ahn, A.J. Alves, J.W. Beach, L.S. Jeong, B.G. Choi, P. Van Roey, R.F. Schinazi and C.K. Chu, *J. Med. Chem.*, 35 (1992) 1987.
- 6 B. Belleau, C.A. Evans, H.L. Allan Tse, H. Jin, D. M. Dixit and T. S. Mansour, *Tetrahedron Lett.*, 33 (1992) 6949.
- 7 *Cyclobond Handbook, a Guide to using Cycodextrin Bonded Phases*, Astec, N.J.

- 8 D.W. Armstrong and W. DeMond, *J. Chromatogr.*, 22 (1984) 411.
- 9 K. Schmid, in F.W. Putman (Editor), *Plasma Proteins*, Academic Press, New York, 1975, pp. 184–222.
- 10 J. Hermansson, *Trends Anal. Chem.*, 8 (1989) 7.
- 11 J. Hermansson and G. Schell, in M. Zief and L.J. Crane (Editors), *Chromatographic Chiral Separations (Chromatographic Science Series, Vol. 40)*, Marcel Dekker, New York, 1988, p. 246.
- 12 J. Hermansson, ChromTech, Norborg, Sweden, personal communication.
- 13 S.G. Allenmark, *Chromatographic Enantioseparation Methods and Applications*, Ellis Horwood, Chichester, 1987.

Characterization of vitamin D₃ metabolites using continuous-flow fast atom bombardment tandem mass spectrometry and high-performance liquid chromatography

Bernice Yeung and Paul Vouros*

Department of Chemistry and The Barnett Institute, Northeastern University, Boston, MA 02115 (USA)

G. Satyanarayana Reddy

Department of Pediatrics, Women and Infants Hospital of Rhode Island, and Brown University School of Medicine, Providence, RI 02905 (USA)

(Received April 5th, 1993)

ABSTRACT

A mass spectrometric method for the detection of vitamin D₃ metabolites is described. This method involves the derivatization of the metabolites by cycloaddition with 4-phenyl-1,2,4-triazoline-3,5-dione, followed by their characterization by continuous-flow fast atom bombardment (CF-FAB) tandem mass spectrometry (MS–MS) and high-performance liquid chromatography (HPLC). Using HPLC, this derivatization has been shown to increase the UV detectability of 25-hydroxyvitamin D₃ by about 5-fold. The FAB spectra of the adducts are dominated by peaks corresponding to a protonated molecule and a fragment ion derived in part from the loss of the side chain. Multiple reaction monitoring (MRM) of this transition by MS–MS may be utilized for trace level analysis of vitamin D metabolites. Sample introduction by flow injection yields detection limits in the low nanogram to high picogram range, whereas the use of on-line capillary LC has been found to decrease the detection limits to the low picogram level.

INTRODUCTION

Vitamin D₃, a seco-steroid involved in the regulation of calcium homeostasis, is synthesized in the skin from 7-dehydrocholesterol on exposure to ultraviolet light. During the past three decades, the metabolism of vitamin D₃ has been extensively investigated [1]. It has been found that vitamin D₃ is first metabolized in the liver to

25(OH)D₃^a, followed by metabolism in the kidney to 24,25(OH)₂D₃ and 1,25(OH)₂D₃. 1,25(OH)₂D₃ is the most active metabolite of vitamin D₃, and is now accepted to be the steroid hormone involved in the maintenance of calcium homeostasis [2]. Recently, it has been found that 1,25(OH)₂D₃ possesses the ability to differentiate several cancer cells [3,4]. *In vitro* studies have shown that 1,25(OH)₂D₃ can suppress the proliferation of leukemic cells and, at the same time, induce their differentiation towards more mature macrophages. These results indicate that 1,25(OH)₂D₃ may have a therapeutic potential in the treatment of leukemia. Unfortunately, dosages required to achieve these

* Corresponding author.

^a Abbreviations: 25(OH)D₃ = 25-hydroxyvitamin D₃; 24,25(OH)₂D₃ = 24,25-dihydroxyvitamin D₃; 1,25(OH)₂D₃ = 1,25-dihydroxyvitamin D₃.

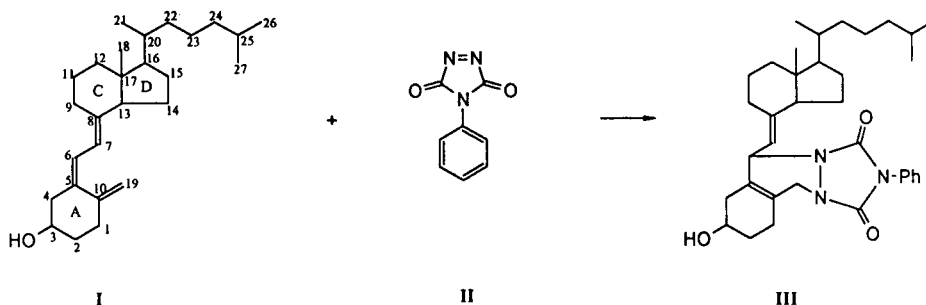
effects were found to cause hypercalcemia. Thus, much interest has arisen in the development of similar analogues as potential anti-cancer agents that are non-calcemic [5].

In the development and testing of new synthetic non-calcemic analogues of $1,25(\text{OH})_2\text{D}_3$, their serum levels in the body need to be closely monitored to avoid overdose. Also, routine quantification and identification of natural vitamin D metabolites in the plasma are equally important. However, the detection of these vitamin D metabolites in plasma has proved to be a difficult task, due to their structural and chemical similarities to one another, and the presence of large quantities of other lipids and sterols in samples. Most importantly, the plasma concentrations of these metabolites in a normal human are extremely low. For example, typical levels are [6]: vitamin D_3 , 8.1 ± 4.8 ng/ml; $25(\text{OH})\text{D}_3$, 27 ± 10 ng/ml; $24,25(\text{OH})_2\text{D}_3$, 1.6 ± 0.6 ng/ml; $1,25(\text{OH})_2\text{D}_3$, 55 ± 10 pg/ml. At such low levels, the detection of the metabolites requires much sensitivity and specificity.

Current methods that are most frequently used for characterizing these metabolites include saturation analysis, high-performance liquid chromatography (HPLC) and gas chromatography–mass spectrometry (GC–MS) measurements. HPLC with UV detection is only sensitive enough for measuring metabolites such as vitamin D_3 and $25(\text{OH})\text{D}_3$ [7] which occur at higher concentration levels. GC–MS with isotope dilution has been applied to the detection of vitamin D_3 metabolites as well. However, the metabolites are not suitable for GC analysis, and some form

of pre-column derivatization must be carried out in order to make them compatible with the high temperature in the column. Typical derivatization employed includes their conversion into trimethylsilyl and *tert*-butyldimethylsilyl ethers [8]. While the electron impact (EI) spectra of these derivatives are often structurally informative, the compounds still suffer from thermal lability. Moreover, the ion peak intensity at the high mass is relatively low and molecular weight information may be obscured. Saturation analysis includes the use of antibodies, plasma binding proteins or receptor proteins. These methods in general have sufficient sensitivity for quantifying the metabolites; however, they lack the necessary specificity [9], and cross reactions often occur. Consequently, each metabolite needs to be completely isolated before reactions with antibodies or proteins can be carried out, thus posing more stringent requirements on the preliminary HPLC separations.

Mass spectrometry (MS) is generally recognized as one of the most definitive analytical techniques currently available. When used in conjunction with a GC or LC system, MS detection can provide excellent sensitivity and specificity. Besides GC–MS, however, there has not been much advancement in such combined techniques in vitamin D research. Yergey *et al.* [10] described a quantitative technique for metabolic assay using thermospray LC–MS with isotope dilution. Although it was successful for many drug metabolites, it did not have a detection limit that is physiologically realistic for $1,25(\text{OH})_2\text{D}_3$. It is therefore deemed important



Scheme 1

to develop a combined LC–MS method that is capable of detecting vitamin D metabolites at biological levels.

In this paper, we describe a MS technique that allows for sensitive detection of vitamin D metabolites by capillary LC–MS. A simple pre-column derivatization step is employed, using the Cookson reagent 4-phenyl-1,2,4-triazoline-3,5-dione (PTAD, II) [11]. PTAD is one of the strongest dienophiles known; it is capable of attacking the 5,7-diene bonds in the vitamin D structure and forms an adduct via a Diels–Alder reaction (Scheme 1). Due to the high UV response of the phenyl ring associated with the PTAD structure, this reaction is found to be promising for the selective labelling of diene compounds for HPLC separation, where large amounts of interferences might be present [12]. PTAD and its methyl analogue, 4-methyl-1,2,4-triazoline-3,5-dione (MTAD), have previously been used as derivatizing reagents for the determination of compounds containing a conjugated diene moiety in an aliphatic chain [13,14]. It has also been examined as a protecting agent for the diene bonds in vitamin D₃ as an approach for A ring derivatization [15]. It is thus quite clear that PTAD is an ideal candidate for the selective labelling of vitamin D metabolites. In our laboratory, we have been examining the utility of these vitamin D₃–PTAD adducts for analysis by MS [16] and HPLC [16,17]. Since the adducts formed are too polar to be ionized by the traditional EI or chemical ionization techniques, fast atom bombardment (FAB) MS operating in the continuous-flow mode has been employed, as reported here.

EXPERIMENTAL SECTION

Chemicals

Vitamin D₃ and PTAD were purchased from Aldrich (Milwaukee, WI, USA). Other metabolites were synthesized by Dr. M.R. Uskokovic of Hoffmann LaRoche (Nutley, NJ, USA). [26,27-³H]-25(OH)D₃ was obtained from Amersham (Arlington Heights, IL, USA) with a specific activity of 20 Ci/mmol. All solvents used were of the highest qualities available.

HPLC conditions

A Waters 600E LC system equipped with a Model 990 photodiode array detector (Waters, Milford, MA, USA) was used. Wavelengths monitored were 226 nm for the adduct, and 265 nm for the metabolite. The column used was a 15 cm × 4.6 mm C₈ column (Rainin, Woburn, MA, USA) with 5 μm particle size. Mobile phase was made up of water–acetonitrile (50:50, v/v) (both HPLC grade and filtered). Flow-rate was maintained at 2.0 ml/min. Fractions were collected using a Retriever II fraction collector. ³H counting was done by a scintillation counter (TM Analytic, Bensenville, IL, USA) using Scintilene (Fisher Scientific, Pittsburgh, PA, USA) as the reagent.

MS conditions

All data were obtained on a Fisons/VG Quattro triple quadrupole mass spectrometer (Fisons/VG Biotech, UK). For CF-FAB, the matrix solution was made up as follows: 1% tetramethylene sulfone, 5% acetonitrile and 19% ethanol in deionized water. This solution was delivered at a flow-rate of 5 μl/min using an Isco μLC-500 pump (Isco, Lincoln, NE, USA) to the dynamic probe tip through a 50 μm I.D. fused-silica capillary (Polymicro Technologies, Phoenix, AZ, USA). A stainless-steel wire mesh [5 μm pore size, 0.003 in. thick (1 in. = 2.54 cm) ≈ 2 mm in diameter] was placed at the tip to stabilize the solution flow. Samples were introduced by flow injection via a Rheodyne injector (No. 7520) equipped with a 0.5-μl internal sample loop (Rheodyne, Cotati, CA, USA). Source temperature was maintained at 35°C in the MS. The collision induced dissociation (CID) (static probe) and multiple reaction monitoring (MRM) data were obtained with a collision energy set at 70 eV. Peak intensity was attenuated by 75% using argon gas.

Capillary LC and LC–MS conditions

A Fisons/Carlo Erba Phoenix 30 capillary LC system (Fisons, Danvers, MA, USA) was used in the isocratic mode at 5 μl/min with the following solvents: (1) Vitamin D₃– and 25(OH)D₃–PTAD: acetonitrile–H₂O–thioglycerol (85:14:1, v/v/v); (2) 24,25(OH)₂D₃– and 1,25(OH)₂D₃–

PTAD: acetonitrile–H₂O–thioglycerol (60:39:1, v/v/v). A C₁₈ Fusica column of 320 μ m I.D. (LC Packings, Switzerland) was used in all work. The LC eluent was delivered to the CF-FAB probe via a 50 μ m I.D. fused-silica capillary.

Reaction of metabolites with PTAD

Samples of metabolites were dissolved and stored in ethanol. Solid PTAD was dissolved in acetonitrile in concentrations in the order of several hundred μ g/ml. The PTAD solution was added directly to each metabolite, until the red color persisted for a few seconds. The reaction mixtures were vortexed for a few minutes, and then left at room temperature for at least 30 min, during which time the color would gradually change to orange or straw-like. For HPLC studies, the samples were first dried down by nitrogen gas and resuspended in the mobile phase before injections. For MS analyses, samples were examined directly in their original solvent mixture.

Tritium counting experiment

For the study of the effect of PTAD derivatization on HPLC–UV sensitivity, 20 μ g of 25(OH)D₃ was spiked with 1 μ Ci of ³H-labelled 25(OH)D₃. A part (3/4) of this solution was reserved for reaction with PTAD, following the conditions as outlined above and using a 1000 molar excess of PTAD to ensure complete conversion. The remaining sample was injected into the HPLC under isocratic conditions. Fractions were collected from 14 to 21 min and peak areas were summed, which contained the eluted 25(OH)D₃ at 17 min. Of each fraction one third was kept for ³H counting, whereas the rest was pooled and reinjected into the HPLC. This procedure was repeated three more times. Similar experiment was carried out with the [³H]-25(OH)D₃–PTAD adduct, with fractions collected between 3 to 8 min. Four sets of readings were also taken of the ³H counts and of the peak areas for the adduct.

RESULTS AND DISCUSSION

Several aspects of the pre-column derivatization with PTAD were evaluated. These included

reaction requirements, potential usefulness of the derivatization for HPLC–UV analysis and detectability of the adducts by MS. Results of these studies are outlined below.

Evaluation of the derivatization reaction

Vitamin D₃ solutions of various concentrations ranging from 10⁻³ to 10⁻⁸ M were allowed to react with different amounts of PTAD. Each reaction product was examined by static FAB-MS, with close attention paid to the protonated molecular ion regions of the vitamin D₃–PTAD adduct (*m/z* 560) and the unreacted vitamin D₃ (*m/z* 385). It was found that at a concentration of 10⁻³ M, a 2-fold molar excess of PTAD was

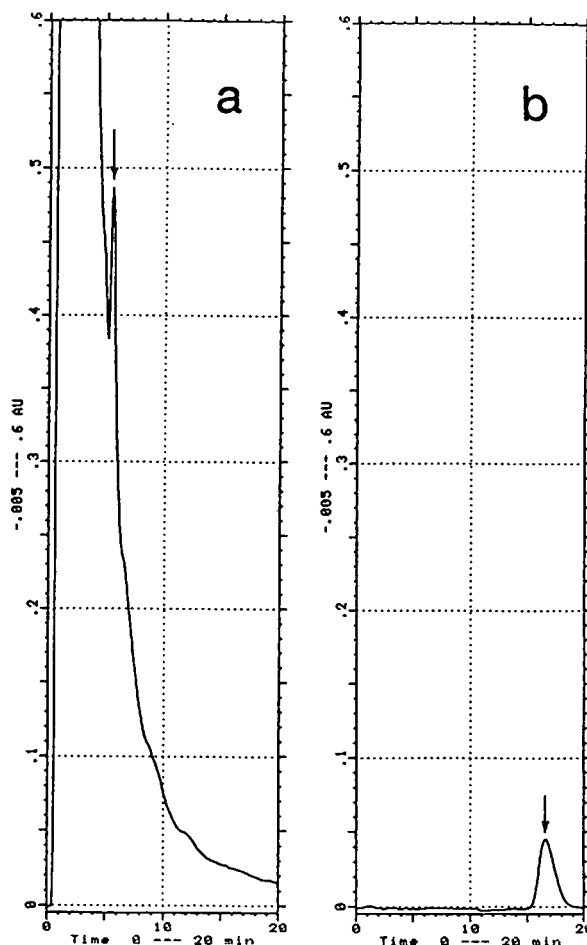


Fig. 1. HPLC chromatograms, shown in the same scale, of (a) ³H-labelled 25(OH)D₃–PTAD, 5 μ g; (b) ³H-labelled 25(OH)D₃, 5 μ g.

sufficient to convert all the vitamin D₃ into the adduct, as no peak was visible at *m/z* 385. At a concentration as low as 10⁻⁸ M, it appeared that the reaction was complete using a 4000-fold molar excess of PTAD. The 10⁻⁸ M concentration would be equivalent to about 3 ng/ml of vitamin D₃ in plasma, which is a physiologically realistic level.

After conversion to the PTAD adducts, it was expected that the phenyl ring in the adduct structure would increase the UV sensitivity of the metabolites. In order to examine this potential increase quantitatively, we used [³H]-25(OH)D₃ as the starting substrate and compared the UV absorbance generated by the [³H]-25(OH)D₃ and its PTAD adduct by HPLC, as outlined in the Experimental section. The advantage of this method is that peak areas from HPLC could be directly related to and quantified by post-column ³H counting, thereby eliminating the need to account for the recovery of sample after HPLC. The chromatograms of labelled 25(OH)D₃ and 25(OH)D₃-PTAD are shown in Fig. 1. A plot of ³H counts vs. peak areas for both compounds indicates that the PTAD adduct of 25(OH)D₃ is about 5 times more UV sensitive than the unreacted metabolite in terms of peak area per ³H count. (Slope = 9.0 × 10⁻⁷ for 25(OH)D₃ with *r* = 0.9745; slope = 5.2 × 10⁻⁶ for 25(OH)D₃-PTAD with *r* = 0.9741). This result further establishes the advantage of pre-column derivatization of the vitamin D₃ metabolites with PTAD for UV detection purposes.

Detectability by FAB-MS

Fig. 2 shows the normal full scan positive ion FAB spectra of PTAD adducts of the four most common vitamin D₃ metabolites. Since the adducts contain nitrogens, protonation by FAB is facilitated and this is advantageous for increasing the detectability of the analytes by MS. In each mass spectrum, the protonated molecules (MH⁺) can be seen clearly, along with the [MH - H₂O]⁺ peaks. Typical of FAB spectra, these spectra are quite simple and contain few fragment ion peaks. Prominent in the spectra of the adducts of vitamin D₃, 25(OH)D₃ and 24,25(OH)₂D₃ is the fragment ion of *m/z* 298. For the A ring hydroxylated metabolite

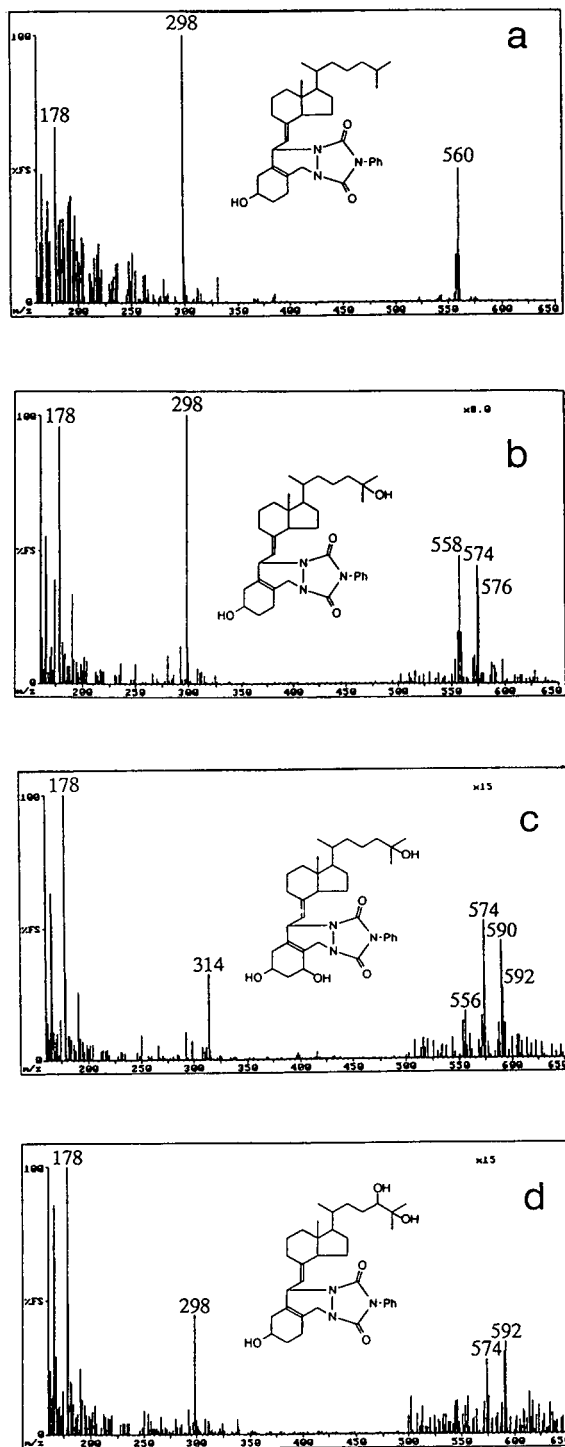
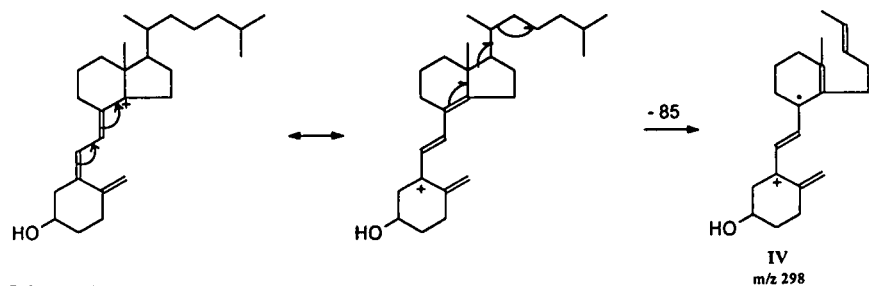
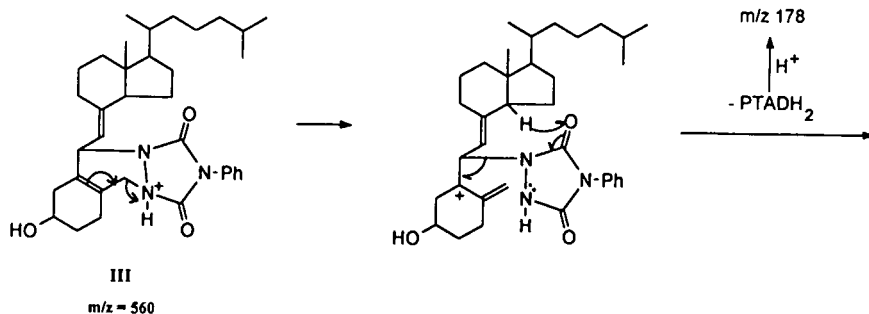


Fig. 2. Full scan FAB spectra of the four adducts studied: (a) vitamin D₃-PTAD, 40.6 ng; (b) 25(OH)D₃-PTAD, 119 ng; (c) 1,25(OH)₂D₃-PTAD, 61 ng; (d) 24,25(OH)₂D₃-PTAD, 50 ng.

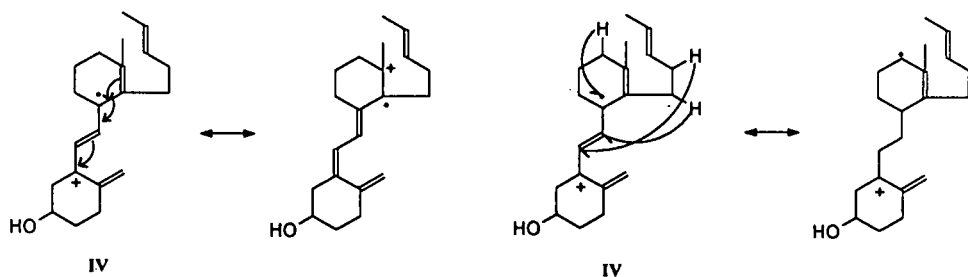


Scheme 2

1,25(OH)₂D₃, this peak is shifted by 16 mass units to *m/z* 314. It may be postulated that this fragment is formed via the process depicted in Scheme 2, starting with a hydrogen transfer which leads to the losses of a reduced PTAD molecule and part of the side chain. Presumably, these ions can undergo a series of rearrangements, resulting in the localization of a charge in the D ring (Scheme 3). The ions of *m/z* 298 and *m/z* 314 have been subjected to CID and the

data (Fig. 3) are consistent with the indicated structural assignments (IV).

The CID data of the MH⁺ ion of all the adducts show high relative abundance for the fragment 298/314 ions. In view of the high abundance of the latter in the normal MS spectra, MRM utilizing these ions appeared to be an attractive detection scheme for the metabolites. In MRM, the transition under collision conditions is monitored in a fashion similar to single-



Scheme 3

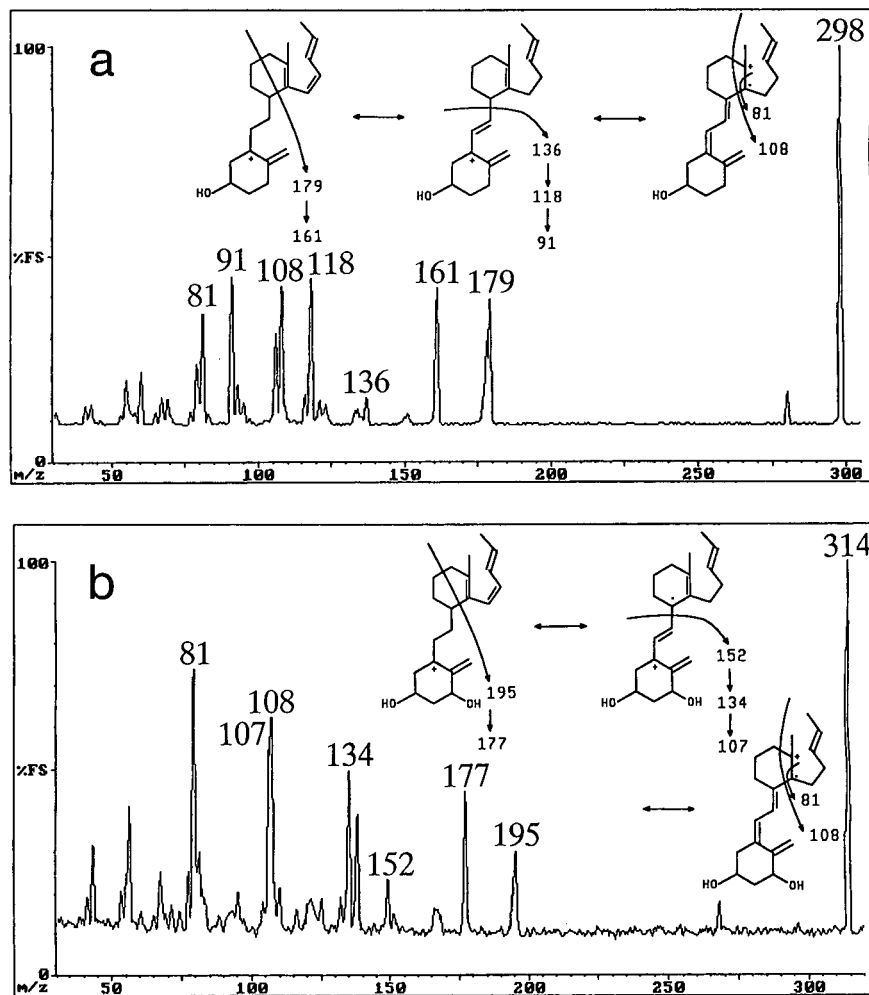


Fig. 3. CID spectra of: (a) m/z 298 and (b) m/z 314. Fragmentation schemes are shown in the inserts.

ion monitoring, and the results are represented as chromatographic profiles. Fig. 4 shows the profiles of the MRM transitions of $MH^+ \rightarrow 298(314)$ for vitamin D_3 - and $1,25(OH)_2D_3$ -PTAD near their detection limits by flow injection. The data of Fig. 4 indicate that detection of low nanogram quantities is readily achievable using this derivative and the appropriate MRM transition.

Given the encouraging results obtained via the flow injection mode, we next considered the analysis of vitamin D-PTAD derivatives by on-line capillary LC-CF-FAB-MS-MS. The focus thus far has been on the further improvement of

the detection limits in view of the concentration effects associated with the use of a chromatographic inlet. Indeed, a significant enhancement in detection limit is indicated for both vitamin D_3 - and $1,25(OH)_2D_3$ -PTAD as shown in Fig. 5. Triplicate injections are shown at 5 pg (13 fmol) for vitamin D_3 -PTAD, indicating a relative standard deviation of 25% in terms of area counts and a S/N ratio of 3.6. As expected, an improvement in signal reproducibility (relative standard deviation = 16%) was observed for analysis at the 50 pg level. For $1,25(OH)_2D_3$ -PTAD, injections of 150 pg (360 fmol) give a S/N of 2.3 and relative standard deviation of

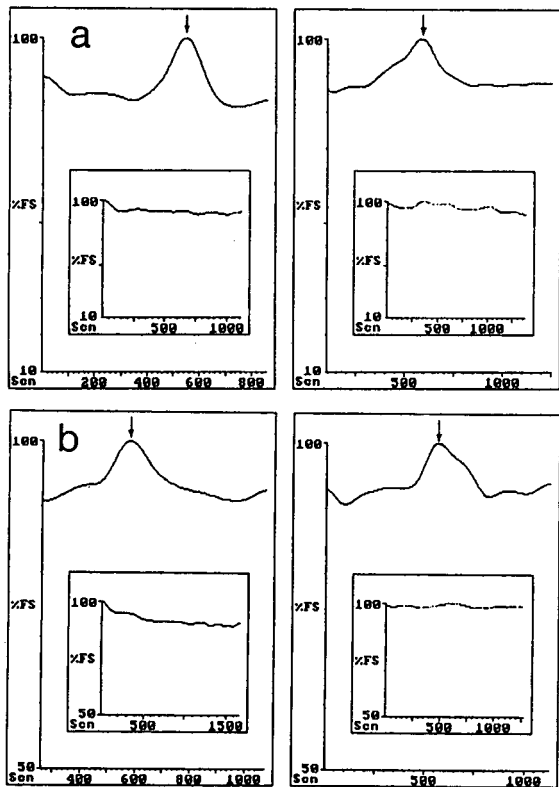


Fig. 4. Detection limits using MRM, by flow injection (in duplicates) of: (a) vitamin D₃-PTAD, 740 pg; (b) 1,25(OH)₂D₃-PTAD, 3 ng. Blanks are shown in the inserts.

6.9% for triplicate injections. In general, the use of a PTAD derivative and analysis by LC-CF-FAB-MS-MS has been found to give detection limits in the range of 100–300 pg for other vitamin D₃ compounds examined thus far.

CONCLUSIONS

Our work in the derivatization of vitamin D₃ metabolites with PTAD has demonstrated the following: (1) The reaction is simple and goes to completion with all the vitamin D₃ metabolites tested in this study, even in very dilute solutions; (2) The 25(OH)D₃-PTAD adduct shows 5 times more UV response than the underivatized metabolite; (3) From the FAB spectra we can distinguish the A ring hydroxylated metabolites from side chain hydroxylated isomeric metabolites, e.g. 1,25(OH)₂D₃ and 24,25(OH)₂D₃; (4)

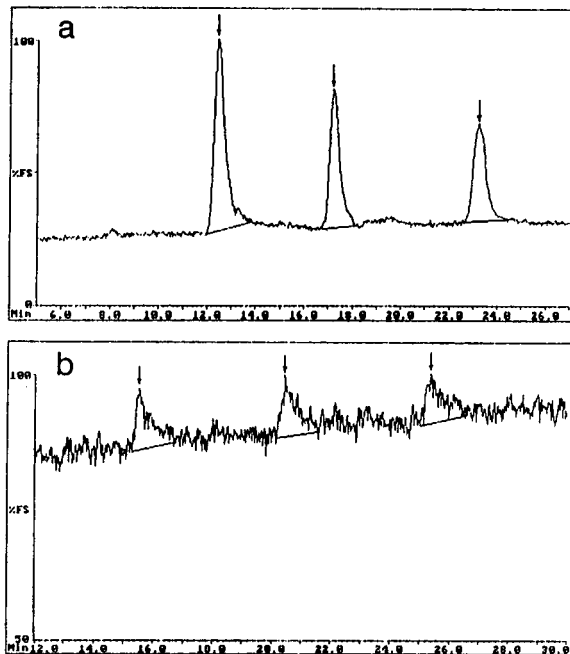


Fig. 5. LC-CF-FAB-MS-MS data, from three injections of: (a) vitamin D₃-PTAD, MRM of m/z 560→298, 5 pg (13 fmol); (b) 1,25(OH)₂D₃-PTAD, MRM of m/z 592→314, 150 pg (360 fmol).

The transition from the protonated molecule to m/z 298/314 can be monitored by MS-MS for trace level detection of specific vitamin D metabolites; (5) Use of capillary LC-CF-FAB-MS-MS has been shown to give detection limits in the mid to low picogram range (mid to high femtomole) for the vitamin D metabolites investigated. These detection limits appear to be in line with the physiologically encountered levels of most commonly occurring metabolites in plasma except for 1,25(OH)₂D₃. Further work to improve on the detectability of this and other vitamin D₃ compounds is currently in progress.

ACKNOWLEDGEMENTS

We would like to thank Ms. Khurshed F. Wankadiya for her assistance with the ³H counting experiment. This work was partially supported by grant number DK-39138 from the National Institute of Health (G.S.R.).

REFERENCES

- 1 J.L. Napoli and R.L. Horst, in R. Kumar (Editor), *Vitamin D: Basic Clinical Aspects*, Martinus Nijhoff Publishing, Boston, MA, 1984, p. 91.
- 2 A.W. Norman, J. Roth and L. Orci, *Endocr. Rev.*, 3 (1982) 331–366.
- 3 E. Abe, C. Miyaura, H. Sakagami, M. Takeda, K. Konno, T. Yamazaki, S. Yoshiki and T. Suda, *Proc. Natl. Acad. Sci. U.S.A.*, 78 (1981) 4990.
- 4 T. Suda, T. Shinki and N. Takahashi, *Annu. Rev. Nutr.*, 10 (1990) 195.
- 5 Y.J. Zhou, A.W. Norman, M. Lübbert, E.D. Collins, M.R. Uskokovic and H.P. Koeffler, *Blood*, 74 (1989) 82.
- 6 R.D. Coldwell, D.J.H. Trafford, M.J. Varley, D.N. Kirk and H.L.J. Makin, *Steroids*, 55 (1990) 418.
- 7 R.D. Coldwell, C.E. Porteous, D.J.H. Trafford and H.L.J. Makin, *Steroids*, 49 (1987) 155.
- 8 G. Jones, D.A. Seemark, D.J.H. Trafford and H.L.J. Makin, in A.P. De Leenheer, W.E. Lambert and M.G.M. De Ruyter (Editors), *Modern Chromatographic Analysis of the Vitamins*, Marcel Dekker, New York, 1985, p.73.
- 9 R.M. Bauwens, J.A. Kint, M.P. Devos, K.A. Van Brussel and A.P. De Leenheer, *Clin. Chim. Acta*, 170 (1987) 37.
- 10 A.L. Yergey, N.V. Esteban and D.J. Liberato, *Biomed. Environ. Mass Spectrom.*, 14 (1987) 623.
- 11 R.C. Cookson, S.S. Gutpe, I.D.R. Stevens and C.T. Watts, *Org. Synth.*, 51 (1971) 121.
- 12 K. Shimada, T. Oe and T. Mizuguchi, *Analyst*, 116 (1991) 1393.
- 13 D.C. Young, P. Vouros, B. Decosta and M.F. Holick, *Anal. Chem.*, 59 (1987) 1954.
- 14 D.C. Young, P. Vouros and M.F. Holick, *J. Chromatogr.*, 522 (1990) 295.
- 15 D.J. Aberhart and A.C.T. Hsu, *J. Org. Chem.*, 41 (1976) 2098.
- 16 B. Yeung, G.S. Reddy and P. Vouros, *Proceedings of the 40th ASMS Conference on Mass Spectrometry and Allied Topics, May 31–June 5, 1992, Washington, D.C.*, p. 1089.
- 17 B. Yeung, G.S. Reddy and P. Vouros, *J. Bone Miner. Res.*, 7 (1982) S 171.

Determination of pesticides in drinking water by on-line solid-phase disk extraction followed by various liquid chromatographic systems

Serge Chiron and Damia Barceló*

Environmental Chemistry Department, CID-CSIC, c/Jordi Girona, 18-26, 08034 Barcelona (Spain)

(First received December 30th, 1992; revised manuscript received April 8th, 1993)

ABSTRACT

C-18 Empore extraction disks were coupled on-line with liquid chromatography–rapid scanning UV–VIS detection and post-column fluorescence detection for the isolation and trace enrichment of various pesticides [carbamates, (aldicarb, carbofuran, carbaryl), carbamate transformation products (TPs) (aldicarb sulfoxide, aldicarb sulfone, 3-hydroxycarbofuran, 3-hydroxy-7-phenol carbofuran, 3-keto-carbofuranphenol and 3-ketocarbofuran) and herbicides (chlortoluron, isoproturon and metolachlor)] spiked at concentration levels of 0.2 and 5 $\mu\text{g/l}$ in drinking water samples. Recoveries were dependent on the pesticide level and pre-concentrated water volume (50 ml to 1000 ml) using LC with rapid scanning UV–VIS detection. The same on-line system coupled with LC–post-column derivatization fluorescence detection has needed only 10 ml of water to achieve similar levels of determination for the carbamate insecticides.

INTRODUCTION

Drinking and ground waters within the European Community were recently reported to be polluted with various pesticides with levels varying from 0.01 $\mu\text{g/l}$ to over 0.1 $\mu\text{g/l}$, the latter of which is the maximum allowable concentration established by the Commission of the European Communities Drinking Water Directive (CEC-DWD) [1]. These pesticides have been also detected at similar concentration levels in various ground waters in the US [2]. The carbamate insecticides aldicarb and carbofuran are rather toxic, and their TPs are even more toxic [1,3]. They are formed both by hydrolysis or photolysis in water under laboratory conditions [3] as well by microbial degradation in soils and hydrolysis in waters [4,5]. It is thus hardly surprising that the National Pesticide Survey (NPS), in a joint

project between EPA's Office of Drinking Water and the Office of Pesticide Programs has included many of these pesticides and TPs in their monitoring programmes [6,7].

A variety of adsorbents (*e.g.*, C-8 or C-18 bonded silica, Carbo-pack B) are currently used in SPE cartridges for concentrating polar pesticides and various TPs [8–15]. On-line systems [SPE coupled on-line with liquid chromatography] have been developed from SPE methods using a precolumn consisting of C-8 or C-18 bonded silica phase or a styrene–divinylbenzene polymer phase (PRP-1 or PLPR-S) [16–20]. One other alternative to trace enrichment uses membrane extraction disks (that contain C-8, C-18 or styrene–divinylbenzene polymer phase) and were used in the off-line [21–26] and on-line [27–28] modes in LC. The 4.6 mm O.D. disks used in the on-line mode are obtained from the conventional 47 mm O.D. disks (500 mg of C-18) by using a cutting device [28].

The aim of this work was to develop an on-line

* Corresponding author.

SPE method using membrane extraction disks to determine various pesticides and their polar TPs at levels below the values fixed by the CEC-DWD of 0.1 $\mu\text{g}/\text{l}$ in drinking water. Development of methods for carbamate TPs was encouraged in a recent report from the CEC [1]. The different compounds were detected by rapid scanning UV-VIS, so confirmation was always possible. However, many of the compounds studied (*e.g.*, aldicarb and carbofuran and their corresponding TPs and metolachlor [3,19]) have their UV maxima below 220 nm, with molar extinction coefficients lower than 10.000, so problems in confirmation from LC-diode array spectra were encountered [3,19,20]. Complementary confirmation could also be achieved for some carbamate pesticides by using post-column derivatization with fluorescence detection. The method is valid for the analysis of water samples containing N-methylcarbamates

and O-(methylcarbomyl)oxime pesticides [29,30]; and it is currently recommended by the US EPA [31] and applied through the NPS [6,7].

EXPERIMENTAL

Chemicals

HPLC-grade water, acetonitrile gradient grade LiChrosolv and methanol from Merck (Darmstadt, Germany) were passed through a 0.45 μm filter before use. Analytical reagent grade standards aldicarb, carbofuran, carbaryl, aldicarb sulfoxide, aldicarb sulfone, 3-hydroxycarbofuran, 3-hydroxy-7-phenol carbofuran, 3-ketocarbofuranphenol, 3-ketocarbofuran, chlortoluron, isoproturon and metolachlor were purchased from Promochem (Wesel, Germany). The names and structures of the pesticides are given in Fig. 1.

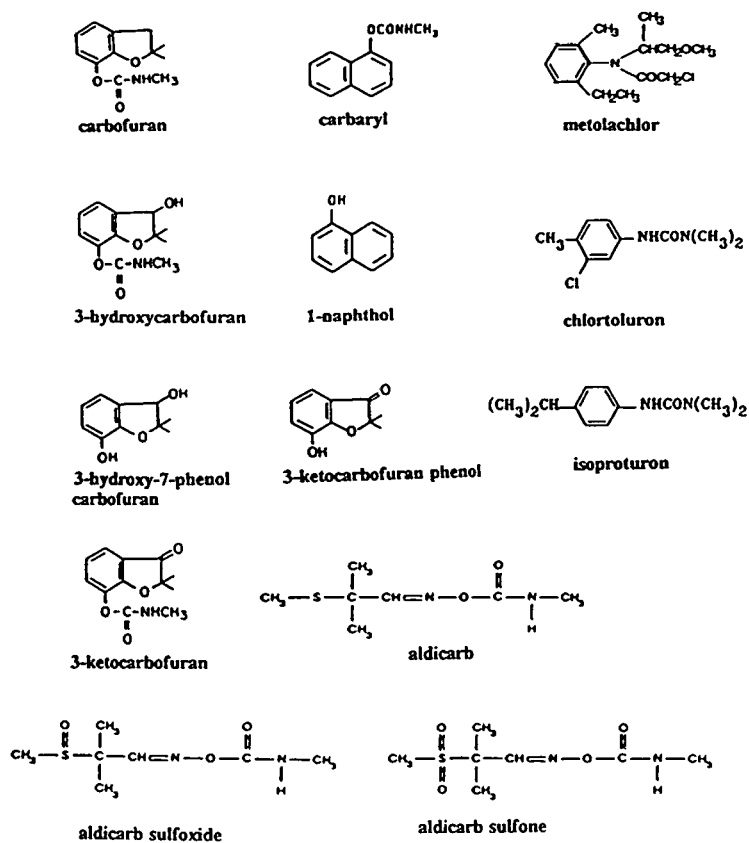


Fig. 1. Chemical structures of the model compounds used.

Rapid scanning UV–VIS detection

The LC eluent was provided by two Knauer 64 high-pressure pumps (Bad Homburg, Germany) coupled to a Chrom-A-Scope rapid scanning UV–VIS detector from Barspec (Rehovot, Israel). Quantitation by LC–UV was performed using UV absorption at 220 nm with external standard calibration methods. The calibration graphs were constructed for eight of the studied analytes (3-hydroxycarbofuran, aldicarb, 3-ketocarbofuran, carbofuran, carbaryl, chlorotoluron, isoproturon and metolachlor) over a concentration range of 0.1–0.7 $\mu\text{g/l}$ using pre-concentration volumes of 250–400 ml. The other analytes were either not recovered (aldicarb sulfoxide, aldicarb sulfone, 3-hydroxy-7-phenol carbofuran) or exhibited recoveries below 70% (3-ketocarbofuranphenol and 1-naphthol).

The system used was similar to one described elsewhere [27,28]. After the membrane disks were placed in the disk holder, this holder was fitted in a MUST column switching device from Spark Holland (AS Emmen, Netherlands) and connected to an SSI Model 300 LC pump from Scientific Systems (State College, PA, USA) which delivered the water samples containing the pesticides. The disks were first conditioned by flushing 10 ml of methanol and then 10 ml of HPLC water at 1 ml/min. Water volumes from 50 to 1000 ml spiked with pesticides and TPs at concentrations of 0.2 and 5 $\mu\text{g/l}$ were pre-concentrated on 10 membrane extraction disks of 4.6 mm diameter at flow-rates varying from 2.5 to 5 ml/min. Following the pre-concentration step, the MUST valve was switched and the components were desorbed and separated in a LiChrocart cartridge column (25 cm x 4.6 mm I.D.) packed with 4- μm Supersphere 60 RP-8 from Merck (Darmstadt, Germany) by using the following gradient elution program: from 5% of A [acetonitrile–methanol–water (40:40:20)] and 95% of B [acetonitrile–water (10:90)] to [20% A/80% B] in 15 min; from [20% A/80% B] to [30% A/70% B] in 20 min; from [30% A/70% B] to [65% A/35% B] in 20 min; and finally from [65% A/35% B] to 100% A in 7 min at a flow-rate of 0.8 ml/min. The column was returned to initial conditions in 5 min and held for post-run, 10 min. By flushing 5 ml of acetonitrile

followed by 5 ml of water through the disks after each analysis, the memory effects in the disks were found to be less than 1%. Desorption of the pesticides from the membrane disk holder was done in the back-flush mode thus preventing chromatographic tailing and thereby enhancing carbamate resolution [16] and preventing extra band-broadening [28]. Since for river water samples the determination of pesticides is in the range of few $\mu\text{g/l}$ [18], the pre-concentrated volumes can also be reduced by a factor of 10 as compared to this work.

Post-column fluorescence derivatization

The above described on-line pre-concentration system was coupled to an LC-post-column fluorescence system. The LC column eluent was delivered by a Model 250 Binary LC pump from Perkin Elmer (Norwalk, Connecticut, USA) coupled to a PCX 5000 carbamate post-column analysis module from Pickering Laboratories (Mountain View, CA, USA). Post-column reaction was carried out as described elsewhere [33]. A difference was the use of thiofluor instead of 2-mercaptoethanol. A Model LC 240 fluorescence detector from Perkin Elmer (Beaconsfield, UK) was used at excitation and emission wavelengths of 330 nm and 465 nm, respectively. A PE Nelson Model 1020 data system was used for data collection. 10-ml drinking water samples were needed for pre-concentration.

RESULTS AND DISCUSSION

Breakthrough volumes

In order to determine the breakthrough volumes of all the test compounds, up to 100–150 ml (depending on the compound) of a solution containing the individual substances at a concentration of 1 mg/l was used. Breakthrough experiments were performed at a flow-rate of 2 ml/min, similar to that described elsewhere [18,19]. The breakthrough volumes were read off the recorded breakthrough curves at 1% of the sample absorbance observed at complete breakthrough; the values thus obtained are given in Table I. As compared to few recent literature data, breakthrough volumes of 1, 30 and >100

TABLE I

ABSORBANCE DATA AND BREAKTHROUGH VOLUMES DURING ON-LINE PRECONCENTRATION

HPLC water containing the individual substances at a concentration of 1 mg/l. Flow-rate: 2 ml/min.

Compound	Peak no.	λ_{\max} (nm)	Breakthrough volume (ml)
Aldicarb sulfoxide	1	235	3
Aldicarb sulfone	2	220	4
3-Hydroxy-7-phenolcarbofuran	3	220	5
3-Hydroxycarbofuran	4	220	80
3-Ketocarbofuran phenol	5	258	40
Aldicarb	6	220	112
3-Keto-carbofuran	7	258	108
Carbofuran	8	220	150
Carbaryl	9	220	123
Chortoluron	10	245	102
1-Naphthol	11	234	80
Isoproturon	12	245	105
Metolachlor	13	200	150

ml were obtained for aldicarb sulfone, aldicarb and metolachlor when using a 10 mm × 2 mm I.D. precolumn of PLRP-S [19]. From these results one can conclude that using 10 membrane

extraction disks of C-18 bonded silica material increases the breakthrough volume of many of the compounds of interest as compared to other conventional packing materials. This can be

TABLE II

AVERAGE % RECOVERY OF PESTICIDES IN WATER USING ON-LINE SPE

SPE with 10 C-18 Empore disks of 4.6 mm O.D. preconcentrating several water volumes at 2 ml/min. Spiking level: 5 $\mu\text{g/l}$. Detection: rapid scanning UV-VIS. R.S.D. (%) varied from 3-6% [calculated for sample volumes of 50 and 80 ml ($n = 5$)].

Compound	Water volume (ml)				
	20	50	50 ^a	80	180
Aldicarb sulfoxide	nd ^b	23	23	18	9
Aldicarb sulfone	nd	27	21	19	10
3-Hydroxy-7-phenolcarbofuran	nd	27	25	20	10
3-Hydroxycarbofuran	78	84	90	70	29
3-Ketocarbofuran phenol	72	71	68	50	19
Aldicarb	85	83	79	72	37
3-Ketocarbofuran	85	75	67	50	25
Carbofuran	95	93	94	70	66
Carbaryl	94	91	89	82	66
Chortoluron	92	91	90	80	69
1-Naphthol	78	74	75	67	37
Isoproturon	94	92	95	80	56
Metolachlor ^c	95	93	95	80	56

^a Drinking water samples spiked with pesticides (see Fig. 2B).

^b Not detected, below detection limits.

^c Calculated after subtraction of spectrum at 220 nm.

ascribed to the higher trapping capacity of C-18 membrane disks of 8 μm particle size in an on-line combination.

Recovery values with rapid scanning UV–VIS detection

Tables II and III show the average recoveries of the studied pesticides at the spiking levels of 5 and 0.2 $\mu\text{g/l}$ as preconcentrated from different volumes (20–1000 ml) of water samples. Table II gives the recoveries obtained with water volumes from 20 to 180 ml. We should note that the highest recoveries for all the compounds were obtained by preconcentrating 50 ml of water spiked with 5 $\mu\text{g/l}$ of each pesticide. Preconcentrating 180 ml of the different pesticides spiked at 5 $\mu\text{g/l}$ will be equivalent to load a maximum of 0.6 μg of each pesticide (at recoveries of 66–69%) onto the disks, so an overall amount of *ca.* 7 μg was loaded. From previous studies it was suggested to use a maximum loading of 15 μg for the sum of all adsorbed species in C-18 or PRP1 precolumns [35]. The difference in the

maximum loading of the disks can be attributed to the water matrix constituents, *e.g.*, detergents in the case of drinking water samples. The recoveries obtained at 180 ml for aldicarb sulfoxide and sulfone were extremely low. In this case the effect of overloading the disks was obviously more important owing to the nature of the solutes.

A volume of < 50 ml would be ideal for compounds with low breakthrough volumes, *e.g.*, aldicarb sulfoxide, sulfone and 3-hydroxy-7-phenol carbofuran. The problem is that these three TPs are not detected by the UV (see Table II). The percent recoveries for the rest of the compounds were all consistent with those obtained by breakthrough measurements. We should also note the absence of remarkable differences in using HPLC and drinking water samples, as can be seen in the chromatograms in Fig. 2, which correspond to 50 ml of HPLC water (A) and 50 ml of drinking water both spiked with all the studied pesticides at 5 $\mu\text{g/l}$ (B) and a blank of 50 ml of drinking water (C).

TABLE III
AVERAGE % RECOVERY OF PESTICIDES IN WATER USING ON-LINE SPE

SPE with 10 C-18 Empore disks of 4.6 mm O.D. preconcentrating several water volumes at flow-rates varying from 2.5 to 5 ml/min. Spiking level: 0.2 $\mu\text{g/l}$. Detection: rapid scanning UV–VIS. R.S.D. (%) varied from 3 to 6% (calculated for sample volumes of 350 and 500 ml ($n = 5$) except for aldicarb sulfoxide, aldicarb sulfone and 3-hydroxy-7-phenolcarbofuran.

Compound Recovery (%)	Water volume (ml)/flow-rate (ml/min)					
	250/2.5	350/3.5	350/5 ^a	400/5	500/5	1000/5
Aldicarb sulfoxide	– ^b	–	–	–	–	–
Aldicarb sulfone	–	–	–	–	–	–
3-Hydroxy-7-phenolcarbofuran	–	–	–	–	–	–
3-Hydroxycarbofuran	94	89	78	92	63	57
3-Ketocarbofuranphenol	–	40	35	46	31	20
Aldicarb	79	92	74	78	62	43
3-Ketocarbofuran	80	85	75	88	68	69
Carbofuran	80	82	71	82	68	74
Carbaryl	74	76	73	79	64	55
Chortoluron	75	73	73	77	66	64
1-Naphthol	62	71	66	66	50	^c
Isoproturon	80	83	76	84	67	70
Metolachlor ^d	95	94	92	95	91	95

^a Drinking water was used.

^b Not detected, below detection limits.

^c Coelution problems (see Fig. 3).

^d Calculated after subtraction of spectrum at 220 nm.

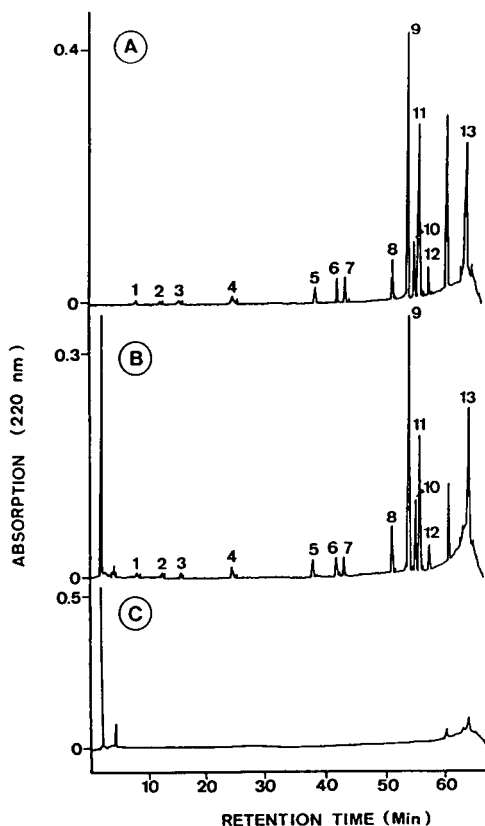


Fig. 2. LC-UV chromatograms obtained after preconcentration on C-18 Empore extraction disks of 50 ml of (A) HPLC water and (B) drinking water both spiked at $5 \mu\text{g/l}$ with the pesticide mixture indicated below, and (C) a drinking water blank. Peaks: 1 = aldicarb sulfoxide; 2 = aldicarb sulfone; 3 = 3-hydroxy-7-phenolcarbofuran; 4 = 3-hydroxycarbofuran; 5 = 3-ketocarbofuranphenol; 6 = aldicarb; 7 = 3-ketocarbofuran; 8 = carbofuran; 9 = carbaryl; 10 = chlortoluron; 11 = 1-naphthol; 12 = isoproturon; 13 = metolachlor. LC gradient elution programme: from 5% of A [acetonitrile-methanol-water (40:40:20)] and 95% of B [acetonitrile-water (10:90)] to [20% A/80% B] in 15 min; from [20% A/80% B] to [30% A/70% B] in 20 min; from [30% A/70% B] to [65% A/35% B] in 20 min; and from [65% A/35% B] to 100% A in 7 min. Back to initial conditions: 5 min; post-run, 10 min; flow-rate: 0.8 ml/min; stationary phase: $4 \mu\text{m}$ Supersphere 60 RP-8.

The blank shows that interferences can only occur in the last part of the gradient elution. The profile of the drinking water blanks analysed in our experiments is more consistent with the on-line preconcentration of other types of drinking waters [17,32,34,35].

Water solutions containing $0.2 \mu\text{g/l}$ of each pesticide were preconcentrated by using water

volumes from 250 up to 1000 ml (Table III). As can be seen from the table, the recoveries obtained for all the compounds were quite similar for 350–400 ml of preconcentrated water. Such recoveries did not change on varying the flow-rate through the precolumn from 3.5 to 5 ml/min. This was also observed previously for several carbamates, the retention of which was not significantly affected by the flow-rate (flow-rates below 6 ml/min were recommended to avoid column back-pressure for precolumns containing $5\text{-}\mu\text{m}$ packing material [32]). As can also be seen from the tables, aldicarb sulfoxide, aldicarb sulfone and 3-hydroxy-phenol carbofuran were not detected at all owing to their low breakthrough volumes (their preconcentration on the disks at this low spiking level of $0.2 \mu\text{g/l}$ was not sufficient to be measured by LC-rapid scanning UV detection).

On comparing Table II and III, it is seen, as already observed in the preconcentration study, that breakthrough volumes increase with decreasing concentration, thus affecting analyte recoveries, similarly as reported previously [34,36]. Thus, in previous studies [36] it was shown that a concentration factor increase of 10 results in a breakthrough volume factor decrease of 5–7. Similarly, in our experiments, for compounds with relatively good recovery values, in preconcentrating water volumes of 50 and 350 ml containing $5 \mu\text{g/l}$ and $0.2 \mu\text{g/l}$, respectively, it is seen that a concentration factor of 25 results in a breakthrough volume factor increase of 7 but a loading decrease of more than a factor of 3 is noticed (obtained from the recovery values). Inasmuch as preconcentration of 350 ml (see Table III) provided reasonable good recoveries for most of the compounds, we can state that the proposed preconcentration system provides good recoveries for loading capacities not exceeding *ca.* $0.064 \mu\text{g}$ (*e.g.*, for aldicarb, 92% recovery) for each compound and for the water type studied in this paper.

One other inference from both Tables II and III involves the recoveries obtained by loading similar amounts of pesticides. If we compare the recoveries obtained by preconcentrating 20 ml of water containing $5 \mu\text{g/l}$ with those achieved by preconcentrating 500 ml of water spiked with $0.2 \mu\text{g/l}$, $0.1 \mu\text{g}$ of each pesticide was loaded in both

cases. The recoveries obtained were better using 20 ml of water for almost all the compounds, except metolachlor, which, owing to its high breakthrough volume (>150 ml), featured identical recoveries with both water volumes and concentrations. Other compounds had recoveries of 85% vs. 68 (3-ketocarbofuran) and 92 vs. 66% (chlortoluron) for 20 ml against 500 ml of water at the same pesticide concentration. These observations are consistent with the results obtained by loading 1 μg of chlortoluron onto a C-18 precolumn, with reported recoveries varying from 100 to 15% for water volumes of 10 to 500 ml, respectively [34]. From Tables II and III we can conclude that the recommended volumes for preconcentration of the different analytes will be 50 ml and 350 ml, for 5 and 0.2 $\mu\text{g}/\text{l}$ spiked pesticides, respectively, since they are the minimum volumes required to achieve acceptable recoveries (>70%) for 10 and 8, respectively, of the studied analytes. Recently [37], 150 ml of enriched Rhine river drinking water was pre-concentrated on-line on PLPR-S cartridges with various spiking levels of pesticides; it was impossible to determine 0.1 $\mu\text{g}/\text{l}$ concentrations for the early eluting compounds (10–35 min), even at such high pre-concentrated water volume. As noted earlier, this can be ascribed to the higher trapping capacity of the membrane C-18 disks relative to polymeric material.

Our on-line system containing 10 membrane extraction disks of 4.6 mm diameter performed well in the analysis of at least ten (six) 350-ml HPLC (drinking) water samples. Since each 47-mm diameter disk provides *ca.* 40 disks of 4.6 mm diameter the cost per analysis is relatively low.

LC-post-column fluorescence detection

By using the on-line system described in the Experimental section, 10 ml of HPLC and drinking water spiked with the carbamate pesticides and their TPs at a concentration of 0.2 $\mu\text{g}/\text{l}$ were pre-concentrated. Fig. 3 shows the different chromatograms obtained following LC-post-column fluorescence detection of spiked HPLC water (A), drinking water (B) and a drinking water blank (C). Two major conclusions can be drawn: (i) only N-methylcarbamates and O-(methylcarbonyl) oxime pesticides can be detected by this

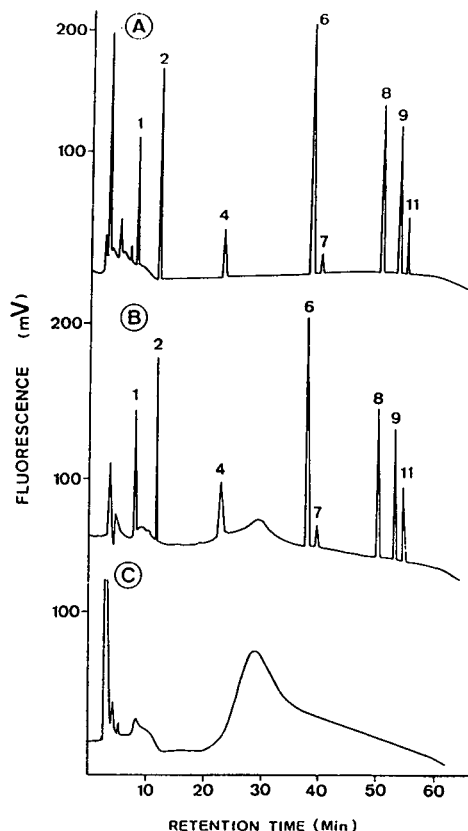


Fig. 3. LC-post column fluorescence detection chromatograms obtained after on-line preconcentration using C-18 Empore extraction disks of 10 ml of (A) HPLC water and (B) drinking water both spiked at 0.2 $\mu\text{g}/\text{l}$ with the pesticide mixture indicated in Fig. 2, and (C) a drinking water blank. Other experimental conditions as in Fig. 2.

technique, which allows 8 of the 13 compounds studied to be determined; and (ii) despite the low breakthrough volumes of aldicarb sulfoxide and aldicarb sulfone (see Table I), the system permits an excellent determination of these compounds at such low concentration level, with recoveries higher than 70% (see Table IV). Fig. 3B and C also shows the interferences from the drinking water matrix, which were not observed with the LC-rapid scanning UV detection. Since the level of interference corresponds to an amount lower than 0.02 $\mu\text{g}/\text{l}$ level, they do not represent a problem in the analysis of the carbamates or their TPs being attributed to either water and/or the disk matrices. Surprisingly, they were never reported in connection with water analyses, *e.g.*, well water [29,30]. Since the

TABLE IV

AVERAGE % RECOVERY AND RELATIVE STANDARD DEVIATION (R.S.D.) OF PESTICIDES IN DRINKING WATER

On-line SPE with 10 C-18 Empore extraction disks of 4.6 mm O.D. diameter at a flow-rate of 2 ml/min. Spiking level: 0.2 $\mu\text{g/l}$. $N = 7$ for each pesticide. Determination by LC post-column fluorescence detection. Water volume: 10 ml.

Compound	Av. (%)	R.S.D. (%)
Aldicarb sulfoxide	73	6
Aldicarb sulfone	71	3
3-Hydroxycarbofuran	73	5
Aldicarb	94	5
3-Ketocarbofuran	74	8
Carbofuran	95	6
Carbaryl	78	3
1-Naphthol	73	5

proposed system also detects compounds with native fluorescence, (e.g., naphthol), matrix interference may arise from such compounds (e.g., humic substances) which were detected by LC-diode array in analyzing surface Rhine river waters [20,37]. The interferences noticed in the fluorescence signal have also been detected in previous studies of preconcentration of drinking water samples [38]. In any case, no problems were observed for the determination of the studied carbamate pesticides or their TPs, as can be seen in the traces of Fig. 3B and more clearly in Fig. 4, where 10 ml of drinking water sample spiked at 0.01 $\mu\text{g/l}$ level was analysed.

Limits of detection

Table V shows the different limits of detection (L.O.D.s) obtained by using the on-line systems described in this paper either followed by rapid scanning UV-VIS detection or by post-column fluorescence. The L.O.D.s were calculated by using a signal-to-noise (S/N) ratio of 3 and assuming that 1 cm was the minimum peak height that could be measured with reasonable confidence. We shall note that, in general, for achieving L.O.D.s of ca. 0.01 $\mu\text{g/l}$ we need to preconcentrate either 350 or 10 ml of water, for rapid scanning UV-VIS or post-column fluorescence detection, respectively. This indicates the

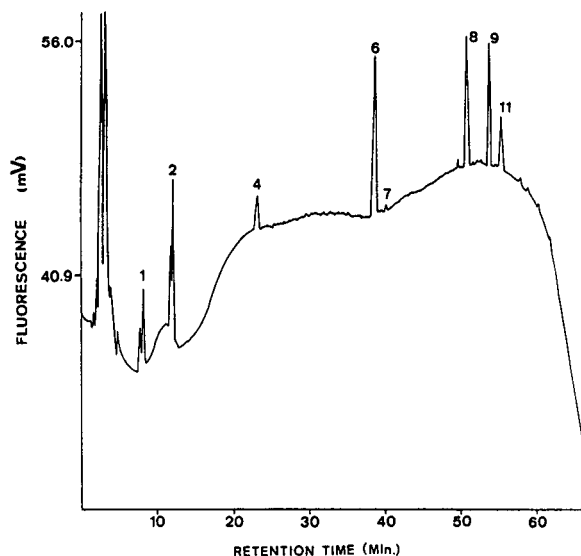


Fig. 4. LC-post-column fluorescence detection chromatogram obtained after preconcentration on C-18 Empore extraction disks of 10 ml of drinking water spiked at 0.01 $\mu\text{g/l}$ with the pesticide mixture indicated in Fig. 2. Other experimental conditions as in Fig. 2.

higher selectivity and sensitivity of the well established method based on post-column reaction with fluorescence detection for N-methylcarbamates and O-(methylcarbonyl)oxime pesticides. In Table V the L.O.D.s obtained with the on-line system proposed in this paper are compared with those afforded by the US EPA method [30,31]. We should note that the L.O.D.s of the EPA methods are higher than those achieved in this work since NPS requirements lie in the low $\mu\text{g/l}$ level, so there is no need to lower them further. An additional advantage of our method is that it is performed on-line whereas in the EPA method a direct injection of 500 ml is performed. Such large injection volumes can cause broad peaks and reduce resolution in early eluting compounds, which may interfere with some of the carbamate TPs. Also the L.O.D.s are somewhat better in ref. 30 than in ref. 31, which may have resulted from using a different fluorescence detector (in ref. 30 they used the same type as in this work, whereas in ref. 31 it was an older type of instrument, a Schoffel Model 970). From the results listed in Table V it is apparent that the LC-post-column fluorescence approach provides

TABLE V

LIMITS OF DETECTION ($\mu\text{g/l}$) AFTER ON-LINE PRECONCENTRATION

(A) 350 ml of drinking water followed by LC with rapid scanning UV–VIS at 220 nm and (B) 10 ml of drinking water followed by LC post-column reaction and fluorescence detection (C) according to US EPA method 531.1 using direct aqueous injection of 500 μl (ref. 31) or (D) 400 μl (ref. 30) at $S/N = 5$.

Compound	A	B	C	D
Aldicarb sulfoxide	5	0.008	2.0	0.4
Aldicarb sulfone	5	0.008	2.0	0.4
3-hydroxy-7-phenolcarbofuran	5	nd ^a	nd	nd
3-Hydroxycarbofuran	0.2	0.010	2.0	0.6
3-Ketocarbofuran phenol	0.2	nd	nd	nd
Aldicarb	0.03	0.005	1.0	0.2
3-Ketocarbofuran	0.03	0.040	ni ^b	ni
Carbofuran	0.02	0.005	1.5	1.5
Carbaryl	0.01	0.005	1.5	0.2
Chortoluron	0.01	nd	nd	nd
1-Naphthol ^c	0.01	0.010	ni	0.6
Isoproturon	0.02	nd	nd	nd
Metolachlor	0.01	nd	nd	nd

^a nd = Not detected.

^b ni = Not investigated.

^c 1-Naphthol was measured by its native fluorescence.

much better L.O.D.s for the carbamate pesticides and their TPs that can be determined by this technique over LC–rapid scanning UV. The proposed method is especially recommended for the determination of aldicarb sulfoxide and aldicarb sulfone.

CONCLUSIONS

We assessed the use in the on-line approach of Empore extraction disks at different water volumes (from 10 to 1000 ml) in order to develop a method capable determining pesticides and some toxic TPs in drinking water at or below the concentrations required by the CEC-DWD (0.1 $\mu\text{g/l}$). From the results it was concluded that 350 ml of drinking water sample are needed to achieve a L.O.D. of 0.01–0.03 $\mu\text{g/l}$ for the complete determination of the 8 compounds with on-line LC–rapid scanning UV detection.

The on-line preconcentration system was also coupled to LC–post-column fluorescence detection, thereby achieving L.O.D.s in the order of ca. 0.005–0.040 $\mu\text{g/l}$ when preconcentrating 10 ml of drinking water containing 8 carbamates

and their TPs. Empore extraction disks proved to have reasonably long lifetimes and to be fairly inexpensive since each conventional 47 mm disk provides ca. 40 4.6-mm disks, and hence various pre-columns can be prepared. The proposed method meets the requirements recently established by the DWD-CEC [1] and in this sense the method developed permits the determination of 10 pesticides and their TPs in drinking water samples at levels below 0.1 $\mu\text{g/l}$ [1].

ACKNOWLEDGEMENTS

One of us (S.C.) acknowledges financial support from the Commission of the European Communities (B/STEP-913011. CEC grant ref. 910212). This work was supported by the Environment R. and D. Programme 1991–94 on the Analysis and Fate of Organic Pollutants in Water, from the Commission of the European Communities (EV5V-CT92-0061). F. Farré, from Perkin Elmer Spain, is acknowledged for kind help in the purchasing the post-column fluorescence derivatization system.

REFERENCES

- 1 M. Fielding, D. Barceló, A. Helweg, S. Galassi, L. Torstensson, P. Van Zoonen, R. Wolter and G. Angeletti, *Pesticides in ground and drinking water. Water Pollution Research Report 27*. Commission of the European Communities, Brussels, 1992, pp. 1-136.
- 2 N. Aharonson, *Pure Appl. Chem.*, 57 (1987) 1419.
- 3 N. De Bertrand and D. Barceló, *Anal. Chim. Acta*, 254 (1991) 235.
- 4 J. Jayaraman, L.P. Celino, K.H. Lee, R.B. Mohamad, J. Sun, N. Tayaputch and Z. Zhang, *Water Air Soil Pollut.*, 45 (1989) 371.
- 5 T.S. Dikshith, S.N. Kumar, R.B. Raizada, M.K. Srivastava and P.K. Ray, *Bull. Environ. Contam. Toxicol.*, 44 (1990) 87.
- 6 D.J. Munch, R.L. Graves, R.A. Maxey and T.M. Engel, *Environ. Sci. Technol.*, 24 (1990) 1446.
- 7 D.J. Munch and Ch. P. Frebis, *Environ. Sci. Technol.*, 26 (1992) 921.
- 8 D. Barceló, *Analyst*, 116 (1991) 681.
- 9 W.E. Johnson, N.J. Fendinger and J.R. Plimmer, *Anal. Chem.*, 63 (1991) 1510.
- 10 E.M. Thurman, M. Meyer, M. Pomes, Ch.A. Perry and P. Schemb, *Anal. Chem.*, 62 (1990) 2043.
- 11 G.A. Junk, and J.J. Richard, *Anal. Chem.*, 60 (1988) 451.
- 12 T.A. Bellar and W.L. Budde, *Anal. Chem.*, 60 (1988) 2076.
- 13 A. de Kok, M. Hiemstra and U.A.Th. Brinkman, *J. Chromatogr.*, 623 (1992) 265.
- 14 R.G. Nash, *J. Assoc. Off. Anal. Chem.*, 73 (1990) 438.
- 15 A. Di Corcia and M. Marchetti, *Environ. Sci. Technol.*, 26 (1992) 66.
- 16 M.W.F. Nielen, R.W. Frei and U.A.Th. Brinkman, in R.W. Frei and K. Zech (Editors), *Selective sample handling and detection in HPLC. Part A*, Elsevier, 1988, Ch. 1.
- 17 V. Coquart and M.C. Hennion, *J. Chromatogr.*, 553 (1991) 329.
- 18 E.R. Brouwer, I. Liska, R.B. Geerdink, P.C.M. Frintrop, W.H. Mulder, H. Lingeman and U.A.Th. Brinkman, *Chromatographia*, 32 (1991) 445.
- 19 I. Liska, E.R. Brouwer, A.G.L. Ostheimer, H. Lingeman, U.A.Th. Brinkman, R.B. Geerdink and W.H. Mulder, *Int. J. Environ. Anal. Chem.*, 47 (1992) 267.
- 20 R. Reupert, I. Zube and E. Plöger, *LC·GC*, 5 (1992) 43.
- 21 C. Markel, D.F. Hagen and V.A. Bunnelle, *LC·GC*, 4 (1991) 10.
- 22 D.F. Hagen, C.G. Markell, G.A. Schmitt and D.D. Blevins, *Anal. Chim. Acta.*, 236 (1990) 157.
- 23 A. Kraut-Vass and J. Thoma, *J. Chromatogr.*, 538 (1991) 233.
- 24 O. Evans, B.J. Jacobs and A.L. Cohen, *Analyst*, 116 (1991) 15.
- 25 D. Barceló, G. Durand, V. Bouvot and M. Nielen, *Environ. Sci. Technol.*, 27 (1993) 271.
- 26 *Determination of organic compounds in drinking water by liquid-solid extraction and capillary column gas chromatography-mass spectrometry. Method 525.1*. US Environmental Protection Agency, National Technical Information Service, Springfield, VA, 1991.
- 27 E.R. Brouwer, H. Lingeman and U.A.Th. Brinkman, *Chromatographia*, 29 (1990) 415.
- 28 E.R. Brouwer, D.J. Van Iperen, I. Liska, H. Lingeman and U.A.Th. Brinkman, *Int. J. Environ. Anal. Chem.*, 47 (1992) 257.
- 29 K.M. Hill, R.H. Hollowell and L.A. Dal Cortivo, *Anal. Chem.*, 56 (1984) 2465.
- 30 M.W. Dong, F.L. Vandemark, W.M. Reuter and M.V. Pickering, *Amer. Env. Lab.*, 2 (6) (1990) 14.
- 31 *Measurement of N-methylcarboxylamines and N-methylcarbamates in water by direct aqueous injection HPLC with post-column derivatization. Method 531.1*. US Environmental Protection Agency, National Technical Information Service, Springfield, VA, 1991.
- 32 C.H. Marvin, I.D. Brindle, C.D. Hall and M. Chiba, *J. Chromatogr.*, 503 (1990) 167.
- 33 M.V. Pickering, *LC·GC*, 6 (1988) 994.
- 34 M.C. Hennion, P. Subra, R. Rosset, J. Lamacq, P. Scribe and A. Saliot, *Int. J. Environ. Anal. Chem.*, 42 (1990) 15.
- 35 P. Subra, M.C. Hennion, R. Rosset and R.W. Frei, *J. Chromatogr.*, 456 (1988) 121.
- 36 C.E. Werkhoven-Goewie, U.A.Th. Brinkman and R.W. Frei, *Anal. Chem.*, 53 (1981) 2072.
- 37 J. Slobodnik, E.R. Brouwer, R.B. Geerdink, W.H. Mulder, H. Lingeman and U.A.Th. Brinkman, *Anal. Chim. Acta*, 268 (1992) 55.
- 38 P. Subra, M.C. Hennion, R. Rosset and R.W. Frei, *Int. J. Environ. Anal. Chem.*, 37 (1989) 45.

Analysis of polyethylene glycols with respect to their oligomer distribution by high-performance liquid chromatography

Thomas Meyer, Dieter Harms and Jürgen Gmehling*

Universität Oldenburg, Technische Chemie, P.O. Box 2503, W-2900 Oldenburg (Germany)

(First received December 2nd, 1992; revised manuscript received February 22nd, 1993)

ABSTRACT

The analysis of average molecular masses and molecular mass distributions by means of liquid chromatography is usually performed with size-exclusion columns. With mathematical methods the average molecular mass of the sample and its distribution are then calculated by comparison with standards. For polyethylene glycols (PEGs), a simple way to separate the oligomer species by isocratic elution with reversed phase columns was found. They can be identified and analysed quantitatively. The measurements were performed for PEGs with molecular masses from 300 up to 2000 g/mol. The results for several commercially available PEGs are presented. A comparison between a large-scale PEG and a PEG standard is shown, which demonstrates that polymer standards must be handled with care.

INTRODUCTION

In recent years, aqueous polymer two-phase systems have become increasingly interesting. These liquid two-phase systems are made by mixing two so-called incompatible polymers such as polyethylene glycol (PEG) and dextran (Dx) or a polymer and a salt in water [1,2]. Two water-rich phases form without the addition of any organic solvents, and these systems have quite interesting properties for the extraction of biochemically manufactured products from fermentation broth. Many efforts have been made to analyse and understand the phase equilibrium behaviour depending on temperature, pH and type of polymer [3–5]. Earlier work reported a fractionation of the polymer between the phases, *i.e.*, the average molecular mass of the polymer used is different in the phases after establishing equilibrium. With a view to the precise analysis

of these type of equilibria, a method has been developed to analyse the PEGs with respect to the type and amount of each oligomer species. In contrast to the frequently used size-exclusion columns, from which the average molecular mass and its distribution can only be estimated with the help of polymer standards and mathematical methods [6,7], a reversed-phase column was used to separate and identify the oligomer species from each other. The separation of the oligomer species is achieved by isocratic elution. This is advantageous because the equipment is cheaper and a refractive index (RI) detector can be used without problems. The separation of the oligomer species is important for the development of thermodynamic models for the aqueous two-phase-systems considering the polydispersity of the PEG.

Throughout this paper, polyethylene glycols are specified as PEG300, PEG1000, etc., where the number is the approximate average molecular mass in g/mol, based on mass fractions as given by the distributor. Single oligomers are

* Corresponding author.

characterized in the same way, but with their precise molecular mass and in addition with the number of their $-\text{CH}_2\text{CH}_2\text{O}-$ monomer units; for example, PEG370(8) means octaethylene glycol.

EXPERIMENTAL

Chemicals

All chemicals used were commercially available. The polyethylene glycols were industrial scale products (trade name Lipoxol) and were obtained from Hüls (Hamburg, Germany), except the PEG standard PEG445, which was purchased from Polymer Standard Service (PSS) (Frankfurt, Germany). Mono-, di-, tri- and tetraethylene glycols were obtained from Merck (Darmstadt, Germany). Methanol was purchased from Riedel-de Haën (Seelze, Germany) and had a purity of better than 99.8%. Demineralized water was used after double distillation.

Equipment

An isocratic HPLC system was set up for the analysis. The solvent was methanol–water with different volume fractions of methanol, depending on the type of polymer to be analysed. The HPLC system consisted of the components listed and described in Table I. As PEG cannot be detected by UV absorption, an RI detector had

to be used. Integration was performed with a simple integrator.

Chromatographic conditions

A high-precision RI detector was used. It was automatically heated to a fixed temperature of 40°C, so that the whole analysis was performed at this temperature. To ensure maximum baseline stability the injection valve and the column were also held at a constant temperature (40°C). The tube connections from the column to the detector were insulated to avoid disturbance from room temperature changes. Before entering the column a side stream of the solvent, which was pumped at 1 cm³/min, was separated by a simple T-piece to supply continuously the reference cell of the detector. The flow through the reference cell was controlled by a needle valve. The samples were detected by measuring the refractive index relative to this reference. To ensure reproducible conditions, the pressure at the pump, which depends naturally on the position of the needle valve, was held constant.

The quality of the separation of the oligomer species depends strongly on the methanol-to-water ratio in the solvent. At a constant ratio in an isocratic system small molecules leave the column first and are detected as sharp more or less separated peaks. With increasing chain length the peaks become wider and show tailing effects. Very large molecules are highly diluted and are only detected with difficulty. This limits the described method to PEGs up to PEG2000. Gradient elution was tested but not taken into account, because this causes problems with the

TABLE I
COMPONENTS OF THE HPLC SYSTEM

Component	Model and company	Description/conditions
Degasser	ERC, Type 3312	Automatic online membrane degasser
Pump	Merck–Hitachi, HPLC pump 6000	0–400 bar, 0.01–9.99 cm ³ /min
Injection valve	Rheodyne, Type 7215	Standard six-way valve, 20- μ l sample loop
Column	Merck, LiChrospher 100 RP-18	Standard reversed-phase column
Thermostat	Merck–Hitachi, Type T-6300	Air thermostat for columns, 30–99°C
Detector	ERC, Type 7511	High-precision RI detector, automatic temperature control at 40°C
Integrator	Merck–Hitachi, Type D-2500	Standard HPLC integrator

RI detector and is not necessary for the smaller PEGs. For every polymer analysed the optimum methanol-to-water ratio had to be found and these are given in Table II. Samples were prepared by dissolving the polymer in an amount of 1–5% (w/w) in the ready-mixed solvent.

Ethylene and di-, tri- and tetraethylene glycols were available as pure substances. Analysing lower-molecular-mass PEG, e.g., PEG300, and comparing the retention times of the peaks with those of the pure components led easily to the identification of these special species in the PEG. From this the other species were identified by sequentially counting the peaks. The retention times increase regularly with increasing chain length. Oligomer species in higher molecular mass PEG were then found by comparison of the retention times with those from PEG300, and so on.

The amount of each oligomer was calculated from the peak area. It was found that the detector signal is linearly dependent on the mass fraction of polymer in the sample, but independent of the molecular mass in the studied range. This could be verified by injecting equally concentrated solutions of different molecular masses and solutions of different concentration and the same molecular mass. Here only a simple calibration relating the total area of all peaks of an analysis to the overall mass fraction of PEG in the sample was needed.

RESULTS AND DISCUSSION

Table II gives the calculated average molecu-

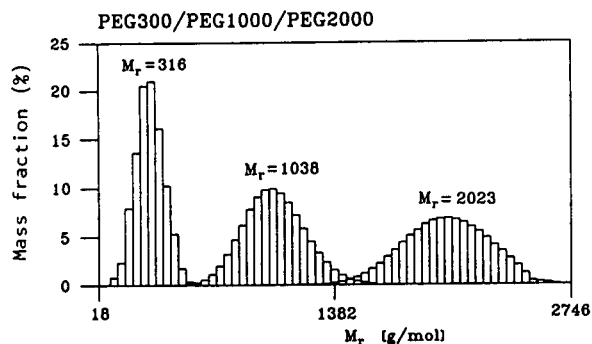


Fig. 1. Histogram of amounts of oligomer species in PEG300, PEG1000 and PEG2000.

lar masses from the analysis and the range of oligomers found. In PEG300 twelve species of oligomers were detected from ethylene glycol to dodecaethylene glycol. The number of species increases with increasing average molecular mass M_r . The error is about 2%. It is convenient to do the calibration runs several times and take the average number of counts to minimize the error.

Fig. 1 demonstrates the distribution of the molecular mass of the oligomers from PEG300, PEG1000 and PEG2000 in the form of histograms. The mass fraction of each species in the polymer (not in the sample solution) is shown as the function of molecular mass. These are results for what we call “clean” polymers. In the chromatograms only a sequence of consecutive oligomer peaks with increasing and subsequently, after a maximum, decreasing peak areas are found. Fig. 2 shows such a run for PEG2000.

TABLE II
METHANOL-TO-WATER RATIOS FOR THE DIFFERENT POLYMERS ANALYSED

Polymer	Methanol in solvent (vol. %)	M_r (g/mol)	Range of oligomers
PEG300	20	316	PEG62(1)–PEG546(12)
PEG400	20	417	PEG150(3)–PEG590(13)
PEG445 (standard)	20	344	PEG194(4)–PEG590(13)
PEG550	45	1034	PEG150(3)–PEG1954(44)
PEG1000	50	1038	PEG502(11)–PEG1602(36)
PEG2000	50	2023	PEG1118(25)–PEG2658(60)

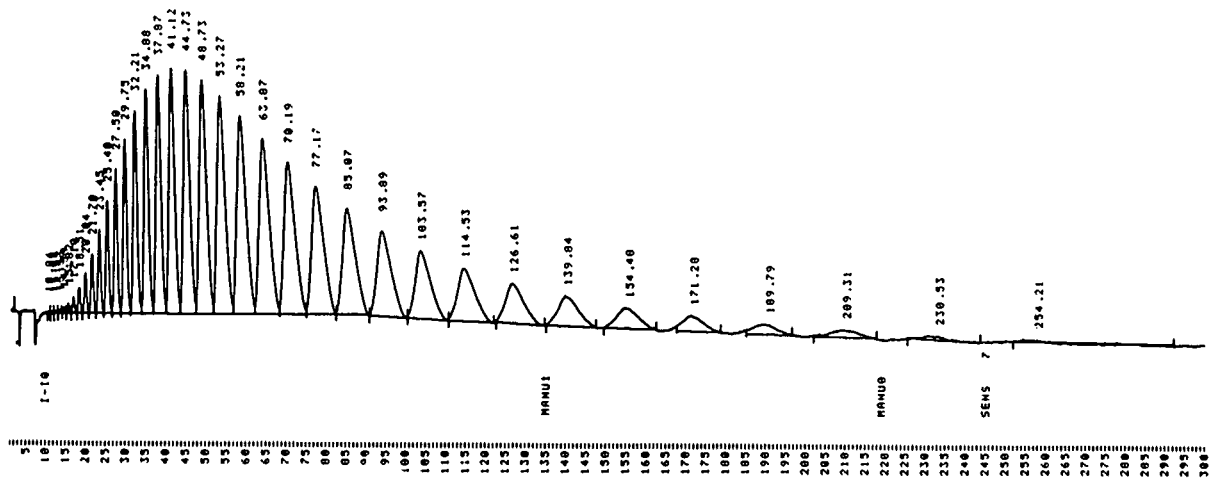
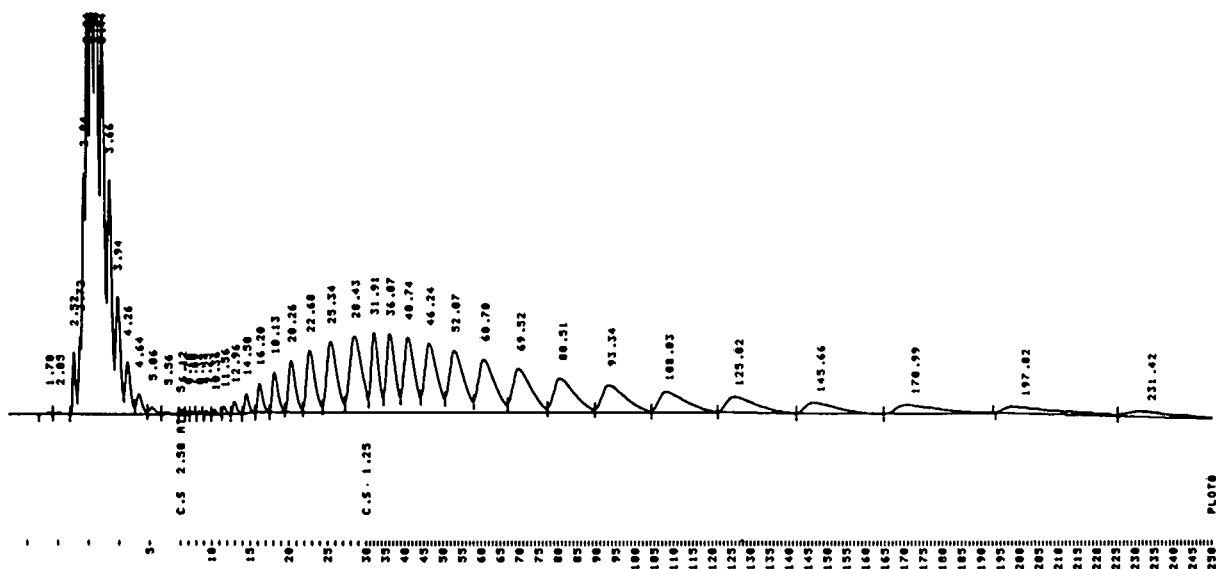


Fig. 2. Chromatogram for PEG2000.

Most of the chromatograms from the Hüls polymers analysed in this work were similar to that in Fig. 2.

Some surprising results were obtained for a few types of polymers. Fig. 3 shows an analysis of PEG550 from Hüls. Here obviously a polymer with a lower molecular weight of around 450 g/mol has been blended with an amount of high-molecular-mass polymer (around 1500 g/mol). As shown in Table II, the obtained weight-average

molecular mass of 1034 g/mol differs significantly from 550 g/mol. To verify this surprising result, the average molecular mass of the PEG sample was determined by the viscosimetric method of Staudinger [8]. With PEG600 and PEG2000 as standards it was found that the average molecular mass of the PEG550 sample was *ca.* 960 g/mol. The molecular mass estimated by the Staudinger method is nearly a weight-average value. An inquiry at Hüls con-



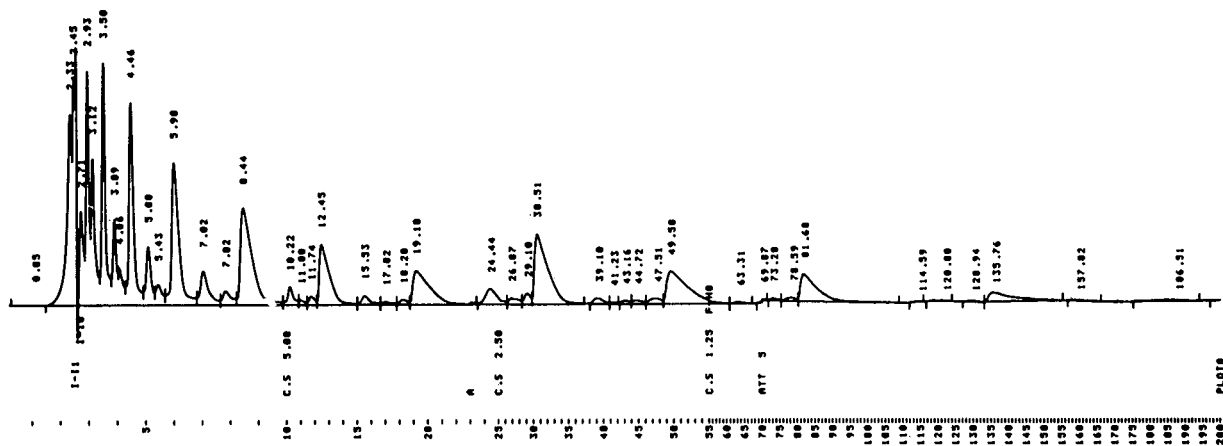


Fig. 4. Chromatogram for PEG445 from PSS.

firmed our measurements. Their PEG550 is a mixture of two different PEGs.

Another example is shown in Fig. 4, where a commercially available PEG445 standard from Polymer Standard Service (PSS) was analysed. Polymer standards are expected to have a narrow molecular mass distribution. Instead, this sample had nearly the same distribution as the Hüls PEG400 (see Table II). In addition, the analysis showed the presence of impurities, which could not be identified. It should be pointed out that an industrial-scale PEG costs less than US\$5 per 1000 g, whereas the price for 1 g of a PEG standard is *ca.* US\$50.

These examples show that even with basic HPLC equipment the composition of polyethylene glycols can be analysed with good accuracy in the range investigated. It is obvious that large amounts of impurities or the use of blends of polymers instead of “clean” products can have significant effects on the behaviour of the aqueous two-phase systems. This and the differences between specified and real molecular masses explain the difficulties that arise when trying to reproduce phase equilibrium measurements published by other workers. Also, researchers who want to develop a thermodynamic model to describe these systems often find large deviations when comparing their calculation results with data from different sources. The average molecular mass and the weight distribution

of the polymers depend strongly on the method of production and can change from batch to batch.

ACKNOWLEDGEMENT

This work was financially supported by the Bundesministerium für Forschung und Technologie, Germany (Grant Nr. 0319276A). We thank Hüls for free samples of all the industrial polyethylene glycols and Mrs. Kerstin Esser for technical assistance.

REFERENCES

- 1 P.-A. Albertsson, *Partition of Cell Particles and Macromolecules*, Wiley-Interscience, New York, 2nd ed., 1971.
- 2 H. Walter, D.E. Brooks and D. Fisher (Editors), *Partitioning in Aqueous Two-Phase Systems*, Academic Press, New York, 1985.
- 3 X. Lei, A.D. Diamond and J.T. Hsu, *J. Chem. Eng. Data*, 35 (1990) 420.
- 4 C.A. Haynes, H.W. Blanch and J.M. Prausnitz, *Fluid Phase Equil.*, 53 (1989) 463.
- 5 B.J. Zaslavsky, A.A. Borovskaya, N.D. Gulaeva and L.M. Milheeva, *J. Chem. Soc., Faraday Trans.*, 87 (1991) 137.
- 6 M. Connemann, J. Gaube, U. Leffrang, S. Müller and A. Pfennig, *J. Chem. Eng. Data*, 36 (1991) 446.
- 7 S.M. Snyder, K.D. Cole and D.C. Szlag, *J. Chem. Eng. Data*, 37 (1992) 268.
- 8 B. Vollmert, *Grundriss der Makromolekularen Chemie*, Vol. 3, E. Vollmert-Verlag, Karlsruhe, 1988.

Solubility parameters of broad and narrow distributed oxyethylates of fatty alcohols

A. Voelkel* and J. Janas

Poznań Technical University, Institute of Chemical Technology and Engineering, Pl. M. Skłodowskiej-Curie 2, 60-965 Poznań (Poland)

(First received February 10th, 1993; revised manuscript received April 27th, 1993)

ABSTRACT

The solubility parameter δ_2 and its components of broad and narrow distributed alcohol oxyethylates were determined by inverse gas chromatography. Corrected values of the solubility parameter δ_T were calculated from the increments of the solubility parameter corresponding to different types of intermolecular solute-solvent interactions. The corrected value of solubility parameter is always lower than that obtained directly from Guillet and co-workers' procedure. The influence of the structure of the examined oxyethylates on the solubility parameter and its components is discussed. Narrow range distributed oxyethylates are characterized by lower values of the solubility parameters than broad range products, but the difference decreases with increase in the average oxyethylation ratio. The increase in the length of oxyethylene chain increases the solubility parameter. The solubility parameter decreases with increase in temperature. Temperature and structural dependences of the solubility parameter increments are also presented and discussed. Relationships between the solubility parameter, corrected solubility parameter, its components and polarity parameters are examined.

INTRODUCTION

Oxyethylene derivatives of fatty alcohols are the main, large group of non-ionic surfactants. Polarity parameters for oxyethylates with broad and narrow distributions of oxyethylene units were reported in a previous paper [1]. It was found that narrow range distributed alcohol oxyethylates exhibit higher polarity at lower temperatures than broad distributed products. This difference decreases with increasing temperature. The retention indices of the first five McReynolds products, the coefficient ρ , polarity index and criterion A properly described the changes in the polarity of oxyethylates with changes in their structure. An increase in the average number of oxyethylene units increased the polarity of the products examined.

According to Hildebrand and Scott [2], the square root of cohesive energy density is called the solubility parameter, δ , having the units $(\text{cal}/\text{cm}^3)^{1/2}$, $(\text{J}/\text{m}^3)^{1/2}$ or $(\text{MPa})^{1/2}$. The solubility of any organic compound in various solvents is largely determined by its chemical structure and increases if the solubility parameters of the compound and solvent are equal. In addition to the chemical structure, the physical state also influences the solubility properties of a compound.

The solubility parameter has seldom been used for the characterization of surface-active compounds. However, the Cohesive Energy Ratio (CER) theory discussed [3] the behaviour of an emulgator in an oil-water system according to the cohesive energies of all components of the system. However, as the data required for most surfactants were not available, the CER theory has seldom been used in practical applications. Determination of the solubility parameter for

* Corresponding author.

surfactants could facilitate the description of water–surfactant–oil systems.

The solubility parameter for volatile compounds is calculated from the basic equation

$$\delta = \left(\frac{\Delta H_v - RT}{V} \right)^{1/2} \quad (1)$$

where ΔH_v = enthalpy of vaporization, R = gas constant, T = temperature and V = molar volume.

For low- or non-volatile species the use of eqn. 1 is impossible. There are two ways to calculate the value of the solubility parameter for this group of compounds: (i) calculation using the structural increments of cohesive energy given by Hoy [4,5] or Hoftyzer and Van Krevelen [6], which results in a *ca.* 10% relative error for the solubility parameter; and (ii) the method of Guillet and co-workers [7,8] with the use of inverse gas chromatography (IGC). Guillet and co-workers presented a procedure for the evaluation of solubility parameters under assumption that the solute–solvent interaction parameter κ^∞ has free energy characteristics with enthalpic (κ_H^∞) and entropic (κ_s^∞) terms:

$$\kappa^\infty = \kappa_H^\infty + \kappa_s^\infty \quad (2)$$

In an IGC process, volatile diluent, injected on to the chromatographic column, has a tendency to be absorbed by the liquid phase, *i.e.*, examined compound (product). This tendency is a function of κ and is measured in terms of retention, *e.g.*, specific retention volume V_g . The interaction parameter was usually obtained in the limit of zero concentration of the solute [9–11] and calculated from the following equation:

$$\begin{aligned} \kappa_{1,2}^\infty = \ln \left(\frac{273.15R}{P_1^0 V_g^0 M_1} \right) - \frac{P_1^0}{RT} (B_{11} - V_1^0) \\ + \ln \left(\frac{\rho_1}{\rho_2} \right) - \left(1 - \frac{V_1^0}{V_2^0} \right) \end{aligned} \quad (3)$$

where M_1 , P_1^0 , B_{11} , V_1^0 , ρ_1 and V_g^0 are the molecular mass, saturated vapour pressure, second virial coefficient, molar volume and specific retention volume of the solute, respectively, ρ_2

and V_2^0 are the density and molar volume of polymer, T is the column temperature, R is the gas constant.

The following equation was used to calculate the solubility parameter of the stationary phase [7,8]:

$$\frac{\delta_1^2}{RT} - \frac{\kappa^\infty}{V_1^0} = \frac{2\delta_2}{RT} \cdot \delta_1 - \left(\frac{\delta_2^2}{RT} + \frac{\kappa_s^\infty}{V_1^0} \right) \quad (4)$$

where δ_1 is the solute solubility parameter. Plotting the left-hand side of eqn. 4 *versus* δ_1 , one obtains a straight line with slope proportional to δ_2 of the polymer [7,12,13].

The use of the Guillet procedure has been reported in a number of papers [7,12,14–17]. Usually excellent linearity of eqn. was found [18]. Price [17] examined organic compounds of relatively low molecular masses: two non-polar alkanes, *n*-hexadecane and squalane, two alkyl phthalates, dinonyl and di-*n*-octyl phthalate, and two compounds having polar groups, *N*-methylpyrrolidone and dibutyl-2-ethylhexamide. Price found a downward curvature of eqn. 4 for the alkane systems, *i.e.*, too low estimates of δ_2 , and upward curvature (overestimates of the solubility parameter) for the other compounds examined. Price separated the contributions to the solubility parameter attributed to dispersive (δ_d) and polar (δ_p) solute–solvent interactions. The total (corrected) solubility parameter was calculated from the equation

$$\delta^2 = \delta_d^2 + \delta_p^2 \quad (5)$$

Although Price reported a significant improvement of the prediction of the solubility parameter, he indicated that the interaction parameter κ for small-molecule systems should include contributions negligible for typical polymeric systems.

We extended the group of polar and non-polar test solutes. Their retention data would allow the calculation of the increments of the solubility parameter according to the following procedure: (i) eqn. 4 would be used separately for three different groups of solutes, the interactions of which with the liquid stationary phase could be attributed to dispersive (alkanes), polar non-hydrogen bonding (aromatic hydrocarbons, ketones, nitropropane) and hydrogen bonding

(alcohols and pyridine) interactions (for details, see Experimental); (ii) the total, corrected solubility parameter would be calculated from an equation similar to those proposed earlier by Hansen [19,20]:

$$\delta_T^2 = \delta_d^2 + \delta_p^2 + \delta_h^2 \quad (6)$$

which corresponds to the contributions of interaction forces to the cohesive energy [2]:

$$E_{\text{coh}} = E_d + E_p + E_h \quad (7)$$

where E_d , E_p and E_h denote the contributions of dispersion, polar forces and hydrogen bonding, respectively, to the cohesive energy of the molecule.

The aim of this work was to: (i) examine the group of oligomeric oligooxyethylene derivatives of cetyl alcohols by inverse gas chromatography; (ii) check the applicability of the Guillet procedure for the oligomers examined and, if possible, to determine their solubility parameter δ_2 by the Guillet procedure; (iii) separate the components of the solubility parameter which could be attributed to dispersive (δ_d), polar (δ_p) and hydrogen bonding (δ_h) interactions; (iv) calculate the corrected value of the solubility parameter from its components according to eqn. 6; and (v) examine structure–solubility parameter relationships for the examined group of compounds.

EXPERIMENTAL

Materials

Cetyl alcohol containing 94% of hexadecanol was used to obtain conventional products with a broad range distribution of homologues (BRD) and narrow range distributed ethoxylates (NRD) having average ethoxylation numbers from 3 to 11. Conventional products were obtained using sodium hydroxide as a catalyst, whereas a proprietary catalyst [18] was utilized to produce narrow range distributed ethoxylates. All products were synthesized at the Institute of Heavy Organic Synthesis “Blachownia”, Kędzierzyn-Koźle, Poland. The contents of components having different lengths of the oligooxyethylene

TABLE I

CONTENT OF COMPONENTS IN THE PAIRS OF BRD AND NRD C₁₆E₆ OXYETHYLATES

Component	Content (%)	
	BRD	NRD
Light components	1.38	2.80
C ₁₆ H ₃₃ OH	5.86	2.28
C ₁₈ H ₃₇ OH	0.11	0.19
C ₁₆ H ₃₃ O(CH ₂ CH ₂ O) ₁ H	5.37	1.48
C ₁₆ H ₃₃ O(CH ₂ CH ₂ O) ₂ H	7.97	3.08
C ₁₆ H ₃₃ O(CH ₂ CH ₂ O) ₃ H	9.62	6.74
C ₁₆ H ₃₃ O(CH ₂ CH ₂ O) ₄ H	10.53	12.70
C ₁₆ H ₃₃ O(CH ₂ CH ₂ O) ₅ H	10.69	18.16
C ₁₆ H ₃₃ O(CH ₂ CH ₂ O) ₆ H	10.37	18.78
C ₁₆ H ₃₃ O(CH ₂ CH ₂ O) ₇ H	7.01	14.57
C ₁₆ H ₃₃ O(CH ₂ CH ₂ O) ₈ H	8.43	8.73
C ₁₆ H ₃₃ O(CH ₂ CH ₂ O) ₉ H	6.86	4.05
C ₁₆ H ₃₃ O(CH ₂ CH ₂ O) ₁₀ H	5.21	1.52
C ₁₆ H ₃₃ O(CH ₂ CH ₂ O) ₁₁ H	3.77	0.35
C ₁₆ H ₃₃ O(CH ₂ CH ₂ O) ₁₂ H	2.13	0.03
C ₁₆ H ₃₃ O(CH ₂ CH ₂ O) ₁₃ H	0.80	0.02
C ₁₆ H ₃₃ O(CH ₂ CH ₂ O) ₁₄ H	0.06	–
Dioxane	–	–
PEG	–	–

chain in the representative pair of oxyethylates is given in Table I. The comparison of homologue distributions for these products indicates a slight shift of the maximum in the NRD products towards the homologues having the higher content of oxyethylene groups. The exact data for GC analysis of oxyethylates were given previously [1].

IGC experiments

The conditions for the IGC experiments were the same as reported previously [1]. To facilitate the determination of the components of solubility parameters, the number of test solutes was significantly increased. The following volatile compounds were used as test probes: *n*-alkanes from *n*-pentane to *n*-decane, the aromatic hydrocarbons benzene, toluene, xylene and ethylbenzene, *n*-alkanols from methanol to 1-butanol, the ketones 2-butanone and 2-pentanone, nitropropane and pyridine.

Solubility parameter and its components

Solubility parameters for the test solutes, δ_1 , were calculated from eqn. 1 using the values of the enthalpy of evaporation [21,22]. These values are presented in Table II. The Flory–Huggins interaction parameter κ_{12}^∞ was calculated from eqn. 3 using the values of the second virial coefficient, B_{11} (Table II), taken from ref. 23 or calculated by the procedure given in refs. 7 and 24. Vapour pressures were taken or compiled from literature data [20,25,26]. The solubility parameter δ_2 , in the first step, was calculated from eqn. 4. The increments of the solubility parameter corresponding to different types of solute–solvent interactions were determined as follows: eqn. 4 was used separately for three groups of solutes, (i) *n*-alkanes, (ii) polar non-hydrogen bonding compounds (aromatic hydrocarbons, ketones and nitropropane) and (iii) alcohols and pyridine; it was assumed that the slope of eqn. 4 for *n*-alkanes is proportional to the dispersive component of the solubility parameter:

$$\delta_d = \frac{\text{slope}_{n\text{-alkanes}} \cdot RT}{2} \quad (8)$$

the polar increment of the solubility parameter, δ_p , was calculated from the difference in the slopes for polar solutes and *n*-alkanes:

$$\delta_p = \frac{(\text{slope}_{\text{polar}} - \text{slope}_{n\text{-alkanes}})RT}{2} \quad (9)$$

and the hydrogen bonding component, δ_h , from the corresponding relationship for *n*-alkanols, pyridine and *n*-alkanes:

$$\delta_h = \frac{(\text{slope}_{\text{alcohols}} - \text{slope}_{n\text{-alkanes}})RT}{2} \quad (10)$$

The corrected value of solubility parameter was calculated from eqn. 6.

RESULTS AND DISCUSSION

The main problem was the applicability of the Guillet procedure for the determination of the solubility parameter of surface-active agents of

TABLE II

SOLUBILITY PARAMETERS, δ_1 , AND VIRIAL COEFFICIENTS, B_{11} , FOR THE TEST SOLUTES

Test solute	Solubility parameter, δ_1 [(J/m ³) ^{1/2}]			Virial coefficient, B_{11} (cm ³ /mol)		
	70°C	80°C	90°C	70°C	80°C	90°C
<i>n</i> -Pentane	12076	11768	11433	-836	-733	-629
<i>n</i> -Hexane	12722	12299	12199	-1275	-1111	-947
<i>n</i> -Heptane	13266	13039	12799	-1899	-1650	-1401
<i>n</i> -Octane	13610	13399	13176	-2660	-2301	-1943
<i>n</i> -Nonane	13953	13746	13548	-3500	-3000	-2570
<i>n</i> -Decane	14229	14035	13841	-4600	-3900	-3300
Methanol	27483	27022	26524	-1157	-944	-731
Ethanol	24043	23664	23542	-1708	-1174	-640
1-Propanol	22064	21741	21370	-1619	-1278	-937
1-Butanol	20504	20262	20019	-1770	-1484	-1199
2-Butanone	17223	16919	16613	-1527	-1239	-952
2-Pentanone	16399	16126	15840	-2450	-1997	-1543
1-Nitropropane	19589	19541	19493	-3272	-2611	-2118
Pyridine	19535	19285	19035	-1303	-1171	-1039
Benzene	17176	16884	16601	-1036	-902	-768
Toluene	16518	16292	16035	-2041	-1681	-1408
Xylene	16183	15955	15715	-3214	-2616	-2164
Ethylbenzene	16483	16441	16400	-2706	-2228	-1863

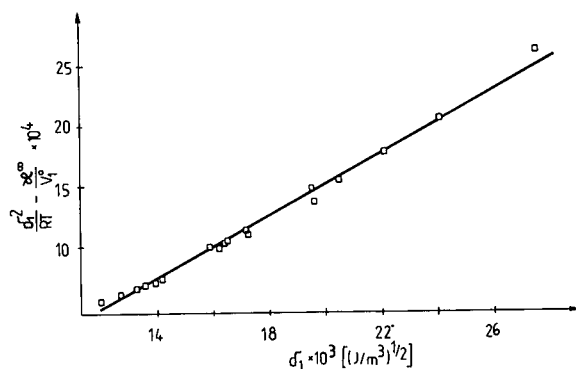


Fig. 1. Example of relationship of $(\delta_1^2/RT - \kappa^0/V_1^0)$ vs. δ_1 for $C_{16}\bar{E}_3$ (BRD type).

relatively low molecular mass. As an example, for the group of surfactants examined the relationship between the left-hand side of eqn. 4 and δ_1 is shown in Fig. 1. Only slight deviations from the straight line are observed and the correlation coefficients are relatively high (>0.9). The deviations are significantly smaller than those reported by Price [17]. Values of the solubility

parameter δ_2 determined directly from eqn. 4 are presented in Tables III–V. However, the deviations from the straight line described by eqn. 4 are large enough to allow the determination of increments of the solubility parameter (Fig. 2). Estimated increments of the solubility parameter are also given in Tables III–V. The experimental error in the determination of δ_2 , increments of the solubility parameter (δ_d , δ_p , δ_h) and corrected solubility parameter never exceeded $0.05 \cdot 10^3$ $(\text{J}/\text{m}^3)^{1/2}$ and generally was in the range 0.01–0.02 units. They were used for the calculation of corrected solubility parameter δ_T by the use of eqn. 6, values for which are also given in Tables III–V. The values of the corrected solubility parameter δ_T are lower than those calculated directly from eqn. 4. The difference changes from $1 \cdot 10^3$ to $3 \cdot 10^3$ $(\text{J}/\text{m}^3)^{1/2}$ depending on the type of compound examined and the average number of oxyethylene units in its molecule.

The solubility parameter δ_2 increases with increase in the average oxyethylation rate of cetyl alcohol for compounds containing up to

TABLE III

SOLUBILITY PARAMETER (δ_2), ITS COMPONENTS (δ_d , δ_p , δ_h) AND CORRECTED SOLUBILITY PARAMETER (δ_T) FOR BROAD AND NARROW DISTRIBUTED OXYETHYLATES [$10^3(\text{J}/\text{m}^3)^{1/2}$] AT 70°C

Type	Average number of EO units	δ_2	δ_d	δ_p	δ_h	δ_T	
BRD	3	16.14	14.88	0.41	0.99	14.92	
	4	16.83	14.68	1.62	3.48	15.17	
	5	16.79	14.92	1.88	2.62	15.26	
	6	16.88	14.86	2.94	1.75	15.25	
	7	17.24	13.30	5.18	6.14	15.54	
	8	18.00	13.17	4.51	7.21	15.67	
	9	17.83	13.85	3.77	6.01	15.56	
	10	17.57	14.08	4.31	5.87	15.84	
	11	17.83	13.68	4.27	8.10	16.46	
	NRD	3	16.64	14.12	2.79	5.76	15.16
		4	17.22	14.12	3.12	5.39	15.20
5		17.06	13.74	3.62	5.78	15.34	
6		17.24	13.24	4.10	6.47	15.30	
7		17.03	13.47	4.10	6.14	15.36	
8		17.40	13.44	4.02	6.69	15.54	
9		17.75	14.46	2.93	5.17	15.63	
10		18.12	14.81	4.21	4.31	15.99	
11		18.40	13.90	6.70	4.10	15.97	

TABLE IV

SOLUBILITY PARAMETER (δ_2), ITS COMPONENTS (δ_d , δ_p , δ_h) AND CORRECTED SOLUBILITY PARAMETER (δ_T) FOR BROAD AND NARROW DISTRIBUTED OXYETHYLATES [$10^3(\text{J}/\text{m}^3)^{1/2}$] AT 90°C

Type	Average number of EO units	δ_2	δ_d	δ_p	δ_h	δ_T	
BRD	3	15.81	14.43	0.22	2.31	14.61	
	4	16.58	14.21	1.77	3.58	14.76	
	5	16.83	14.28	2.11	3.84	14.94	
	6	16.82	14.43	1.96	3.73	15.04	
	7	17.12	14.25	2.32	4.13	15.02	
	8	17.13	14.27	2.39	4.38	15.12	
	9	17.37	13.73	3.36	5.28	15.09	
	10	17.26	14.10	2.70	4.75	15.12	
	11	17.81	13.34	4.09	6.49	15.39	
	NRD	3	16.89	13.94	2.60	4.36	14.84
		4	17.01	13.90	2.55	4.59	14.85
5		17.41	13.46	3.47	5.79	15.06	
6		17.44	13.48	3.42	6.04	15.03	
7		17.38	13.49	3.56	5.67	15.06	
8		17.74	13.33	4.58	5.83	15.25	
9		17.25	13.79	3.17	5.24	15.09	
10		17.50	13.39	4.13	5.82	15.17	
11		17.79	13.13	4.39	6.86	15.45	

TABLE V

SOLUBILITY PARAMETER (δ_2), ITS COMPONENTS (δ_d , δ_p , δ_h) AND CORRECTED SOLUBILITY PARAMETER (δ_T) FOR BROAD AND NARROW DISTRIBUTED OXYETHYLATES [$10^3(\text{J}/\text{m}^3)^{1/2}$] AT 110°C

Type	Average number of EO units	δ_2	δ_d	δ_p	δ_h	δ_T	
BRD	3	15.54	14.51	0.15	1.19	14.26	
	4	16.28	14.19	0.91	2.54	14.28	
	5	16.29	13.92	1.88	2.62	14.28	
	6	16.29	13.76	1.96	3.39	14.30	
	7	16.77	13.04	3.52	5.08	14.43	
	8	16.57	12.83	4.58	5.50	14.41	
	9	16.99	12.68	3.58	6.02	14.49	
	10	16.88	13.07	3.34	5.30	14.49	
	11	17.52	12.59	4.60	6.78	14.99	
	NRD	3	16.21	12.92	2.85	5.53	14.34
		4	16.62	13.28	2.73	4.61	14.32
5		17.13	12.90	3.58	5.95	14.65	
6		17.18	12.54	4.20	6.37	14.68	
7		17.05	13.01	3.49	5.60	14.59	
8		17.09	12.96	3.89	5.58	14.64	
9		17.06	13.12	3.42	5.47	14.62	
10		17.25	12.66	4.10	6.39	14.76	
11		17.57	12.59	4.50	6.78	15.07	

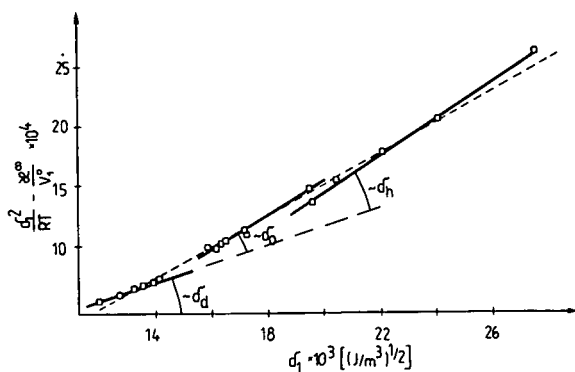


Fig. 2. Determination of increments of the solubility parameter.

7–8 oxyethylene units in both the BRD and NRD groups of surfactants. For BRD compounds having more than 7–8 oxyethylene units some decrease in δ_2 is observed. This effect is observed only at 70°C. The influence of the number of oxyethylene chain length on the solubility parameter δ_2 is less significant (Fig. 3) than for BRD analogues. Values of the solubility parameter δ_2 are higher for NRD products, but the difference decreases with increase in the oxyethylation ratio.

The examined parameters are characterized by δ_2 values ranging from $16 \cdot 10^3$ to $18 \cdot 10^3$ $(J/m^3)^{1/2}$ at 70°C, which correspond to 7.8–9 $(cal/cm^3)^{1/2}$ [note that $10^3 (J/m^3)^{1/2} = (MPa)^{1/2} =$

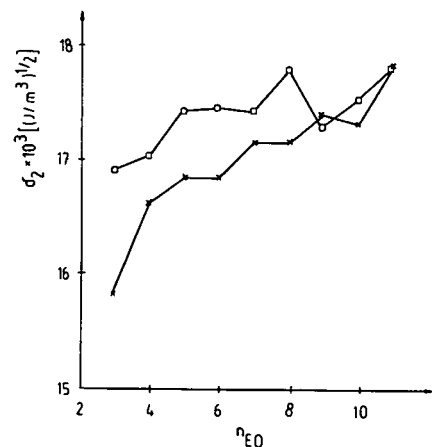


Fig. 3. Influence of the number of oxyethylene units on the values of the solubility parameter δ_2 for (x) BRD and (□) NRD oxyethylates.

$0.4888 (cal/cm^3)^{1/2}$]. These values are higher than or equal to those reported for polystyrene of $7.6 (cal/cm^3)^{1/2}$ [7], poly(methyl acrylate) of $8.7 (cal/cm^3)^{1/2}$ [7] and silicone stationary phases, OV-101 of $6.49 (cal/cm^3)^{1/2}$ and OV-105 of $6.83 (cal/cm^3)^{1/2}$ [15]. Sanetra *et al.* [27] reported δ_2 values for poly(styrene–divinylbenzene) copolymers containing 5, 10 and 20% of divinylbenzene of 14.8, 15.7 and 17.8 $(MPa)^{1/2}$, respectively. Becerra *et al.* [15] explained the increase in the solubility parameter by the presence of 5% of cyanopropyl groups in the molecule of a dimethylsilicone. Hence the increase in the content of polar groups increases the solubility parameter. Therefore, we could discuss the increase in the solubility parameter for BRD and NRD cetyl alcohol oxyethylates as being due to an increase in their polarity.

As indicated previously, corrected values of the solubility parameter δ_T are always lower than those predicted directly by the Guillet procedure. The difference varies from $1 \cdot 10^3$ to $3 \cdot 10^3$ $(J/m^3)^{1/2}$ depending on the type of oxyethylate (BRD or NRD product), the number of oxyethylene units in the molecule and the temperature of GC experiment. Values of the corrected solubility parameter δ_T increase with increase in the oxyethylene chain length but the differences between the two groups of compounds examined are very small. Slightly higher values are observed for NRD products (by 0.2–1.0 units), but the differences diminish for homologues containing more than 7–8 oxyethylene units in their molecules (Fig. 4).

The corrected solubility parameter δ_T is calculated from increments corresponding to different types of intermolecular interactions. These increments depend also on the composition of the materials examined. The dispersive component of the solubility parameter δ_d tends to decrease with increasing oxyethylation ratio for both groups of compounds examined. However, the relationships are not monotonic, *e.g.*, linear (Fig. 5a). Generally, for a lower content of oxyethylene units δ_d is higher for BRD products, whereas for $n_{EO} \geq 7-8$ these values are similar for both groups of oxyethylates or, in some instances, higher for NRD analogues.

The polar component of the solubility parameter δ_p increases with increase in the length of the

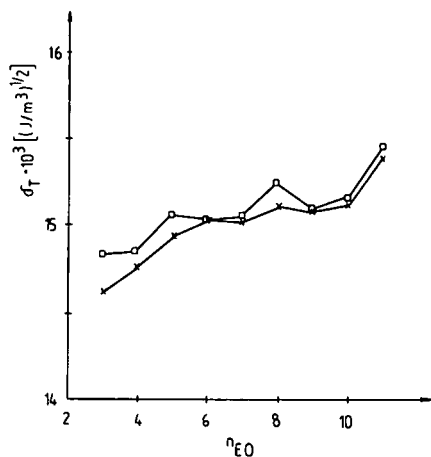


Fig. 4. Influence of the number of oxyethylene units on corrected values of solubility parameter δ_T for (x) BRD and (□) NRD oxyethylates.

oxyethylene chain. Generally, δ_p is higher for NRD products. However, for $n_{EO} \geq 7-8$ δ_p is higher for BRD oxyethylates (at 70°C, Fig. 5b). At higher temperatures, i.e. 90 and 110°C, this effect disappears and the δ_p values are very similar for both series of compounds.

The same behaviour is observed for the hydrogen bonding component of the solubility parameter δ_h . Significantly higher δ_h values are observed for compounds having a short oxyethylene chain (Fig. 5c). Higher homologues are characterized by similar values of this parameter.

In each instance large and significant changes in the values of the solubility parameter components are observed for BRD products, whereas the changes for the NRD analogues are much lower. As an example, the difference between the maximum and minimum values of δ_p (at 70°C) for BRD products is $4.5 \cdot 10^3$ (J/m³)^{1/2}, whereas the difference for NRD oxyethylates is $1.42 \cdot 10^3$ (J/m³)^{1/2}. Moreover, for higher contents of oxyethylene units the values for all types of solubility parameter increments are similar. As a result, the corrected values of the solubility parameter δ_T are similar for both groups of oxyethylates and slightly higher values for NRD products are observed only for $n_{EO} \leq 5$. In this region the δ_d -component is much higher for BRD products, but it does not compensate for the

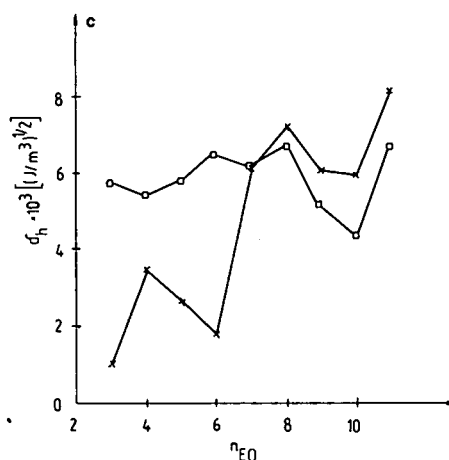
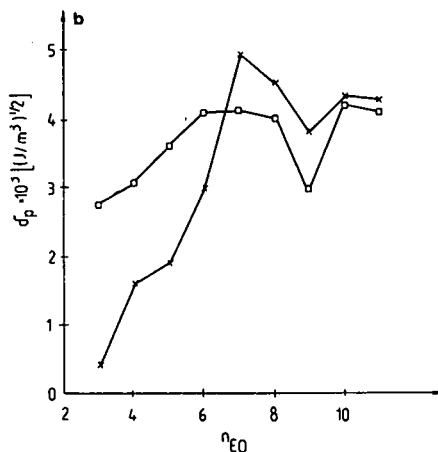
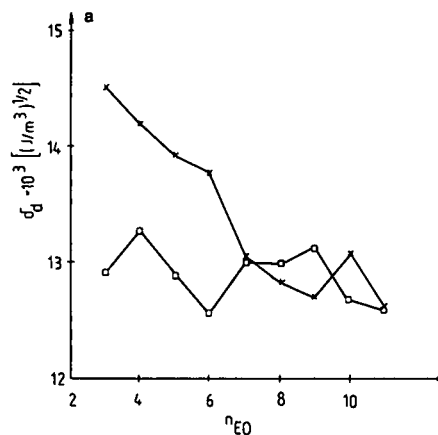


Fig. 5. Influence of the number of oxyethylene units on increments of the solubility parameter for (x) BRD and (□) NRD oxyethylates: (a) δ_d vs. n_{EO} at 110°C; (b) δ_p vs. n_{EO} at 70°C; (c) δ_h vs. n_{EO} at 70°C.

differences in δ_p and δ_h between the two series of compounds.

The solubility parameter δ_2 and its corrected value δ_T decrease with increasing column temperature. It is contradiction with statements by Becerra *et al.* [15] but agrees with the findings of Fernandez-Sanchez *et al.* [16]. The decrease in the solubility parameter seems to be approximately linear (Fig. 6a), but the evaluation of statistically significant relationships requires more experimental data than are available. Similar behaviour was observed with typical polarity parameters determined previously for the examined oxyethylates [1]. The polarity index, *PI*, the coefficient ρ and the retention indices of polar test solutes also decreased with increasing temperature. A detailed analysis of the temperature dependence of the solubility parameter's

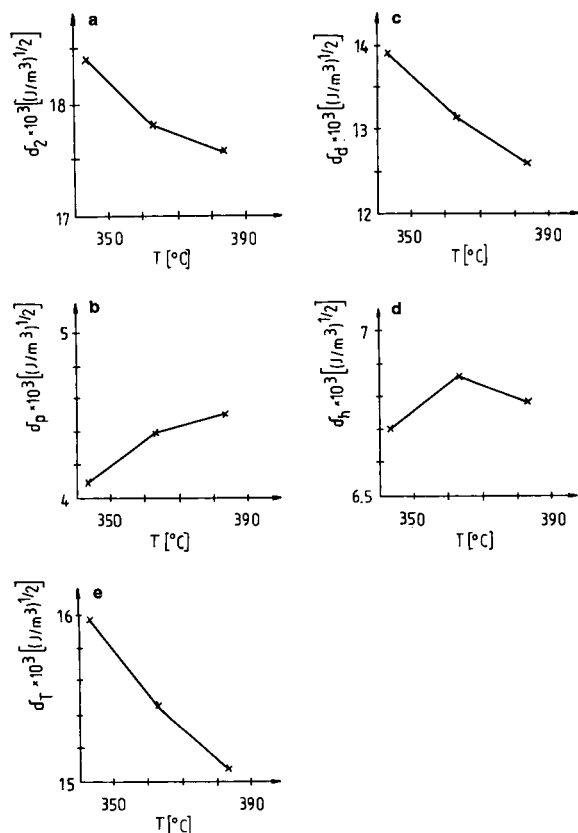


Fig. 6. Temperature dependence of (a) the solubility parameter δ_2 , (b) dispersive component δ_d , (c) polar component δ_p , (d) hydrogen bonding component δ_h and (e) corrected solubility parameter δ_T for $C_{16}\bar{E}_{11}$ narrow range distributed oxyethylate.

components should answer the question of what the reason is for the decrease in a compound's polarity. The most significant changes are observed for the dispersive components of the solubility parameter δ_d (Fig. 6b). The decrease in this increment varies from $0.24 \cdot 10^3$ to $1.31 \cdot 10^3$ (J/m³)^{1/2}, depending on the type of oxyethylate and the length of the oxyethylene chain. The polar component δ_p varies or increases with increasing temperature. There is no general rule that could describe the temperature. There is no general rule that could describe the temperature behaviour of this increment of the solubility parameter (Fig. 6c). For BRD having $n_{EO} = 11$ the lowest value of δ_p is observed at 90°C and increases at 110°C. In contrast, for $C_{16}\bar{E}_4$ BRD oxyethylate (\bar{E}_n denotes average number of oxyethylene units) the maximum value is measured at 90°C. A monotonic decrease in δ_p was found, e.g., for $C_{16}\bar{E}_7$ NRD oxyethylate. However, a monotonic increase was observed for the $C_{16}\bar{E}_{11}$ NRD analogue.

The hydrogen bonding increment of the solubility parameter also varies with increasing temperature. A representative example is given in Fig. 6d for an NRD homologue having $n_{EO} = 11$. Only in a few instances does the change in δ_h have a monotonic character, as for $C_{16}\bar{E}_7$ NRD oxyethylate.

The influence of temperature on the corrected solubility parameter is a result of temperature variations of its components. The sum of these variations gives an almost linear decrease in δ_T with increasing temperature (Fig. 6e). This decrease in δ_T is mainly caused by the significant decrease in the dispersive component δ_d with increase in temperature.

It was mentioned previously that one may discuss the solubility parameter and/or corrected solubility parameter as a measure of a compound's polarity. The polarity of surfactants is often expressed with the use of parameters determined by GC [18,28]. These parameters determined for broad and narrow range distributed oxyethylates of cetyl alcohol have been reported previously [1].

Both the solubility parameter δ_2 and corrected solubility parameter δ_T increase with increase in representative polarity parameters such as the

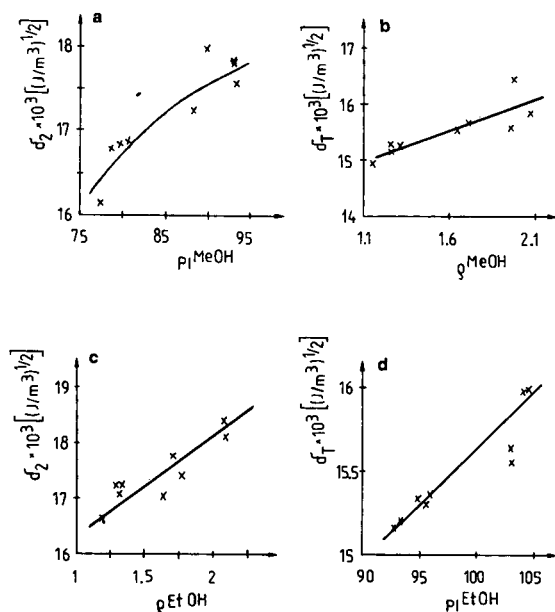


Fig. 7. Relationships between solubility and polarity parameters: (a) solubility parameter δ_2 vs. polarity index (methanol as polar solute); (b) δ_T vs. coefficient ρ (methanol as polar solute); (c) δ_2 vs. coefficient ρ (methanol as polar solute); (d) δ_T vs. polarity index (ethanol as polar solute).

polarity index PI and coefficient ρ (Fig. 7). However, these relationships are not linear. The relationship between polar (δ_p) and hydrogen bonding (δ_h) components of the solubility parameters and previously determined polarity parameters are presented in Fig. 8. Both increments of the solubility parameter increase with increasing polarity of the compounds examined. In other

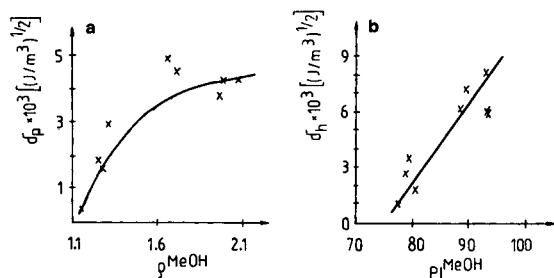


Fig. 8. Relationships between increments of solubility parameter and polarity parameters: (a) δ_p vs. coefficient ρ (methanol as polar solute); (b) δ_h vs. polarity index (methanol as polar solute).

words, the observed and measured increases in polarity are a result of increasing polar and hydrogen bonding interactions between the liquid stationary phase and test solutes in IGC.

CONCLUSIONS

Two series of cetyl alcohol oxyethylates with broad and narrow range distributions of oxyethylene units were characterized in terms of solubility parameters. The values of the solubility parameters were determined by IGC. It was found that the Guillet procedure is applicable also for compounds having relatively low molecular masses. However, some deviations from the straight line described by eqn. 4 were observed. This allows a procedure for the determination of the solubility parameter increments from IGC data to be proposed. Dispersive, polar and hydrogen bonding components were calculated and their structural dependence was examined. Corrected solubility parameters were calculated from these increments. Generally, the solubility parameter δ_2 , the corrected solubility parameter δ_T and the polar and hydrogen bonding components increase with increasing oxyethylation ratio. The dispersive component decreases with increase in the number of oxyethylene units. The increase in the corrected solubility parameter is a result of increases in the polar and hydrogen bonding components. Although both solubility and corrected solubility parameters describe the compounds examined in a similar way, the use of the corrected solubility parameter δ_T is suggested. This parameter is calculated according to the accepted Hansen's equation using the increments determined from IGC experiments. A significant temperature dependence was found for all the parameters examined. Both the solubility parameter and corrected solubility parameter decrease with increasing temperature. It seems that this decrease is mainly caused by a decrease in the dispersive increment of the solubility parameter with increasing column temperature in IGC. The increase in the solubility parameters is accompanied by an increase in the polarity parameters, e.g., the polarity index and the coefficient ρ .

ACKNOWLEDGEMENT

This work was supported by KBN Grant No. 7 0487 91 01, which is gratefully acknowledged.

REFERENCES

- 1 A. Voelkel, J. Szymanowski and W. Hreczuch, *J. Am. Oil. Chem. Soc.*, in press.
- 2 J.H. Hildebrand and R.L. Scott, *The Solubility of Nonelectrolytes*, Van Nostrand, Princeton, NJ, 1950.
- 3 A. Beerbower and M.W. Hill, in *McCutcheon's Detergents and Emulsifiers*, Allured, Ridgewood, 1971, pp. 223–232.
- 4 K.L. Hoy, *J. Paint Technol.*, 42 (1970) 76.
- 5 K.L. Hoy, *Tables of Solubility Parameters, Solvent and Coatings*, Materials Research and Development Department, Union Carbide, 1985.
- 6 P.J. Hoftyzer and D.W. Van Krevelen, in *Properties of Polymers*, Butterworth, London, 2nd ed., 1976, Ch. 7, pp. 152–155.
- 7 G. DiPaola-Barányi and J.E. Guillet, *Macromolecules*, 11 (1978) 228.
- 8 J.E. Guillet, *J. Macromol. Sci. Chem.*, 4 (1970) 1669.
- 9 O. Smidsrød and J.E. Guillet, *Macromolecules*, 2 (1969) 272.
- 10 D. Patterson, Y.B. Tewari, H.P. Schreiber and J.E. Guillet, *Macromolecules*, 4 (1971) 356.
- 11 Y.-K. Leung and B.E. Eichinger, *J. Phys. Chem.*, 78 (1974) 60.
- 12 E. Fernandez-Sanchez, A. Fernandez-Torrez, J.A. Garcia-Dominguez and J.M. Santiuste, *J. Chromatogr.*, 457 (1988) 55.
- 13 J.M. Barrales-Rienda and J. Vidal Gancedo, *Macromolecules*, 21 (1988) 220.
- 14 Y. Ren and P. Zhu, *J. Chromatogr.*, 457 (1988) 354.
- 15 M.R. Becerra, E. Fernandez-Sanchez, A. Fernandez-Torrez, J.A. Garcia-Dominguez and J.M. Santiuste, *J. Chromatogr.*, 547 (1991) 269.
- 16 E. Fernandez-Sanchez, A. Fernandez-Torrez, J.A. Garcia-Dominguez and M.D. Salvador Moya, *J. Chromatogr.*, 556 (1991) 485.
- 17 G.J. Price, in D.R. Lloyd, T.C. Ward and H.P. Schreiber (Editors), *Inverse Gas Chromatography. Characterization of Polymers and Other Materials (ACS Symposium Series, No. 391)*, American Chemical Society, Washington, DC, 1989, Ch. 5, pp. 48–58.
- 18 A. Voelkel, *CRC Crit. Rev. Anal. Chem.*, 22 (1991) 411.
- 19 C.M. Hansen, *Ind. Eng. Chem., Prod. Res. Dev.*, 8 (1969) 2; 13 (1974) 218.
- 20 C.M. Hansen, *J. Paint Technol.*, 39 (1967) 104 and 505.
- 21 R.C. Wilhoit and B.J. Zwolinski, *Handbook of Vapor Pressures and Heats of Vaporization of Hydrocarbons and Related Compounds*, Thermodynamic Research Center, Texas A&M University, College Station, TX, 1971.
- 22 *Poradnik Fizykochemiczny*, WNT, Warsaw, 1974.
- 23 J.H. Dymond and E.B. Smith, *The Virial Coefficients of Pure Gases and Mixtures. A Critical Compilation*, Clarendon Press, Oxford, 1980.
- 24 R.C. Reid, J.M. Prausnitz and T.K. Sherwood, *The Properties of Gases and Liquids*, McGraw-Hill, New York, 3rd ed., 1977.
- 25 T. Boublik, V. Fried and E. Hala, *The Vapour Pressures of Pure Substances*, Elsevier, Amsterdam, 1975.
- 26 M. Hirata, S. Ohe and K. Nagahama, *Computer Aided Data Book of Vapor-Liquid Equilibria*, Kodansha Elsevier, Tokyo, 1975.
- 27 R. Sanetra, B. Kolarz and A. Wlochowicz, *Polymer*, 28 (1987) 1753.
- 28 J. Szymanowski, *CRC Crit. Rev. Anal. Chem.*, 21 (1990) 407.

Parallel cryogenic trapping multidimensional gas chromatography with directly linked infrared and mass spectral detection

Kevin A. Krock, N. Rangunathan and Charles L. Wilkins*

Department of Chemistry, University of California, Riverside, Riverside, CA 92521 (USA)

(First received February 23rd, 1993; revised manuscript received May 3rd, 1993)

ABSTRACT

This paper describes successful implementation of multiple trap multidimensional gas chromatography (GC) directly linked with parallel Fourier transform infrared (FT-IR) and mass spectroscopy (MS) detectors. For complex mixture separation, six parallel cryogenic traps are interposed between a first-stage GC pre-column and a second-stage GC analytical column. With proper choices of heart cut time intervals, this multiple parallel cryogenic trap approach allows expansion of the practical analytical dynamic range and accommodates the separation constraints of a combined GC–FT-IR–MS system. An unleaded gasoline sample is analyzed with respect to the degree of secondary separation and to the reproducibility of adjusted retention times. The results of cryogenically trapping heart cuts using both with 72- and 12-s trapping times are presented. Shortening the trapping times from 72 to 12 s results in a significant improvement in the analytical column separation and identification with infrared and mass spectra. Thus, use of multidimensional separation coupled with multispectral detection may provide increased reliability of complex mixture component identification.

INTRODUCTION

Combination of multiple types of spectroscopic detection with gas chromatographic separation is a powerful method for analysis of complex mixtures [1]. There have been several recent applications of GC–FT-IR–MS ranging from environmental component analyses [2–4] to essential oil [5,6], biochemical, and clinical analyses [7,8]. When combined infrared and mass spectral detection are used, the specific gas chromatographic separation method used is dictated, to some degree, by the constraints of detector dead volume and sensitivity. As a

consequence, use of narrow-bore capillary GC columns is precluded and chromatographic performance is therefore limited. Thus, it is necessary to address the problem of reduced resolution that is inherent when one uses larger bore capillary columns that are compatible with these information-rich detectors. Obviously, if mixtures, rather than pure compounds reach the infrared and mass spectral detectors, the quality of combined spectroscopic library searches will be compromised and could lead to incorrect or ambiguous identification of mixture components. It is therefore clear that, in order to realize the true analytical potential of a combined separation and multi-spectral analysis system, an improved separation strategy is mandatory.

Recently, a multi-valve based multidimension-

* Corresponding author.

al gas chromatography (MDGC) system with two parallel cryogenic traps interposed between a first stage GC precolumn and a second stage GC analytical column with infrared and mass spectral detection was successfully implemented [9]. That study demonstrated the feasibility of carrying out a valve-based MDGC separation employing two parallel cryogenic traps for heart cutting. Here it is demonstrated that use of a new experimental setup, incorporating *multiple* parallel cryogenic traps, allows much improved performance for MDGC, in the context of a GC-FT-IR-MS analysis system.

Although MDGC [10–13] is a conceptually attractive method for complex mixture analysis, its applications to practical analytical problems has been relatively limited. However, it appears that use of multiple cryogenic traps allowing parallel heart cutting, combined with computer automation should obviate some of the previous difficulties. This paradigm, in the limit of short heart cut trapping times and a very large number of traps is conceptually equivalent to the approach of Phillips *et al.* [14]. The difference between the two methods is analogous to the difference between dispersive and Fourier infrared spectrometry. Depending on the nature of analysis, one can utilize a multiple parallel cryogenic trapping system to carry out heart cutting using 1–3 min trapping periods or higher resolution heart cuts employing 10–20-s trapping times. With longer heart cut times, the system behavior would be closer to a coupled column technique and, with a shorter heart cut time, the system would behave as a true multidimensional system [15]. Either approach has its advantages and disadvantages. With longer cut times an analyst can quickly estimate the approximate nature and number of components present in a complex mixture. Use of shorter trapping periods not only provides detailed information about the number and nature of the components, but can permit sample enrichment for trace components, and can reduce the required dynamic range within individual second stage chromatograms. In one sense, the choice can be described as a trade-off between increased information and longer analysis time versus less information and shorter total analysis time.

EXPERIMENTAL

Apparatus

The parallel cryogenic trap system was designed around a Hewlett-Packard GC-FT-IR-MS system, which was utilized as the basic instrument. The details of the instrument modifications and chromatographic conditions have been previously described [9]. Fig. 1 shows the schematic of the multidimensional system used in the work described here. This system employs two six-port rotary selection valves (Rheodyne, Cotati, CA, USA; 300°C maximum temperature) with one common input line and six individual output lines for routing analyte to selected traps and subsequent reinjection of trapped analytes onto the analytical column. Unlike the high performance on/off valves previously utilized for trap selection [9], the present valves allow selection of only one trap at a time. The six traps are fabricated from 1/16-in. (1 in. = 2.54 cm) stainless-steel tubing. Control of liquid nitrogen flow through the traps is accomplished by means of quick acting toggle valves (Supelco, Bellefonte, PA, USA).

Reinjection technique

Reinjection is carried out by selecting an unfilled trap to use as a trap bypass and then

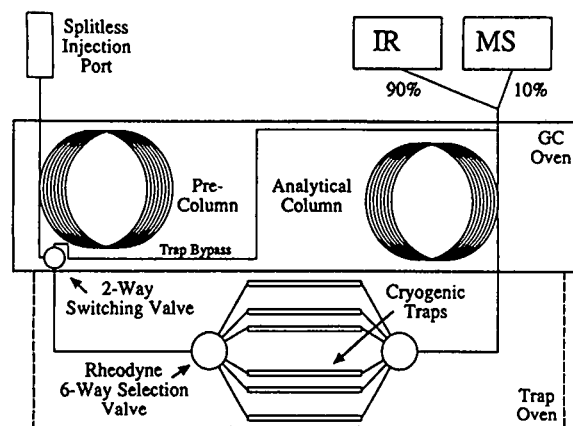


Fig. 1. Schematic diagram of the six-trap multidimensional gas chromatography system. The pre-column is a 30 m \times 0.32 mm \times 1.0 μ m DB-1701, and the analytical column is a 30 m \times 0.32 mm \times 1.0 mm DB-5 column. The parallel traps are placed in an external oven located on the top of the HP 5890 gas chromatograph.

turning off the liquid nitrogen to all the traps and delaying any reinjections until the traps equilibrate to the external oven temperature (250°C).

Rotary valves

The present design significantly reduces dead volume and metal wall contact area. Valve rotors are made from an inert polymer with an internal volume of approximately 2 μ l.

Sample

The sample analyzed in the present study is a unleaded gasoline sample which, for analysis, was injected using 0.5 μ l splitless injections with a 50 ml/min purge at 55 s into the run. Fig. 2a shows the first 20 min of the precolumn chromatogram of this sample. The secondary separation of the segments chosen for heart cutting are shown in Fig. 2b. In the first set of experiments, five segments were chosen for heart cutting. Trapped sequentially were components eluting from the precolumn consecutive 72-s periods beginning at 6 min after sample injection. A

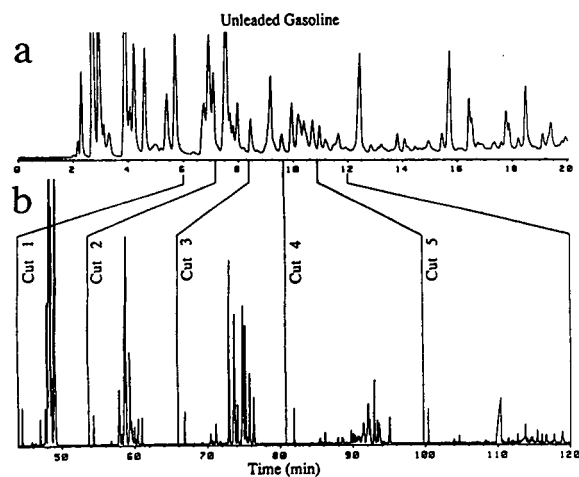


Fig. 2. (a) The first 20 min of the Gram-Schmidt reconstructed total IR response chromatogram from the precolumn separation of the unleaded gasoline sample. The areas between the lines and labeled are the 72-s heart cuts that were selected for a second stage of separation. (b) Total ion chromatogram (TIC) of the five heart cuts for run A. The five heart cuts were released to the analytical column from the traps in the sequence they were collected by the oven equilibrated method.

second set of experiments explored higher resolution analysis by sequential cryogenic trapping, for 12-s periods of precolumn eluents emerging between 7.5 and 8.5 min.

Retention time data

Two separate experiments were performed to estimate the average adjusted retention time variation. The adjusted retention time was taken as $t_R - t_M$ where t_R is the retention time of a component peak and t_M is the retention time of unretained CO_2 . Both experiments were performed by making five consecutive injections and trapping the precolumn region from 8.4 min to 9.7 min in five different traps per experiment. In experiment A, the secondary separation of each of the trapped sections was performed isothermally at 30°C, and in experiment B the separations were performed isothermally at 50°C. Adjusted retention time data were derived by the Hewlett-Packard data acquisition computers from the Gram-Schmidt reconstructed chromatograms [16]. Five peaks were chosen for analysis in experiment A, and eight peaks for experiment B.

RESULTS AND DISCUSSION

The primary focus of this investigation is the design of a simple multiple parallel cryogenic trap MDGC system, the reproducibility of retention times relative to CO_2 (which served as an internal standard), and other experimental features that are unique to a multi-parallel cryogenic trap MDGC system. The unleaded gasoline sample used here for evaluation purposes is chosen because it has a conveniently large number of components and is well-suited for the experimental questions posed, rather than as a test of the qualitative analysis capabilities of the system. Because it is a hydrocarbon mixture containing primarily C_3 to C_{12} species, it does not contain components representing a wide range of polarity or functionality. Thus, the issue of qualitative analysis is secondary in this study. The first peak in each heart cut section in Fig. 2b corresponds to the unretained CO_2 peak and retention times are mea-

sured relative to that. It is interesting to note that this CO₂ is roughly the same height peak in all the cuts. This uniformity of height reveals that there are no significant leaks in the capillary–valve interface. If there were, the relative quantity of CO₂ detected when the contents of different traps were analyzed would be non-uniform. It appears that the source of CO₂ in these analyses is a minor impurity in the carrier gas which is accumulated in the traps during the trapping time. In Fig. 2a, 30 observable peaks are seen in precolumn chromatogram over the period for which heart cuts were subsequently taken. After MDGC separation using the analytical column to further separate these five cuts total approximately 93.

Figs. 3a and b show the secondary separation of the 72-s cuts 1 and 2. The numbers above the peaks represent the cut number in which that peak appears in the series of 12-s cuts shown in

Fig. 3c. Fig. 3c shows analytical column chromatograms obtained by trapping five 12-s segments from the region of the precolumn chromatogram corresponding to the second heart cut (components eluting between 6 and 7.2 min). As expected, the sum of the five chromatograms in Fig. 3c compares well with the corresponding chromatogram presented in Fig. 3b. However, when the analytical column chromatogram in Fig. 3b is compared with the individual chromatograms in Fig. 3c, it is obvious that much improved chromatographic resolution is obtained.

Qualitative infrared and mass spectral library search identification of the separated components appearing in Fig. 3c was carried out using procedures previously described [17,18]. In most cases structural classifications, rather than specific identifications, result (See Table I). A combination of factors can account for the fail-

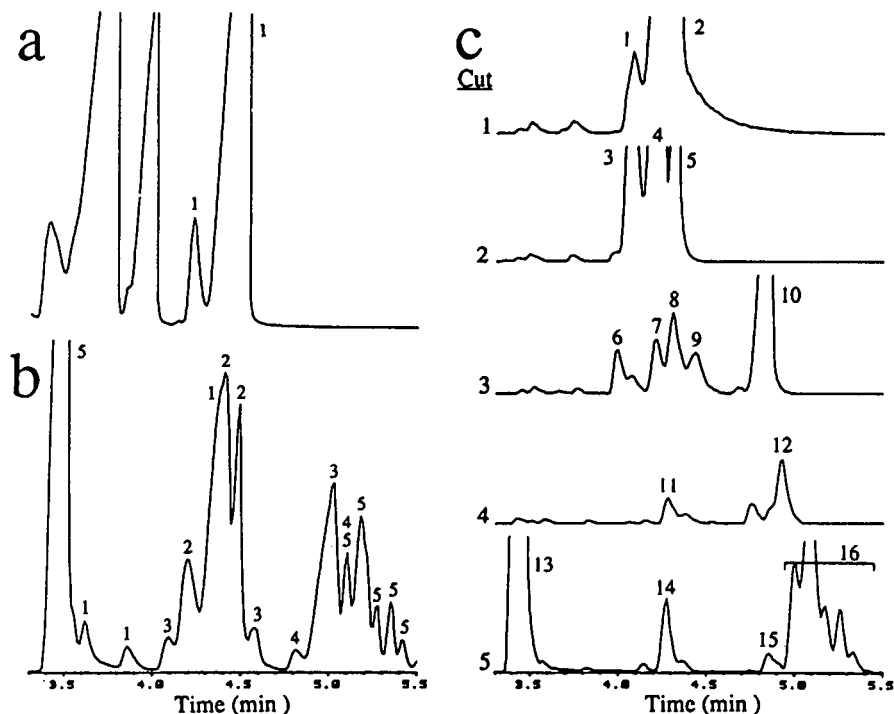


Fig. 3. An expanded view of the total ion chromatograms of the 72-s cuts 1(a) and 2(b). The peak labels represent the cut in which that particular peak appears in (c). (c) Total ion chromatograms of the five 12-s cuts over the 7.5–8.5-min range. Peak labels correspond to the component designations in Table I.

TABLE I

LIST OF COMPOUNDS IDENTIFIED IN FIG. 3 BY IR AND MS

The IR and MS libraries contain spectra of approximately 3000 and 42 000 compounds, respectively.

1	<i>trans</i> -1,3-Dimethylcyclopentane
2	2,2-Dimethylhexane
3	<i>trans</i> -1,3-Dimethylcyclopentane
4	<i>cis</i> -1,3-Dimethylcyclopentane
5	1,2-Dimethylcyclopentane
6	Cyclohexene
7	Straight-chain hydrocarbon, alkane
8	Cyclic hydrocarbon
9	Alkene
10	Heptane
11	Straight-chain hydrocarbon, alkane
12	Alkene
13	Benzene
14	Straight-chain hydrocarbon, alkane
15	Heptane isomer
16	Hexene, heptene isomers

ure to precisely identify each mixture component. Obviously, the absence of requisite library spectra could be one source of this problem. A second possibility is that inadequate chromatographic resolution, the problem addressed here, has resulted in coelution of components, thereby compromising the spectral library search approach. In any event, the demonstrably better resolution available by MDGC, which is obvious from Fig. 2, can only improve analytical reliability.

Total analysis times

As is evident from Fig. 2b, the time required to carry out complete analytical separation of the five heart cuts was 2 h. This time is significantly less than would be required if cuts were done sequentially, using multiple sample injections and a single cryogenic trap. For example, the time required for each cut, if performed sequentially, would be between 40 and 50 min to obtain both precolumn and analytical column chromatograms. Thus, complete analysis of five cuts would require between 200 and 250 min. In this example, by carrying out MDGC experiments in

parallel one saves a minimum of 80 min. Although a single high-resolution narrow-bore capillary column (≤ 0.1 mm) could permit shorter separation times, that would be at the expense of lower dynamic range and forfeiture of the ability to use the infrared detector.

Chromatographic resolution

The results presented in Figs. 2 and 3 show that the presence of a rotary valve with a small dead volume instead of glass press-tight connectors after the traps has not degraded the chromatographic resolution through peak broadening. The peak widths, as measured as the full peak width at half height, obtained in the present investigation are comparable to those obtained previously, where glass press-tight connectors were used after the traps [9].

Retention time reproducibility

As mentioned earlier, the presence of the CO₂ peak at the beginning of each heart cut analytical chromatogram provides a convenient internal standard for the measurement of adjusted retention times. Thus, it is readily possible to cross correlate retention times between adjacent heart cuts to detect possible component carry over. Furthermore, if retention time data are accurate and precise, they can further augment the analytical information available from the infrared and mass spectra data [19]. Obviously, such use of retention time information coupled with spectroscopic detection and appropriate computer software has the potential for providing a quick and automated means of analyzing complex chromatograms generated from MDGC separations. For the experiment A data, the average variation of the adjusted retention time was 0.05 min, and for experiment B, the average was 0.02 min (see Table II). This difference in average variation may be linked to the inability of the GC oven to maintain a constant temperature near ambient, but it appears that the variations are small enough that the adjusted retention time data may be used for preliminary qualitative analysis based on retention time.

TABLE II
ADJUSTED RETENTION TIME RESULTS

Experiment A, precolumn trap from 8.4 to 9.7 min, isothermal secondary separation at 30°C; experiment B, precolumn trap from 8.4 to 9.7 min, isothermal secondary separation at 50°C. The standard deviations were obtained from five replicate runs.

Experiment	Peak No.	Average adjusted retention time (min)	Standard deviation (min)
A	1	6.73	0.04
	2	10.06	0.05
	3	12.02	0.05
	4	13.48	0.07
	5	14.23	0.05
	Average		0.05
B	1	3.24	0.01
	2	4.52	0.02
	3	5.01	0.02
	4	5.49	0.02
	5	5.71	0.02
	6	5.84	0.02
	7	6.00	0.02
	8	6.27	0.02
	Average		0.02

CONCLUSIONS

A multi-parallel cryogenic trapping scheme developed for multidimensional GC–FT-IR–MS analysis of complex mixtures has been successfully demonstrated. The system developed has the potential to analyze complex mixtures without sacrificing sample dynamic range, which is essential in environmental, essential oil and petroleum chemistry. In addition, the technique can take advantage of both the information provided by multiple retention times in addition to the infrared and mass spectra for analysis of complex mixtures. Thus, multidimensional detection combined with the multi-dimensional separation could increase the reliability of identifying of components in a complex mixture. The improvements in analysis could be further enhanced by use of multiple analytical columns with different selectivities, incorporating techniques to carry out (GC)ⁿ separations, and by performing parallel sample enrichment of different segments.

REFERENCES

- 1 C.L. Wilkins, *Anal. Chem.*, 59 (1987) 571A.
- 2 K.A. Krock and C.L. Wilkins, *Anal. Chim. Acta*, 272 (1993) 381.
- 3 D.M. Hembree, N.R. Smyrl, W.E. Davis and D.M. Williams, *Analyst*, 118 (1993) 249.
- 4 D.T. Williams, Q. Tran, P. Fellin and K.A. Brice, *J. Chromatogr.*, 549 (1991) 297.
- 5 C. Bicci, C. Frattini, G. Pellegrino, P. Rubiolo, V. Raverdino and G. Tsoupras, *J. Chromatogr.*, 609 (1992) 305.
- 6 L.M. Hedges and C.L. Wilkins, *J. Chromatogr. Sci.*, 29 (1991) 345.
- 7 G.E. Platoff, D.W. Hill, T.R. Koch and Y.H. Caplan, *J. Anal. Toxicol.*, 16 (1992) 389.
- 8 W.P. Duncan and D.G. Deutsch, *Clin. Chem.*, 35 (1989) 1279.
- 9 N. Rangunathan, K.A. Krock and C.L. Wilkins, *Anal. Chem.*, 65 (1993) 1012.
- 10 W. Bertsch, in H.J. Cortes (Editor), *Multidimensional Chromatography—Techniques and Applications (Chromatographic Science Series, Vol. 50)*, Marcel Dekker, New York, Basel, 1990, Ch. 3, p. 74.
- 11 H. Himberg, E. Sippola and M.L. Riekkola, *J. Microcol. Sep.*, 1 (1989) 271.

- 12 Z. Liu and J.B. Phillips, *J. Chromatogr. Sci.*, 29 (1991) 227.
- 13 B.M. Gordon, M.S. Uhrig, M.F. Borgerding, H.L. Chung, W.M. Coleman, III, J.F. Elder, Jr., J.A. Giles, D.S. Moore, C.E. Rix and E.L. White, *J. Chromatogr. Sci.*, 26 (1988) 174.
- 14 J.B. Phillips, D. Luu, J.B. Pawliszyn and G.C. Carle, *Anal. Chem.*, 57 (1985) 2779.
- 15 J.C. Giddings, in H.J. Cortes (Editor), *Multidimensional Chromatography —Techniques and Applications (Chromatographic Science Series, Vol. 50)*, Marcel Dekker, New York, Basel, 1990, Ch. 1, p. 15.
- 16 J.A. de Haseth and T.L. Isenhour, *Anal. Chem.*, 49 (1977) 1977.
- 17 J.R. Cooper, I.C. Bowater and C.L. Wilkins, *Anal. Chem.*, 58 (1986) 2791.
- 18 J.R. Cooper and C.L. Wilkins, *Anal. Chem.*, 61 (1989) 1571.
- 19 H.F. Yin and Y.L. Sun, *Chromatographia*, 29 (1990) 39.

Rapid synthesis of isoprenoid diphosphates and their isolation in one step using either thin layer or flash chromatography

R. Kennedy Keller*

Department of Biochemistry and Molecular Biology, University of South Florida, College of Medicine, Box 7,
12 901 N. 30th Street, Tampa, FL 33612-4799 (USA)

Robert Thompson

Department of Medicine, University of South Florida College of Medicine, Tampa, FL 33612 (USA)

(First received April 1st, 1993; revised manuscript received May 10th, 1993)

ABSTRACT

A rapid procedure for the preparation of short-chain (C_5 - C_{20}) isoprenoid diphosphates is described. It is based on the method of Cornforth and Popjak [*Methods Enzymol.*, 15 (1969) 359-390] which utilizes bis-triethylammonium phosphate in trichloroacetonitrile as the phosphorylating reagent. The reaction takes place in 15 min, and product isolation, previously requiring several steps, is done in a single step using either preparative thin-layer chromatography or flash chromatography on silica. From a single TLC plate, up to 50 μ mol of pure farnesyl diphosphate (*i.e.*, *ca.* 20 mg) can be isolated, while up to 1200 μ mol can be isolated using a standard flash chromatography column.

INTRODUCTION

Isoprenoid diphosphates [*e.g.*, isopentenyl diphosphate (IPP), dimethylallyl diphosphate (DMAPP), geranyl diphosphate (GPP), farnesyl diphosphate (FPP), and geranylgeranyl diphosphate (GGPP)] are key intermediates in the branched pathway of mevalonate metabolism [1]. This pathway includes the biosynthesis of cholesterol, dolichol, ubiquinone, prenylated proteins, heme A, and isopentenyl tRNA. Accordingly, isoprenoid diphosphates are required in both radioactive and non-radioactive forms in order to carry out *in vitro* studies. Of the various procedures described for the preparation of these compounds [2-4] all require considerable

time for synthesis; further, several steps are involved in product isolation. In the present report, we describe a procedure for the rapid preparation of pure isoprenoid diphosphates. The original procedure of Cornforth and Popjak [2] has been modified such that the reaction is much more rapid; in addition, product isolation is carried out in a single step using either preparative silica TLC for reactions in which up to 200 μ mol of alcohol are phosphorylated, or flash chromatography for large-scale reactions using up to 4000 μ mol of alcohol.

EXPERIMENTAL

[3 H]Farnesol was prepared according to Adair *et al.* [5]. Orthophosphoric acid (HPLC grade) was from Fisher Chemical (Pittsburgh, PA, USA). Triethylamine was from Sigma (St. Louis

* Corresponding author.

MO, USA). Trichloroacetonitrile, 3-methyl-3-buten-1-ol (isopentenol), 3-methyl-2-buten-1-ol (dimethylallyl alcohol), geraniol, and farnesol [95% *trans* (*E,E*), 5% *cis* (*Z,E*)] were from Aldrich (Milwaukee, WI, USA). Geranylgeraniol was from TCI Chemicals (Seattle, WA, USA). All solvents were HPLC grade from Fisher Chemical. Solution A is prepared by diluting 25 ml of concentrated phosphoric acid (HPLC grade) into 94 ml acetonitrile. Solution B is prepared by diluting 110 ml triethylamine into 100 ml acetonitrile. Mobile phase 1 is isopropanol–conc. NH_4OH – H_2O (6:2.5:0.5). Mobile phase 2 is isopropanol–conc. NH_4OH – H_2O (6:3:1). All commercial chemicals were used without further purification. All glassware was treated with Sigmacote (Sigma) prior to use.

HPLC

HPLC was carried out on a Waters 501 instrument equipped with on-line UV monitoring (210 nm). The stationary phase was a 22 cm silica (5 μm) column from Brownlee Labs (obtained through Alltech, Deerfield, IL, USA). The mobile phase was 2% reagent alcohol in hexane and the flow-rate was 1 ml/min. “Reagent alcohol” is a mixture of 5% methanol, 90% ethanol, 5% 2-propanol from Fisher Chemical.

TLC

Analytical TLC was carried out using plastic-backed silica gel 60 plates from E. Merck (cat. No. 5735-7, obtained from Alltech). Preparative TLC was carried out using linear K plates (see below). Detection was achieved by spraying with either water (see below) anisaldehyde solution or molybdenum reagent. Anisaldehyde solution is 90 volumes ethanol, 5 volumes *p*-anisaldehyde (Sigma), and 5 volumes concentrated H_2SO_4 . Molybdenum spray reagent was from Sigma.

Flash chromatography

CAUTION! Due to the noxious nature of the mobile phase, all steps must be carried out in a well ventilated hood.

Chromatography was carried out using a Chromaflex chromatography column (48 cm \times 5.5 cm O.D.) from Kontes Glass, Vineland, NJ, USA. Seven hundred cm^3 of silica resin (40 μm “Flash”, Universal Scientific, Atlanta, GA,

USA) was heated in a vacuum oven for 3–4 h at 100°C, allowed to cool, and suspended in mobile phase 1 to a final volume of 1000 ml. The bottom of the column was filled with approximately 1 cm of 50–70 mesh sand (Aldrich) and wetted with the mobile phase. The suspended silica was poured into the column via a funnel and allowed to settle with the stopcock closed. After settling, the stopcock was opened and solvent was applied with house air pressure to give a flow-rate of 10 ml/min. When the resin was finished packing (5–10 min), air pressure was applied until the mobile phase just reached the top of the column bed. The top of the column was opened and 1 cm of sand was applied to the stationary phase. The mobile phase was pumped using air pressure until the sand was packed evenly over the top of the resin. Air pressure was then applied until the mobile phase reached the top of the silica bed. The column was then opened again and the entire reaction mixture (40 ml, see below) was directly applied. Air pressure was applied until the entire sample had been absorbed into the silica. The sample was washed onto the column with a small amount (5–10 ml) of isopropanol. The mobile phase then was begun at a flow-rate of 10 ml/min. Generally, 150 fractions of 16–18 ml each were collected.

Small-scale preparation of isoprenoid diphosphates

The reaction is carried out in a fume hood. Approximately 200 μmol of the neat alcohol (e.g., 52 μl farnesol for preparation of FPP) is transferred to a 75 \times 12 mm polypropylene tube. Trichloroacetonitrile (0.5 ml, *ca.* 5 mmol) is then added followed by the addition of 0.5 ml of a solution of bis-triethylammonium phosphate (TEAP) in acetonitrile. The TEAP solution is prepared by slowly mixing 0.91 ml of solution A with 1.5 ml solution B while stirring. The sample is placed in a 37°C bath for 5 min. Two more additions of TEAP are added as before with 5 min incubations after each addition. The entire reaction is then streaked onto the application zone (about 2 cm from the bottom of the plate) of a 20 \times 20 cm silica preparative TLC plate (Whatman Linear K, 1000 μm , with fluorescent indicator, obtained through Fisher Chemical). A 2-ml “Pi-Pump” (Fisher Chemical) connected to

a Pasteur pipette is ideal for streaking the sample. The plate is allowed to dry (*ca.* 15 min) and then placed in a TLC tank containing 125 ml mobile phase 2. Two plates can be run in a single tank if desired. A quick check of the reaction can be carried out by diluting 1 μl into 10 μl of methanol and streaking 3 μl on a 8 \times 2 cm analytical TLC plate (silica). This plate, which can be developed in a small TLC tank in about 20 min, is stained with anisaldehyde solution (see Fig. 1). Development of the preparative plates requires about 8 h, but plates can be left overnight without deleterious effects. TLC takes place in a well ventilated hood. Following removal of the preparative plates, they are placed flat in the hood and allowed to dry until the odor of ammonia is no longer present (*ca.* 1 hour). Upon viewing with an ultraviolet light, fluorescent bands are seen at 4, 6, 8, 13.5, and 15 cm from the bottom of the plate (the chemical nature of these bands is not known). In addition, a yellow band is seen about 12 cm from the bottom of the plate. Plates containing TEAP reactions of geraniol, farnesol, or geranylgeraniol are sprayed liberally with water using a typical TLC sprayer. About 10 ml of water are required to soak a single plate. During spraying, the monophosphate (close to the solvent front), diphosphate and triphosphate appear as thick white bands, with the diphosphate appearing around 9–11 cm from the origin ($R_F = 0.5$). The diphosphate band is scraped into a 50 ml graduated screw-capped polypropylene centrifuge tube. A plastic "cell lifter" (cat. No. 3008, Costar Scientific, Cambridge, MA, USA) is ideal for scraping. The sample is treated with 20 ml of 10 mM ammonium hydrogen carbonate (pH 8), the tube capped, and vortexed vigorously for 1 min. Following centrifugation in swinging bucket rotor for 10 min at 3000 *g*, the supernate, which still contains fine particles of silica, is passed through a 50-ml disposable sterilization filter (0.2 μm) connected to a 50-ml polypropylene centrifuge tube (Costar No. 8301) under reduced pressure. The pellet is washed with 10 ml of the same buffer, centrifuged and the supernate filtered through the same filter as before. The concentration is determined on 10- and 25- μl aliquots of the pooled filtrate by assaying for phosphate according to the method of Ames [6] using 1 mM adenosine diphosphate (molar ab-

sorbance $15.4 \times 10^3 \text{ l mol}^{-1} \text{ cm}^{-1}$ at 259 nm) as standard. The yield at this point should be 30–70 μmol , depending on the isoprenoid diphosphate (see below). If a more concentrated solution is desired, samples can be flash evaporated or lyophilized. Care must be taken to keep solutions of the allylic diphosphates alkaline during these steps. The final product is filtered again if necessary and stored in 10 mM ammonium hydrogencarbonate–methanol (1:1). Such samples are stable for months when kept at -20°C . Samples of FPP and GGPP prepared using the above procedure can be concentrated by applying them to a C_{18} sorbent extraction column (*e.g.*, Bond Elut, Analytichem International, Harbor City, CA, USA or Sep-Pak, Waters/Millipore, Milford, MA, USA) and eluting with 2 ml methanol. Such samples are diluted with an equal volume of 10 mM ammonium hydrogencarbonate and stored at -20°C .

Large-scale preparation of isoprenoid diphosphates

The phosphorylation reaction is carried out exactly as described for TLC except that it is scaled up 20-fold (*i.e.*, 4000 μmol of starting material is used). A 50-ml screw-capped centrifuge tube is a convenient reaction vessel. After completion of the reaction, the entire sample is subjected to flash chromatography as described above. Aliquots (2 μl) of every fifth fraction are analyzed by silica TLC using mobile phase 2. Appropriate fractions are pooled and concentrated to a volume of *ca.* 25 ml on a standard rotary evaporator (bath temperature 30°C) connected to a water aspirator pumping at 20 mmHg (1 mmHg = 133.322 Pa). The sample is then diluted to 50 ml with 10 mM ammonium hydrogencarbonate and an equal volume of methanol is added. Samples are stored at -20°C in 50 ml polypropylene centrifuge tubes. A small amount silica may precipitate upon storage; it is easily removed by centrifugation or filtration.

RESULTS

Rapid small-scale synthesis of isoprenoid diphosphates

In preliminary studies, several different con-

concentrations of TEAP and ratios of TEAP–trichloroacetonitrile were tested. The effect of reaction temperature was also investigated. The conditions chosen, which involve three additions of relatively concentrated TEAP and 5 min incubations at 37°C, yield *ca.* 30% diphosphate product when farnesol is reacted, as judged by anisaldehyde spray and by radioscanning when [³H]farnesol is used as substrate (Fig. 1). We found no advantage to crystallizing the TEAP

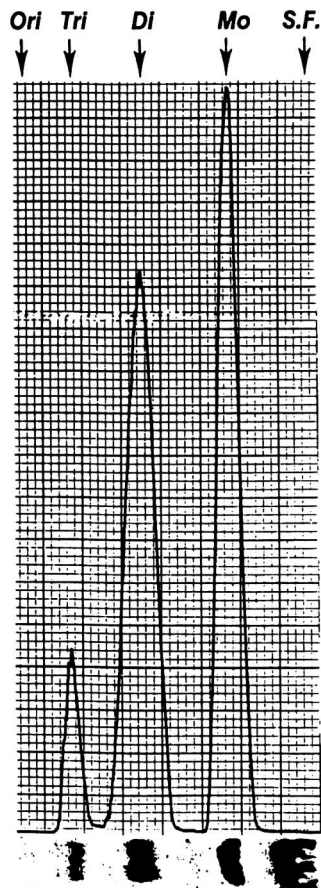


Fig. 1. Analytical TLC of reaction products. Farnesol (2 μ mol) was mixed with 10^7 dpm [³H]farnesol and reacted under the standard conditions scaled down 100-fold (*i.e.*, 20 μ l total volume). After reaction, 1 μ l was diluted into 10 μ l methanol and 3 μ l spotted onto a TLC plate and chromatographed using mobile phase 2. After development, the plate was radioscanned (top) and then sprayed with anisaldehyde (bottom). Positions of the origin (Ori), triphosphate (Tri), diphosphate (Di), monophosphate (Mo), and solvent front (S.F.) are indicated.

prior to reaction, as described by Cornforth and Popjak [2]. The pattern observed in Fig. 1 is reproducible: it was consistently observed in over 100 reactions during the course of a year. In addition, under the conditions described, phosphodiester of farnesol (farnesol–phosphate–farnesol; farnesol–pyrophosphate–farnesol) are not observed, as evidenced by a lack of side products on TLC and by the complete hydrolysis of the isolated diphosphates by alkaline phosphatase (see below).

The procedure of Danilov *et al.* [4] using tetrabutylammonium phosphate was also investigated. These workers reported that, if the concentration of trichloroacetonitrile–alcohol is greater than 5, the main products of moraprenol phosphorylation are the mono- and diphosphates in about 45% yield for each. Fig. 2 shows the

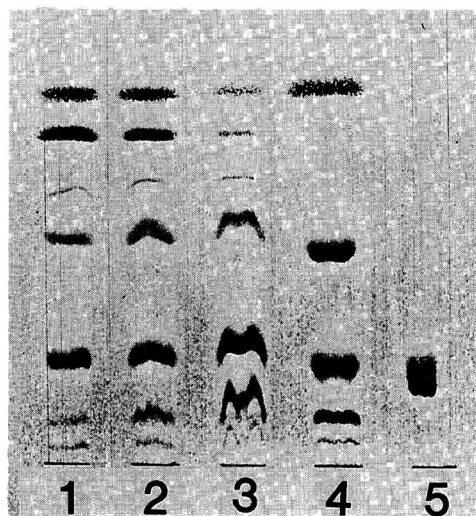


Fig. 2. Comparison of procedure of Danilov *et al.* and current method. Lanes 1, 2, and 3, reactions carried out according to Danilov *et al.* [4]. Farnesol (12.7 μ mol) was treated with 50 μ l trichloroacetonitrile and either 70 (lane 1), 140 (lane 2) or 280 μ l (lane 3) of 360 mM tetrabutylammonium phosphate in acetonitrile. Aliquots of 5, 8, and 12 μ l (representing 0.5 μ mol of original farnesol) were diluted into methanol to give a final volume of 30 μ l. Aliquots (3 μ l) were streaked on an analytical TLC and chromatographed as described in Experimental. Lane 4: 12.7 μ mol of farnesol was reacted under the standard conditions with 33 μ l trichloroacetonitrile and three portions of 33 μ l TEAP in acetonitrile (see Experimental). An aliquot (5 μ l, representing *ca.* 0.5 μ mol of farnesol) of this reaction was diluted with 25 μ l of methanol and 3 μ l were streaked on the TLC plate. Lane 5: FPP (25 nmol).

results of a phosphorylation reaction of farnesol according to the conditions described by Danilov *et al.* [4] using varying amounts of tetrabutylammonium phosphate. A standard reaction as described in the Experimental was added for comparison. It is clear that the procedure of Danilov *et al.* [4] also yields the tri- and tetraphosphate species. In addition, the yield of diphosphate is not significantly greater than that obtained using the procedure described in Experimental. Since the workup of the reaction described by Danilov *et al.* is considerably more lengthy than that described below, this procedure was deemed unsuitable for the rapid preparation of small or large amounts of the isoprenoid diphosphates.

Isolation of isoprenoid diphosphates using preparative TLC

As described in the Experimental section, the entire TEAP reaction can be applied to a preparative thin-layer plate. After overnight chromatography, the desired products can be detected by subjecting a lateral portion of the plate to either anisaldehyde or molybdate spray solutions. However, since we desired maximum yield, we attempted to detect the products by simply spraying with water. As shown in Fig. 3, water spray yields strong white bands corresponding to the mono-, di-, and triphosphates.

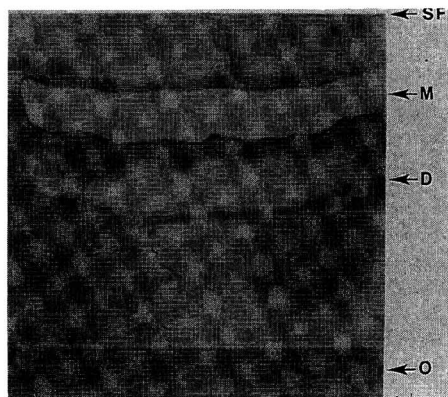


Fig. 3. Preparative TLC of reaction products. A typical reaction mixture containing 200 μmol farnesol was applied to preparative TLC and developed overnight in mobile phase 2. After drying 1 h, the plate was sprayed with *ca.* 10 ml water. Bands representing the monophosphate (M) and diphosphate (D) are indicated.

Each of these can be subsequently eluted using the procedure described in Experimental. Yield of farnesyl diphosphate from the plate is around 80%, giving an overall yield of *ca.* 24% from the alcohol. It is to be noted that the water spray technique is only applicable to the phosphorylated derivatives longer than C_{10} ; isopentenol and dimethylallyl alcohol phosphates can only be detected by spraying a “guide lane” with either anisaldehyde or molybdenum spray (note: the plate must be free of ammonia in order for these sprays to work).

Large-scale preparation of isoprenoid diphosphates

For the isolation of larger quantities of isoprenoid diphosphates, the same reaction conditions described for the isolation on TLC are employed except that the volumes are scaled up 20-fold. Following incubation, the entire reaction is subjected to flash chromatography as described in Experimental. Fig. 4 shows that the mono-, di-, and triphosphates are well resolved using this procedure. Following localization of the desired product, appropriate fractions are pooled and concentrated by rotary evaporation using an aspirator pump.

Yield and purity of isolated products

Table I shows the yield obtained of the isoprenoid diphosphates using the small-scale and large-scale procedures. Analytical TLC (Fig. 5)

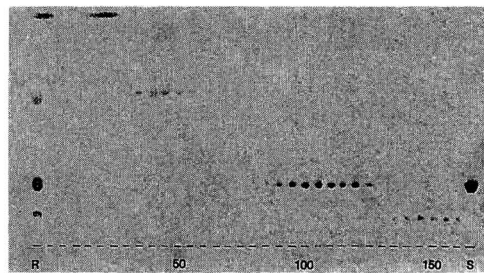


Fig. 4. Monitoring of flash chromatography column elution by analytical TLC. Farnesol (4000 μmol) was subjected to the TEAP reaction as described in Experimental and chromatographed using flash chromatography. Fractions (18 ml each) were collected and 2- μl aliquots of every fifth fraction were spotted for TLC. R: 0.3 μl of the reaction mixture was spotted; S: 15 nmol standard FPP.

TABLE I

YIELD OF ISOPRENOID DIPHOSPHATES PREPARED BY PREPARATIVE TLC AND FLASH CHROMATOGRAPHY

The indicated products were prepared and assayed for organic phosphate according to the procedure described in Experimental. Results are expressed as the mean \pm S.D. with the number of preparations in parentheses.

Isoprenoid diphosphate	Yield (%)	
	TLC	Flash
IPP	35.6 \pm 1.6 (<i>n</i> = 3)	25 (<i>n</i> = 1)
DMAPP	36 (<i>n</i> = 1)	
GPP	28.6 \pm 1.7 (<i>n</i> = 3)	30 (<i>n</i> = 1)
FPP	24.0 \pm 1.0 (<i>n</i> = 3)	31 \pm 1 (<i>n</i> = 2)
GGPP	17.1 \pm 2.5 (<i>n</i> = 3)	35 (<i>n</i> = 1)

shows the high degree of purity of the isoprenoid diphosphates prepared using the TLC procedure. To further test purity of the prepared products, we carried out enzymatic dephosphorylation of FPP and subjected the resultant extract to HPLC. Analysis by reversed-phase HPLC indicated a single peak coeluting in the position of farnesol (not shown). Analysis of the same sample by silica HPLC (Fig. 6) revealed the presence of a small amount of the α -*cis* species (*i.e.*, *Z,E*) which was present in the starting compound prior to phosphorylation.

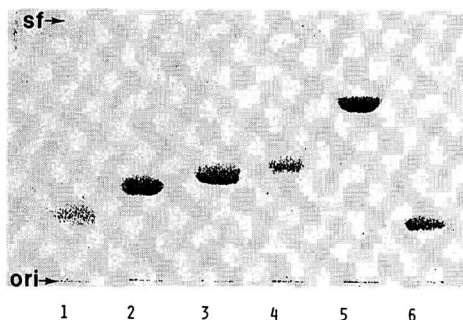


Fig. 5. Analytical TLC of purified isoprenoid phosphates. Isoprenoid phosphates were prepared by preparative TLC and *ca.* 20 nmol were applied to analytical TLC plates. Detection was with anisaldehyde. 1 = IPP; 2 = GPP; 3 = FPP; 4 = GGPP; 5 = farnesyl monophosphate; 6 = farnesyl triphosphate.

DISCUSSION

The present study was prompted by our desire to have available a rapid procedure for the preparation of both labeled and unlabeled isoprenoid diphosphates. Such a procedure would greatly facilitate our ongoing studies of mevalonate metabolism in rat liver. We found that the original procedure of Cornforth and Popjak [2] was both tedious and time consuming. The procedure of Danilov *et al.* [4] also involves several steps prior to resolution of the products on DEAE-cellulose using gradient elution. The procedure of Davisson *et al.* [3] has the advantage of generating only the diphosphate product. However, it requires preparation of an intermediate halide, and a low temperature reaction (-40°C) using dry solvents in an inert atmosphere. In addition, the diphosphorylating agent must be prepared using ion exchange chromatography. Following a 24-h reaction, isolation of the diphosphate involves ion-exchange chromatography, lyophilization, and flash chromatography on cellulose.

In developing a rapid procedure to synthesize isoprenoid diphosphates, we reasoned that there was really no disadvantage to generating the mono- and triphosphate side products, since neither the cost nor availability of the starting alcohols was a limiting factor. In addition, it is often useful to have available the mono- and triphosphate derivatives for control experiments and chromatography standards. We therefore decided to use TEAP in trichloroacetonitrile as the phosphorylating reagent. After many modifications of the original procedure [2], the conditions chosen were found to generate the expected products in good yield after a 15-min incubation in the absence of side products.

A major advance in the small-scale procedure is the single step isolation of the reaction products on commercially available preparative TLC plates. In the isolation of FPP described by Cornforth and Popjak [2], several steps are required, including extraction with diethyl ether, absorption onto Amberlite XAD-2 (an overnight procedure) and DEAE-cellulose chromatography. In the procedure described here, the product can be used after elution from TLC

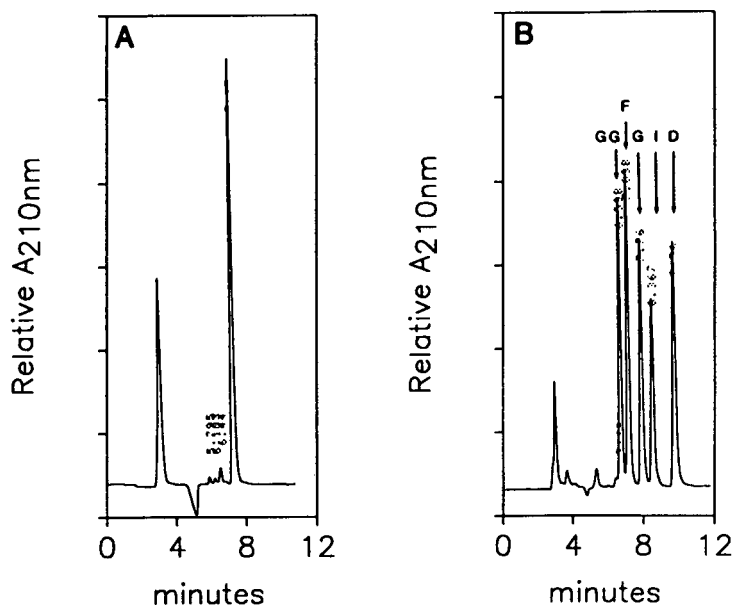


Fig. 6. (A) Silica HPLC of dephosphorylated FPP. FPP (50 nmol) was subjected to dephosphorylation in 1 ml 0.1 M sodium glycinate, 1 mM ZnCl₂, 1 mM MgCl₂, pH 10.7, using 1 unit bovine intestinal alkaline phosphatase (Sigma). After 1 h at 37°C, the reaction was extracted with 1 ml methylene chloride. An aliquot (100 μl) of the extract was mixed with 10 μl reagent alcohol and reduced to about 10 μl using a gentle stream of argon. Hexane (0.2 ml) was then added and the sample subjected to HPLC on a 22 cm silica column. Mobile phase: 2% reagent alcohol in hexane. Flow-rate: 1 ml/min. Detection: A_{210nm}. Right panel, standard alcohols: 1 μg each geranylgeraniol (GG), farnesol (F), and geraniol (G), 10 μg isopentenol (I), and 2 μg dimethylallyl alcohol (D).

without further purification. Product analysis indicates that the isoprenoid diphosphates are essentially pure (Fig. 5) and generate the expected alcohols after dephosphorylation (Fig. 6, and data not shown). In addition, they have been found to be biologically active in enzymatic assays (*e.g.*, squalene synthetase [7]).

For the preparation of isoprenoid diphosphates in amounts greater than 40 μmol, either multiple TLC plates or flash chromatography can be employed. Under the conditions described herein, flash chromatography is completed in about 3 h and yields 800–1200 μmol of pure material.

ACKNOWLEDGEMENTS

Supported in part by funds from the Division of Technology Transfer, University of South Florida.

The technical assistance of Fequiere Vilsaint, Alison Rhinehart, and Gary Sessums is gratefully acknowledged.

REFERENCES

- 1 J.L. Goldstein and M.S. Brown, *Nature*, 343 (1990) 425–430.
- 2 R.H. Cornforth and G. Popjak, *Methods Enzymol.*, 15 (1969) 359–390.
- 3 V.J. Davisson, A.B. Woodside and C.D. Poulter, *Methods Enzymol.*, 110 (1985) 130–144.
- 4 L.L. Danilov, T.N. Druzhinina, N.A. Kalinchuk, S.D. Maltsev and V.N. Shibaev, *Chem. Phys. Lipids*, 51 (1989) 191–203.
- 5 W.L. Adair, N. Cafmeyer and R.K. Keller, *J. Biol. Chem.*, 259 (1984) 4441–4446.
- 6 B.N. Ames, *Methods Enzymol.*, 8 (1966) 115–118.
- 7 R.K. Keller, A. Cannons, F. Vilsaint, Z. Zhihong and G.C. Ness, *Arch. Biochem. Biophys.*, 302 (1993) 304–306.

Application of capillary electrophoresis to the analysis of the oligomeric distribution of polydisperse polymers

John Bullock

Sterling-Winthrop Pharmaceuticals Research Division, Malvern, PA 19355 (USA)

(First received February 16th, 1993; revised manuscript received May 11th, 1993)

ABSTRACT

Capillary electrophoresis was investigated for characterizing the oligomeric distribution of some model ionic and non-ionic synthetic polymers. Ionic poly(alkyl oxide) oligomers in the molecular mass range from a few hundred to over 4000 were separated into as many as 60 individual oligomers and detected using an indirect UV approach. Neutral Triton X series oligomers from $n = 1$ to $n = 46$ were separated in under 20 min using a sodium dodecyl sulfate matrix with high levels of acetonitrile. Separations have also been obtained on neutral poly(ethylene glycol) polymers after derivatization with phthalic anhydride. In all cases the analyses were conducted in the open tube CE format without the aid of sieving media. Separations of individual oligomers were achieved by incorporating additives into the electrophoretic buffer to modulate either the charge on the surface of the capillary or the charge properties of the oligomeric analytes.

INTRODUCTION

The techniques typically used to characterize the molecular mass properties of synthetic polymers encompass a broad spectrum of physical, spectroscopic and separation methods. In the area of separations, size exclusion chromatography [1,2] and, to a lesser extent, different modes of sorption (reversed-phase, normal-phase and ion-exchange) chromatography [3–6] are used to determine average molecular mass values, molecular mass distributions and compositional heterogeneity in the case of copolymers. Except in the case of lower oligomers, size-exclusion chromatography is not able to completely resolve the various oligomers that might be found in a typical polydisperse polymer. Instead, molecular mass distribution analysis is achieved by calibrating the system with well characterized standards and deconvolution of the polymer sample chromatogram using appropriate data analysis software. Alternatively, molecular mass-sensitive detectors can be used to directly obtain this information from the chromatogram

without relying on external calibration. Separation of individual oligomers in polymeric materials has been achieved, in a few instances, using normal- and reversed-phase HPLC [3–5], supercritical fluid chromatography [7], as well as ion-exchange chromatography [6].

Capillary electrophoresis (CE) has rapidly emerged as a fast high-resolution separation technique applicable to a wide variety of charged and uncharged compounds. Given the high resolution that has been demonstrated with CE, it would be anticipated that this technique would have utility for analyzing polydisperse polymers. While numerous reports exist demonstrating the application of CE to the analysis of various types of biopolymers including peptides [8], proteins [9], oligonucleotides [10] and DNA fragments [11], much less work has been reported in the area of CE analysis of other types of synthetic polymers. Poli and Schure [12] described the separation of polystyrene sulfonates using CE. Separation of polymers of different average molecular mass was achieved by incorporating a sieving medium into the buffer, although in-

dividual oligomers were not resolved. Garcia and Henion [13] recently reported on the interfacing of capillary gel electrophoresis to an ion spray mass spectrometer. The authors demonstrated the separation of poly(acrylic acid) oligomers from $n = 7$ to $n = 14$ using this system. Amankwa *et al.* [14] examined the oligomeric distribution of poly(oxyalkylene) diamine polymers. Samples were derivatized with 2,3-naphthalenedialdehyde and detected by fluorescence detection. And Braud and Vert [15] used CE to resolve several low-molecular-mass oligomeric fragments of poly(malic acid).

In this work, CE in the open tube format with conventional UV detection was investigated for characterizing the oligomeric distribution of different types of polymers. Several different amine-terminated ionic poly(alkyl oxide) polymers were examined encompassing a molecular mass range from several hundred up to 4000. Fast high-resolution separations of individual oligomers were achieved using relatively simple buffer matrices. Triton oligomers from $n = 1$ to $n = 46$ corresponding to a mass range from 200 to 2000 were separated in under 20 min using a sodium dodecyl sulfate (SDS)-buffer matrix containing high levels of acetonitrile. And separations of oligomers of neutral poly(ethylene glycol) in the molecular mass range from about 1000 to over 3500 were also achieved. A different separation and detection strategy was required for the different types of polymers examined. Preliminary results demonstrate that CE will have utility for characterizing molecular mass and sample polydispersion for these polymeric materials. This work addresses some of the separation and detection strategies useful for analyzing these different polymers.

EXPERIMENTAL

Materials

Water was purified using a Milli-Q system (Millipore). Triton X series oligomers were purchased from Sigma. Poly(ethylene oxide) (PEO) molecular mass standards were from Polymer Labs. and poly(ethylene glycols) (PEGs) were purchased from Sigma. Jeffamine ED series polymers (polyoxypropylene-polyoxyethylene

oxide diamine copolymers) were from Texaco Chemical. Poly(ethylene oxide) diamine of average molecular mass 3350 was from Sigma. Creatinine, phthalic anhydride and 1,3-diaminopropane were obtained from Aldrich and electrophoresis-grade SDS was from J.T. Baker. All other chemicals were of reagent grade and were obtained from J.T. Baker.

Derivatization of poly(ethylene glycols)

To 1.0 g of poly(ethylene glycol) polymer dissolved in 2 ml of acetonitrile was added an amount (g) of phthalic anhydride equivalent to $600/(\text{average molecular mass of the polymer})$. The solution contained in a capped 5-ml glass vial was placed in a heating block at 100°C for 15 h. Samples were diluted 5 to 1000 with a mixture of acetonitrile-5 mM borate buffer (30:70) at pH 8.7 prior to analysis by capillary zone electrophoresis (CZE).

Instrumentation

A Spectra-Physics Model 1000 CZE instrument was used for this work. The instrument was controlled using an IBM model 70386 personal computer. Data were collected and processed with PENelson Access★Chrom software. All capillary tubing (50 μm I.D. \times 375 μm O.D.) was from Polymicro Technologies. Capillaries were conditioned with 1 M NaOH for 15 min prior to use. All experiments were conducted in the constant voltage mode at 25°C. Hydrodynamic injections were accomplished using vacuum.

For the analyses of Tritons, a buffer consisting of 25 mM boric acid, 50 mM SDS adjusted to pH 8.6 in acetonitrile-water (35:65) was used. Samples were prepared in this buffer at concentrations from 0.5 to 3 mg/ml. Typical injection times were 1–2 s. Samples were separated in a 67 cm capillary (60 cm separation distance) at 25 kV (27 μA) and 25°C and detected at 200 nm.

Poly(alkyl oxide) diamines were analyzed in a 30 mM creatinine buffer adjusted to pH 4.8 with acetic acid. Various PEO molecular mass standards were added to the electrophoretic buffer at a level of 1 mg/ml to enhance separation of individual oligomers. Polymer samples were prepared in a 1 in 5 dilution of the run buffer at

concentrations from 0.5 to 2 mg/ml and injected for 5 s. Separations were performed in a 44 cm capillary (37 cm separation distance) at 25°C and 25 kV (13 μ A). Indirect UV detection at 220 nm was used.

CE separations of phthalic anhydride derivatized samples of poly(ethylene glycol) were separated in a 44 cm (37 cm separation distance) \times 50 μ m I.D. capillary with a buffer of 57 mM boric acid +35 mM 1,3-diaminopropane, pH 9.7–acetonitrile (70:30). Samples were injected for 1 s and separated at 25°C and 25 kV (14 μ A). Detection was at 205 nm.

RESULTS AND DISCUSSION

Synthetic polymers come in a wide variety of forms differing in shape (linear, branched, cross-linked, star-burst, etc.), sizes (from molecular masses of hundreds to over a million) and chemical characteristics (ionic, non-ionic, hydrophobic, hydrophilic, etc.). Due to this tremendous diversity in the properties of synthetic polymers, no one electrophoretic technique will be universally applicable to all polymers. Therefore, the particular approach used to analyze different types of polymers will often need to be uniquely tailored to the specific properties of the polymer. Additional considerations in relation to CE are the solubility properties of the polymer and mode of detection available. UV detection is by far the most prevalent detection mode available on commercial CE systems. Many polymers of interest are soluble only in non-aqueous solvents. Since many polymers exhibit very weak or no UV absorbance and show poor aqueous solubility, there are limitations on the use of CE for polymer analysis. The focus of this work is on the CE analysis of some common water-soluble ionic and non-ionic polymers and the different approaches useful for characterizing their oligomeric distributions.

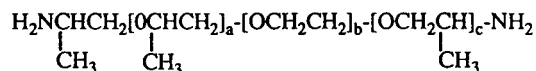
CE analysis of Jeffamine ED series polymers

A series of different poly(alkyl oxide) diamine polymers were used as model compounds to examine the utility of CE for characterizing polymers terminated with ionic groups. This includes diamine homo and copolymers of poly-

propylene oxide and polyethylene oxide (refer to Fig. 1). The mixed poly(propylene oxide)–poly(ethylene oxide) diamine polymers (Jeffamine ED series) have been analyzed previously [14]. However, the procedure described in this reference entailed the use of a derivatizing agent (2,3-naphthalenedialdehyde) and the use of laser induced fluorescence detection. In the present work, a simpler approach was sought that would allow separation and detection without derivatization and without the need for fluorescence detection which is not available on most commercial instruments. In addition, derivatization would preclude the possibility of detecting monoamine oligomers in these samples, if present as by-products. Since these polymers have negligible native UV absorbance, an indirect UV approach was used as described by Foret *et al.* [16] for the analysis of rare earth metal ions. This entails the use of a UV absorbing back-

I. Polyoxyethylene/polyoxypropylene Diamines

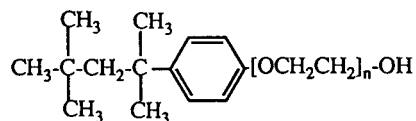
(Jeffamine ED Series Polymers)



II. Polyethylene Oxide Diamines



III. Triton X Series Oligomers



IV. Poly(ethylene glycol) Derivatized With Phthalic Anhydride

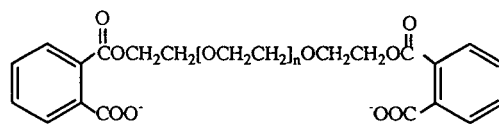


Fig. 1. Structures of polymeric compounds analyzed in this work.

ground electrolyte (creatinine) which carries a positive charge. Other types of UV-absorbing background electrolytes have also been demonstrated for indirect detection of cations [17,18]. The positively charged oligomers partially displace the creatinine in the separation capillary creating a negative UV signal as the analyte zones migrate through the detector. By reversing the leads from the detector, these negative signals produce positive peaks. Using this approach a very fast separation of three Jeffamine polymers of different average molecular mass was achieved in under 5 min as depicted in Fig. 2.

In an attempt to resolve the individual oligomers present in these polymers, several different buffer modifiers capable of reducing the electroosmotic flow were investigated. It was found that neutral PEO polymers were effective for this purpose. The effectiveness of a series of PEO additives of different average molecular mass was evaluated for enhancing the separation of the oligomers in the Jeffamine polymer of average molecular mass 600. The electropherograms in Fig. 3 shows that the higher the molecular mass of the PEO buffer additive, the greater is the reduction in the electroosmotic flow resulting in better resolution of individual oligomers. Optimal separations for the Jeffamine polymers of average molecular mass 600 and 900 are displayed in Fig. 4. The distinctive pattern of peaks observed in these electropherograms is indicative of the compositional distribution of the individual oligomers in terms of relative

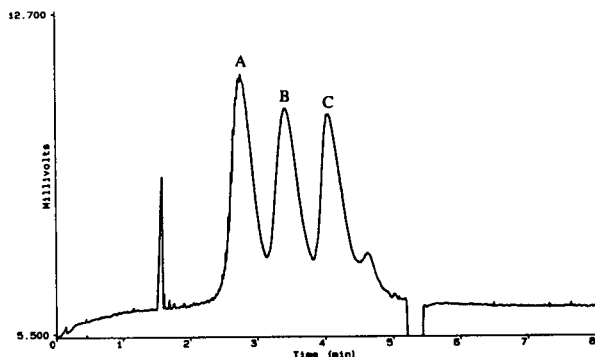


Fig. 2. CE separation obtained on a mixture of Jeffamine ED series polymers of average molecular mass (A) 900, (B) 2000 and (C) 4000. Conditions as given in the Experimental section using a buffer with no PEO additive.

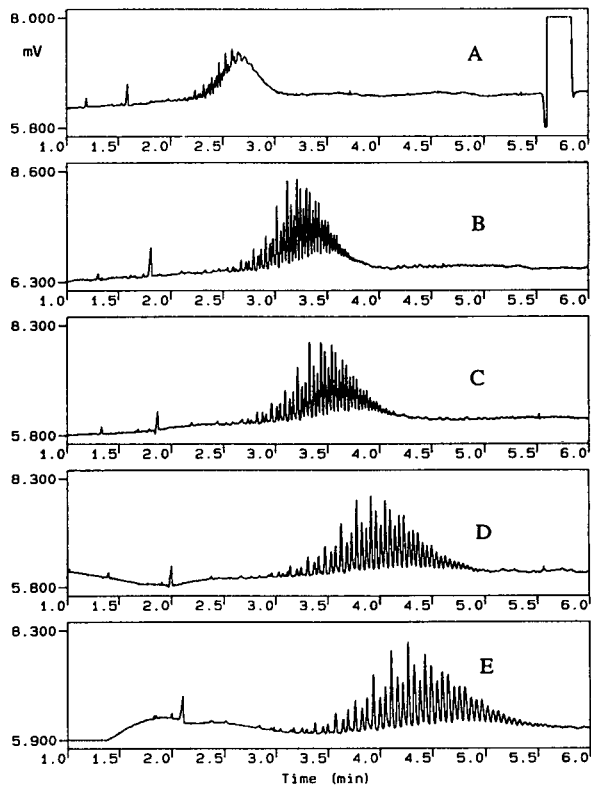


Fig. 3. CE separation of Jeffamine ED series polymer of average molecular mass 600 with (A) no buffer additive, (B) 1 mg/ml PEO-10 000, (C) 1 mg/ml PEO-20 000, (D) 1 mg/ml PEO-42 000 and (E) 1 mg/ml PEO-86 000 added to the buffer. Refer to Experimental section for additional conditions.

proportions of poly(propylene oxide) and poly(ethylene oxide) in each polymer chain.

To demonstrate that this enhancement in the resolution of Jeffamine oligomers with the addition of PEO to the buffer is due solely to reduced electroosmotic flow and not a sieving mechanism, the following experiment was performed. First, the capillary was equilibrated with buffer containing 1 mg/ml of the PEO additive. This buffer was then replaced with a similar buffer that did not have the PEO additive just prior to injecting the sample. The separation achieved in this experiment (data not shown) was virtually identical to that obtained when the PEO was present in the buffer. This is due to the fact that the PEO that was initially absorbed to the capillary surface is very slowly desorbed from the capillary. This maintains the significantly

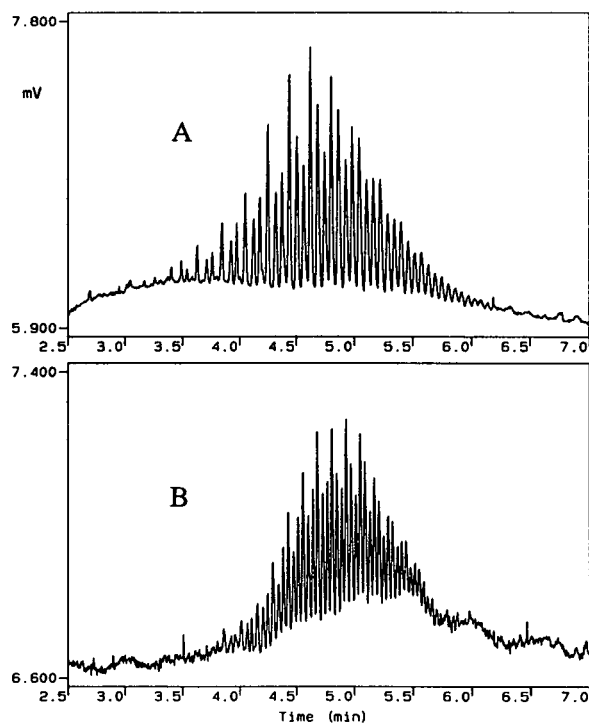


Fig. 4. Optimal CE separation for Jeffamine ED series polymers of average molecular mass (A) 600 and (B) 900. Conditions as given in the Experimental section with 1 mg/ml PEO-86 000 buffer additive.

reduced electroosmotic flow which produces the enhanced resolution of individual oligomers. It is conceivable that this dynamic coating of PEO also aids in reducing any interaction of the polymeric diamines with the surface of the capillary.

Poly(ethylene oxide) diamine polymers

A series of poly(ethylene oxide) diamine oligomers encompassing a molecular mass range from 1100 to 4000 were separated using a similar separation/detection protocol as depicted in the electropherogram in Fig. 5. Baseline resolution of oligomers from $n = 26$ to $n = 90$ were achieved in 16 min using a buffer containing 1 mg/ml PEO-86 000. Tentative assignment of oligomer numbers in this electropherogram is based on the peak average molecular mass values (determined by size-exclusion chromatography) for the three respective PEO-diamine polymers (molecular masses 1500, 2000 and 3350) composing this sample. The dependence of the migration time

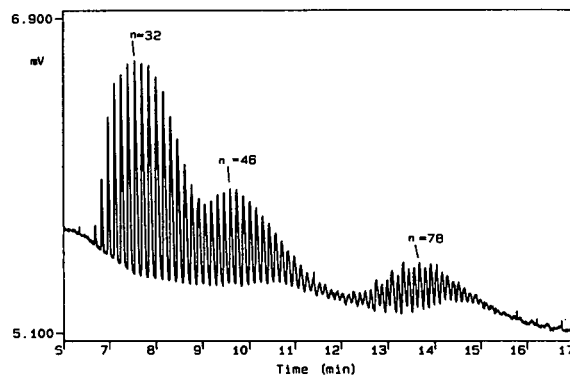


Fig. 5. CE separation of poly(ethylene oxide) diamine oligomers of molecular masses from 1100 to 4000. Conditions as given in the Experimental section using a buffer with 1 mg/ml PEO-86 000.

of the poly(ethylene oxide) diamine oligomers on their molecular mass is depicted in the plot in Fig. 6. The data (migration time *versus* log molecular mass) was fit to a third order polynomial resulting in an R^2 value of 1.000. Table I contains precision of migration time data for selected oligomers for replicate injections of this sample. R.S.D.s for migration times were all under 1.0%. This data suggests that this technique will be useful for molecular mass distribution analysis. Fig. 7 contains an electropherogram of a poly(ethylene oxide) diamine polymer of average molecular mass 1500. Using

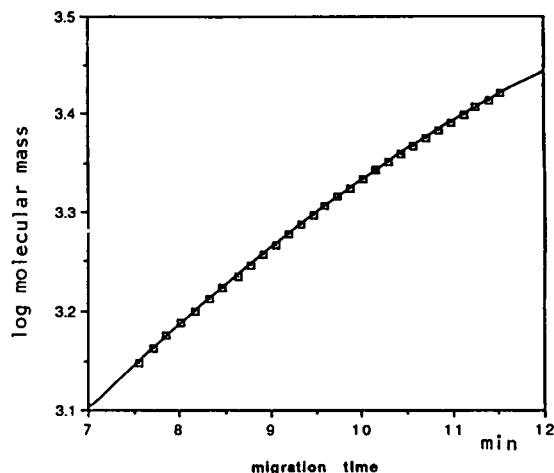


Fig. 6. Plot of the log of molecular mass of poly(ethylene oxide) diamine oligomers *versus* migration time. Data fit to a third-order polynomial. $y = 2.3534 + 0.11975x - 1.0690 \cdot 10^{-3}x^2 - 1.1161 \cdot 10^{-4}x^3$; $R^2 = 1.000$.

TABLE I

PRECISION OF MIGRATION TIMES FOR POLYETHYLENE OXIDE DIAMINE OLIGOMERS BY CE

CE conditions as given in Fig. 5. Mean, etc. are of 7 determinations.

	Migration times (min) for oligomers					
	$n = 27$	$n = 30$	$n = 33$	$n = 36$	$n = 39$	$n = 42$
Mean (min)	6.67	7.07	7.49	7.94	8.41	8.86
S.D. (min)	0.0430	0.0465	0.0522	0.0604	0.0641	0.0826
R.S.D. (%)	0.644	0.658	0.696	0.761	0.763	0.933

this technique, monoamine by-product oligomers present in this sample can be separated from the corresponding diamine oligomers.

CE analysis of Tritons

CE analysis of neutral polymers such as Triton X series oligomers which contain significant hydrophobic character is more problematic. Since they do not contain any charge, separation in the free solution mode is precluded. The related technique of micellar electrokinetic capillary chromatography is available but is of limited utility for these types of compounds due to the large size of the polymer and the strong interaction of the hydrophobic portions of the polymer with the SDS micelle. Separation of these types of polymers was achieved here using an alternative approach. By incorporating high concentrations of acetonitrile (>30%) into an SDS-

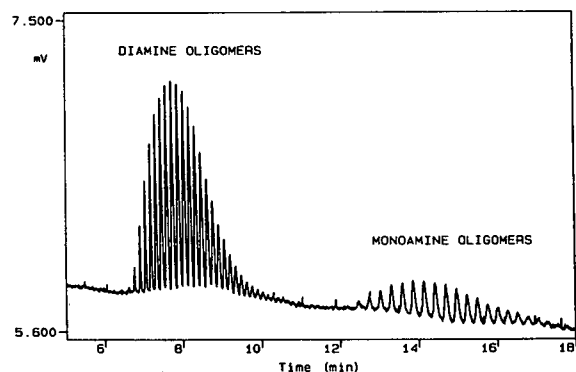


Fig. 7. CE separation of poly(ethylene oxide) diamine polymer of average molecular mass 1500 showing the separation of the monoamine oligomer by-products. Conditions as described in the Experimental section using 1 mg/ml PEO-86 000 in the buffer.

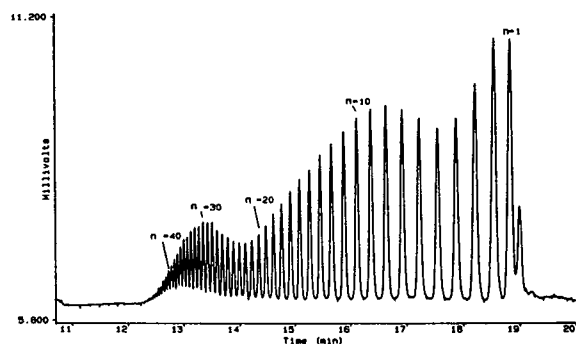


Fig. 8. CE separation of Triton X series oligomers from $n = 1$ to $n = 46$. Conditions as given in the Experimental section.

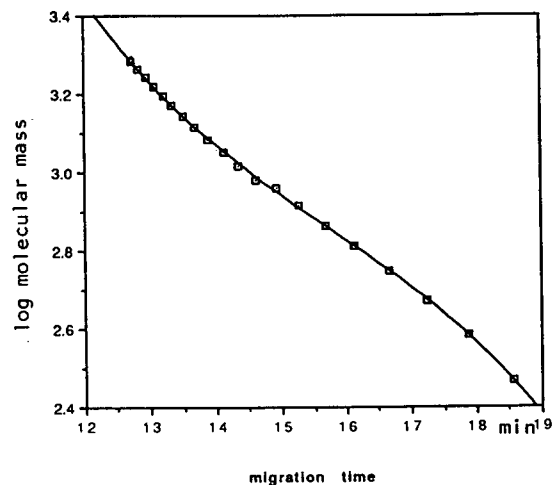


Fig. 9. Plot of the log of the molecular mass of Triton X series oligomers versus migration time. Data fit to a third-order polynomial. $y = 16.652 - 2.3997x + 0.14509x^2 - 3.0695 \cdot 10^{-3}x^3$; $R^2 = 1.000$.

containing buffer, the micelle structure is essentially broken down. The hydrophobic portions of individual SDS molecules can still associate with the hydrophobic portions of the Triton oligomers. This type of mechanism has been described as solvophobic association by Walbroehl and Jorgenson [19]. Individual Triton oligomers will, to a first approximation, associate with the same amount of SDS due to an apparent strong interaction with the alkylaryl portion of the molecule. Individual oligomers can then be separated based on differences in the lengths of the poly(ethylene oxide) chains. Fig. 8 shows the separation of Triton X series oligomers from $n = 1$ to $n = 46$. The dependence of the migration times on molecular mass is depicted in the plot of migration time *versus* log molecular mass shown in Fig. 9. Data were fit to a third-order polynomial resulting in an R^2 value of 1.000. The precision of the migration times for selected oligomers was determined for replicate injections. The data are compiled in Table II. The precision for absolute migration times achieved here is not as good as obtained for the poly(alkyl oxide) diamines, although the precision of relative migration times was quite good. It is anticipated that the precision of absolute migration times will be improved by incorporating an appropriate capillary regeneration protocol into the analysis. Fig. 10 shows the separation obtained on the oligomers in a sample of Triton X-100 surfactant which indicates about 20 oligomers.

To elucidate the mechanism of this separation (micellar or solvophobic association) conductivity measurements were obtained on solutions con-

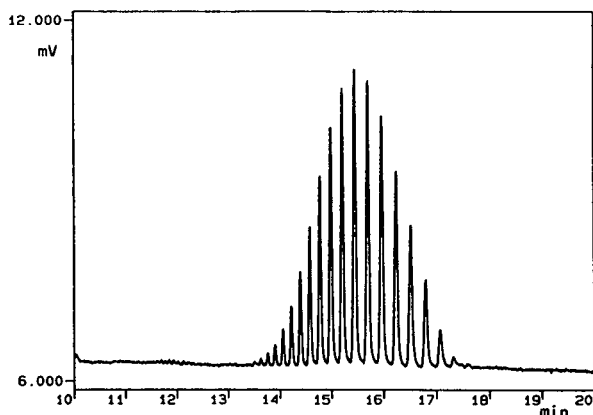


Fig. 10. CE separation of Triton X-100. Conditions as given in the Experimental section.

taining 25 mM boric acid pH 8.6, 35% acetonitrile with different amounts of SDS from 0 to 50 mM. A linear increase in conductivity ($57.1 \mu\text{S}/\text{mM}$ SDS, $R^2 = 1.000$) was observed with increasing concentration of SDS. A similar experiment conducted in water without any acetonitrile revealed a sharp break in the conductivity relationship at about 7 mM which is consistent with the formation of micelles. These data indicate the absence of micelles in the presence of 35% acetonitrile and, therefore, a solvophobic association mechanism.

CE analysis of neutral poly(ethylene glycol) polymers

Neutral PEG polymers were not directly amenable to CE analysis due to a lack of charge as well as the absence of a UV chromophore. In order to impart these two characteristics to the PEG, a modification of the classical phthalic

TABLE II

PRECISION OF CE MIGRATION TIMES FOR TRITON X SERIES OLIGOMERS

Conditions as given in Fig. 8. Mean, etc. are of 7 determinations.

	Migration times (min) for oligomers					
	$n = 1$	$n = 5$	$n = 10$	$n = 20$	$n = 30$	$n = 40$
Mean (min)	18.40	17.18	15.83	14.13	13.17	12.56
S.D. (min)	0.4155	0.3517	0.2866	0.2182	0.1842	0.1646
R.S.D. (%)	2.26	2.05	1.80	1.54	1.40	1.31

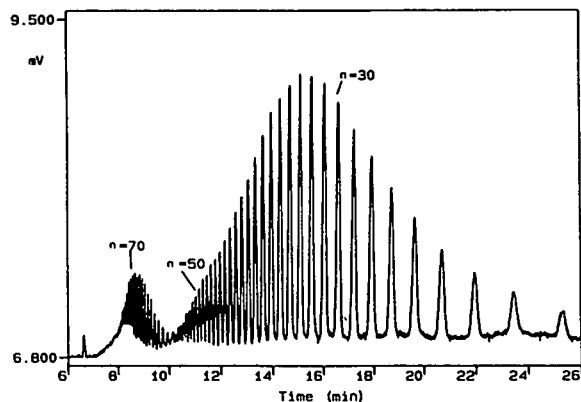


Fig. 11. CE separation of PEG oligomers derivatized with phthalic anhydride. Conditions as given in the Experimental section.

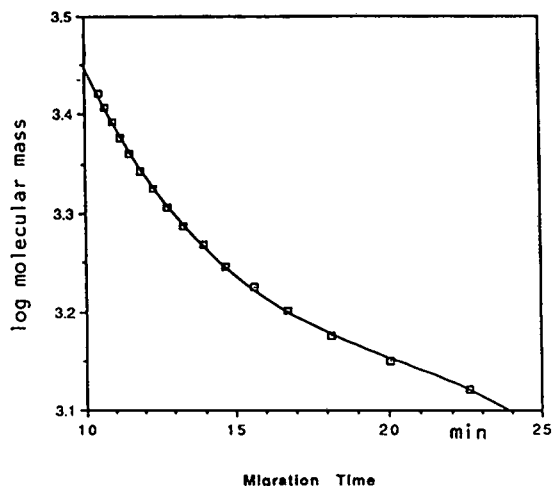


Fig. 12. Plot of the log of the molecular mass of PEG oligomers versus migration time. Data fit to a third-order polynomial. $y = 4.7042 - 0.20473x + 9.4356 \cdot 10^{-3}x^2 - 1.5388 \cdot 10^{-4}x^3$; $R^2 = 1.000$.

TABLE III

PRECISION OF CE MIGRATION TIMES FOR PEG PHTHALATES

Conditions as given in Fig. 11. Mean, etc. are of 7 determinations.

	Migration times (min) for oligomers					
	$n = 25$	$n = 30$	$n = 35$	$n = 40$	$n = 50$	$n = 65$
Mean (min)	20.02	16.15	13.94	12.51	10.79	8.88
S.D. (min)	0.1992	0.1343	0.1056	0.0877	0.0670	0.0486
R.S.D. (%)	0.995	0.831	0.758	0.701	0.621	0.547

anhydride derivatization chemistry [20] was used. By reacting the terminal hydroxyl groups of the PEG with phthalic anhydride, a phthalate ester is tagged onto each end of the polymer giving it a chromophore (phenyl group) and ionic termini (carboxylic acids).

Fig. 11 shows a free solution CE separation of a mixture of a series of derivatized PEG oligomers with molecular masses from about 1000 to over 3500. In this case separation of individual oligomers was achieved by incorporating acetonitrile and 1,3-diaminopropane into the separation buffer. Both of these modifiers act to reduce the electroosmotic flow which correlated with improved resolution of individual oligomers. Fig. 12 shows a plot of the dependence of migration time on the molecular mass of the PEG oligomers. Again, the data were fit to a third-order polynomial resulting in an R^2 value of 1.000. To gauge the reproducibility of the separation, migration times for individual oligomers were measured for multiple injections. The data contained in Table III demonstrates R.S.D.s of under 1.0%.

CONCLUSIONS

This work has examined the utility of CE for characterizing the oligomeric distribution of different types of polydisperse polymers. Success has been achieved for polymers in which a difference in charge-to-size ratio for the oligomers exists (terminal ionic polymers) or where a hydrophobic tail is present at the ends of hydrophilic polymer chains (Tritons). For neutral

PEG polymers, separation was achieved after derivatizing the polymer to impart charge and a UV chromophore. Each different type of polymer can present a different set of problems related to the separation and detection schemes needed for the analysis. Future plans include analysis of larger-sized polymers and the incorporation of sieving media to extend the utility of the technique to other types of polymers.

ACKNOWLEDGEMENT

The author thanks David Ladd of the Medicinal Chemistry Department of Sterling-Winthrop for the preparation of poly(ethylene oxide) diamines.

REFERENCES

- 1 H.G. Barth and B.E. Boynes, *Anal. Chem.*, 64 (1992) 428R.
- 2 C.G. Smith, R.A. Nyquist, P.A. Smith, A.J. Pasztor and S.J. Martin, *Anal. Chem.*, 63 (1991) 11R.
- 3 S. Mori, *J. Chromatogr.*, 507 (1990) 473.
- 4 R.E.A. Escott and N. Mortimer, *J. Chromatogr.*, 553 (1991) 423.
- 5 P. Jandera, *J. Chromatogr.*, 449 (1988) 361.
- 6 T. Okada, *Anal. Chem.*, 62 (1990) 327.
- 7 B. Gemmel, B. Lorenschat and F.B. Schmitz, *Chromatographia*, 27 (1989) 605.
- 8 P.D. Grossman, K.J. Wilson, G. Petrie and H.H. Lauer, *Anal. Biochem.*, 173 (1988) 265.
- 9 H.H. Lauer and D. McManigill, *Anal. Chem.*, 58 (1986) 166.
- 10 A. Guttman, A.S. Cohen, D.N. Heiger and B.L. Karger, *Anal. Chem.*, 62 (1990) 137.
- 11 D.N. Heiger, A.S. Cohen and B.L. Karger, *J. Chromatogr.*, 516 (1990) 33.
- 12 J.B. Poli and M.R. Schure, *Anal. Chem.*, 64 (1992) 896.
- 13 F. Garcia and J.D. Henion, *Anal. Chem.*, 64 (1992) 985.
- 14 L.N. Amankwa, J. Scholl and W.G. Kuhr, *Anal. Chem.*, 62 (1990) 2189.
- 15 C. Braud and M. Vert, *Polym. Bull.*, 29 (1992) 177.
- 16 F. Foret, S. Fanali, A. Nardi and P. Boček, *Electrophoresis*, 11 (1990) 780.
- 17 A. Weston, P.R. Brown, P. Jandik, A.L. Heckenberg and W.R. Jones, *J. Chromatogr.*, 608 (1992) 395.
- 18 M. Chen and R.M. Cassidy, *J. Chromatogr.*, 602 (1992) 227.
- 19 Y. Walbroehl and J. Jorgenson, *Anal. Chem.*, 58 (1986) 479.
- 20 *Standard Test Methods for Chemical Analysis of Alcohol Ethoxylates and Alkylphenol Ethoxylates*, American Society for Testing and Materials, Philadelphia, PA, methods D4252–D4289.

Short Communication

Determination and confirmation of benomyl and carbendazim in water using high-performance liquid chromatography and diode array detection

Jagdev S. Dhoot* and Aurora R. del Rosario

California State Department of Health Services, Sanitation and Radiation Laboratory, 2151 Berkeley Way, Berkeley, CA 94704 (USA)

(First received April 20th, 1993; revised manuscript received May 25th, 1993)

ABSTRACT

This paper describes a direct determination of benomyl and carbendazim in a single analytical run and their confirmation by absorption spectra using diode array detection. A simple technique has been developed for preparation of benomyl calibration standard. Benomyl was dissolved in chloroform prior to a high dilution in water for HPLC.

Detection limits, precision, and accuracy of data are presented. The method is simple, rapid, accurate, and precise.

INTRODUCTION

Benomyl [methyl 1-(butylcarbamoyl)-2-benzimidazolecarbamate] is used as a systemic fungicide and miticide in agricultural crops. It is marketed with the trademark of Benlate which contains 50% benomyl. It is stable in the dry state but splits into butyl isocyanate to form carbendazim (methyl 2-benzimidazolecarbamate) or MBC in acid solution and organic solvents. Both benomyl and MBC are considered to be fungitoxic.

Most of the analytical methods used for determining benomyl involve conversion of benomyl to carbendazim [1–4] or formation of its derivative [5]. Direct analysis of benomyl as

parent molecule has been difficult because of its instability in solvents [6,7] and poor solubility in water [8].

EXPERIMENTAL

Apparatus

Analytical procedures were performed using a Hewlett-Packard 1090 liquid chromatograph equipped with a Hewlett-Packard diode array detector, PV5 solvent delivery system, autoinjector and a Hewlett-Packard 79994A "Chem Station" for data acquisition. A Brownlee cyano column (25 cm × 4.6 mm × 5 μm) was obtained from Rainin (Emeryville, CA, USA). A filter (0.45 μm particle size) and a guard column of the same composition were used on-line before the column.

* Corresponding author.

Reagents

Benomyl (99.9%) was purchased from Ultra Scientific (North Kingston, RI, USA). Carbendazim (99.0%) was obtained from the Pesticides and Industrial Chemical Repository, United States Environmental Protection Agency Repository. Chloroform and ammonium acetate were obtained from Aldrich (Milwaukee, WI, USA).

Procedure

Carbendazim stock standard solution was prepared by weighing 10 mg of pure carbendazim and dissolving in 10 ml methanol. This stock standard, when stored at 4°C and protected from light, is stable for six months. Aqueous standards ranging from 5 µg/l to 2 mg/l were prepared by spiking 10 ml of water with different volumes of stock standard. A calibration curve of concentration versus area counts was prepared.

Standard solution of benomyl (1000 or 100 mg/l) was prepared by dissolving 10 mg in 10 or 100 ml chloroform. Immediately 20 µl of the 1000 mg/l standard solution were spiked into 10 ml reagent water and shaken vigorously for 20 s to dissolve the chloroform solution and then 200 µl of this aqueous calibration standard (2 mg benomyl/l) were injected immediately into the HPLC system for analysis. Similarly, each aqueous standard ranging in concentration from 5 µg/l to 2 mg/l was prepared from neat benomyl powder and analyzed immediately so that contact of benomyl with chloroform and water before injection into the HPLC system was achieved in 1–2 min. Only 1 to 20 µl chloroform for aqueous standard preparation was used because chloroform has limited solubility (0.5% V/V) in water. The standard solution of benomyl (100 mg/l) mentioned above was used for the preparation aqueous calibration standards at concentration levels of <200 µg/l. The benomyl calibration curve was established after adjusting the benomyl loss by conversion to carbendazim, if any, as follows:

benomyl concentration that gives response (mg/l) = benomyl concentration prepared (mg/l) – [carbendazim concentration (mg/l) × 1.52]

Carbendazim concentration refers to the concentration of carbendazim peak which appeared in the benomyl standard chromatogram as calculated from the carbendazim calibration curve prepared above.

The standard solutions, spiked reagent water, drinking water, and wastewater were analyzed using 200 µl injections with methanol–0.05 M ammonium acetate (35:65, v/v) as the mobile phase at 1 ml/min and 25°C temperature. The diode array detector was scanned from 210 to 400 nm wavelength to get the absorption spectra and the 286 nm wavelength was used to monitor the quantitation. Molar absorptivities for benomyl and carbendazim, dissolved in chloroform and methanol respectively, were determined at 286 nm wavelength. The detection limit was established by using the lowest concentration of the analyte that gives a 2:1 signal-to-noise ratio.

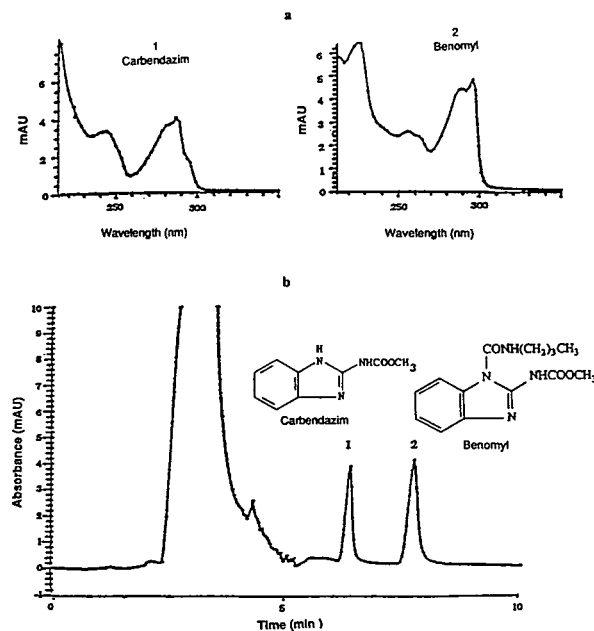


Fig. 1. (a) Diode array spectra for carbendazim and benomyl corresponding to chromatographic peaks 1 and 2, respectively, in (b) UV absorption chromatogram at 286 nm showing carbendazim (1) and benomyl (2) in wastewater at 100 µg/l each using Brownlee cyano column (25 cm × 4.6 mm × 5 µm particle size), solvent methanol–0.05 M ammonium acetate (35:65, v/v), 1 ml/min flow-rate, 25°C.

TABLE I
RECOVERY OF BENOMYL AND CARBENDAZIM FROM SPIKED DRINKING WATER AND WASTE WATER

Analyte	Concentration ($\mu\text{g/l}$)	Number of replicates	Average recovery (%)	Relative standard deviation (%)
<i>Tap drinking water</i>				
Benomyl	5.0	7	109	9.0
	50	7	106	10
Carbendazim	5.0	7	115	10
	50	7	119	14
<i>Waste Water</i>				
Benomyl	50	7	97	9.5
	100	7	93	11
Carbendazim	50	7	107	9.2
	100	7	103	14

RESULTS AND DISCUSSION

Separation and quantitation

Fig. 1 illustrates the separation of benomyl and carbendazim in wastewater. The separation was achieved in 10 min. The high molar absorptivities of benomyl (1.9×10^4) and carbendazim (1.3×10^4) at 286 nm wavelength facilitated an otherwise sensitive assay. The limits of detection for benomyl and carbendazim were 1 $\mu\text{g/l}$ each. Benomyl standard solutions in all solvents, including water, always show some degree of conversion to carbendazim; a correction therefore has to be made. When each calibration aqueous standard at different concentration level was analyzed, only $3.5 \pm 1\%$ ($n = 5$) conversion of benomyl to carbendazim had occurred. Chloroform was used as a solvent because it dissolves benomyl quickly and yet does not accelerate its decomposition [9]. Instrumental response was demonstrated to be sufficiently linear over a range of 1 ng to 4 μg for both benomyl and carbendazim with a correlation coefficient of > 0.99 .

Method evaluation

In Table 1 the recovery and precision data for the wastewater samples compared favourably

with that from the drinking water samples. This shows that the matrix effect in these cases was minimal. Confirmation of peak identity with a high degree of confidence is possible by comparing the retention times and UV spectra of benomyl and carbendazim (Fig. 1a). The minimum amounts of these analytes required by diode array detection to provide a UV spectra of sufficient quality to permit identification were determined to be 2 ng for carbendazim and 10 ng for benomyl, respectively.

ACKNOWLEDGEMENT

We appreciate the careful review of a draft of the manuscript by Dr. Michael G. Volz, Chief, Division of Laboratories, California Department of Health Services, Berkeley, CA, USA.

REFERENCES

- 1 J.J. Kirkland, *J. Agric. Food Chem.*, 21 (1973) 171.
- 2 J.J. Kirkland, R.F. Holt and H.L. Pease, *J. Agric. Food Chem.*, 21 (1973) 368.
- 3 G. Zweig and R.Y. Gao, *Anal. Chem.*, 55 (1983) 1448.
- 4 G.M. Jett, *Test Methods for Nonconventional Pesticides Analysis of Industrial and Municipal Wastewater*. Environmental Protection Agency, Washington, DC, 1983, pp. 33 and 596.

5 M. Chiba, *J. Agric. Food Chem.*, 34 (1986) 108.

6 M. Chiba, *J. Agric. Food Chem.*, 25 (1977) 368.

7 M. Chiba and E.C. Cherniak, *J. Agric. Food Chem.*, 26 (1978) 573.

8 R.P. Singh and M. Chiba, *J. Agric. Food Chem.*, 33 (1985) 63.

9 J.P. Calmon and D.R. Sayag, *J. Agric. Food Chem.*, 24 (1976C) 426.

Short Communication

Structure-gas chromatographic retention time models of tetra-*n*-alkylsilanes and tetra-*n*-alkylgermanes using topological indexes

A correction

Eugene J. Kupchik

Department of Chemistry, St. John's University, Grand Central and Utopia Parkways, Jamaica, NY 11439 (USA).

(Received April 27th, 1993)

ABSTRACT

Previously reported [*J. Chromatogr.*, 630 (1993) 223] structure-gas chromatographic retention time models for 26 tetra-*n*-alkylsilanes, 26 tetra-*n*-alkylgermanes, and the mixed set of silanes and germanes have been corrected. Most of the previously reported equations are improved. The general conclusions of the previous paper remain unchanged.

INTRODUCTION

In the author's previous paper [1] the topological indexes for compounds 15, 21, 41 and 47 in Table III were incorrectly computed. The analyses have been repeated using the correct topological indexes for these compounds.

RESULTS

Equations 14, 15, 17 and 18 in the previous paper [1] are virtually unchanged. The other previously reported equations are improved and are given below. The numbers of the equations correspond to those in the previous paper [1]. The intercorrelation results are given after each multivariable equation. The results of the analysis using eqn. 20 are given in corrected Table III,

which corresponds to Table III in the previous paper [1]:

$$\log T = -0.455(0.040) + 0.514(0.007)^1\chi \quad (12)$$

$$n = 26 \quad r = 0.998 \quad s = 0.045 \quad F = 5448$$

$$\log T = -0.165(0.053) + 0.493(0.006)^1\chi - 0.193(0.031)^3\chi_c \quad (13)$$

$$n = 26 \quad r = 0.999 \quad s = 0.028 \quad F = 6959$$

The intercorrelation between $^1\chi$ and $^3\chi_c$ is: $r = 0.627$

$$\log T = -0.029(0.052) + 0.490(0.006)^1\chi - 0.174(0.031)^3\chi_c \quad (16)$$

$$n = 26 \quad r = 0.999 \quad s = 0.027 \quad F = 7180$$

TABLE III

LOGARITHMS OF RETENTION TIMES OF TETRA-*n*-ALKYLSILANES AND TETRA-*n*-ALKYLGERMANES AND TOPOLOGICAL INDEXES

No.	Compound ^a	¹ χ	³ χ _c	S	TTV	Log T ^b	Calc. ^c	Res. ^d
1	Me ₃ BuSi	3.5607	1.5607	-0.6782	14.3584	1.29	1.31	-0.02
2	MeEt ₃ Si	3.6820	0.9286	-0.6713	14.1734	1.43	1.48	-0.05
3	Me ₂ Pr ₂ Si	4.1213	1.2071	-0.7033	17.2755	1.60	1.65	-0.05
4	Me ₂ EtBuSi	4.1213	1.2071	-0.6982	17.2958	1.61	1.64	-0.03
5	MeEt ₂ PrSi	4.1820	0.9268	-0.6973	17.2185	1.70	1.72	-0.02
6	Et ₄ Si	4.2426	0.7071	-0.6914	17.1717	1.80	1.79	0.01
7	Me ₂ PrBuSi	4.6213	1.2071	-0.7243	20.3554	1.90	1.89	0.01
8	MeEtPr ₂ Si	4.6820	0.9268	-0.7234	20.2999	1.95	1.97	-0.02
9	Et ₃ PrSi	4.7426	0.7071	-0.7174	20.2666	2.05	2.04	0.01
10	Me ₂ Bu ₂ Si	5.1213	1.2071	-0.7453	23.4573	2.15	2.13	0.02
11	MePr ₃ Si	5.1820	0.9268	-0.7494	23.4178	2.20	2.21	-0.01
12	Et ₂ Pr ₂ Si	5.2426	0.7071	-0.7434	23.3979	2.29	2.28	0.01
13	Et ₃ BuSi	5.2426	0.7071	-0.7384	23.3913	2.32	2.28	0.04
14	MePr ₂ BuSi	5.6820	0.9268	-0.7704	26.5620	2.47	2.46	0.01
15	MeEtBu ₂ Si	5.6820	0.9268	-0.7653	26.5546	2.49	2.46	0.03
16	EtPr ₂ Si	5.7426	0.7071	-0.7695	26.5656	2.52	2.53	-0.01
17	Pr ₄ Si	6.2426	0.7071	-0.7955	29.7698	2.74	2.77	-0.03
18	EtPr ₂ BuSi	6.2426	0.7071	-0.7905	29.7462	2.77	2.77	0.00
19	Et ₂ Bu ₂ Si	6.2426	0.7071	-0.7854	29.7254	2.82	2.77	0.05
20	MeBu ₂ Si	6.6820	0.9268	-0.8123	32.9167	2.99	2.94	0.05
21	Pr ₃ BuSi	6.7426	0.7071	-0.8165	32.9782	2.99	3.02	-0.03
22	EtPrBu ₂ Si	6.7426	0.7071	-0.8114	32.9489	3.03	3.01	0.02
23	Pr ₂ Bu ₂ Si	7.2426	0.7071	-0.8375	36.2088	3.24	3.26	-0.02
24	EtBu ₃ Si	7.2426	0.7071	-0.8324	36.1737	3.30	3.26	0.04
25	PrBu ₃ Si	7.7426	0.7071	-0.8584	39.4616	3.49	3.50	-0.01
26	Bu ₄ Si	8.2426	0.7071	-0.8794	42.7365	3.72	3.75	-0.03
27	Me ₃ BuGe	3.5607	1.5607	-1.1086	13.4109	1.42	1.43	-0.01
28	MeEt ₃ Ge	3.6820	0.9268	-1.1250	13.0229	1.57	1.60	-0.03
29	Me ₂ Pr ₂ Ge	4.1213	1.2071	-1.1597	16.1384	1.77	1.77	0.00
30	Me ₂ EtBuGe	4.1213	1.2071	-1.1503	16.1933	1.77	1.77	0.00
31	MeEt ₂ PrGe	4.1820	0.9286	-1.1632	15.9902	1.84	1.85	-0.01
32	Et ₄ Ge	4.2426	0.7071	-1.1667	15.8485	1.94	1.92	0.02
33	Me ₂ PrBuGe	4.6213	1.2071	-0.1885	19.1749	2.04	2.02	0.02
34	MeEtPr ₂ Ge	4.6820	0.9268	-1.2014	18.9886	2.09	2.10	-0.01
35	Et ₃ PrGe	4.7426	0.7071	-1.2049	18.8569	2.18	2.17	0.01
36	Me ₂ Bu ₂ Ge	5.1213	1.2071	-1.2172	22.2309	2.31	2.26	0.05
37	MePr ₃ Ge	5.1820	0.9268	-1.2396	22.0178	2.35	2.35	0.00
38	Et ₂ Pr ₂ Ge	5.2426	0.7071	-1.2431	21.8963	2.42	2.42	0.00
39	Et ₃ BuGe	5.2426	0.7071	-1.2336	21.9310	2.45	2.42	0.03
40	MePr ₂ BuGe	5.6820	0.9268	-1.2683	25.1095	2.61	2.60	0.01
41	MeEtBu ₂ Ge	5.6820	0.9268	-1.2589	25.1429	2.64	2.59	0.05
42	EtPr ₂ Ge	5.7426	0.7071	-1.2813	24.9666	2.66	2.67	-0.01
43	Pr ₄ Ge	6.2426	0.7071	-1.3194	28.0678	2.89	2.92	-0.03
44	EtPr ₂ BuGe	6.2426	0.7071	-1.3100	28.0891	2.91	2.91	0.00
45	Et ₂ Bu ₂ Ge	6.2426	0.7071	-1.3006	28.1125	2.95	2.91	0.04
46	MeBu ₂ Ge	6.6820	0.9268	-1.3258	31.3514	3.14	3.09	0.05
47	Pr ₃ BuGe	6.7426	0.7071	-1.3482	31.2146	3.13	3.16	-0.03
48	EtPrBu ₂ Ge	6.7426	0.7071	-1.3388	31.2313	3.16	3.16	0.00
49	Pr ₂ Bu ₂ Ge	7.2426	0.7071	-1.3769	34.3810	3.38	3.41	-0.03
50	EtBu ₃ Ge	7.2426	0.7071	-1.3675	34.3930	3.40	3.41	-0.01
51	PrBu ₃ Ge	7.7426	0.7071	-1.4057	37.5670	3.61	3.65	-0.04
52	Bu ₄ Ge	8.2426	0.7071	-1.4344	40.7725	3.85	3.90	-0.05

^a Me = Methyl; Et = ethyl; Pr = *n*-propyl; Bu = *n*-butyl.^b Logarithm of retention time taken from ref. 24.^c Calculated from eqn. 20.^d Residual = Log T - calc.

The intercorrelation between ${}^1\chi$ and ${}^3\chi_c$ is: $r = 0.627$

$$\log T = -0.468(0.022) + 0.485(0.004){}^1\chi + 0.023(0.001){}^3\chi^v \quad (19)$$

$$n = 52 \quad r = 0.999 \quad s = 0.033 \quad F = 9810$$

The intercorrelation between ${}^1\chi$ and ${}^3\chi^v$ is: $r = -0.420$

$$\log T = -0.290(0.040) + 0.476(0.004){}^1\chi - 0.183(0.023){}^3\chi_c - 0.277(0.016)S \quad (20)$$

$$n = 52 \quad r = 0.999 \quad s = 0.029 \quad F = 8850$$

The intercorrelation results are: $r = 0.218$ for S and ${}^1\chi$, $r = -0.001$ for S and ${}^3\chi_c$, and $r = 0.612$ for ${}^1\chi$ and ${}^3\chi_c$.

$$\log T = -1.265(0.030) + 0.372(0.003){}^0\chi^r + 0.040(0.002){}^4\chi_{pc}^v \quad (21)$$

$$n = 52 \quad r = 0.999 \quad s = 0.034 \quad F = 9478$$

The intercorrelation between ${}^0\chi^r$ and ${}^4\chi_{pc}^v$ is: $r = 0.010$.

REFERENCE

- 1 E.J. Kupchik, *J. Chromatogr.*, 630 (1993) 223.

Short Communication

Adsorption chromatography on cellulose

X. Adsorption of tryptophan and derivatives from CuSO_4 -containing eluents

Huynh Thi Kieu Xuan and M. Lederer*

Institut de Chimie Minérale et Analytique, Université de Lausanne, Boîte Postale 115, Centre Universitaire, CH-1015 Lausanne 15 (Switzerland)

(First received December 11th, 1992; revised manuscript received April 29th, 1993)

ABSTRACT

The adsorption of tryptophan and substituted tryptophans on cellulose thin layers developed with CuSO_4 solutions is reported. The presence of CuSO_4 decreases the chiral discrimination of cellulose for tryptophan and substituted tryptophans. The results are compared with those from previously reported work where chiral separations were obtained.

INTRODUCTION

In a study of the effect of various metal salts on the separation of optical isomers of tryptophan on cellulose [1] with aqueous solvents, it was noted that only Cu^{2+} had an effect on this separation, resulting in a diminution of the separation effect. Copper (II) yields the most stable complexes with amino acids with stability constants of the order of 10^{15} , so that an effect was to be expected. What was of interest was that the tryptophan was still adsorbed and did not travel with the liquid front although both the amino and the carboxylic groups were not free.

In the eluent used, namely 0.05 M CuSO_4 , there would be a large excess of Cu^{2+} ions and in view of the high stability constants one can assume that the tryptophan would be present as a 1:1 complex with the two free coordination groups of the copper occupied by water molecules. We felt that this observation merited more attention.

EXPERIMENTAL

Merck cellulose (Art. No. 5577) (consisting of microcrystalline cellulose) was used throughout. The chromatograms were developed at room temperature in small, well stoppered glass jars. After drying, the spots were revealed by exposure to iodine vapour, which gave good contrast when copied with a photocopier.

* Corresponding author.

RESULTS

A number of fluoro-, hydroxy- and methyl-tryptophans was examined, in addition to tyrosine, tyrosine peptides, tryptophan peptides, kynurenine and a series of glycine peptides. The results are given in Tables I and II, where a comparison is made between copper sulphate

and non-complexing eluents such as sodium chloride and sodium sulphate.

DISCUSSION

The separation of enantiomers is diminished or non-existent with CuSO_4 as eluent in all instances (Table I). The fact that there is a slight

TABLE I

R_F VALUES OF AMINO ACIDS AND PEPTIDES ON CELLULOSE THIN LAYERS WITH 0.1 M SODIUM CHLORIDE AND 0.05 M COPPER(II) SULPHATE SOLUTIONS AS ELUENTS

Compound ^a	0.1 M NaCl		0.05 M CuSO_4	
	R_F	ΔR_F	R_F	ΔR_F
L-Tyr	0.75	0.06	0.78	0.04
D-Tyr	0.81		0.82	
L-(Tyr) ₂	0.75		0.77	
L-(Tyr) ₃	0.71		0.73	
DL-Kynurenine	0.48 } 0.55 }	0.07	0.71	One spot only
L-Trp	0.57	0.05	0.70	0.04
D-Trp	0.62		0.74	
L-(Trp) ₂	0.48		0.38	
DL-4-Methyl-Trp	0.29 } 0.36 }	0.07	0.48	One spot only
DL-5-Methyl-Trp	0.37 } 0.46 }	0.09	0.50 } 0.53 }	0.03
DL-6-Methyl-Trp	0.32 } 0.39 }	0.07	0.52	One spot only
DL-7-Methyl-Trp	0.34 } 0.41 }	0.07	0.54	One spot only
DL-4-Fluoro-Trp	0.38 } 0.44 }	0.06	0.55	One spot only
DL-5-Fluoro-Trp	0.39 } 0.45 }	0.06	0.575	One spot only
DL-6-Fluoro-Trp	0.41 } 0.46 }	0.05	0.565	One spot only
DL-5-hydroxy-Trp	0.31 } 0.36 }	0.05	0.45	One spot only
Trp-Tyr	0.595		0.545	
Gly-Trp	0.68		0.74	
Gly	} Move with the solvent front		} Move with the solvent front	
(Gly) ₂				
(Gly) ₃				
(Gly) ₄				
(Gly) ₅				
(Gly) ₆				

^a Trp = Tryptophan; Tyr = tyrosine; Gly = glycine.

TABLE II

R_F VALUES OF SUBSTITUTED TRYPTOPHANS ON CELLULOSE THIN LAYERS WITH VARIOUS CONCENTRATIONS OF COPPER(II) SULPHATE SOLUTION AS ELUENTS

Compound ^a	0.1 M NaCl	0.5 M Na ₂ SO ₄	1 M Na ₂ SO ₄	0.05 M CuSO ₄	0.5 M CuSO ₄	1 M CuSO ₄																																																																												
DL-4-Fluoro-Trp	0.38	0.33	0.24	0.55	0.61	0.51																																																																												
	0.44	0.37	0.28				DL-5-Fluoro-Trp	0.39	0.38	0.28	0.57	0.64	0.56	0.45	0.43	0.33	DL-6-Fluoro-Trp	0.41	0.35	0.28	0.58	0.63	0.55	0.46	0.40	0.31	DL-5-Hydroxy-Trp	0.31	0.25	0.22	0.45	0.53	0.46	0.46	0.30	0.26	DL-4-Methyl-Trp	0.29	0.23	0.14	0.48	0.50	0.44	0.36	0.24	0.20	DL-5-Methyl-Trp	0.37	0.27	0.18	0.50	0.55	0.47	0.46	0.34	0.225	DL-6-Methyl-Trp	0.32	0.26	0.15	0.52	0.55	0.37	0.39	0.33	0.21	DL-7-Methyl-Trp	0.34	0.26	0.16	0.54	0.58	0.45	0.41	0.31	0.20	DL-Kynurenine	0.48			0.71	0.77
DL-5-Fluoro-Trp	0.39	0.38	0.28	0.57	0.64	0.56																																																																												
	0.45	0.43	0.33				DL-6-Fluoro-Trp	0.41	0.35	0.28	0.58	0.63	0.55	0.46	0.40	0.31	DL-5-Hydroxy-Trp	0.31	0.25	0.22	0.45	0.53	0.46	0.46	0.30	0.26	DL-4-Methyl-Trp	0.29	0.23	0.14	0.48	0.50	0.44	0.36	0.24	0.20	DL-5-Methyl-Trp	0.37	0.27	0.18	0.50	0.55	0.47	0.46	0.34	0.225	DL-6-Methyl-Trp	0.32	0.26	0.15	0.52	0.55	0.37	0.39	0.33	0.21	DL-7-Methyl-Trp	0.34	0.26	0.16	0.54	0.58	0.45	0.41	0.31	0.20	DL-Kynurenine	0.48			0.71	0.77	0.74	0.55								
DL-6-Fluoro-Trp	0.41	0.35	0.28	0.58	0.63	0.55																																																																												
	0.46	0.40	0.31				DL-5-Hydroxy-Trp	0.31	0.25	0.22	0.45	0.53	0.46	0.46	0.30	0.26	DL-4-Methyl-Trp	0.29	0.23	0.14	0.48	0.50	0.44	0.36	0.24	0.20	DL-5-Methyl-Trp	0.37	0.27	0.18	0.50	0.55	0.47	0.46	0.34	0.225	DL-6-Methyl-Trp	0.32	0.26	0.15	0.52	0.55	0.37	0.39	0.33	0.21	DL-7-Methyl-Trp	0.34	0.26	0.16	0.54	0.58	0.45	0.41	0.31	0.20	DL-Kynurenine	0.48			0.71	0.77	0.74	0.55																		
DL-5-Hydroxy-Trp	0.31	0.25	0.22	0.45	0.53	0.46																																																																												
	0.46	0.30	0.26				DL-4-Methyl-Trp	0.29	0.23	0.14	0.48	0.50	0.44	0.36	0.24	0.20	DL-5-Methyl-Trp	0.37	0.27	0.18	0.50	0.55	0.47	0.46	0.34	0.225	DL-6-Methyl-Trp	0.32	0.26	0.15	0.52	0.55	0.37	0.39	0.33	0.21	DL-7-Methyl-Trp	0.34	0.26	0.16	0.54	0.58	0.45	0.41	0.31	0.20	DL-Kynurenine	0.48			0.71	0.77	0.74	0.55																												
DL-4-Methyl-Trp	0.29	0.23	0.14	0.48	0.50	0.44																																																																												
	0.36	0.24	0.20				DL-5-Methyl-Trp	0.37	0.27	0.18	0.50	0.55	0.47	0.46	0.34	0.225	DL-6-Methyl-Trp	0.32	0.26	0.15	0.52	0.55	0.37	0.39	0.33	0.21	DL-7-Methyl-Trp	0.34	0.26	0.16	0.54	0.58	0.45	0.41	0.31	0.20	DL-Kynurenine	0.48			0.71	0.77	0.74	0.55																																						
DL-5-Methyl-Trp	0.37	0.27	0.18	0.50	0.55	0.47																																																																												
	0.46	0.34	0.225				DL-6-Methyl-Trp	0.32	0.26	0.15	0.52	0.55	0.37	0.39	0.33	0.21	DL-7-Methyl-Trp	0.34	0.26	0.16	0.54	0.58	0.45	0.41	0.31	0.20	DL-Kynurenine	0.48			0.71	0.77	0.74	0.55																																																
DL-6-Methyl-Trp	0.32	0.26	0.15	0.52	0.55	0.37																																																																												
	0.39	0.33	0.21				DL-7-Methyl-Trp	0.34	0.26	0.16	0.54	0.58	0.45	0.41	0.31	0.20	DL-Kynurenine	0.48			0.71	0.77	0.74	0.55																																																										
DL-7-Methyl-Trp	0.34	0.26	0.16	0.54	0.58	0.45																																																																												
	0.41	0.31	0.20				DL-Kynurenine	0.48			0.71	0.77	0.74	0.55																																																																				
DL-Kynurenine	0.48			0.71	0.77	0.74																																																																												
	0.55																																																																																	

^a For abbreviations see footnote to Table I.

separation between D- and L-tryptophan and between D- and L-5-methyltryptophan indicates that also other pairs could have small chiral effects, which are too small to be detected in thin-layer chromatography, however.

In CuSO₄ solutions the R_F values of the tryptophan derivatives are always higher than in non-complexing solvents by about 0.10–0.15 units, except for tryptophan peptides, which either adsorb more strongly (as in the case of Trp–Trp and Trp–Tyr) or increase only by 0.06 (in the case of Gly–Trp). Tyrosine and tyrosine peptides hardly differ in the presence and absence of Cu²⁺ ions. Kynurenine is desorbed with an R_F increase of 0.2 with a simultaneous loss of enantiomer separation.

Copper ions are not retained on cellulose from aqueous solutions and there is no retardation of the “copper front” in these chromatograms. A size-exclusion effect due to the larger size of the copper complexes is unlikely as much larger molecules such as peptides adsorb well. Except for Dalglish [2], no specific discussion of the mechanism of chiral separations on cellulose

seems to have been published, but it seems likely from the extensive work on the very similar cyclodextrins (see, e.g., ref. 3) that hydrophobic adsorption and hydrogen bonding are the important contributors to it.

A loss of chiral resolution and an increase in R_F value was also observed when the amino group of tryptophan is methylated. Although an additional methyl group usually increases hydrophobicity, DL- α methyltryptophan moves as a single spot with an R_F value about 0.1–0.15 higher than that for tryptophan [4].

Both results seem to agree with Dalglish's theory [2] that a “three-point” adsorption is necessary for chiral separations. As soon as the NH₂ (in the case of the α -methyltryptophan) or both the NH₂ and the COOH groups (in the case of the Cu²⁺ complexes) are unable to participate in the adsorption, the R_F value increases and the chiral separation diminishes.

Several concentrations of CuSO₄ were examined (see Table II) and we attempted to correlate the results with R_F values obtained with NaCl and Na₂SO₄. In CuSO₄ the R_F values

increase with increase in concentration from 0.05 to 0.5 *M* and then decrease from 0.5 to 1 *M*. There is no similar behaviour with sodium or ammonium salts (see ref. 4). It could be that with increase in the Cu^{2+} concentration from 0.05 to 0.5 *M* there is also an increase in complex formation, which is unlikely in view of the high stability constants, or that there is a considerable concentration gradient along the chromatogram in 0.05 *M* CuSO_4 . Both are rather unlikely from previous experience. Hence this behaviour cannot be explained at present.

The decrease in R_f values with increase in concentration from 0.5 to 1 *M* is consistent with the usual salting-out effect on increasing the electrolyte concentration.

REFERENCES

- 1 M. Lederer, *J. Chromatogr.*, 510 (1990) 367.
- 2 C.E. Dalgliesh, *J. Chem. Soc.*, (1952) 3940.
- 3 S. Fanali and P. Boček, *Electrophoresis*, 11 (1990) 757.
- 4 A.O. Kuhn, M. Lederer and M. Sinibaldi, *J. Chromatogr.*, 469 (1989) 253.

Short Communication

Quantitation of 5-methylcytosine by one-dimensional high-performance thin-layer chromatography

Sherry A. Leonard, So Chun Wong and Jonathan W. Nyce*

Department of Molecular Pharmacology and Therapeutics, School of Medicine, East Carolina University, Greenville, NC 27858 (USA)

(First received September 2nd, 1992; revised manuscript received May 24th, 1993)

ABSTRACT

A method for the quantitative analysis of DNA 5-methylcytosine by one-dimensional high-performance thin-layer chromatography using alkylamino modified silica (HPTLC-NH₂) plates is described. The preparative method is simple, involving enzymatic digestion of DNA with micrococcal nuclease and phosphodiesterase II to 3'-monophosphate nucleosides, conversion by T₄ polynucleotide kinase to ³²P-labeled 3',5'-bisphosphate nucleosides, and chromatographic separation of nuclease P₁-cleaved 5'-monophosphate nucleosides. The weak, basic anion exchanger property of the HPTLC-NH₂ plate enables separation of multiple samples in one dimension, whereas traditional polyethyleneimine cellulose plates require development of individual samples in two dimensions for analysis of 5-methylcytosine.

INTRODUCTION

The presence of 5-methylcytosine (5mC)^a in nucleic acids was first described in *Mycobacterium tuberculosis* by Johnson and Coghill [17] in 1925. Since then, many studies have sought to determine its biological role, resulting in a variety of methods for the analysis of this minor base. Past techniques for measuring 5mC required sophisticated instrumentation such as high-performance liquid chromatography [1,2], gas chro-

matography-mass spectrometry [3,4], or antibodies specific for 5mC [5,6]. Other procedures utilizing thin-layer chromatography coupled with a postlabeling technique [7,8] required development in two dimensions such that only a single sample could be analyzed on one plate. Using HPTLC-NH₂ plates [9], we have developed a one-dimensional technique for 5mC determination that permits the simultaneous analysis of ten samples. In contrast to HPLC, this method allows the analysis of large batches of samples in a shorter period of time. The results obtained through this method are comparable with several HPLC methods and are within the range of previously published results for V79 cells [10]. Since changes in DNA methylation represent an early marker for neoplastic transformation [11] and exposure to cytotoxic drugs [12,13], this procedure could facilitate the screening of large

* Corresponding author.

^a Abbreviations: 5mC = 5-methylcytosine; HPTLC = high-performance thin-layer chromatography; 5mdCMP = 5-methyl-2'-deoxycytidine 5'-monophosphate; dCMP = 2'-deoxycytidine 5'-monophosphate; dAMP = 2'-deoxyadenosine 5'-monophosphate; dGMP = 2'-deoxyguanosine 5'-monophosphate; dTMP = thymidine 5'-monophosphate; dH₂O = deionized distilled water.

numbers of patients or monitoring the effects of drug treatment upon DNA methylation.

EXPERIMENTAL

Materials

Isobutyric acid and 5'-monophosphate nucleosides 5mdCMP, dCMP, dAMP, dGMP, dTMP, ATP and TLC chambers (inside dimensions 121 mm × 108 mm × 83 mm) were obtained from Sigma (St. Louis, MO, USA) as were the enzymes micrococcal nuclease and phosphodiesterase II. T₄ polynucleotide kinase and nuclease P₁ were purchased from Boehringer Mannheim (Indianapolis, IN, USA). Glass-based HPTLC plates, 10 × 10 cm, coated with silica gel NH₂ F254s were obtained from EM Separations (Gibbstown, NJ, USA). Radiolabeled [γ -³²P]ATP (6000 Ci/mmol) was purchased from DuPont (Boston, MA, USA) and [2-¹⁴C]deoxycytidine (45–55 mCi/mmol) was from Moravsek Biochemicals (Brea, CA, USA) Kodak Diagnostic Film X-Omat RP was purchased from Eastman Kodak (Rochester, NY, USA).

Cell line

V79 Chinese hamster cells were a kind gift of Morgan Harris, University of California, Berkeley, CA, USA. Cells were grown in Dulbecco's Modified Eagle's Medium (Sigma) supplemented with 10% dialyzed fetal bovine serum (JRH Biosciences, Lenexa, KS, USA).

DNA preparation

Total cellular DNA was extracted using a modified Marmur procedure as previously described [14]. Only DNA samples with an A₂₆₀/A₂₈₀ ratio of 1.8 were used since protein contamination was found to result in poor chromatographic separation. For each sample, 6 μ g of DNA was precipitated using 1/50th volume of 5 M sodium chloride and two volumes of ethanol at -20°C.

Nucleic acid digestion and kinase reactions

DNA (6 μ g) from each sample was digested into 3'-monophosphate nucleosides with micrococcal nuclease (5 units) and phosphodiesterase II (0.25 units) for 3 h at 37°C in 30 μ l of 2.5

mM Tris pH 8.8 containing 2.5 mM CaCl₂. The 3'-monophosphate nucleosides were converted to ³²P-labeled 3',5'-bisphosphate nucleosides by reacting 5 μ l of the above digest with T₄ polynucleotide kinase (5 units) and 25 μ Ci of [γ -³²P]ATP in 50 mM Tris pH 7.6, 10 mM MgCl₂, 5 mM dithiothreitol, 10 μ M ATP, and 1 mM spermidine in a total volume of 25 μ l for 3 h at 37°C. The labeled 3',5'-bisphosphate nucleosides were then converted to 5'-[³²P]monophosphate nucleosides by adding nuclease P₁ (5 units) in a volume of 5 μ l of 0.6 mM ZnCl₂ (for a final concentration of 0.1 mM ZnCl₂) for 1 h at 70°C. This enzymatic hydrolysis is essentially identical to that published by Wilson *et al.* [8]. The digests were then frozen at -20°C until HPTLC analysis.

HPTLC separation and quantitation of the 5'-monophosphate nucleosides^a

Using a 10 × 10 cm glass HPTLC-NH₂ plate with fluorescent indicator, unlabeled dCMP and 5mdCMP were first applied (1 and 2 μ l of 1 mg/ml stocks, respectively) to facilitate the detection of the nucleotides of interest. After centrifuging the digest at 10 000 g for 10 min, 0.5 μ l of the labeled sample was applied over the standards. The plate was developed in isobutyric acid:dH₂O:NH₄OH (17.7:8.0:0.3, v/v) until the solvent front was within 2 mm of the top of the plate. The plate was then dried to completeness (under vacuum at 80°C for 30 min). The plate was again developed in the same dimension in fresh solvents, dried and exposed to X-ray film for ten minutes for sample evaluation. The dCMP and 5mdCMP spots were identified (Fig. 1A) by UV-induced fluorescence (254 nm). Spots corresponding to the standards were marked on the glass side of the plate, excised with a diamond scribe and subjected to scintillation counting with aqueous cocktail. The 5mC content of the DNA was determined from the radioactivity found in the dCMP and 5mdCMP

^a While we found this HPTLC technique useful for the analysis of 5'-monophosphate nucleosides, the 3'-monophosphate nucleosides did not produce sufficient resolution for analysis.

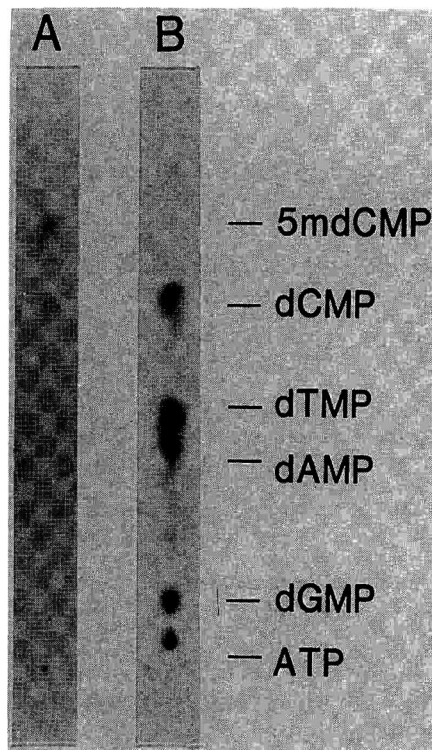


Fig. 1. (A) Postlabeled V79 cell DNA digest on HPTLC-NH₂ after one-dimensional development in isobutyric acid-dH₂O-NH₄OH (17.7:8.0:0.3, v/v/v). The dCMP and 5mdCMP standards were detected under UV light (254 nm). (B) Autoradiogram of the above lane. *R_f* values are: ATP, <0.01; dGMP, 0.05; dAMP, 0.26; dTMP, 0.29; dCMP, 0.45; 5mdCMP, 0.54.

using the following equation: % 5mC = [5mdCMP/(5mdCMP + dCMP)] × 100.

HPLC analysis

For the purpose of comparison, 5mC content of V79 cells was also determined by treating log phase cells with [2-¹⁴C]deoxycytidine and the DNA was analyzed as described previously [16]. Briefly, V79 cells were exposed to [2-¹⁴C]deoxycytidine for 24 h, and DNA was purified and subsequently hydrolyzed to free bases in 88% formic acid for 30 min at 180°C. Formic acid was removed by evaporation under a stream of nitrogen gas and each sample was taken up in a small volume of 0.1 M HCl. Using a Bio-Rad

HPLC system, the labeled bases were separated on an Aminex A-9 column (Bio-Rad) at 60°C using 0.2 M ammonium acetate pH 5.5 at a flow of 1.0 ml/min. Fractions were collected at 30-s intervals and assessed for radioactivity by scintillation counting as above.

RESULTS AND DISCUSSION

The HPTLC-NH₂ plate offers an alternative procedure for the separation of 5'-monophosphate nucleosides. This one-dimensional method, which allows up to ten samples to be analyzed per plate, permits reproducible determination of the percent of 5mC in total DNA. The postlabeling procedure and HPTLC conditions resulted in high incorporation of label and adequate separation of product so that a 0.5 μl application gave average counts of 155 000 and 2300 dpm against a background of <100 dpm for dCMP and 5mdCMP, respectively. The percent of 5mC in total V79 cell DNA as determined by postlabeling and HPTLC was 1.50 ± 0.05. As seen in Table I, this compares favorably with HPLC values reported earlier by Citti *et al.* [10], and with values obtained in our laboratory. As can be seen by the autoradiogram in Fig. 1B, the four major nucleotides dCMP, dTMP, dAMP and dGMP are present in sufficient amounts for quantitation by standard densitometric methods. However, since 5mC normally represents only a small percentage of the total cytosines in mammalian DNA, it was not possible to produce a sufficient exposure of the 5mdCMP spot without

TABLE I
5mC CONTENT OF V79 CELL DNA

Method	%5mC ± standard error
HPTLC	1.50 ± 0.05 ^a
HPLC	1.42 ± 0.20 ^b
HPLC	1.52 ± 0.04 ^c

^a *n* = 4, mean of means.

^b Results from Citti *et al.* [10], number of determinations unknown.

^c Results from V79 cell DNA pre-labeled with [2-¹⁴C]deoxycytidine, *n* = 4.

saturation of the film over the other nucleotide spots.

The limits of this one-dimensional HPTLC technique have yet to be fully defined. We have measured 5mC levels of clinical tumor specimens from patients receiving various chemotherapy agents which tend to alter methylation levels over a wide range. Concentrations of 5mC measured in these samples ranged between 1.0 and 8.5% of total cytosines (data to be published elsewhere). The method reported here thus produces reliable quantitation over at least this range of 5mC concentrations, which encompasses values which could be reasonably expected in mammalian DNA. With the emergence of storage phosphor technology, the overall sensitivity and accuracy could likely be increased [15].

CONCLUSIONS

HPTLC using alkylamino-modified silica plates offers a simple, practical method for the determination of 5mC content in microgram quantities of postlabeled DNA. This technique is different from earlier two-dimensional TLC procedures since the HPTLC-NH₂ plate offers the advantage of multiple sample analysis on a single plate.

ACKNOWLEDGEMENT

The authors wish to acknowledge the technical efforts of Dawn Canupp. This work was sup-

ported by National Cancer Institute Grant R29-CA47217 to JN.

REFERENCES

- 1 K.C. Kuo, R.A. McCune, C.W. Gehrke, R. Midgett and M. Erlich, *Nucl. Acids Res.*, 8 (1980) 4763.
- 2 D. Eick, H. Fritz and W. Doerfler, *Anal. Biochem.*, 135 (1983) 165.
- 3 J. Singer, W.C. Schnute, J.E. Shively, C.W. Todd and A.D. Riggs, *Anal. Biochem.*, 94 (1979) 297.
- 4 P.F. Crain and J.A. McCloskey, *Anal. Biochem.*, 132 (1983) 124.
- 5 C.W. Achwal, C.A. Iyer and H.S. Chandra, *FEBS Lett.*, 158 (1983) 353.
- 6 B.H. Vasilikaki and Y. Nishioka, *Exp. Cell Res.*, 147 (1983) 226.
- 7 M.V. Reddy, R.C. Gupta and K. Randerath, *Anal. Biochem.*, 117 (1981) 271.
- 8 V.L. Wilson, R.A. Smith, H. Autrup, H. Krokan, D.E. Musci, N. Le, J. Longoria, D. Ziska and C.C. Harris, *Anal. Biochem.*, 152 (1986) 275.
- 9 W. Jost and H.E. Hauck, *J. Chromatogr.*, 261 (1983) 235.
- 10 L. Citti, G. Gervasi, G. Turchi and L. Mariani, *J. Chromatogr.*, 261 (1983) 315.
- 11 J. Nyce, S. Weinhouse and P.N. Magee, *Br. J. Cancer*, 48 (1983) 463.
- 12 J. Nyce, L. Liu and P.A. Jones, *Nucl. Acids Res.*, 14 (1986) 4353.
- 13 J. Nyce, *Cancer Res.*, 49 (1989) 5829.
- 14 J. Marmur, *J. Mol. Biol.*, 3 (1961) 208.
- 15 R.F. Johnston, S.C. Pickett and D.L. Barker, *Electrophoresis*, 11 (1990) 355.
- 16 J. Nyce, D. Mylott, S. Leonard, L. Willis and A. Katarina, *J. Liq. Chromatogr.*, 12 (1989) 1313.
- 17 T.B. Johnson and R.D. Coghill, *J. Am. Chem. Soc.*, 47 (1925) 2838.

Short Communication

Validation of a capillary electrophoresis method for the enantiomeric purity testing of fluparoxan

K.D. Altria* and A.R. Walsh

Pharmaceutical Analysis, Glaxo Group Research, Park Road, Ware, Herts. SG12 0DP (UK)

N.W. Smith

Chemical Analysis Department, Glaxo Group Research, Greenford, Middlesex (UK)

(First received March 23rd, 1993; revised manuscript received May 11th, 1993)

ABSTRACT

A free solution capillary electrophoresis method has been validated for the enantiomeric purity determination of either enantiomer of fluparoxan. The method allowed determination of 1% of either enantiomer in the presence of its stereoisomer. Method validation showed adequate detector linearity over the required range. The method also gave good performance in terms of sensitivity for trace levels of the undesired enantiomers, injection precision and recovery.

INTRODUCTION

Free solution capillary electrophoresis (FSCE) methods employing cyclodextrins as chiral recognition agents have been reported for a number of racemic pharmaceuticals [1–4]. However, few reports have considered quantitative aspects of chiral analysis and none have reported the successful validation of a method. Separation conditions have previously been reported [5] for the FSCE chiral separation of the racemic phar-

maceutical fluparoxan (structure shown in Fig. 1). This paper describes the validation of a chiral FSCE method for the determination of the enantiomeric purity of both the (+)- and (–)-enantiomers of fluparoxan.

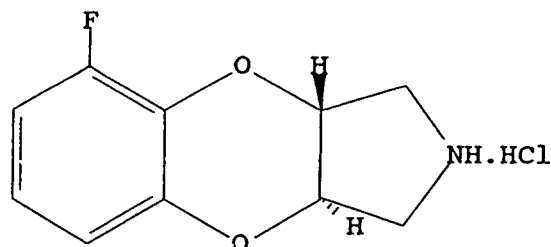


Fig. 1. Structure of fluparoxan.

* Corresponding author.

EXPERIMENTAL

Inorganic chemicals were obtained from Aldrich (Poole, UK). Water was obtained from a Millipore Q system (Watford, UK). Capillary electrophoresis was performed on a P/ACE 2000 CE instrument (Beckman, Palo Alto, CA, US) which was connected to a Hewlett-Packard (Bracknell, UK) data collection system. The fused-silica capillaries used were purchased from Metal Composites, Hallow, UK.

The separation conditions are given below, the method consists of five automated steps: (i) pre-separation rinse 1: 1 min with 0.1 M NaOH; (ii) pre-separation rinse 2: 2 min with electrolyte; (iii) set detector: UV at 214 nm; (iv) sample introduction: 5 s pressure; (v) typically +16 kV applied for 30 min. Operating temperature set at 25°C; 57 cm × 50 μm fused-silica capillary.

Sample concentration (1.25 mg/ml) dissolved in water containing 10% (v/v) electrolyte. Fluparoxan samples were obtained from within Glaxo Group Research.

Electrolyte: (10 mM borax, 10 mM Tris, 150 mM β-cyclodextrin, 6 M urea)-isopropanol (80:20, v/v), the pH of the resulting solution was adjusted to 2.5 with concentrated H₃PO₄.

Normalisation of peak areas to their migration times was performed prior to calculation of %area/area. If this is not performed the later eluting enantiomer is overestimated [6] as it migrates more slowly through the detector.

RESULTS AND DISCUSSION

Capillary electrophoresis separation conditions for the chiral resolution of fluparoxan have been reported [5] which employed 100 mM β-cyclodextrin as the chiral selector. These conditions were shown to be capable of achieving acceptable baseline resolution of the fluparoxan racemate. This method was modified to enable enantiomeric purity detector at a 1% level for each of the single enantiomers. These variations involved use of a higher β-cyclodextrin concentration. The cyclodextrin concentration was raised to 150 mM which improved chiral separation. Cyclodextrin concentrations of as high as 250 mM have been employed elsewhere [7]. However, excessive cyclodextrin concentrations

can have a deleterious effect upon certain separations [8]. A lower ionic strength electrolyte was employed to improve resolution by reducing internal heating within the capillary as resolution decreases at higher temperature [3]. The sample was prepared with dilute electrolyte to improve peak shape by increasing sample stacking [9].

The optimised method was validated for the enantiomeric purity testing of either enantiomer. The validation criteria applied were similar to those applicable to the validation of a HPLC method.

Specificity

A sample of racemic fluparoxan was spiked with the (+)-enantiomer to produce a 60:40 ratio of (+)- to (–)-enantiomers. This sample was analysed to confirm the migration order. Fig. 2 shows a typical separation of this mixture with

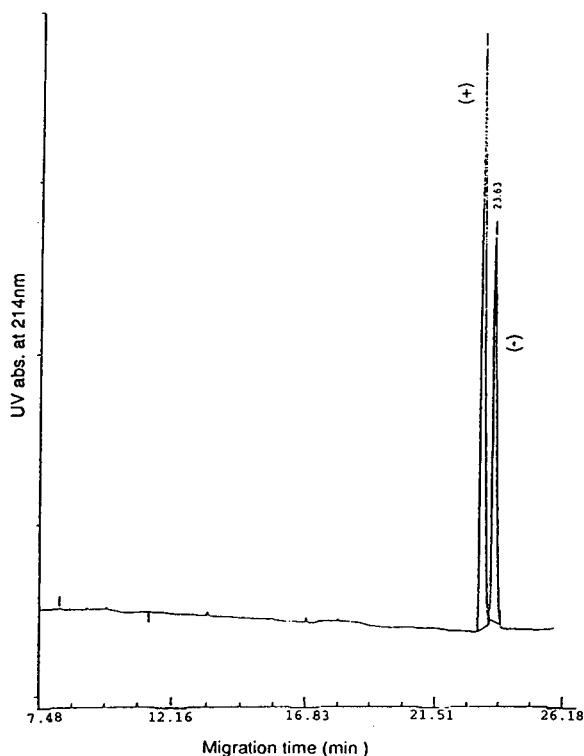


Fig. 2. Electropherogram of 60:40 (w/w) mixture of (+)- and (–)-fluparoxan enantiomers. Separation conditions: 57 cm × 50 μm fused-silica capillary (10 mM borax, 10 mM Tris, 150 mM β-cyclodextrin, 6 M urea)-isopropanol (80:20, v/v), the pH of the resulting solution was adjusted to 2.5 with concentrated H₃PO₄, 25°C, UV detection at 214 nm, +16 kV for 30 min.

TABLE I
QUANTITATIVE ANALYSIS OF AN ENANTIOMER MIXTURE

	(+)-Enantiomer	(-)-Enantiomer
Spiking level (% w/w)	60.1	39.9
% Height	60.3	39.7
% Normalised areas	60.2	39.8

the (+)-enantiomer migrating first. Peak height and normalised peak area measurements quantitatively confirmed the spiking levels (Table I).

Linearity

Detector linearity (peak area) for the CE method was demonstrated over the range 1.5–125% of the nominal target concentration (1.25 mg/ml), a correlation coefficient of 0.994 and an intercept value of 0.2% of the nominal concentration were achieved (Table II).

TABLE II
DETECTOR LINEARITY AND DETECTION LIMITS

Concentration range	Correlation coefficient
1.25–125% nominal	0.994 (intercept 0.2% of nominal value)
1–8% (w/w) of spiked (-)	0.992
1–8% (w/w) of spiked (+)	0.970
Limit of quantitation	1.0%
Limit of detection	0.3%

TABLE III
PRECISION OF INJECTION FOR 1% (w/w) SPIKED SAMPLES ($n = 6$)

	1% (+)-Enantiomer	1% (-)-Enantiomer
Main peak (R.S.D.) for other enantiomer	1.6	2.0
%Area/area for trace enantiomer	0.8	0.9
	0.9	0.9
	1.0	1.0
	0.9	1.0
	1.1	1.0
	0.9	1.2
Average (%area/area)	1.0	0.9

In two further separate exercises solutions of each of the enantiomers were spiked with 1–8% (w/w) of their stereoisomers. In both instances acceptable levels of linearity were obtained (correlation coefficient values of 0.992 and 0.970 for the (-)- and (+)-enantiomers respectively).

Precision of injection

Solutions (1.25 mg/ml) of both single enantiomers were spiked with 1% of their stereoisomers and analysed 6 times. Acceptable levels of precision were obtained for the main peak and for the trace enantiomer (Table III). Good recovery was indicated by the agreement between observed enantiomer level and the % (w/w) spiking. Figs. 3 and 4 show representative separations from the two analysis sets.

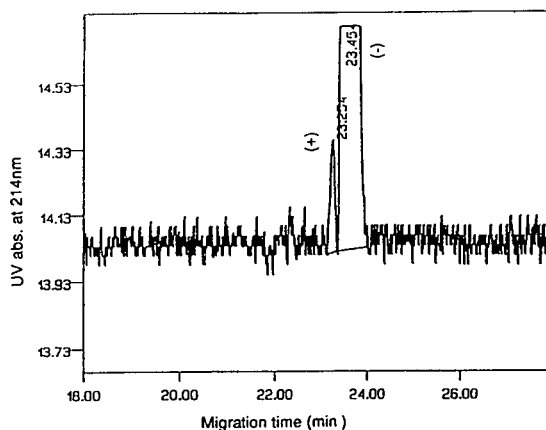


Fig. 3. Typical electropherogram of 1% (+)-enantiomer in presence of (-)-enantiomer. Separation conditions as in Fig. 2.

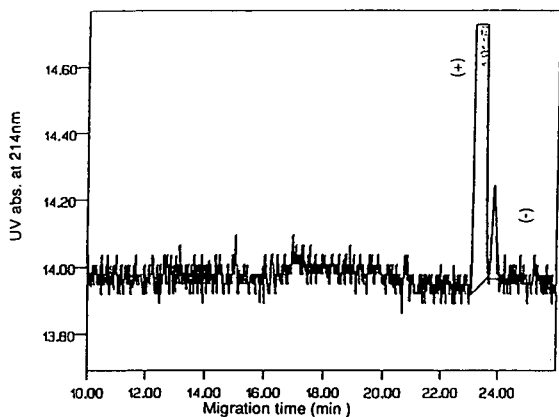


Fig. 4. Typical electropherogram of 1% (–)-enantiomer in presence of (+)-enantiomer. Separation conditions as in Fig. 2.

Limit of detection (LOD)

The method is capable of performing enantiomeric purity testing to the required 1% level for both enantiomers. Figs. 3 and 4 show that signal-to-noise ratios of greater than 3 were obtained for the undesired enantiomers. A limit of detection of 0.3% was calculated giving a limit of quantitation of 1.0% for the undesired enantiomer.

Freedom from interference

A solution of the dissolving solution was injected onto the system, in duplicate, and no interfering peaks were observed.

Stability of sample solutions

Solutions of both the (+)- and (–)-enantiomers were stored for 7 days at 30°C and retested

by the CE method. No racemization had occurred indicating a minimum sample solution shelf-life of 7 days.

CONCLUSIONS

A low-pH FSCE method has been validated for the enantiomeric purity determination of both the (+)- and (–)-enantiomers of fluparoxan. To maximise performance a previously reported method was modified in terms of electrolyte ionic strength, cyclodextrin concentration and the sample dissolving solution. Method validation showed good levels of performance in terms of precision, linearity, recovery and the required LOD. No interfering peaks were obtained from the dissolving solvent.

REFERENCES

- 1 J. Snopek, H. Soini, M. Novotony, E. Smolková-Keulemansová and I. Jelinek, *J. Chromatogr.*, 559 (1991) 215.
- 2 M.J. Sepaniak, R.O. Cole and B.K. Clark, *J. Liq. Chromatogr.*, 15 (1992) 1023.
- 3 K.D. Altria, D.M. Goodall and M.M. Rogan, *Chromatographia*, 34 (1992) 19.
- 4 R. Kuhn, F. Stoecklin and F. Erni, *Chromatographia*, 33 (1992) 32.
- 5 N.W. Smith, poster presented at *HPCE'93, Orlando, January 1993*; *J. Chromatogr. A*, 652 (1993) in press.
- 6 K.D. Altria, *Chromatographia*, 35 (1993) 177.
- 7 A. Shibukawa, D.K. Lloyd and I.W. Wainer, *Chromatographia*, 35 (1993) 419.
- 8 S.A.C. Wren and R.C. Rowe, *J. Chromatogr.*, 603 (1992) 235.
- 9 D.S. Burgi and R.L. Chien, *Anal. Chem.*, 63 (1991) 2042.

Short Communication

Determination of total vitamin C in fruits by capillary zone electrophoresis

Marcella Chiari and Marina Nesi

Istituto di Chimica degli Ormoni, CNR, Via Mario Bianco 9, Milano 20133 (Italy) and Faculty of Pharmacy and Department of Biomedical Sciences and Technologies, University of Milan, Via Celoria 2, Milan 20133 (Italy)

Giacomo Carrea

Istituto di Chimica degli Ormoni, CNR, Via Mario Bianco 9, Milan 20133 (Italy)

Pier Giorgio Righetti*

Faculty of Pharmacy and Department of Biomedical Sciences and Technologies, University of Milan, Via Celoria 2, Milan 20133 (Italy)

(First received February 25th, 1993; revised manuscript received April 26th, 1993)

ABSTRACT

A simple capillary zone electrophoretic (CZE) method is described for the rapid determination of ascorbic acid and dehydroascorbic acid, the physiologically active forms of vitamin C, in fruits. The electrophoretic run was accomplished in 9 min on a coated capillary column using 20 mM phosphate buffer (pH 7.0). Total ascorbic acid was determined by first reducing the dehydroascorbic acid to ascorbic acid by treatment with DL-homocysteine. This reaction was complete in 15 min and total ascorbic acid determination was performed immediately. The data obtained by CZE were in good agreement with HPLC data.

INTRODUCTION

Vitamin C is widely distributed in both animals and plants, probably in equilibrium with dehydro-L-ascorbic acid. Plants rapidly synthesize L-ascorbic acid from carbohydrates, some of which is metabolized into carbohydrates and re-converted into L-ascorbic acid for storage in the metabolic pool. Its content in most plants rarely

exceeds 100 mg% of fresh mass, except for a few species that accumulate it in their tissues. The vitamin C content in oranges is about 50 mg per 100 g [1]. Ascorbic acid is also very important in food technology, where it is used as a stabilizer for processing of beverages, wines and meat products.

L-Dehydroascorbic acid occurs in biological materials in relatively low concentrations and it is formed in a redox system in the presence of ascorbic acid. The amounts of ascorbic acid and dehydroascorbic acid are therefore regarded as

* Corresponding author.

criteria for the initial concentration of ascorbic acid in foodstuffs. Ascorbic acid is mainly determined in fruits and vegetables for judging the storage quality whereas dehydroascorbic acid is only determined in vegetable foodstuffs for assessing the ascorbic acid concentration and its total balance.

Degradation reactions of L-ascorbic acid in aqueous solution depend on several factors, such as pH, temperature and the presence or absence of oxygen and of metals [2–4]. Numerous methods have been developed for the determination of both ascorbic acid (AA) and dehydroascorbic acid (DAA). These include: (1) determination of DAA by condensation with 2,4-dinitrophenylhydrazine and determination of total ascorbic acid (TAA) by oxidation of AA to DAA and subsequent osazone formation [5–7]; (2) the procedure of Tillmans *et al.* [8] based on the titration of AA with 2,6-dichloroindophenol [8,9], reduction of DAA and final titration for evaluation of TAA; and (3) treatment of DAA with *o*-phenylenediamine to produce an easily detectable fluorophore [10]. Each of these methods has been adapted for the semiautomated continuous-flow determination of ascorbic acid in pharmaceuticals and food products. However, these procedures are not specific for ascorbic acid, require the preparation and analysis of blanks and are time consuming. Several HPLC methods have also been described for the determination of TAA, based on UV, fluorimetric or electrochemical detectors [11–13]. Among them, Dennison *et al.* [11] described a method for the determination of vitamin C in beverages by UV measurement of AA after reduction of DAA with homocysteine.

Capillary zone electrophoresis (CZE) offers many advantages for the separation of ionic substances [14–18]. In CZE, the analytes are separated according to their net electrophoretic mobility under the influence of a high potential field. In a coated capillary the electroosmotic flow is strongly reduced and the neutral products exhibit a negligible mobility under an electric field. In this context the separation is only affected by the differences in charges. A procedure for the rapid determination of AA and TAA based on the observation that

homocysteine reduces DAA completely to AA was adopted in this work. The reduction of DAA was necessary because of its low molar absorptivity. Thus, ascorbic acid was determined before and after reduction, the difference representing the amount of DAA in the sample. The same samples were also injected into an HPLC system under the conditions described by Dennison *et al.* [11] in order to compare the quantitative results.

After this paper has been submitted, a paper was published [19] dealing with the analysis of vitamin C in biological fluids and fruit beverages by CZE. However, in that work no mention was made of the equilibrium between reduced and oxidized vitamin C, and we therefore assume that Koh *et al.* [19] were unable to determine dehydroascorbic acid.

EXPERIMENTAL

Materials

DL-Homocysteine and dehydroascorbic acid were obtained from Aldrich (Steinheim, Germany), L-ascorbic acid from Merck (Darmstadt, Germany), acrylamide, ammonium peroxodisulphate and N,N,N',N'-tetramethylethylenediamine (TEMED) from Bio-Rad Labs. (Richmond, CA, USA) and phthalic acid from Carlo Erba (Milan, Italy). A fused-silica capillary (100 μm) was supplied by Polymicro Technologies (Phoenix, AZ, USA).

Methods

CZE was performed in a Waters Quanta 4000 capillary electrophoresis system (Millipore, Millford, MA, USA). The analysis was carried out with 20 mM phosphate buffer (pH 7.0) at 6 kV and 60 μA in a 40 cm \times 100 μm I.D. capillary. The samples were loaded by hydrostatic pressure for 6 s. The detector was set at 254 nm and the run was carried out at room temperature under reversed polarity (cathode at the injection port and anode at the detection side). The capillary was washed with 20 mM phosphate buffer (pH 7.0) after each run.

HPLC separation of ascorbic acid was achieved with a Jasco HPLC instrument. The column effluents were monitored at 254 nm. A

column of 150 mm \times 4.6 mm I.D., packed with Erbasil NH₂ spheres of 5 μ m diameter, efficiently separated AA isocratically by using methanol–0.25% KH₂PO₄ buffer (pH 3.5) (1:1, v/v) as the mobile phase. The flow-rate was 0.5 ml/min and the sample injection volume was 10 μ l.

Coating the capillary inner wall

The following procedure gave the best results. The capillary was first treated with 100 μ l of 1 M NaOH for 5 h, then rinsed and flushed with 100 μ l of 0.1 M HCl followed by 100 μ l of 0.1 M NaOH. After 1 h it was rinsed with water and acetone, filled with a 1:1 solution of acetone in Bind Silane [3-(trimethoxysilyl)propyl methacrylate] and then incubated overnight. After this treatment, the capillary was rinsed with acetone, flushed with air for 5 min and then washed with 20 mM phosphate buffer (pH 7.0). The capillary was filled with 6% acrylamide solution in the same buffer, degassed and containing the appropriate amount of catalyst (0.5 μ l TEMED and 0.5 μ l of 40% ammonium peroxodisulphate per millilitre of gelling solution). Polymerization was allowed to proceed overnight at room temperature and then the capillary was emptied by means of a syringe.

Sample extraction and treatment procedures

For determination of total vitamin C, 5 ml of 12.5% trichloroacetic acid were added to a 15-g portion of freshly squeezed orange juice, the solution was centrifuged and filtered and the filtrate was assayed for AA. The sample solution was then diluted with distilled water so as to provide an estimated ascorbic acid concentration of 10–100 μ g/ml, and the pH was adjusted to 7.0. The reduction of DAA was performed by adding 2.0 ml of 0.8% DL-homocysteine solution to 0.5 ml of the sample extract (a minimum of a 40:1 molar excess of homocysteine to dehydroascorbic acid). After 15 min, the sample was filtered and assayed immediately.

Standardization

Serial dilutions containing 5–80 μ g/ml were prepared by dissolving reference grade ascorbic acid mixed with phthalic acid used as an internal standard. Aliquots of each standard were ana-

lysed and a calibration graph was obtained by plotting peak height *versus* concentration. The ascorbic acid concentration of the sample extract was calculated by interpolation on the calibration graph and by application of dilution factors. The AA concentration of the sample was expressed as mg per 100 ml.

RESULTS AND DISCUSSION

The determination of total ascorbic acid required a rapid method of converting DAA into AA, as only AA possessed the strong UV absorption necessary for detection. The reduction of DAA to AA by DL-homocysteine was described in 1956 by Hughes [20] and verified by Dennison *et al.* [11]. The reaction is highly efficient and provided a rapid method of reducing DAA for total ascorbic acid determination.

Standards and orange juice samples, when injected into the CZE system, gave a typical electropherogram as shown in Fig. 1. In a coated capillary, owing to the migration conditions adopted, only AA is visible (peak 2), peak 1 corresponding to the phthalic acid used as internal standard in the quantitative analysis. The response was linear between 3 and at least 80

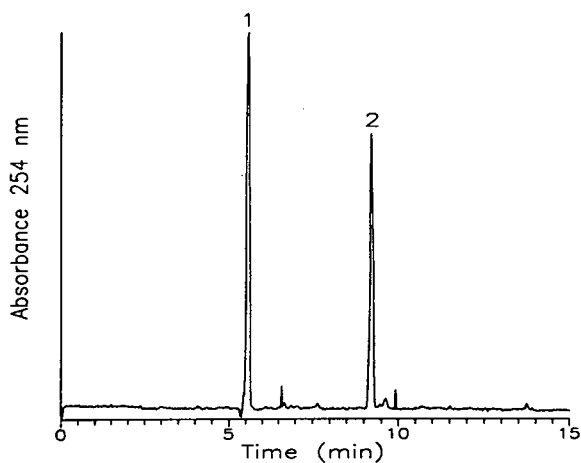


Fig. 1. CZE profile of a homocysteine-reduced orange juice sample. Sample injection: 6 s by hydrostatic pressure. Coated capillary of 40 cm \times 100 μ m I.D. Run in 20 mM phosphate buffer (pH 7.0) at 6 kV and 60 μ A. Detection at 254 nm; anodic migration (reverse polarity). Peaks: 1 = internal standard (phthalic acid); 2 = ascorbic acid.

$\mu\text{g/ml}$. The amounts assessed in two different samples of orange juice were 44.7 ± 1.3 and 57.5 ± 1.7 mg per 100 ml ($n=6$ in both instances), in excellent agreement with the HPLC results (45.2 ± 2.2 and 56.5 ± 3.1 mg per 100 ml, respectively; $n=6$). Although we have not evaluated the stability of the coating over an extended period of time, we did not experience any deterioration of the results after at least 100 sample analyses. A typical HPLC elution profile of a diluted and reduced freshly squeezed orange juice is shown in Fig. 2. The HPLC procedure affords an excellent separation among AA (peak with retention time of 8.718) and the reacted and unreacted DL-homocysteine (4.722 and 5.940 min, respectively).

In conclusion, the CZE procedure proposed here for ascorbic acid is simple, requires a minimum of sample preparation and provides a good method for the rapid determination of total

vitamin C. In addition, the CZE method measures the ascorbic acid directly, eliminating the need for organic solvents and expensive chromatographic columns. The combined treatment and analysis time required for any sample does not exceed 25 min, with complete recovery from the food matrices examined.

ACKNOWLEDGEMENTS

This work was supported in part by a grant from the Progetto Finalizzato Chimica Fine II (CNR, Rome, Italy). M. Nesi is the recipient of a fellowship from CNR, Rome.

REFERENCES

- 1 G.M. Jaffe, in L.J. Machlin (Editor), *Handbook of Vitamins*, Marcel Dekker, New York, 1984, pp. 199–244.
- 2 K. Mikova and J. Davidele, *Chem. Listy*, 68 (1974) 715–720.
- 3 F.E. Uelin, *Food Res.*, 18 (1953) 633–639.
- 4 J. Campbell and W.G. Tubb, *Can. J. Res.*, 28E (1947) 19–25.
- 5 J.H. Roe, M.B. Mills, M.J. Oesterling and C.M. Dawson, *J. Biol. Chem.*, 174 (1948) 201–205.
- 6 C.F. Bourgeois and P.R. Nainguy, *Int. J. Vitam. Nutr. Res.*, 44 (1974) 70–76.
- 7 O. Pelletier and R. Brossard, *J. Food Sci.*, 42 (1977) 1471–1476.
- 8 J. Tillmans, P. Hirsch and F. Siebert, *Z. Unters. Lebensm.*, 63 (1932) 21–30.
- 9 K. Hiromi, C. Kuwamoto and M. Ohnishi, *Anal. Biochem.*, 101 (1980) 421–430.
- 10 M.J. Deutsch and C.E. Weeks, *J. Assoc. Off. Anal. Chem.*, 48 (1965) 1248–1253.
- 11 D.B. Dennison, T.G. Browley and G.L.K. Hunter, *J. Agric. Food Chem.*, 29 (1981) 927–929.
- 12 W. Kneifel and R. Sommer, *Z. Lebensm.-Unters.-Forsch.*, 181 (1985) 107–110.
- 13 K. Brunt and H.C.P. Bruins, *J. Chromatogr.*, 172 (1979) 37–47.
- 14 F.E.P. Mikkers, F.M. Everaerts and Th.P.E.M. Verheggen, *J. Chromatogr.*, 169 (1979) 11–20.
- 15 J.W. Jorgenson and K.D. Lucacs, *Anal. Chem.*, 53 (1981) 1298–1303.
- 16 J.W. Jorgenson and K.D. Lucacs, *Science*, 222 (1983) 266–268.
- 17 E. Gassman, J.E. Kuo and R.N. Zare, *Science*, 230 (1985) 813–816.
- 18 H.H. Lauer and D. McManigill, *Anal. Chem.*, 58 (1986) 166–172.
- 19 E.V. Koh, M.G. Bissell and R.K. Ito, *J. Chromatogr.*, 633 (1993) 145–150.
- 20 R.E. Hughes, *Biochem. J.*, 64 (1956) 203–208.

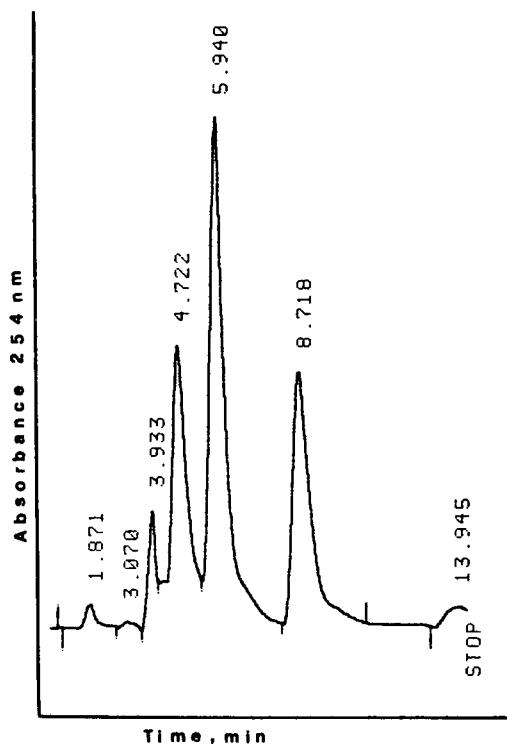


Fig. 2. HPLC profile of the orange juice sample in Fig. 1. Sample injection volume: $10 \mu\text{l}$. Column: $150 \text{ m} \times 4.6 \text{ mm}$ I.D., packed with Erbasil NH_2 spheres of $5 \mu\text{m}$ diameter. Isocratic elution with methanol–0.25% potassium phosphate buffer (pH 3.5) as mobile phase at a flow-rate of 0.5 ml/min . Detection at 254 nm. Vitamin C is the peak with an elution time of 8.718 min.

CATALOGUE 1993 ON CD-ROM

Elsevier Science Publishers - the world's largest scientific publisher - presents for the first time details of all its publications on CD-ROM

ADVANTAGES

- Easy to use.
- Get more comprehensive information than ever before.
- Make fast and effective searches.
- Find what you want even with incomplete information.
- Compile special lists of products without typing.
- Improve your control of scientific product information.
- Enhance service to clients.

PRODUCT DESCRIPTION

The CD-ROM contains descriptions of all Elsevier products.

- All the journals, with complete information about journal editors and editorial boards
- Listings of recently published papers for many journals
- Complete descriptions and contents lists of book titles
- Independent reviews of published books
- Forthcoming title information
- Book series
- All other products, e.g. software, CDs, dictionaries, wallcharts.

In addition, the CD-ROM features easy-to-use search tools, making the information

accessible and useful. For example, searches can be made by subject area, by year of publication, by author/editor or title and by "free text" search.

Full book and journal information can be printed to initiate your order.

If you do not find what you need, or wish to know more about Elsevier's publishing programme, the CD-ROM can supply you with the name, address and fax number of the correct person to contact.

AUDIENCE

Librarians, booksellers, researchers, agents and information specialists.

SYSTEM REQUIREMENTS

The CD-ROM has been designed to run under Microsoft® Windows™ 3.0, on IBM PC-ATs and compatibles. The CD-ROM is Microsoft® Windows™ 3.1 compatible.

The minimum requirements are:

- IBM or IBM-compatible PC with a 80286 or higher processor
- 2 MB or more RAM
- MS-DOS® 3.3 or higher installed
- Microsoft® Windows™ 3.0 (or 3.1) installed
- Microsoft® Windows™ compatible mouse or other pointing device
- VGA graphics adapter (colour or monochrome)
- Hard disk with at least 2 MB free disk space
- CD-ROM drive which is accessible from Microsoft® Windows™
- For faster operation a 80386SX or higher processor is recommended, as well as a fast CD-ROM drive (access time less than 0.4 seconds).

The CD-ROM can be installed in a local area network.

For further information please contact

ELSEVIER SCIENCE PUBLISHERS
Attn. Vivian Wong Swie San
Marketing Services Department
P.O. Box 211
1000 AE Amsterdam
The Netherlands
FAX: (020) 5862 425
In the USA & Canada
Journal Information Center
P.O. Box 882
Madison Square Station
New York, NY 10159, USA
FAX: (212) 633 3764



ELSEVIER
SCIENCE PUBLISHERS

Intelligent Software for Chemical Analysis

Edited by L.M.C. Buydens and P.J. Schoenmakers

Data Handling in Science and Technology Volume 13

Various emerging techniques for automating intelligent functions in the laboratory are described in this book. Explanations on how systems work are given and possible application areas are suggested. The main part of the book is devoted to providing data which will enable the reader to develop and test his own systems. The emphasis is on expert systems; however, promising developments such as self-adaptive systems, neural networks and genetic algorithms are also described.

The book has been written by chemists with a great deal of practical experience in developing and testing intelligent software, and therefore offers first-hand knowledge. Laboratory staff and managers confronted with commercial intelligent software will find information on the functioning, possibilities and limitations thereof, enabling them to select and use modern software in an optimum fashion. Finally, computer scientists and information scientists will find a wealth of data on the application of contemporary artificial intelligence techniques.

Contents:

1. Introduction. Automation and intelligent software. Expert systems. Neural networks and genetic algorithms. Reader's guide. Concepts. Conclusions.
2. Knowledge-based Systems in Chemical Analysis (P. Schoenmakers). Computers in analytical chemistry. Sample preparation. Method selection. Method development. Instrument control and error diagnosis. Data handling and calibration. Data

interpretation. Validation. Laboratory management. Concluding remarks. Concepts. Conclusions. Bibliography.
3. Developing Expert Systems (H. van Leeuwen). Introduction. Prerequisites. Knowledge acquisition. Knowledge engineering. Inferencing. Explanation facilities. The integration of separate systems. Expert-system testing validation and evaluation. Concepts. Conclusions. Bibliography.

4. Expert-System-Development Tools (L. Buydens, H. van Leeuwen, R. Wehrens). Tools for implementing expert systems. Tool selection. Knowledge-acquisition tools. Concepts. Conclusions. Bibliography. **5. Validation and Evaluation of Expert Systems for HPLC Method Development - Case Studies** (F. Maris, R. Hindriks). Introduction. Case study I: Expert systems for method selection and selectivity optimization. Case study II: System-optimization expert system. Case study III: Expert system for repeatability testing, applied for trouble-shooting in HPLC. Case study IV: Ruggedness-testing expert system. General comments on the evaluations. Concepts. Conclusions. Bibliography.
6. Self-adaptive Expert Systems (R. Wehrens). Introduction -

maintaining expert systems. Self-adaptive expert systems: Methods and approaches. The refinement approach of SEEK. Examples from analytical chemistry. Concluding remarks. Concepts. Conclusions. Bibliography.
7. Inductive Expert Systems (R. Wehrens, L. Buydens). Introduction. Inductive classification by ID3. Applications of ID3 in analytical chemistry. Concluding remarks. Concepts. Conclusions. Bibliography. **8. Genetic Algorithms and Neural Networks** (G. Kateman). Introduction. Genetic algorithms. Artificial neural networks. Concepts. Conclusions. Bibliography. **9. Perspectives.** Limitations of Intelligent Software. Dealing with intelligent software. Potential of intelligent software. **Index.**

© 1993 366 pages Hardbound
Price: Dfl. 350.00 (US \$ 200.00)
ISBN 0-444-89207-9

ORDER INFORMATION

For USA and Canada
ELSEVIER SCIENCE PUBLISHERS
Judy Weislogel, P.O. Box 945
Madison Square Station
New York, NY 10160-0757
Fax: (212) 633 3880

In all other countries
ELSEVIER SCIENCE PUBLISHERS
P.O. Box 330
1000 AH Amsterdam
The Netherlands
Fax: (+31-20) 5862 845

US\$ prices are valid only for the USA & Canada and are subject to exchange rate fluctuations; in all other countries the Dutch guilder price (Dfl.) is definitive. Customers in the European Community should add the appropriate VAT rate applicable in their country to the price(s). Books are sent postfree if prepaid.



ELSEVIER
SCIENCE PUBLISHERS

PUBLICATION SCHEDULE FOR THE 1993 SUBSCRIPTION

Journal of Chromatography and Journal of Chromatography, Biomedical Applications

MONTH	1992	J-A	M	J	J	A	S	O	N	D
Journal of Chromatography	Vols. 623-627	Vols. 628-636	637/1 637/2 638/1 638/2	639/1 639/2 640/1 + 2	641/1 641/2 642/1 + 2 643/1 + 2 644/1	644/2 645/1 645/2 646/1	646/2 647/1 647/2	648/1 648/2		
Cumulative Indexes, Vols. 601-650 ^a										
Bibliography Section		649/1		649/2			650/1		650/2	
Biomedical Applications		Vols. 612, 613 and 614/1	614/2 615/1	615/2 616/1	616/2 617/1	617/2 618/1 + 2	619/1 619/2	620/1 620/2	621/1 621/2	622/1 622/2

^a To appear in 1994.

INFORMATION FOR AUTHORS

(Detailed *Instructions to Authors* were published in Vol. 609, pp. 437-443. A free reprint can be obtained by application to the publisher, Elsevier Science Publishers B.V., P.O. Box 330, 1000 AH Amsterdam, Netherlands.)

Types of Contributions. The following types of papers are published in the *Journal of Chromatography* and the section on *Biomedical Applications*: Regular research papers (Full-length papers), Review articles, Short Communications and Discussions. Short Communications are usually descriptions of short investigations, or they can report minor technical improvements of previously published procedures; they reflect the same quality of research as Full-length papers, but should preferably not exceed five printed pages. Discussions (one or two pages) should explain, amplify, correct or otherwise comment substantively upon an article recently published in the journal. For Review articles, see inside front cover under Submission of Papers.

Submission. Every paper must be accompanied by a letter from the senior author, stating that he/she is submitting the paper for publication in the *Journal of Chromatography*.

Manuscripts. Manuscripts should be typed in **double spacing** on consecutively numbered pages of uniform size. The manuscript should be preceded by a sheet of manuscript paper carrying the title of the paper and the name and full postal address of the person to whom the proofs are to be sent. As a rule, papers should be divided into sections, headed by a caption (e.g., Abstract, Introduction, Experimental, Results, Discussion, etc.) All illustrations, photographs, tables, etc., should be on separate sheets.

Abstract. All articles should have an abstract of 50-100 words which clearly and briefly indicates what is new, different and significant. No references should be given.

Introduction. Every paper must have a concise introduction mentioning what has been done before on the topic described, and stating clearly what is new in the paper now submitted.

Illustrations. The figures should be submitted in a form suitable for reproduction, drawn in Indian ink on drawing or tracing paper. Each illustration should have a legend, all the *legends* being typed (with double spacing) together on a *separate sheet*. If structures are given in the text, the original drawings should be supplied. Coloured illustrations are reproduced at the author's expense, the cost being determined by the number of pages and by the number of colours needed. The written permission of the author and publisher must be obtained for the use of any figure already published. Its source must be indicated in the legend.

References. References should be numbered in the order in which they are cited in the text, and listed in numerical sequence on a separate sheet at the end of the article. Please check a recent issue for the layout of the reference list. Abbreviations for the titles of journals should follow the system used by *Chemical Abstracts*. Articles not yet published should be given as "in press" (journal should be specified), "submitted for publication" (journal should be specified), "in preparation" or "personal communication".

Dispatch. Before sending the manuscript to the Editor please check that the envelope contains four copies of the paper complete with references, legends and figures. One of the sets of figures must be the originals suitable for direct reproduction. Please also ensure that permission to publish has been obtained from your institute.

Proofs. One set of proofs will be sent to the author to be carefully checked for printer's errors. Corrections must be restricted to instances in which the proof is at variance with the manuscript. "Extra corrections" will be inserted at the author's expense.

Reprints. Fifty reprints will be supplied free of charge. Additional reprints can be ordered by the authors. An order form containing price quotations will be sent to the authors together with the proofs of their article.

Advertisements. The Editors of the journal accept no responsibility for the contents of the advertisements. Advertisement rates are available on request. Advertising orders and enquiries can be sent to the Advertising Manager, Elsevier Science Publishers B.V., Advertising Department, P.O. Box 211, 1000 AE Amsterdam, Netherlands; courier shipments to: Van de Sande Bakhuyzenstraat 4, 1061 AG Amsterdam, Netherlands; Tel. (+31-20) 515 3220/515 3222, Telefax (+31-20) 6833 041, Telex 16479 els vi nl. UK: T.G. Scott & Son Ltd., Tim Blake, Portland House, 21 Narborough Road, Cosby, Leics. LE9 5TA, UK; Tel. (+44-533) 753 333, Telefax (+44-533) 750 522. USA and Canada: Weston Media Associates, Daniel S. Lipner, P.O. Box 1110, Greens Farms, CT 06436-1110, USA; Tel. (+1-203) 261 2500, Telefax (+1-203) 261 0101.

Statistical Treatment of Experimental Data

by J. R. Green and D. Margerison

This book is primarily intended for researchers wishing to analyse experimental data using statistical methods. Statistical concepts and methods which may be employed to treat experimental data are explained, and the ideas and reasoning behind statistical methodology are clarified. Formal results are illustrated by many numerical worked examples mainly taken from the laboratory. Concepts, practical methodology, and worked examples are integrated in the text.

Consideration is given in this work to a large number of practical topics which are often omitted from standard texts. These include; obtaining an approximate confidence interval for a function of some unknown parameters; testing for outliers, stabilization of heterogeneous variances, and significant differences between means; estimation of parameters after performing tests; deciding what numbers of significant figures to quote for sample means and variances; straight-line and polynomial regression, through the origin or not, using weighted points, and testing the homogeneity of a set of such lines or curves.

The numerous examples which are provided throughout the text will serve as models for the various problems encountered by the readers when

employing statistical methods to treat experimental data. Neither a strong mathematical background nor a prior knowledge of probability or statistics is required in order to make use of this work.

In addition to research workers in universities and industry, the book will be of use for first-year students of statistics, and would be especially suitable as the basis of a graduate course in experimental sciences.

Contents: 1. Introduction. 2. Probability. 3. Random Variables and Sampling Distributions. 4. Some Important Probability Distributions. 5. Estimation. 6. Confidence Intervals. 7. Hypothesis Testing. 8. Tests on Means. 9. Tests on Variances. 10. Goodness of Fit Tests. 11. Correlation. 12. The Straight Line Through the Origin or Through Some Other Fixed Point. 13. The Polynomial Through the Origin or Through Some Other Fixed Point. 14. The General Straight Line. 15. The General Polynomial. 16. A Brief Look at Multiple Regression. Appendices: 1. Drawing a Random Sample Using a Table of Random Numbers. 2. Orthogonal Polynomials in x . References. Index.

1977 5th imp. 1988 x + 382 pages
Price: US \$ 96.00 / Dfl. 168.00
ISBN 0-444-41725-7



Elsevier Science Publishers

P.O. Box 211, 1000 AE Amsterdam, The Netherlands
P.O. Box 882, Madison Square Station, New York, NY 10159, USA



0021-9673(19930813)645:1;1-X